RETURN TO ANL (IDAHO) LIBRARY.

ANL-7770

Argonne National Laboratory

Division of Biological and Medical Research

Annual Report

1970

The facilities of Argonne National Laboratory are owned by the United States Government. Under the terms of a contract (W-31-109-Eng-38) between the U. S. Atomic Energy Commission, Argonne Universities Association and The University of Chicago, the University employs the staff and operates the Laboratory in accordance with policies and programs formulated, approved and reviewed by the Association.

MEMBERS OF ARGONNE UNIVERSITIES ASSOCIATION

The University of Arizona
Carnegie-Mellon University
Case Western Reserve University
The University of Chicago
University of Cincinnati
Illinois Institute of Technology
University of Illinois
Indiana University
Iowa State University
The University of Iowa
Kansas State University
The University of Kansas
Loyola University
Marquette University
Michigan State University
The University of Michigan
University of Minnesota
University of Missouri
Northwestern University
University of Notre Dame
The Ohio State University
Ohio University
The Pennsylvania State University
Purdue University
Saint Louis University
Southern Illinois University
The University of Texas at Austin
Washington University
Wayne State University
The University of Wisconsin

NOTICE

This report was prepared as an account of work sponsored by the United States Government. Neither the United States nor the United States Atomic Energy Commission, nor any of their employees, nor any of their contractors, subcontractors, or their employees, makes any warranty, express or implied, or assumes any legal liability or responsibility for the accuracy, completeness or usefulness of any information, apparatus, product or process disclosed, or represents that its use would not infringe privately-owned rights.

Printed in the United States of America
Available from
National Technical Information Service
U.S. Department of Commerce
5285 Port Royal Road
Springfield, Virginia 22151
Price: Printed Copy $3.00; Microfiche $0.95

ANL-7770

Biology and Medicine

Argonne National Laboratory
9700 South Cass Avenue
Argonne, Illinois 60439

Division of Biological and Medical Research

Annual Report 1970

December 1970

Warren K. Sinclair, Director
John F. Thomson, Associate Director

Preceding Report
ANL-7635, December 1969

FOREWORD

This report represents a departure from the format followed in previous years. On the one hand, we are faced with the necessity of reducing publication costs; on the other, we wish to preserve a primary function of the report, viz., a medium for information about work in progress in this Division. The 1970 report is a compromise between these aims. Individual submissions generally are shorter, and somewhat less detailed than formerly; research that has reached the stage of submission of a manuscript to a journal has been represented only by the abstract.

We expect that further changes in our annual report will take place in future years. We would appreciate comments from our readers on the format and scope of this report.

TABLE OF CONTENTS

EFFECTS OF RADIATION ON LIVING ORGANISMS

ACUTE AND CHRONIC EFFECTS OF EXTERNAL X-RAY AND GAMMA RADIATIONS

1 Study of cell proliferation of the hair follicle
R. J. Michael Fry, Charlotte L. Weber, Walter E. Kisieleski, Melvin L. Griem, and Frederick D. Malkinson

1 The influence of route of administration on the uptake of tritiated thymidine
R. J. Michael Fry, Walter E. Kisieleski, and Anthony R. Sallese

2 Explanting the 3-day chick embryo for the study of radiation injury to the microcirculation
Emily J. B. Christian and S. Phyllis Stearner

3 A technique to visualize the peripheral microcirculation in the young chicken
Emily J. B. Christian and S. Phyllis Stearner

3 Microvasculature and loose connective tissue in freeze-fracture preparations
S. Phyllis Stearner and Margaret H. Sanderson

Mechanisms of acute radiation damage and repair

3 Introduction
S. Phyllis Stearner

4 I. *In vivo* observations of microvascular injury in the gamma-irradiated chicken
S. Phyllis Stearner and Emily J. B. Christian

5 II. Ultrastructure of the chick mesentery and early effects of gamma irradiation
S. Phyllis Stearner and Margaret H. Sanderson

6 III. Toward an interpretation of the increase and decay of resistance to early lethal radiation injury
S. Phyllis Stearner, Sylvanus A. Tyler, and Merlin H. Dipert

7 IV. Long-term effects of ionizing radiations in the chicken: A. Survival
S. Phyllis Stearner and Emily J. B. Christian

9 Hydroxyurea and cell-cycle kinetics of cultured antibody-forming cells
Bernard N. Jaroslow and Librado Ortiz-Ortiz

9 Late effects of irradiation on immune responsiveness of aging mice
Bernard N. Jaroslow and Marietta M. Miller

Laboratory animal medicine

10 Statement of program objectives
Robert J. Flynn, Thomas E. Fritz, Calvin M. Poole and Patricia C. Brennan

I. The supply and maintenance of defined animals

10 A. Status of the colony
Calvin M. Poole, Thomas E. Fritz, Patricia C. Brennan, and Robert J. Flynn

11 B. The development of inbred catalase mutant mice
Calvin M. Poole, Ronald W. Camden, Robert J. Flynn, and Robert N. Feinstein

12 C. *Rattus rattus* as an experimental animal
Thomas E. Fritz, David V. Tolle, Robert J. Flynn, and Patricia C. Brennan

II. Laboratory animal diseases

14 A. Murine pneumonia
Patricia C. Brennan, Thomas E. Fritz, and Robert J. Flynn

15 B. Survival of *Pseudomonas aeruginosa* in acidified water
Patricia C. Brennan

15 C. Throat flora of a closed colony of beagle dogs
Patricia C. Brennan and Richard C. Simkins

16 D. The use of the scanning electron microscope as an aid in the identification of mites affecting laboratory animals
Robert J. Flynn and George T. Chubb

III. Laboratory animal management

17 A. Frequency of cage cleaning and the survival of mice
Robert J. Flynn and Calvin M. Poole

18 B. Effects of acidified water on health of mice
Calvin M. Poole, Thomas E. Fritz, and Robert J. Flynn

18 C. Long-distance air transport of aged laboratory mice
Robert J. Flynn, Calvin M. Poole, and Sylvanus A. Tyler

THEORETICAL BIOLOGY

19 Do band cells follow "first in-first out" kinetics?
Ernesto Trucco
22 The "fall" of intracellular particles on a horizontal-axis clinostat
Ernesto Trucco, Sylvanus A. Tyler, Merlin H. Dipert, and Richard R. Dedolph
23 The determination of cell-cycle parameters from measurements of the fraction of labeled mitoses
Peter J. Brockwell, Ernesto Trucco, and R. J. Michael Fry
23 A method for the mathematical definition of rhythmic biological responses
Merlin H. Dipert, William Chorney, and Richard R. Dedolph
24 Binomial-sequential model of photoreactivation
Sylvanus A. Tyler and David J. G. Davies

NEUTRON AND GAMMA-RAY TOXICITY STUDIES

26 Completion and dosimetry of the JANUS High Flux Exposure Room
Frank S. Williamson, Gordon L. Holmblad, and Joseph E. Trier
29 The effect of fission neutrons from the JANUS reactor upon Chinese hamster cells in culture
Warren K. Sinclair
32 Relative biological effectiveness of neutrons from the JANUS reactor: Survival of mice, colony-forming units, and intestinal microcolonies
E. John Ainsworth, R. J. Michael Fry, Frank W. Williamson, Donn L. Jordan, Mary P. O'Malley and Anthony R. Sallese
33 Strain differences of gut and bone marrow and their relation to radiosensitivity
R. J. Michael Fry, Walter E. Kisieleski, E. John Ainsworth, and Anthony R. Sallese
34 Properties of colony-forming units—studies in progress
E. John Ainsworth and Mary P. O'Malley
36 Hematopoietic injury and recovery: Evaluation by granulocyte mobilization
E. John Ainsworth, Eugenia M. Cooke, Marietta Miller, and Mary P. O'Malley
38 Neutron and gamma-ray toxicity studies: Further analysis of survival and cause of death statistics for mice under duration-of-life gamma irradiation
Douglas Grahn, Ruth Ann Lea, Katherine Allen, R. J. Michael Fry, John Rust, and George Sacher
40 Pathological findings after single dose neutron irradiation
R. J. Michael Fry, John H. Rust, Janet E. Newlin, and Everett Staffeldt
41 Studies of long-term irradiated survivors and aged mice
E. John Ainsworth, R. J. Michael Fry, Patricia C. Brennan, Donn L. Jordan, and Mary P. O'Malley
44 Bacteriology on irradiated mice in the JANUS program
E. John Ainsworth, Patricia C. Brennan, Donn L. Jordan, Mary P. O'Malley, Richard C. Simkins, and Calvin M. Poole

MECHANISMS OF CARCINOGENESIS

48 Mechanisms of carcinogenesis
Austin M. Brues, Donald D. Grube, and Harry Auerbach
50 Retention of radiostrontium in soft tissues
Austin M. Brues, Donald D. Grube, and Harry Auerbach
51 Promotion by phenobarbital of hepatocarcinogenesis induced by acetylaminofluorene in rats
Carl Peraino, R. J. Michael Fry, and Everett Staffeldt
52 Dietary and hormonal interplay in the regulation of rat-liver ornithine aminotransferase
Carl Peraino
53 Functional properties of the ornithine aminotransferase molecule
Carl Peraino
54 Cerenkov radiation and liquid scintillation counting
Walter E. Kisieleski
54 Concerning the uptake of lipid by the nucleus
Ambrose D. Barton, Walter E. Kisieleski, and Friedrich Wassermann
54 Experimental modification of structures at the periphery of the liver cell nucleus
Ambrose D. Barton, Walter E. Kisieleski, Friedrich Wassermann, and Faustina Mackevicius

MOLECULAR AND CELLULAR LEVEL BIOLOGY

BIOCHEMISTRY

55 Effects of radioprotective thiols *in vivo* on the sedimentability of mitochondria
John F. Thomson, Sharron L. Nance, and Sandra L. Tollaksen
55 Stable isotope analysis of organic molecules using combined gas chromatography-mass spectroscopy: Application to clinical measurements of bile acid pool size
Peter D. Klein, Otto W. Berngruber, Patricia A. Szczepanik, Rudy G. Danziger, Alan F. Hofmann, and Leslie J. Schoenfield

56 Analysis of deuterium-labeled compounds by gas chromatography-mass spectroscopy: Instrument modifications and analysis of test mixtures
Peter D. Klein, Joseph Haumann, Otto W. Berngruber, and William J. Eisler
59 Through darkest quench with analyser and camera
Peter D. Klein and William J. Eisler
59 Biological assay of bile salt purity
Roger Lester, Otto W. Berngruber, Joanna M. Little, and Peter D. Klein
59 Fatty acid composition of *Pseudomonas angulata*, *Pseudomonas phaseolica*, and *Pseudomonas tabaci*
Paul Sacco, James J. McNeill, Patricia A. Szczepanik, and Peter D. Klein
60 Identification and characterization of fully deuterated fatty acids isolated from *Scenedesmus obliquus* cultured in deuterium oxide
Gustav Graff, Patricia Szczepanik, Peter D. Klein, and Ralph T. Holman
60 Preparation of tritium-labeled sterols and the synthesis of labeled 24-azacholesterol
Malcolm J. Thompson, Otto W. Berngruber, and Peter D. Klein
Membrane-bound enzymes in mammalian cells
60 Introduction
Yueh-Erh Rahman, Elizabeth A. Cerny, Carl Peraino, Faustina Mackevicius, Betty Jean Wright, Theodore N. Tahmisian, Sarmukh S. Brar, and Donald M. Nelson
61 I. Studies of phospholipases A
Yueh-Erh Rahman, Elizabeth A. Cerny, Carl Peraino, Faustina Mackevicius, Betty Jean Wright, Theodore N. Tahmisian, Sarmukh S. Brar, and Donald M. Nelson
A. Phospholipases A in cellular and intracellular membranes of rat liver
B. Studies of phospholipase A in rat spleen endoplasmic reticulum
C. Purification of phospholipase A from rat spleen
D. Biological regulation(s) of membrane-bound phospholipases A
64 II. Studies of membrane components
Yueh-Erh Rahman, Elizabeth A. Cerny, Carl Peraino, Faustina Mackevicius, Betty Jean Wright, Theodore N. Tahmisian, Sarmukh S. Brar, and Donald M. Nelson
A. Electron microscopic studies of isolated intracellular organelles and their purified membranous components
B. Thermal neutron activation analysis of purified biological membranes
66 The specificity of deamination of adenosine sulfur compounds
Fritz Schlenk, Cynthia R. Zydek-Cwick, and Nancy K. Hutson
67 Stabilization of mutant catalase by complex formation with antibody to normal catalase
Robert N. Feinstein, Bernard N. Jaroslow, Judith B. Howard, and Joann T. Faulhaber
68 Effect of high doses of gamma radiation on survival and certain blood parameters of normal and acatalasemic mice
Robert N. Feinstein and Donald Michael Nelson
Biochemistry of catalase
68 Introduction
Robert N. Feinstein
69 I. Catalase decrease in liver after subcutaneous injection of talc
Robert N. Feinstein and Judith B. Howard
69 II. Effect of compounds related to aminotriazole on blood and liver catalase
Robert N. Feinstein, Judith B. Howard, and Rosanne Savol
70 III. Heat stability and urea stability of catalatic activity in blood and various tissues
Robert N. Feinstein and Judith B. Howard
71 IV. Age variation in catalatic activity of leg and breast muscle of mallard ducks
Robert N. Feinstein and Charles W. Dane
71 V. Attempts at direct separation of catalase from mouse blood
Robert N. Feinstein, Rosanne Savol, Judith B. Howard, and Carl Peraino
72 Cytological effects of lethal X irradiation on yeast cells
George Svihla, Julia L. Dainko, and Fritz Schlenk
73 Cryostat cut, freeze-dried tissues for microscopic investigations
Per Freitag, Milton B. Engel, and George Svihla
73 The biochemistry of development
Richard E. Ecker
74 I. Uterine suppression of biochemical and morphogenetic events in *Rana pipiens*
L. Dennis Smith and Richard E. Ecker
74 II. Influence of exogenous ions on the events of maturation in *Rana pipiens* oocytes
Richard E. Ecker and L. Dennis Smith
74 III. The nature and fate of *Rana pipiens* proteins synthesized during maturation and early cleavage
Richard E. Ecker and L. Dennis Smith
75 IV. The action of steroid hormones on isolated oocytes of *Rana pipiens*
L. Dennis Smith and Richard E. Ecker
75 V. RNA synthesis during the development of the large milkweed bug, *Oncopeltus fasciatus*
Richard E. McDowell

BIOPHYSICS

Studies with mammalian cells in culture
I. Basic studies on cell generation cycles
76 A. Cell cycle compartment analysis of Chinese hamster cells in stationary phase cultures
Dennis W. Ross and Warren K. Sinclair
77 B. Synchrony by mitotic selection alone or with colcemid in Chinese hamster cells
Warren K. Sinclair
78 C. Variation in sulfhydryl content of Chinese hamster cells during the cell cycle
Warren K. Sinclair and Melvin D. Long
II. Radiation effects on cell division
79 A. Cycloheximide and radiation induced division delay in synchronized Chinese hamster cells
Silvia Bacchetti and Warren K. Sinclair
79 B. Ultraviolet induced division delay in synchronized Chinese hamster cells
Antun Han, Warren K. Sinclair, and C. K. Yu
80 C. Effect of X rays on DNA, RNA, and protein synthesis in synchronized Chinese hamster cells
Silvia Bacchetti and Warren K. Sinclair
III. Effects of protective agents and sensitizers on Chinese hamster cells
80 A. Sensitization of Chinese hamster cells to X rays by N-ethylmalemide
Warren K. Sinclair
81 B. Recovery from sublethal damage induced by X irradiation in cysteamine protected Chinese hamster cells
Warren K. Sinclair
82 C. Protective effect of certain agents against X irradiation in mammalian cells
Warren K. Sinclair
IV. Cytological effects
82 A. Polyploidy induced by X rays in G_1 cells of Chinese hamster *in vitro*
C. K. Yu and Warren K. Sinclair
83 B. Effect of hydroxyurea on the chromosome repair process
C. K. Yu and Warren K. Sinclair
84 Magnetic resonance studies of the structures and interactions of biologically active molecules
Steven S. Danyluk, David B. Davies, George E. Chapman, and William A. Bernhard
I. Nucleic acids: Structure and conformation
85 A. Assignment and conformational properties of the sugar-ring hydroxyl protons of the common nucleosides
David B. Davies and Steven S. Danyluk
85 B. A complete conformational model for uridine-5′-monophosphate in aqueous solution
David B. Davies and Steven S. Danyluk
86 C. Complete analysis of the proton spectrum of uridylyl-(3′ → 5′)-adenosine: Conformational structure
David B. Davies and Steven S. Danyluk
86 II. Antibiotic structure: Analysis and conformational properties of actinomycin D
Thomas A. Victor, Frank E. Hruska, Charles L. Bell, and Steven S. Danyluk
87 III. The hydration structure of collagen
George E. Chapman and Steven S. Danyluk
88 IV. A superconducting multinuclei nuclear magnetic resonance spectrometer system
George E. Chapman, Steven S. Danyluk, Joseph R. Haumann, and Bruno S. Kotula
90 V. Solvent dependence of the chemical shifts and coupling constants of 1,2-dichlorofluorethylenes
Charles L. Bell and Steven S. Danyluk
90 The photobiology of circadian rhythms in protozoa and other eukaryotic microorganisms
Charles F. Ehret and John J. Wille, Jr.
91 Testing the chronon theory of circadian timekeeping
Audrey Barnett, Charles F. Ehret, and John J. Wille, Jr.
91 Molecular biology of circadian rhythms in eukaryotic cells
Charles F. Ehret and Audrey Barnett
93 Two classes of postirradiation oxygen effect in *Staphylococcus aureus*
Robert B. Webb
94 An X-ray crystallographic study of a Bence-Jones protein
Allen B. Edmundson, Marianne Schiffer, Mical K. Wood, Karl D. Hardman, and Kathryn R. Ely
96 Chemical studies of concanavalin A
Allen B. Edmundson, Kathryn R. Ely, Dayle A. Sly, Florence A. Westholm, and Dennis A. Powers
96 An X-ray crystallographic study of the structure of concanavalin A
Karl D. Hardman, Mical K. Wood, Marianne Schiffer, and Clinton F. Ainsworth
98 A chemical study of the carbohydrate binding sites of concanavalin A
Karl D. Hardman and Clinton F. Ainsworth
99 The primary structure of sucker hemoglobins
Dennis A. Powers and Allen B. Edmundson

CELLULAR FINE STRUCTURE AND RELATED FUNCTION

100 Morphological changes in cellular organelles of X-irradiated bacteria-free grasshopper diapause embryos
THEODORE N. TAHMISIAN AND BETTY JEAN WRIGHT
101 The structure of paramecium as viewed from its constituent levels of organization
CHARLES F. EHRET AND EUGENE W. MCARDLE

PLANT RADIOBIOLOGY

101 Correlative determinants of RNA metabolism in the gamma-irradiated Coleus leaf
SOLON A. GORDON AND EVELYN M. BUESS
102 Development of a capacitance auxanometer for the measurement of growth rates
SOLON A. GORDON AND WILLIAM A. DOBRA
103 Growth and constituents of oat plants grown under single- and multidimensional gravity compensation
SOLON A. GORDON
105 Comparative morphology of normal and callus initiated carrot roots
RAY R. HINCHMAN
105 Plastid morphology and ontogeny in the oat seedling
RAY R. HINCHMAN AND SOLON A. GORDON
106 Participation of Golgi apparatus in geotropism
JANE SHEN-MILLER AND CAROL MILLER
108 Kinetics and periodicity of auxin transport, geotropic curvature and growth
JANE SHEN-MILLER, NELEEN G. NOACK, AND JUDITH E. BAKER
The physiological effects of environmental stress on plants
110 I. The effect of gravity on the soluble carbohydrate economy of oat seedlings
RICHARD R. DEDOLPH AND LOUIS H. DECKER
112 II. Quantitative extraction, separation, and measurement of fructose, glucose, and sucrose in plant tissue
RICHARD R. DEDOLPH, LOUIS H. DECKER, AND WILLIAM CHORNEY
112 III. The physical basis of gravity stimulus nullification by clinostat rotation
RICHARD R. DEDOLPH AND MERLIN H. DIPERT
113 IV. The removal of lead from air by soils
RICHARD R. DEDOLPH, ROBERT H. STAMPS, AND WILLIAM CHORNEY
113 V. Rest period reduction in non-stored onion (*Allium cepa*) sets
HERBERT J. HOPEN, RICHARD R. DEDOLPH, WILLIAM F. WHITESIDE, AND WILLIAM CHORNEY
Photobiology studies in mammals
114 I. X radiation and the circadian thermoperiodicity of *Perognathus penicillatus*
SOLON A. GORDON, JOHN L. CARRIGAN, AND JAMES C. LIANG
115 II. Spectral sensitivities for the phasing of circadian temperature rhythms in *Perognathus penicillatus*
SOLON A. GORDON AND GERALD A. BROWN
115 III. The induction of chromosome aberrations in pig kidney cells by far-red light
SOLON A. GORDON, AGNES N. STROUD, AND CHEN H. CHEN

RADIATION GENETICS

MAMMALIAN GENETICS

116 Determination of the radiation induced mutation rate for sex-linked lethals and detrimentals in the mouse
DOUGLAS GRAHN, RUTH ANN LEA, AND JANE L. HULESCH
118 Genetic location of a sex chromosome controller gene on the normal *X* of the mouse
DOUGLAS GRAHN, RUTH ANN LEA, AND JANE L. HULESCH

MICROBIAL GENETICS

118 The growth-duplication cycle. XII. The distribution of cell generation times and its relationship to linear cell growth
HERBERT E. KUBITSCHEK
119 Potassium uptake in *E. coli*
HERBERT E. KUBITSCHEK, MICHAEL L. FREEDMAN, AND SIMON SILVER
119 Chromosome replication in slowly growing bacteria
HERBERT E. KUBITSCHEK, MICHAEL L. FREEDMAN, AND DAVID VALDEZ
121 Regulation of chromosome replication in *Bacillus subtilis:* Marker frequency analysis after amino acid starvation
JAMES C. COPELAND
121 Regulation of chromosome replication in *Bacillus subtilis:* Effects of amino acid starvation in strain W23
JAMES C. COPELAND
121 Regulation of chromosome replication in *Bacillus subtilis:* Modulation control of DNA replication
JAMES C. COPELAND

123 Evaluation of different scintillation cocktails for the counting of tritiated ribonucleic acid separated by sucrose gradient centrifugation
Richard E. McDowell and James C. Copeland
123 Repair of damage induced by near UV and visible radiations
Robert B. Webb, John R. Lorenz, and Mickey S. Brown
125 Photoreactivation of 365-nm lethality
Mickey S. Brown and Robert B. Webb
127 The lethal effects of ^{125}I decay in *E. coli* and in bacteriophages
Robert E. Krisch, Sandra A. Drick, and Wayne T. Kickels
128 Changes in the mean cell volume of *Escherichia coli* after bacteriophage infection
Michael L. Freedman and Robert E. Krisch

THE METABOLISM AND TOXICITY OF FISSION PRODUCTS

130 Toxicity and metabolism of radionuclides: Program objectives and introduction
William P. Norris

STUDIES OF RADIATION-INDUCED CHANGES

The response of ANL beagles to protracted exposure to ^{60}Co gamma rays at 5 to 35 R/day
130 I. Survival and clinical observations
William P. Norris and Calvin M. Poole
132 II. Estimation of the LD_{50} at 35 R/day
William P. Norris and Calvin M. Poole
132 III. Pathologic changes in dogs exposed at 10 R/day
Thomas E. Fritz, David V. Tolle, and Ruth C. Zeman
134 IV. Bone marrow cell ultrastructure in dogs continuously exposed to ^{60}Co gamma rays
Theodore N. Tahmisian, Rosemarie L. Devine, William P. Norris, Thomas E. Fritz, Ruth C. Zeman, and David V. Tolle
135 V. Beta-hemolytic streptococci in the throats of beagles receiving continuous ^{60}Co gamma radiation
Patricia C. Brennan, Richard C. Simkins, and William P. Norris
Effects of irradiation on the beagle thyroid gland
135 I. Effect of X irradiation on the thyroid gland of beagles fed a restricted iodide diet
Thomas E. Fritz, William P. Norris, James A. Taylor, and Norbert D. Kretz
137 II. Thyroid response to protracted whole-body exposure to ^{60}Co gamma rays
William P. Norris, Thomas E. Fritz, and Norbert D. Kretz
139 Radiation dosimetry in beagles given intravenous doses of ^{137}Cs
William P. Norris
141 Beagles: Inbreeding, ancestry, and radiosensitivity
Carl E. Rehfeld and William P. Norris
143 Comparison of certain hematologic effects in beagles given cesium-137, cerium-144, or exposed to cobalt-60
Carl E. Rehfeld, Donald E. Doyle, and Donald L. Pearson

CHARACTERIZATION OF THE ANL BEAGLE

144 Source of beta-hemolytic streptococci in beagle pups
Patricia C. Brennan, Richard C. Simkins, and William P. Norris
145 Clinical chemistry of the normal beagle dog
Lillian V. Kaspar and William P. Norris
146 Analysis of heritable influence on mean erythrocyte volume in beagles
Carl E. Rehfeld, Max R. Zelle, Donald E. Doyle, and Merlin H. Dipert
147 History of a beagle colony
Carl E. Rehfeld, Jeanne Blomquist, and Glenn N. Taylor

MODIFICATION OF RADIATION EFFECTS

149 Determination of ^{239}Pu and ^{241}Am in animal tissues by liquid scintillation spectrometry
Arthur Lindenbaum and Marguerite A. Smyth
149 Metabolic and therapeutic studies of plutonium and americium
Arthur Lindenbaum, Marcia W. Rosenthal, John J. Russell, Elizabeth S. Moretti, and Dorothy Chladek
152 Biochemistry and ion binding of connective tissue. V.
Arthur Lindenbaum and Nancy Egan
153 Supralethally X-irradiated amoebae treated with nonirradiated, homogenized protoplasm
Edward W. Daniels and Evelyn P. Breyer
153 Ultrastructure of spermatozoa from the American oyster, *Crassostrea virginica* Gmelin
Edward W. Daniels, Arlene C. Longwell, and Judith M. McNiff
154 Ultrastructure of oocytes from the American oyster, *Crassostrea virginica* Gmelin
Edward W. Daniels, Arlene C. Longwell, and Judith M. McNiff

154 Treatment of X- or UV-irradiated amoebae with injections of homogenate made from nonirradiated amoebae at 2° C
EDWARD W. DANIELS AND JUDITH M. MCNIFF

157 EDUCATIONAL ACTIVITIES

159 PUBLICATIONS

163 STAFF OF THE DIVISION OF BIOLOGICAL AND MEDICAL RESEARCH

165 AUTHOR INDEX

Acute and Chronic Effects of External X-Ray and Gamma Radiations

STUDY OF CELL PROLIFERATION OF THE HAIR FOLLICLE*

R. J. Michael Fry, Charlotte L. Weber, Walter E. Kisieleski, Melvin L. Griem,† and Fredrick D. Malkinson‡

The matrix of the hair follicle provides a cell population suitable for the study of changes in kinetics with changes in growth and for the study of effects of irradiation in both a rapidly proliferating and a quiescent population. A technique by which follicles of known hair types can be isolated both for squash preparations and assay of radioactivity by a combustion-scintillation counting method has been used. The precise duration of anagen (growth phase) has been determined by assay of uptake of ^{3}HTdR both autoradiographically and by scintillation counting. At the end of anagen, cell production ceases but it was not known precisely what changes in cell kinetics took place. We have determined the cell cycle and the number of cells proliferating near the end of anagen. The backs of CF_1/Anl female mice about 90 days old were plucked and 24 days later replucked and the mice were injected with ^{3}HTdR 0.5 μCi/g, 0.36 Ci/mM, 2, 4, 8, 12, 14, 16, 18, and 20 days later. Other mice plucked a single time were injected on days 3, 6, 10, 16, 17, 18, 19, and 20. All mice were sacrificed one hour after injection. Small pieces of skin were fixed in cold acid alcohol, hydrolyzed and stained by the Feulgen reaction. Individual hair follicles were dissected out for squash preparations for autoradiography and groups of 10, 20, 30, and 40 follicles were collected for scintillation counts. The salient findings were:

1. Squash preparations and ^{3}H content assay of individual hair types are useful and practical methods for the study of hair follicles.
2. Grouping of follicles into large and small is not sufficiently precise for some experiments.
3. The duration of induced anagen depends on the definition of the growth phase, but it is clear that proliferative activity has ceased in all hair types 19 days after plucking. The number of cells in cycle increases for several days initially and the decrease in proliferation starts at about 15 days. The duration for differing hair types appears to be similar. The fraction of cells either differentiating or returning to cycle is varying throughout anagen.
4. The cell cycle time does not alter in the initial period of reduction in the number of proliferative cells at the end of induced anagen.

* Abstract of paper to appear in the Proceedings of the Fourth International Congress of Radiation Research, Evian, France, on June 29–July 4, 1970.

† Department of Radiology, Argonne Cancer Research Hospital.

‡ Department of Medicine (Section of Dermatology), University of Chicago, Department of Medicine (Section of Dermatology), Presbyterian-St. Luke's Hospital, Department of Medicine (Section of Dermatology), University of Illinois, College of Medicine, Chicago, Illinois.

THE INFLUENCE OF ROUTE OF ADMINISTRATION ON THE UPTAKE OF TRITIATED THYMIDINE

R. J. Michael Fry, Walter E. Kisieleski, and Anthony R. Sallese

PURPOSE AND METHODS

Previously we reported on various factors involved in the uptake of tritiated thymidine.[1] It was shown that the uptake of tritiated thymidine by crypt cells measured by grain counts was greater after intraperitoneal than intravenous injections. The duration of availability of label to crypt cells appeared to be longer by the intraperitoneal route. These results raised the question of the suitability of the commonly used intraperitoneal route for our future labeling experi-

TABLE 1. THE NUMBER OF LABELED CELLS AND TRITIUM CONTENT IN THE CRYPTS OF THE JEJUNUM OF BCF_1/ANL [ANL 66] MICE

Route	1400 hr				2400 hr			
	Labeled cells/ crypt		Tritium content, cpm/crypt		Labeled cells/ crypt		Tritium content, cpm/crypt	
	Mean	S.D.	Mean	S.D.	Mean	S.D.	Mean	S.D.
Intraperitoneal	58	14	0.083	0.016	75	14	0.131	0.023
Intravenous	64	15	0.068	0.011	74	17	0.082	0.012

ments involving determinations of the proliferation in the gut. We therefore have determined the number of labeled nuclei and the tritium content of crypts after (1) intraperitoneal and (2) intravenous injections of ^{3}HTdR. Sixteen male BCF_1/Anl [Anl 66] mice, 100 days of age were used; injections by each route of administration at either 1400 or 2400 hr were given to four mice; 0.5 μCi/g ^{3}HTdR (Spec. Act. 0.36 Ci/mM) and sacrificed one hour later. The times of injection were chosen to determine whether any influence of the route of administration was dependent on other factors, such as the degree of proliferative activity and, therefore, the time of the day. Standard techniques for obtaining autoradiographs of crypt squashes and assaying tritium content were used.

PROGRESS REPORT

The results shown in Table 1 are as follows:

1. The route of administration has no effect upon the number of labeled nuclei/crypt at either time interval.

2. The number of labeled nuclei is greater at 0.01% level of significance at 2400 hr than at 1400 hr after an intraperitoneal injection. The differences after intravenous injection are significant only at the 5% level.

3. This latter finding is perhaps reflected in that there is no significant difference in the cpm/crypt at the two time intervals when the label is given intravenously.

4. At midnight the cpm/crypt is greater after intraperitoneal injection.

CONCLUSIONS

It appears that when ^{3}HTdR injected mice are sacrificed within one hour there is little difference between the two routes of injection. The proliferative activity appears to be greater at midnight than at mid-day, though with intravenous injection the difference is only significant at the 5% level.

REFERENCE

1. Fry, R. J. M., W. E. Kisieleski, A. B. Reiskin, A. R. Sallese, and C. L. Weber. Argonne National Laboratory Biological Medical Research Division Annual Report, 1969. ANL-7635, pp. 11–14.

*EXPLANTING THE 3-DAY CHICK EMBRYO FOR THE STUDY OF RADIATION INJURY TO THE MICROCIRCULATION**

Emily J. B. Christian and S. Phyllis Stearner

A new technique was developed to explant the microscopically inaccessible 3-day chick embryo and the entire area vasculosa onto a solid agar-albumen medium. The extraembryonic membranes of such explanted embryos provide excellent optical conditions for the microscopic study of the circulation in the living animal and for the identification of experimentally-induced lesions. Lethal doses of X radiation delivered in a few minutes resulted in rapid structural and functional changes in the vascular system. These changes led to generalized stasis and death within a few hours. If the exposure time was increased from a few minutes to a few hours, a larger amount of radiation was required to produce the same mortality. In such lethally irradiated embryos, lesions appeared rapidly and were similar to those that followed a lethal exposure given in a few minutes. Mortality of embryos irradiated in explant was comparable to that of embryos irradiated *in ovo*.

The technique and radiation effects on the microcirculation are illustrated in two films.

* Abstract of paper to be published in the *Microscope*.

A TECHNIQUE TO VISUALIZE THE PERIPHERAL MICROCIRCULATION IN THE YOUNG CHICKEN*

Emily J. B. Christian and S. Phyllis Stearner

Early circulatory collapse in the lethally irradiated chicken is characterized by edema, hemorrhage, and hypotension. In the explanted 3-day chick embryo, we have described the rapid structural and functional changes in the microcirculation that occur after X irradiation. Death may result within a few hours. Vascular collapse in the lethally irradiated chicken resembles that in the young embryos. To extend our *in vivo* studies to the more differentiated vascular system of the older bird, we have developed a procedure for observation and cinemicrographic recording of the microcirculation in the 3-week chicken. At this age, the relatively transparent skin fold that extends between the coracoid and carpal bones of the wing is sufficiently large, yet still thin enough to provide for microscopic observations of the vascular network. Although maximum resolution in this region is less than that obtained in the extraembryonic membranes of the explanted chick embryo, details of the microvascular network can be examined without the trauma associated with surgical procedures.

With this method, we have observed the microcirculation in individual birds over several hours. Considerable detail of the vessel wall as well as intracellular structures were distinguished with higher power objectives (up to 70 ×). Results of observation on untreated and irradiated chickens are described in a separate report.

* Abstract of paper to be submitted for publication in *Microvascular Research*.

MICROVASCULATURE AND LOOSE CONNECTIVE TISSUE IN FREEZE-FRACTURE PREPARATIONS*

S. Phyllis Stearner and Margaret H. Sanderson

Tissues of the young chick and chick embryo were prepared in a relatively unaltered condition by the freeze-fracture technique. The ultrastructure of the microvasculature and surrounding interstitial region is compared with that seen in conventional thin-sectioned material. In the undifferentiated vessels of the 3-day chick embryo, no distinct basement lamina can be distinguished in either type of preparation. In the 3-week chick, a continuous basement lamina is present beneath the endothelium only in chemically fixed and sectioned tissue; it cannot be distinguished from the remaining interstitial substance in freeze-fracture preparations. Blood-tissue exchange may depend on permeability characteristics of the entire interstitial region rather than on the basement lamina alone.

* Abstract of paper to be published in *Z. Zellforsch.*

MECHANISMS OF ACUTE RADIATION DAMAGE AND REPAIR: INTRODUCTION

S. Phyllis Stearner

Microvascular damage, a significant factor in radiation injury mechanisms associated with acute lethality, is expressed within a few hours after exposure in a variety of vertebrates. Vascular damage also contributes to the radiation sensitivity of tumor tissue and is important in radiation therapy procedures. The relationship of vascular damage and surrounding connective tissue injury to later degenerative changes is difficult to evaluate. Although delayed effects of early vascular injury can be expected, there are obvious problems in distinguishing between primary and secondary damage to parenchymal cells of various organs. *In vivo* observations and ultrastructural studies in the chicken reveal that circulatory stasis from endothelial damage, degeneration, and collapse of small vessels is the principal cause of death within 24 hours after ionizing irradiations. Of special concern in our studies is the relation of vascular injury to radiation dose and

time (during or between exposures) and to possible radioprotective procedures. From the observed variation in degree of vascular injury, the endothelium appears to respond as a cell population, exhibiting a distribution of sensitivities. These findings suggest that the methodolgy of compartmental model theory might be employed to advantage toward a description of the observed phenomena.

MECHANISMS OF ACUTE RADIATION DAMAGE AND REPAIR. I. IN VIVO OBSERVATIONS OF MICROVASCULAR INJURY IN THE GAMMA-IRRADIATED CHICKEN

S. Phyllis Stearner and Emily J. B. Christian

PURPOSE AND METHODS

The early circulatory response resembles an inflammatory reaction with increased permeability and localized degenerative changes in blood vessels. Vascular degeneration within a few hours after irradiation has been described in the chick embryo.[1-3] Similar studies, now in progress in the young chick, relate microvascular effects with quantitative differences in the early radiation mortality after protracted and fractionated exposure schedules. The relatively thin fold of skin between the coracoid and carpal bones in the wing of the young chick provides the best optical conditions available in the intact bird for *in vivo* study of the microcirculation. The 3-week-old chick was selected because at this age the wing skin fold is sufficiently large yet still thin enough to provide satisfactory resolution of microvascular structure. The method for microscopic study of the circulation is described in greater detail in another report.[4] Chicks were observed for several hours after ^{60}Co γ irradiation and the sequence of events associated with the early radiation injury were recorded on 16-mm motion picture film.

The skin area of the wing in which we observed the microcirculation contains a network of superficial arterioles, capillaries, and venules. Larger vessels as well as additional small vessels occur in the subdermal loose connective tissue. Cellular details of the vessel wall as well as the circulating cells can be distinguished at high magnifications, and it is possible to make extended observations without trauma to the microcirculation.

PROGRESS REPORT

Early damage to the microcirculation follows irradiation in the lethal range, i.e., a 15-min exposure to 1000–1200 R. Within 30 to 60 min, there are stasis and occlusion in a few superficial venules and capillaries, and the circulation may become sluggish in other vessels. Leucocytes and thrombocytes frequently roll along the vessel wall or are firmly attached. At this time, circulation is rapid in the larger peripheral vessels and in the deeper vasculature. Within 2 to 3 hr, however, occlusion and collapse of the capillaries and small venules frequently are widespread; these vessels then are lysed and rapidly disappear, and stasis of superficial vessels is complete within a few hours. Usually the deeper circulation soon fails also and the chick dies within 4 to 6 hr. A rapid circulation continues in the deeper wing vessels of some birds, and they survive the early (24 hr) period. Endothelial cells in damaged vessels are seen at higher magnifications to be swollen and an occasional circulating cell has been observed to penetrate the vessel wall. Combined with these changes in circulation, occlusion of vessels by thrombi also contributes to the rapid development of stasis.

Colloidal carbon injected into the circulation at various times after irradiation serves to indicate the location of damaged and leaking vessels. Increased permeability is identified by the accumulation outside the endothelium of carbon masses sufficiently large to be visible with the light microscope. Thrombocytes, the most numerous circulating cells without hemoglobin, readily take up carbon particles and tend to aggregate. Such labeled aggregates are very easily identified in occluded vessels. In some apparently nonfunctioning larger vessels, the circulation frequently is restored suddenly by the flush of red cells preceded by a labeled thrombus. Carbon is retained in the circulation for relatively short periods after injection; visible amounts will accumulate in the walls of injured vessels for only a short time after it is introduced. Furthermore, carbon is carried only to vessels in which there is an active circulation when it is introduced. In the control chick, vascular leakage usually is not present and only rarely are labeled vessels seen. Carbon accumulations in the walls of a few capillaries and venules are identified within ½ to 1 hr after lethal irradiation and are frequently ob-

served in the superficial vascular bed in chicks injected within 2 to 3 hr after exposure.

Observations of the microvascular network in the mesentery (surviving tissue) reveals a similar pattern of labeled vessels within 2 to 3 hr after irradiation. The mesentery is a more favorable tissue for high resolution study, but the compact arrangement of the visceral organs makes such studies quite difficult in the living chick.

CONCLUSIONS

In contrast to the uniform labeling pattern observed after localized vascular trauma (e.g., heat or crushing), irradiation results in a nonuniform distribution of injury severe enough to produce carbon leakage. The most extensive damage occurs in the superficial vessels of the dermis. Occlusion and degeneration of the deeper vascular bed as well as of the superficial vessels results in death within a few hours.

MECHANISMS OF ACUTE RADIATION DAMAGE AND REPAIR. II. ULTRASTRUCTURE OF THE CHICK MESENTERY AND EARLY EFFECTS OF GAMMA IRRADIATION

S. Phyllis Stearner and Margaret H. Sanderson

PURPOSE AND METHODS

This study in the 3-week chick is concerned with the fine structure of blood vessels in perivascular loose connective tissue, especially of the mesentery, and with the effects of lethal irradiation. Ultrastructural changes are related to those we have described in association with early radiation damage in the 3-day chick embryo.[5] These studies are also correlated with *in vivo* observations of the microcirculation in the skin of the lethally irradiated chick.

Three-week-old male white Leghorn chicks were exposed to 1000 to 1200 R ^{60}Co γ rays (exposure time 15 min). Two to 3 hr after exposure, birds were anesthetized and loops of small intestine surgically exteriorized. The attached mesenteries were spread gently, fixed *in situ* with Karnovsky's solution for 5 min, dissected from the intestinal wall and processed for electron microscopic study.[5] At similar times after exposure, other birds were injected intravenously with 0.1 ml of colloidal carbon (Pelikan "biological ink", C11/1431a, particle size, 250Å) in order to label areas of increased vascular permeability. After a 10-min circulation time, the mesenteries were prepared for study as above. Mesenteries from control chickens were similarly prepared.

PROGRESS REPORT

Mesenteric blood vessels of the 3-week chick, in contrast to the vasculature of the young embryo, are differentiated into the principal types: arteries, arterioles, capillaries, venules, and veins. In the mesentery, the endothelium is continuous and has a well-defined basement lamina. An occasional pericyte partially surrounds smaller vessels. Endothelial cells have characteristics of greater differentiation than do those of the 3-day embryo. Cytoplasmic activity is indicated by the presence of smooth and rough endoplasmic reticulum (ER) cisternae filled with electron-dense material and increased numbers of pinocytotic vesicles.

The arterial wall has the typical four layers: endothelium, elastica interna, muscularis, and elastica externa. Endothelial cells of arteries are rounded or pyramidal and project into the lumen. The elastica interna has an undulant appearance, presumably due to agonal contraction of the arterial wall as it is fixed. The muscularis (smooth muscle) and the elastica externa vary in thickness in relation to the size of the artery. The adventitia that adjoins the elastica externa contains fibroblasts, tissue mast cells, collagen, elastic fibers, and numerous capillaries. Capillaries and smaller venules have only endothelium and pericytes. Veins have an endothelium and one, or several layers of fibroblast-like cells. In the chick embryo, blood vessels of all sizes resemble the capillaries of the chick mesentery; they are undifferentiated and have only endothelium and pericytes.

Circulating blood cells in the 3-week chicken include nucleated erythrocytes (normal hemoglobin concentration), lymphocytes, monocytes, heterophils, eosinophils, basophils, and thrombocytes. Granulocyte types are distinguished from each other by their nuclear shape and cytoplasmic granules. Thrombocytes take up colloidal carbon from the circulation and store it in membrane-limited vacuoles, as do mammalian platelets. These cells tend to adhere both to each other and to endothelial cells, especially after foreign material (e.g., colloidal carbon) has been introduced into the circulation.

Within 2 to 3 hr after γ-ray exposures to 1000 to 1200 R given in 15 min, birds are somewhat inactive and at 24 hr there is >75% mortality. At 3 hr after exposure, the endothelial cells are swollen, and have a

pale-staining cytoplasm, dilated ER cisternae and swollen mitochondria. In some areas, the endothelium may be disrupted. Some capillaries and venules are occluded with erythrocytes or aggregated thrombocytes. Leucocytes showing degenerative changes occasionally appear to be attached to the vessel wall. Colloidal carbon is accumulated in endothelial gaps and within the wall of small vessels, usually venules.

Loose connective tissue of the adventitia also shows damage 2 to 3 hr after a lethal exposure. There are degeneration and lysis of fibroblasts and degranulation of tissue mast cells. Displacement and disordering of the cellular and fibrillar structures suggest interstitial edema.

CONCLUSIONS

The principal vessel types seen in the 3-week chick mesentery are similar ultrastructurally to those seen in mammals. Lethal γ irradiation produces extensive injury to the endothelium of arterioles, venules, capillaries, and to the adventitial loose connective tissue within 3 hr after exposure. Early lesions in irradiated chickens, including dilated ER cisternae and condensed mitochondria, resemble lesions produced when energy metabolism is inhibited.[6] The dilated ER cisternae contain electron-dense material, suggesting accumulation of unreleased product.

Accumulations of colloidal carbon within the walls of occluded vessels, at no more than 10 min after injection of the tracer, locate endothelial leakage and indicate vessels that were at least partially functional at the time of injection. In such instances, occlusion of the vessel must occur suddenly, between the time of carbon injection and sacrifice of the animal.

General condition of the bird at time of sacrifice is related to the amount of vascular damage. There is much variation in damage to adjacent vessels, however, and also to different segments of the same vessel. In addition, alterations of the surrounding adventitia frequently cannot be correlated with vascular damage. As in the chick embryo,[5] vascular injury appears to be due to direct damage to individual cells of the vessel wall, as well as to the adjacent loose connective tissue.

MECHANISMS OF ACUTE RADIATION DAMAGE AND REPAIR. III. TOWARD AN INTERPRETATION OF THE INCREASE AND DECAY OF RESISTANCE TO EARLY LETHAL RADIATION INJURY

S. Phyllis Stearner, Sylvanus A. Tyler, and Merlin H. Dipert

A kinetic model is presented of repair and resistive processes that act to reduce the radiation injury leading to circulatory collapse and death of the chicken.

The salient facts extracted from acute mortality data collected over two decades, to which the model conforms, are:

1. In response to single, protracted exposures, the radiation dose required to produce a given level of mortality increases with length of exposure. A linear function approximately describes this dependence.[7]

2. In response to high-rate, split exposures, resistance develops within 3 hr of the first dose, reaches a maximum between 4 and 8 hr, and decays by 24 hr.[8]

3. In response to high-rate, split exposures, the initial rate of build-up of resistance and the maximum resistance attained are increasing functions of conditioning dose, and also are correlated with age of animal.[9]

4. A significant amount of resistance *does not* develop when a high-rate, conditioning dose is followed immediately by a low-rate protracted exposure.[8]

5. A measurable resistance *does* develop when a low-rate, protracted exposure is followed immediately by a high-rate challenging dose.[8]

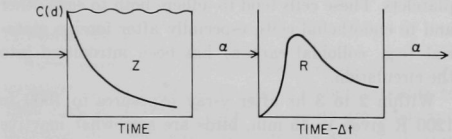

FIG. 1.—Illustration of transit between adjacent compartments.

PROGRESS REPORT

Two adjacent compartments of an n-chain compartmental system are assumed that have equal and irreversible out-put rates (Fig. 1). We postulate that some component, Z (upon which radiosensitivity depends) is activated by the initial exposure and decays at a rate α. The initial amount, $C(d)$, of Z (pool size) is dependent on the size of the first dose (d). Resistance in compartment, R, is given by the

expression:

$$R = A(t-\Delta t)\,\mathrm{Exp}\{-\alpha(t-\Delta t)\}, \qquad (1)$$

where A is the initial rate of increase of R, Δt is the time-translation constant, and α is the output rate.

The mathematical analysis is based on treatment groups listed in Table 2, and radiosensitivity is estimated by the LD_{50} values for single and split dose groups within each treatment group. Estimates of the parameters in expression (1) for each treatment group were obtained. α was relatively constant, A and Δt varied with treatment.

TABLE 2. TREATMENT GROUPS INCLUDED IN ANALYSIS

Age	First dose, R
Rooster (6-month)	150
	300
	600
3-week chick	700
3-day chick	300
	500
	700
14-day embryo	300
	600
12-day embryo	600
6-day embryo	700

CONCLUSIONS

1. The output rate (α) is an invariant of the process.
2. The initial rate (A) of increase in resistance varies exponentially with the first dose.
3. The value of A increases with age.
4. The time at which resistance begins (Δt) is negatively correlated with age and with the first dose, and the later relationship is approximately linear.

We will use this model in connection with the large volume of data already accumulated in formulating testable assumptions of radiation injury mechanisms.

MECHANISMS OF ACUTE RADIATION DAMAGE AND REPAIR. IV. LONG-TERM EFFECTS OF IONIZING RADIATIONS IN THE CHICKEN: A. SURVIVAL

S. Phyllis Stearner and Emily J. B. Christian

PURPOSE AND METHODS

In evaluating radiation effects comparisons are made of the relative contribution of dose and exposure time to long-term effects on survivors after the 30-day acute response period.

Male, white leghorn chickens were maintained for duration of life in order to determine the effects of γ and X radiations on survival and weight. Variables associated with egg production precluded use of the female. Because no length-of-life information on caged chickens has been published, survival and weight data on unirradiated (control) birds are valuable, independent contributions to information on longevity under laboratory conditions. A limited number of birds could be maintained throughout their lifetime in our animal facilities because of available space. Survival time tends to decrease with increased γ-ray dose (within each exposure time group), but variations are so large that groups have been combined into lethal and sublethal (long exposures only) ranges. Weights of chicks irradiated at 3 days after they hatched have been used to analyze irradiation effects on growth over the first year;[10] weights after the first year remain to be analyzed. Only survival data are presented in this preliminary report.

Newly-hatched white leghorn cockerels obtained from Kerr Chickeries, Frenchtown, New Jersey were irradiated at 3 to 4 days of age with either ^{60}Co γ rays or 200 kVp X rays. Gamma-ray exposures were for either 6 to 60 min or 24 hr. Doses ranged from 700 to 1000 R for short exposures and 700 to 1600 R for 24-hr exposures. Acute (30-day) mortality did not exceed 60%. X-irradiated (30-min exposures) chicks also received prophylactic treatments to reduce the acute mortality (7% O_2, epinephrine in peanut oil, and partial body shielding). These treatments were most effective against the early (<2 day) deaths, although later mortality (3 to 30 day) also was reduced. X-irradiated chicks that survived the acute period then were available for study of long term effects. Exposure of prophylactically treated chicks to 1200 R resulted in <75% mortality during the 30-day acute period, compared with more than 99% expected after 1200 R without other treatment. Thirty days after exposure, survivors were caged individually and observed daily for duration of their lives. Chicks were introduced into the experiment several times over a period of 7 years, as part of this study which has continued for more than 17 years. Table 3 shows the number of chickens in each group.

The control survival curve (Fig. 2) approximates an arithmetic straight line, except for slightly higher mortality during the first and seventh years. Only the last decile survived beyond 9 years (maximum survival 10½ years). During the first two years, more than half the mortality involved the leukosis complex. The incidence of leukosis was still high between 2 and 5 years, but in the latter half of the life span (>5 years) degenerative lesions (especially of liver and kidneys), apparent cardiac failure, and teratomas were the most prominent abnormalities.

TABLE 3. MAJOR TREATMENT GROUPS INCLUDED IN LONG TERM OBSERVATIONS

	N	Dose range, R	30-day survival, %
Control	95	—	100
γ Rays: 6- to 60-min exposures	53	700–1000	30–90
24-hr exposures	43	700–1000	>97
	24	1200–1600	50–90
X Rays: 30-min exposures	68	1200	20–60

In γ-irradiated groups, there was little correlation between dose and long term survival (>30 days) after exposures in the 30-day lethal range. Shorter exposure doses ranged from 700 to 1000 R; 1200 to 1600 R protracted over 24 hr was of comparable effectiveness. Survival curves for these groups (Fig. 2) were similar and the time to 50% survival was 2.6 and 2.8 years, respectively, compared to about 5 years for the non-irradiated control. The leukosis complex was identified in all short-exposure groups but only in the lower dose groups (700 to 1000 R) exposed over 24 hr. Although most cases appeared within the first 2 years, the disease was observed at necropsy even in 5- and 6-year-old birds.

In X-irradiated groups, prophylactic treatments apparently resulted in a different pattern of long term survival. Comparison of the X-ray survival curve with the control curve suggests that a specific protective action is involved rather than a general dose reduction. Although mortality during the first year was high

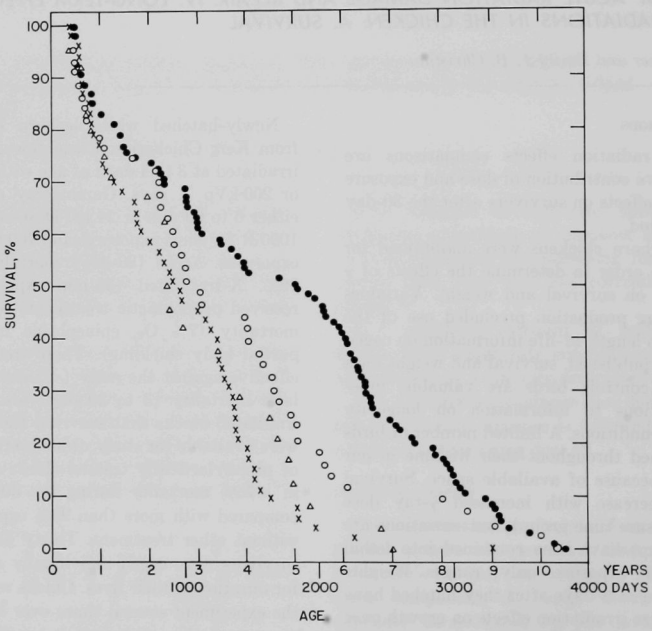

FIG. 2.—Survival of roosters γ irradiated at 3 days after hatching; effects of exposure time. Survival based on those living at 30 days after exposure. ● Control; × 6- to 60-min exposure; 700 to 1000 R; ○ 24-hr exposure; 700 to 1000 R; △ 24-hr exposure; 1200 to 1600 R.

(>35%), few birds died during the second and third years. Thereafter, the survival curve roughly paralleled that of sublethally γ-irradiated groups.

CONCLUSIONS

The arithmetic straight line mortality curve for roosters raised in cages under laboratory conditions resembles that reported for zoo populations. In irradiated groups, mortality between the third and sixth years was most markedly increased within the dose range investigated. Vascular injury, leading to cardiac failure, has been reported in X- and γ-irradiated mice[11] and rabbits.[12] In rabbits, fatal "heart disease" within 3 months after exposure was shown to be influenced by dose fractionation. The time-dependent vascular injury that develops within a few hours after irradiation in the chicken also may be relevant to the effect of exposure time on the long-term survival.

The leukosis complex, a virus-induced neoplasia, occurs in various strains of chickens with varying frequencies. In our experience, the incidence in nonirradiated controls has been variable (usually 10 to 20%). It occurred most frequently between 4 months and one year, and was not observed in chickens older than 6 years of age. Leukosis, less common in irradiated groups, was not observed in birds receiving the highest doses.

REFERENCES

1. Stearner, S. P. and E. J. B. Christian. *Radiat. Res.* **34**, 138–152 (1968).
2. Stearner, S. P. and E. J. B. Christian. *Radiat. Res.* **38**, 153–160 (1969).
3. Stearner, S. P. and E. J. B. Christian. *Microvasc. Res.* **2**, 202–211 (1970).
4. Christian, E. J. B. and S. P. Stearner. A Technique to Visualize the Peripheral Circulation on the Young Chicken. To be submitted for publication in *Microvascular Research*.
5. Stearner, S. P. and M. H. Sanderson. *J. Path.* **99**, 312–318 (1969).
6. Croker, B. P., Jr., A. J. Saladino and B. F. Trump. *Am. J. Pathol.* **59**, 247–278 (1970).
7. Stearner, S. P. and S. A. Tyler. *Radiat. Res.* **7**, 253–266 (1957).
8. Stearner, S. P., S. A. Tyler, M. H. Sanderson, and E. J. B. Christian. *Radiat. Res.* **14**, 732–747 (1961).
9. Stearner, S. P. Argonne National Laboratory Biological and Medical Research Division Annual Report, 1969. ANL-7635, pp. 35–38.
10. Tyler, S. A. and S. P. Stearner. *Radiat. Res.* **29**, 257–266 (1966).
11. Barnes, D. W. H., G. T. Bungay and R. H. Mole. *Int. J. Radiat. Biol.* **11**, 409–427 (1966).
12. Fajardo, I. F. and J. R. Steward. *Am. J. Pathol.* **59**, 299–315 (1970).

HYDROXYUREA AND CELL-CYCLE KINETICS OF CULTURED ANTIBODY-FORMING CELLS*

Bernard N. Jaroslow and Librado Ortiz-Ortiz

The cell cycle kinetics of precursors to antibody-forming cells was studied in mouse spleen-cell cultures immunized with sheep red cells. The cultures were treated with 0.5 mM hydroxyurea for 1 to 24 hr. The shape of the survival curve showed the proportion of cells killed in S (0.74), the duration of S (6–7.5 hr) and generation time (8.5–10 hr). This technique is particularly useful for the study of a very small population of differentiating cells prior to the expression of the unique character by which they are detected.

* Abstract of paper submitted to *Cellular Immunology*.

LATE EFFECTS OF IRRADIATION ON IMMUNE RESPONSIVENESS OF AGING MICE*

Bernard N. Jaroslow and Marietta M. Miller

Immunologic responsiveness, measured by the number of antibody-forming cells (AFC) produced in mouse spleens against sheep red blood cells, decreases with age to give $t_{1/2}$ for 19S AFC ~9 months and $t_{1/2}$ for 7S AFC ~6 months. When immunization is initiated in spleen cell cultures, the $t_{1/2}$ for 19S AFC is 6 months. A low dose of neutrons (150 rads) resulted in a marked loss of responsiveness 580 days after irradiation, whereas a comparable dose of ^{60}Co γ radiation (206 rads) did not result in such a loss. Post-radiation recovery from 730 to 1000 rads of ^{60}Co γ radiation did not exceed 60% of normal 2 years after exposure.

* Abstract of a paper to be published in the Proceedings of the Symposium on Late Effects at the IVth International Congress on Radiation Research, Evian, France, June 29–July 4, 1970.

LABORATORY ANIMAL MEDICINE: STATEMENT OF PROGRAM OBJECTIVES

Robert J. Flynn, Thomas E. Fritz, Calvin M. Poole, and Patricia C. Brennan

The Division's research program in laboratory animal medicine is aimed at developing methods for the improved production and management of animals used in the Division's diverse research programs. Our research directed toward providing sufficient and appropriate animal models is illustrated by reports on the development of inbred catalase mutant mice and on *Rattus rattus* as a research animal. Refinement of controlled management is presented in reports on effects of frequency of cage cleaning on the survival of mice, the effects of acidification of water on the health of mice, and the effects of long-distance air transport on the health of aged mice. Special effort is devoted to studying management of laboratory animal disease, particularly those that represent hazards to the Division's research programs. These studies are described by reports on murine pneumonia, survival of *Pseudomonas aeruginosa* in acidified water, throat flora of a closed colony of beagle dogs and the use of the scanning electron microscope as an aid in the identification of mites affecting laboratory animals.

Animal facilities' personnel also provide cooperative, specialized professional assistance (pathology, microbiology, roentgenography, surgery) to the Division's overall research program. This support can be identified in reports found elsewhere in this Annual Report (see the sections on Cellular Fine Structure and Related Function, Toxicity and Metabolism of Radionuclides, and JANUS).

LABORATORY ANIMAL MEDICINE. I. THE SUPPLY AND MAINTENANCE OF DEFINED ANIMALS

Defined animals are necessary for effective biomedical research. Specific animal requirements for different research projects vary, but the general trend is toward the use of animals that are more highly controlled and defined. The animal facilities' group provides the animals needed by the Division's research program through production or acquisition, and furnishes compatible maintenance.[1, 2]

A. Status of the Colony

Calvin M. Poole, Thomas E. Fritz, Patricia C. Brennan, and Robert J. Flynn

The June 30, 1970, animal inventory, including the number and kinds of animals produced or acquired and maintained in the Division's animal facilities during the past fiscal year is presented in Table 4.

The studies involving these animals during this period may be identified by referring to other parts of this report. Animals produced within the Division's facilities are designated with the suffix "Anl" (for Argonne National Laboratory).

Although the overall effort within the animal facilities has been reduced during the past year, in keeping with budgetary restrictions and realignment of research priorities, the production and quality control of strains of mice needed for the JANUS program have been increased. Several cesarean-derived, barrier-maintained mouse colonies have been established, and others are planned.

There were two episodes of increased incidence of *Pseudomonas aeruginosa* infection in the mouse colonies during the past year. Both were detected and controlled by the facilities' routine quality and disease control procedures. Concern over the possible interfering effects of any future episodes on the JANUS program led to a decision to acidify the water bottles used for JANUS animals as a prophylactic measure. Studies related to the effectiveness and possible harmful effects of hydrochloric acid in the drinking water are described in this section.

Pitting and clouding of clear polycarbonate rodent cages, resulting in decreased life and usefulness of these cages, has been experienced for some time. Because the deterioration is primarily related to autoclaving for sterilization, a series of tests were completed involving variations in autoclaving and pre-autoclaving procedures. Deterioration of the cages

TABLE 4. ANIMAL INVENTORY

Common name	Scientific name	Inventory as of June 30, 1970	Total acquired July 1, 1969–June 30, 1970	Total produced at Argonne July 1, 1969–June 30, 1970
Mouse	*Mus musculus*			
Germfree		120	72	75
SPF		6,091	0	51,897
Conventional		6,677	5,661	11,018
Whitefooted mouse	*Peromyscus leucopus*	227	0	100
Brush mouse	*Peromyscus boyleyi*	27	0	0
California mouse	*Peromyscus californicus*	126	0	105
Canyon mouse	*Peromyscus crinitus*	32	0	0
Cactus mouse	*Peromyscus eremicus*	18	0	0
Florida mouse	*Peromyscus floridans*	51	0	30
Cotton mouse	*Peromyscus gossypinus*	99	0	8
Desert pocket mouse	*Perognathus penicillatus*	25	25	0
Harvest mouse	*Reithrodontymus humilus*	52	0	64
Dormouse	*Glis glis*	3	6	0
Northern pygmy mouse	*Baiomys taylori*	28	30	0
Vole	*Microtus* sp.	9	0	0
Tunisian jird	*Meriones lybycus*	1	0	0
Rat	*Rattus norvegicus*	1,912	2,400	5,112
Black rat	*Rattus rattus*	584	0	832
Multimammate mouse	*Praomys* (Mastomys) *natalensis*	190	0	1,009
Cotton rat	*Sigmodon hispidus*	18	0	0
Pack rat	*Neotoma albigulo*	2	0	0
Rice rat	*Oryzomus palustris*	50	0	51
Treeshrew	*Tupia terruginea*	1	0	0
Syrian hamster	*Mesocricetus auratus*	235	0	2,647
Chinese hamster	*Cricetulus barabensis*	70	0	541
Chinchilla	*Chinchilla laniger*	72	131	0
Chipmunk	*Tamias striatus*	6	0	0
Ground squirrel	*Citellus tridecemlineatis*	9	50	0
Tropical red squirrel	*Sciurus granatensis*	2	0	0
Rabbit	*Oryctolagus cuniculus*	24	10	0
Dog (beagle)	*Canis familiaris*	624	0	88
Chicken	*Gallus domesticus*	314	3,900	0
Frog	*Rana pipiens*	0	200	0
Snail	*Helix aspersa*	45	0	0
Grasshopper	*Melanoplus differentialis*	1,200	0	3,600

appears to be related to the alkalinity of the rinse solution and steam condensate. Attempts to find a solution to this problem continue.

The Division's animal facilities, fully accredited by the American Association for the Accreditation of Laboratory Animal Care since 1965, were visited by a site inspection team during August, 1970; and again they have been fully accredited.

B. The Development of Inbred Catalase Mutant Mice

Calvin M. Poole, Ronald W. Camden, Robert J. Flynn, and Robert N. Feinstein

The original program to introduce the acatalasemic locus (Cs^b) into the C3Hf/Anl mouse to provide an acatalasemic animal of uniform coat color, size and growth rate with good reproductive performance,[3-5] was expanded during the year by the introduction of the Cs^b locus into the C57BL/6Anl mouse and the Cs^c (hypocatalasemic) locus into the same two inbred strains. When the program is completed, studies between mutants as well as between different genetic backgrounds will be possible. The C57BL/6Anl mouse

was selected because of its low tumor incidence and wide use for the maintenance of mutations.

Development of these inbred mutant strains involves initial crosses between the mutants and the selected inbred strains with subsequent backcrosses between mutant carriers and stocks from the appropriate strain. Mutant carriers are determined by tests of the blood catalase levels. Whenever possible, only mutant carriers from large litters (8 or more weaned) with the physical appearance of the inbred strain are used for further breeding. Eight generations of backcrosses and eight subsequent sibling matings between mutant homozygotes are required to produce an inbred mutant that is genetically comparable to the catalase normal inbred strain.

The eight backcross generations and five of the eight sibling mated generations in the C3Hf/Anl-Cs^b program have been completed. The second backcross generation has been reached in the C57BL/6Anl-Cs^b program and three backcross generations have been completed in both the C3Hf/Anl-Cs^c and C57BL/6Anl-Cs^c programs. About 20 breeding pairs of each mutant inbred line are being maintained. All animals appear uniform in size, reproduce well and have shown no signs of disease.

C. Rattus rattus as an Experimental Animal

Thomas E. Fritz, David V. Tolle, Robert J. Flynn, and Patricia C. Brennan

The identification of animal species that develop spontaneous diseases or that have physiological responses similar to man has allowed biological research to make great advances through studies of these animal model systems of human diseases.[6, 7] The albino rat (*Rattus norvegicus*), which has been a standard laboratory animal for many decades, is unacceptable for some types of biological research.[8] Few studies of the black rat (*R. rattus*) in captivity have been published.[9] We have established a breeding colony of this species and are attempting to characterize it and examine its value as an experimental animal.[10]

During the past year, this breeding colony was expanded—a total of 99 monogamous pairs were set up. Table 5 presents data obtained from these 99 pairs during the period August 1, 1969–October 1, 1970. All animals produced have had a consistent coat color, which has been described as the standard wild-type, i.e., agouti dorsum with a white venter.[11] One female among the original stock with dark grey (black) pilage failed to reproduce.

Although our records are presently limited, it appears that our animals mate late and that reproduction of these rats does not begin before they are 4 to 5 months of age. This pattern is somewhat different from that reported for *R. rattus*,[9] and very different from *R. norvegicus*.[12]

TABLE 5. Breeding Performance of *Rattus rattus* (14 months)

Total breeding pairs	99
Pairs producing litters	48 (48.5%)
Total litters produced	169
Mean number of litters per pair	3.52 (range 1–12)
Total born	1169
Mean litter size at birth	6.97
Total weaned	832 (70.6%)
Mean litter size at weaning	5.04

TABLE 6. Peripheral Blood Values (under Sodium Pentobarbital Anesthetic; Samples Taken from Axillary Artery)

	Female	Male
WBC, $\times 10^3$	11.37 ± 0.79[a]	11.98 ± 1.99
Hb, gm/100 ml	13.0 ± 0.3	13.6 ± 0.4
PCV, %	42.5 ± 0.8	44.0 ± 1.4
Immature neutrophils, %	None	0.4 ± 0.2
Mature neutrophils, %	13.4 ± 2.1	28.8 ± 4.1
Lymphocytes, %	81.8 ± 2.4	65.6 ± 2.9
Monocytes, %	2.2 ± 0.7	1.0 ± 0.3
Eosinophils, %	2.2 ± 0.5	4.2 ± 0.9

[a] Mean ± S.E. for 5 animals.

As shown in Table 5, 48 of 99 pairs produced litters during the 14-month period. The sexes are segregated at weaning and mated as monogamous pairs at approximately 100 days of age. Because most females have nonpatent vaginas as late as 90 days of age, we routinely open the vagina by manual massage at the time of mating. Breeding pairs are left mated until at least 6 months of age before they are culled for infertility.

To further characterize our *R. rattus*, hemograms, bone marrow differential cell counts and organ weights were collected. These data are presented in Tables 6, 7 and 8. In differential counts of the peripheral blood the male has a higher percentage of mature neutrophils and a lower percentage of lymphocytes than the

female. This is an important finding because *R. norvegicus* is reported to have no differences in number or differential counts of the leukocytes between the sexes.[13] More data are needed to confirm this finding because only five animals of each sex were examined.

A preliminary study of the radiation sensitivity of *R. rattus* and *R. norvegicus* has also been completed. One hundred 100-day-old animals of each species (50 males and 50 females) were irradiated by exposure to γ radiation from a ^{60}Co source. The doses were 700, 750, 800, 850, or 900 R at a dose rate of 20 R/minute.

Before irradiation, the water bottles from all cages of animals were cultured three times, at weekly intervals, for *Pseudomonas aeruginosa*. Samples of heart blood were also cultured from all animals dying during the first 14 days after exposure. Table 9 lists the 30 day mortality for each species. When subjected to probit analysis, these data give an $LD_{50/30}$ of 899 ± 122 R for *R. rattus*. This dose range was too low to permit calculation of an $LD_{50/30}$ for *R. norvegicus;* only 4 animals died. It is obvious from these results, however, that *R. rattus* is more sensitive to whole-body irradiation than *R. norvegicus*.

TABLE 7. Femoral Bone Marrow Differential Cytology

	Female, %	Male, %
Rubriblast	—	—
Prorubricyte	2.0 ± 0.5[a]	3.2 ± 0.9
Rubricyte	7.8 ± 0.5	10.4 ± 2.8
Metarubricyte	13.8 ± 1.4	13.8 ± 1.4
Myeloblast	1.6 ± 0.5	2.2 ± 0.4
Promyelocyte	4.2 ± 0.7	4.8 ± 0.9
Myelocyte	23.0 ± 1.0	24.4 ± 2.1
Metamyelocyte	9.8 ± 0.7	7.4 ± 1.4
Band neutrophil	13.4 ± 1.4	11.4 ± 1.2
Mature neutrophil	19.4 ± 3.1	19.4 ± 2.7
Plasma cell	1.6 ± 0.2	1.6 ± 0.5
Megakaryocyte	0.4 ± 0.2	0.4 ± 0.2
Lymphocyte	3.0 ± 0.5	0.8 ± 0.6
Myeloid-erythroid ratio (M:E)	2.1:1.0 ± 0.1	2.8:1.0 ± 0.2

[a] Mean ± S.E. for 5 animals.

TABLE 8. Total Body and Organ Weights in Grams

	Female	Male
Total body	156.5 ± 11.2[a]	203.2 ± 12.0
Brain	1.6 ± 0.04	1.8 ± 0.04
Pituitary	0.0072 ± 0.0006	0.0054 ± 0.0004.
Heart	0.77 ± 0.11	0.90 ± 0.08
Lung	0.79 ± 0.06	0.90 ± 0.08
Liver	8.7 ± 0.9	10.1 ± 0.7
Spleen	0.21 ± 0.04	0.24 ± 0.01
Kidneys	1.3 ± 0.10	1.3 ± 0.03
Adrenals	0.1 ± 0.01	0.1 ± 0.008
Gonads	0.06 ± 0.005	2.9 ± 0.09
Stomach	0.9 ± 0.05	1.0 ± 0.06
Small intestine	2.8 ± 0.9	2.1 ± 0.2
Large intestine (incl. cecum)	1.5 ± 0.14	1.9 ± 0.11
Eyes	0.3 ± 0.02	0.3 ± 0.02
Thyroids	0.01 ± 0.001	0.01 ± 0.0005
Pancreas	0.3 ± 0.09	0.5 ± 0.02
Uterus	0.4 ± 0.07	—

[a] Mean ± S.E. for 5 animals.

TABLE 9. Comparison of Radiation Sensitivity of *R. rattus* and *R. norvegicus* to Single Brief Doses of ^{60}Co γ Rays

Dose, R	*R. rattus*			*R. norvegicus*		
	Male	Female	Total	Male	Female	Total
900	6/10[a]	6/11	12/21	0/10	2/10	2/20
850	2/10	4/10	6/20	0/10	1/10	1/20
800	1/10	2/10	3/20	0/10	1/10	1/20
750	4/11	7/11	11/22	0/10	0/10	0/20
750	0/10	0/11	0/21	0/10	0/10	0/20
Total	13/51	19/53	32/104	0/50	4/50	4/100

[a] Number dead/number irradiated.

Probit analysis, $LD_{50/30}$ for *Rattus rattus* = 899 ± 122 R. Insufficient data of probit analysis $LD_{50/30}$ for *Rattus norvegicus*.

Chromosomes from bone marrow preparations from 3 animals had a diploid number ($2n$) of 38. This number is the same as that reported for this species from Australia, but is different from the karyotype reported from Japan, Southeast Asia,[14] and a laboratory colony once maintained in North America.[15]

Studies of *R. rattus* to be completed during the coming year will include additional bone marrow and peripheral blood cell examinations, testicular chromosome examinations, studies to determine the age at which the first fertile breeding for each sex occurs, and additional radiation studies to establish more precisely the radiation response.

REFERENCES

1. Flynn, R. J., T. E. Fritz, C. M. Poole, R. W. Camden, and P. C. Brennan. Argonne National Laboratory Biological and Medical Research Division Annual Report, 1967. ANL-7409, pp. 232–233.
2. Poole, C. M., R. W. Camden, T. E. Fritz, P. C. Brennan, and R. J. Flynn. Argonne National Laboratory Biological and Medical Research Division Annual Report, 1969. ANL-7639, pp. 55–56.
3. Flynn, R. J., R. W. Camden, R. N. Feinstein, and D. Grahn. Argonne National Laboratory Biological and Medical Research Division Annual Report, 1967. ANL-7409, p. 119.
4. Camden, R. W., R. J. Flynn, and R. N. Feinstein. Argonne

National Laboratory Biological and Medical Research Division Annual Report, 1968. ANL-7535, pp. 189–190.
5. Camden, R. W., R. N. Feinstein, and R. J. Flynn. Argonne National Laboratory Biological and Medical Research Division Annual Report, 1969. ANL-7635, p. 58.
6. Frenkel, J. K. *Fed. Proc.* **28**, 160–161 (1969).
7. Jones, T. C. *Fed. Proc.* **28**, 162–169 (1969).
8. Lochard, R. B. *Am. Psychol.* **23**, 734–742 (1968).
9. Kilway, P. *Care and Management of Laboratory Animals*, 2nd ed., Ed. A. N. Worden and W. Lane-Petter. The Universities Federation for Animal Welfare, London, 1957, pp. 378–383.
10. Fritz, T. E., D. V. Tolle, P. C. Brennan, R. C. Simkins, and R. J. Flynn. Argonne National Laboratory Biological and Medical Research Division Annual Report, 1969, ANL-7635, pp. 58–59.
11. Tomich, P. Q., and H. T. Kami. *J. Mammal.* **47**, 423–431 (1966).
12. Camden, R. W., R. J. Flynn, and C. M. Poole. Argonne National Laboratory Biological and Medical Research Division Annual Report, 1969. ANL-7635, p. 57.
13. Creshoff, A. J., T. Fitz-Hugh, Jr., and E. J. Farris. *The Rat in Laboratory Investigation*, 2nd ed., Ed. E. J. Farris and J. Q. Griffith, Jr. Lippincott, Philadelphia, 1959, pp. 406–420.
14. Yoshida, T. H., K. Tsuchiya. H. Imai, and K. Moriwaki. *Japan J. Genetics* **44**, 89–91 (1969).
15. Pincus, G. *J. Morphol. Physiol.* **44**, 515–537 (1937).

LABORATORY ANIMAL MEDICINE. II. LABORATORY ANIMAL DISEASES

High quality animal research requires healthy animals. Thus, a rigid disease control program is essential. Unfortunately, the cause of many of the diseases of laboratory animals is unknown and, even when known, knowledge of effective control is lacking. For these reasons, the animal facilities' group actively studies laboratory animal diseases.

A. Murine Pneumonia

Patricia C. Brennan, Thomas E. Fritz, and Robert J. Flynn

We previously showed that germfree mice infected with both *Pasteurella pneumotropica* and *Mycoplasma pulmonis* develop a pneumonia which clinically resembles spontaneous murine pneumonia in conventional mice.[1] We also reported that mice presumably free from infection with either organism were latently infected with small numbers of both organisms. Recently, Nelson[2] suggested that a difference in virulence between strains of *M. pulmonis* might account for our failure to produce severe pneumonia with *M. pulmonis* unless we also infected the mice with *P. pneumotropica*. In our report, we suggested that a difference between strains of mice might account for the differences.[1] Although our studies of murine pneumonia have been curtailed because of a shortage of time and personnel, we are continuing them on a limited basis to clarify this point.

Three experiments are in progress: *Experiment I.* To determine if *P. pneumotropica* is pathogenic for conventionally reared mice, 20 CF⅜1/Anl[Anl 66] female mice 28 days of age were instilled intranasally with 3×10^7 viable *P. pneumotropica* cells and 20 control mice were instilled with 0.05 ml sterile broth. Ten mice from each group were killed 5 days after infection and the rest were killed 10 days after infection. Examination and culture procedures have been described.[1] *Experiment II.* To determine if experimental infection with either *P. pneumotropica* or *M. pulmonis* can reveal latent infection with either organism, 30, 9-month-old CF⅜1/CF female mice were necropsied. Their lungs, trachea, nasal passages and middle ears were cultured for *P. pneumotropica* and *M. pulmonis*. As part of this experiment, 20 additional mice of the same age and strain will be infected with *M. pulmonis* and 20 with *P. pneumotropica* and 20 will be instilled intranasally with 0.05 ml sterile broth. Ten of each group will be killed and examined 30 days after infection and the other ten after 60 days. *Experiment III.* A small breeding nucleus of Swiss mice and Princeton mice has been obtained from Dr. J. B. Nelson of The Rockefeller University. Offspring from these mice will be used in experiments to determine if the strains of mice used can account for the differences in susceptibility to pneumonia observed by Nelson and us.

All the mice given *P. pneumotropica* in the first experiment had consolidated lungs at necropsy. The lesions were identical to those observed in germfree mice infected with *P. pneumotropica*,[1] and the organism was recovered from all the lungs. *M. pulmonis* was not isolated. No control mice had lesions and neither organism was recovered.

None of the uninoculated old CF⅜1/CF mice in the

second experiment had lesions and neither *M. pulmonis* nor *P. pneumotropica* was recovered from the sites cultured.

A preliminary conclusion to be drawn is that *P. pneumotropica* is pathogenic for conventionally reared mice as well as for germfree mice.

B. Survival of Pseudomonas aeruginosa in Acidified Water

Patricia C. Brennan

A number of investigators have reported the control of *Pseudomonas aeruginosa* infection in mouse colonies by acidifying the drinking water;[3-5] however, they only used one pH level. Because acidification of the drinking water for the Division's rodent colonies is planned, studies were initiated to determine the highest pH at which *P. aeruginosa* will not survive in tap water and in water containing mouse feces and other organic matter and bacteria.

Eight flasks containing 250 ml of tap water from the bottle filler were prepared. The pH of the water in seven flasks was adjusted with 1.0 N HCl to pH 3.9, 3.4, 2.9, 2.7, 2.4, 2.2 and 2.0. One flask served as an unacidified control. Its pH was 9.1. Washed *P. aeruginosa* cells were added to each flask to a final concentration of 2×10^6/ml. The flasks were incubated at room temperature and samples were withdrawn at 24-hr intervals for one week. One 1-ml sample was serially diluted and pour plates were made to determine the number of viable cells. A second 1-ml sample was inoculated directly into Wensincks glycerol broth[6] to test for pyocyanin production. At the end of one week, the water remaining in those flasks that had been negative for *P. aeruginosa* in glycerol broth was filtered through a 0.45-μ Millipore filter. The filter was incubated in glycerol broth.

In a second experiment, seven cages of 5 mice each were given acidified water at the above pH values and one cage of 5 mice was given tap water. All of the bottles were inoculated with 10^9 viable *P. aeruginosa*/ml. Plate counts were made from each bottle after 24 and 72 hours and at the end of one week. Glycerol broth was inoculated with 1 ml from each bottle every day. After one week the acidified water was removed and replaced with tap water, and this water was cultured daily for another week for *P. aeruginosa*. At the end of the second week the mice were killed and throat and fecal cultures for *P. aeruginosa* were made.

After 24 hr the number of viable bacteria had fallen to 2×10^3 in both unacidified water and in water at pH 3.9. There were less than 10 viable cells/ml at the other pH values, and this number remained constant throughout the course of the experiment. At times later than 24 hr *P. aeruginosa* grew in unacidified water and, after a week, reached a population of 10^6/ml. Although tests of the 1-ml samples were negative for *P. aeruginosa* below pH 3.9, tests of the membrane filters were positive at pH 3.4, 2.9 and 2.7, indicating that at least one viable cell survived in each flask.

When acidified water containing *P. aeruginosa* was placed on mouse cages, the organism survived at all pH levels tested. The mice did not become "shedders" of *P. aeruginosa* because tests of unacidified, uncontaminated water placed on the cages after the water containing the organism was removed were negative. *P. aeruginosa* was recovered from neither the throats nor the feces of the mice.

Thus, *P. aeruginosa* can survive at pH 2.7 for one week, but it cannot survive at pH 2.4 or less in the absence of organic matter. In the presence of feces, other organic matter and bacteria, *P. aeruginosa* can survive for at least one week in water of pH 2.0.

C. Throat Flora of a Closed Colony of Beagle Dogs

Patricia C. Brennan and Richard C. Simkins

Our survey of the throat flora of the beagle colony in the Division of Biological and Medical Research now includes results for a second one-year period. Four hundred thirty-nine dogs have been cultured, using the methods previously described.[7, 8] Our study of the incidence of β hemolytic streptococci by age, sex, pedigree and kennel location of the dogs and by the month in which the culture was obtained has also been extended.

The kinds of bacteria recovered and their incidence are presented in Figure 3. Although the kinds of bacteria isolated this year closely parallel those isolated

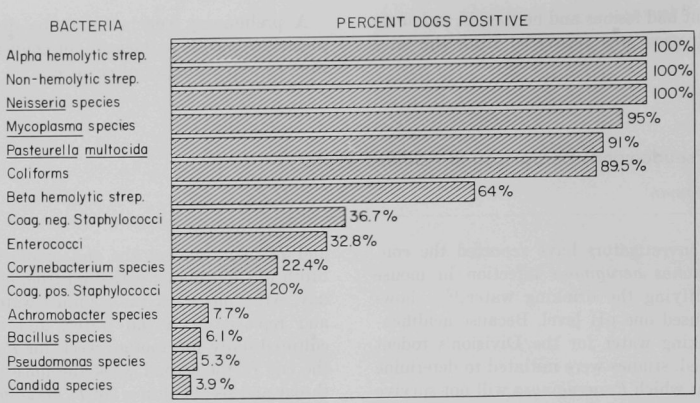

FIG. 3.—Throat flora of a closed colony of beagle dogs.

last year,[8] the incidence of some potential pathogens has increased. The incidence of β hemolytic streptococci increased significantly from 41.8% to 64% ($P < 0.01$). Similarly, the incidence of *Pasteurella multocida* increased from 80% to 91% and the incidence of coagulase-positive staphylococci increased from 3.3% to 20%. *Mycoplasma* species decreased from 100% to 95%, a decrease which is probably not a *real* change but due to technical difficulties associated with its isolation. Organisms considered nonpathogenic remained fairly constant, although an increase was noted in the incidence of *Pseudomonas, Bacillus* and *Candida* species.

Although younger dogs (1–4 years old) continued to show a significantly lower incidence than older dogs (over 4 years of age), this difference was not as marked as that reported previously. The incidence of β hemolytic streptococci was similar for all months, except March, when the lowest incidence (38.5%) was noted. The low incidence in October and November last year was not repeated during those months this year. Breeding adults and young stock dogs, again, showed a lower incidence than experimental or control dogs. No sex differences were noted, nor were differences observed between the two strains of beagle dogs in the colony.

Thus, the throat flora of these beagles has been generally stable over a two-year period (1968 to 1970); the incidence of some potential pathogens during this period has increased.

D. The Use of the Scanning Electron Microscope as an Aid in the Identification of Mites Affecting Laboratory Animals

Robert J. Flynn and George T. Chubb

The high magnification, excellent resolution and depth of focus available with scanning electron microscopy permits one to investigate surface structures of living organisms in detail not possible previously. Diagnostically important surface characteristics of mites, sometimes difficult to see by transmitted light microscopy, are readily recognized with the scanning electron microscope. Reports of first attempts at scanning electron micrography of house-dust mites[9] and plant mites[10] have been published but, to date, no reports refer to this technique as used to describe or identify mites of importance as ectoparasites on animals.

Procedures for scanning electron micrography of most biological materials are still being developed. This study, too, is presently concerned principally with development of techniques.

A first attempt using gold coating was reasonably successful; photographs of useful quality were obtained. Subsequent efforts, using vacuum and freeze-

drying procedures were less successful. Scanning microscopy of unfixed living mites, coated and uncoated, is now being tried.

The scanning electron microscope, which only "sees" surface characteristics of materials, appears to be a highly effective instrument for the study of the morphology of animals with exoskeletons such as mites. Essential surface details, now often lacking in descriptions of mites of medical importance, will be described.

REFERENCES

1. Brennan, P. C., T. E. Fritz and R. J. Flynn. *J. Bacteriol.* **97,** 337–349 (1969).
2. Nelson, J. B. *Lab. Animal Care* **20,** 670–674 (1970).
3. McPherson, C. W. *Lab. Animal Care* **13,** 737–744 (1963).
4. Trentin, J. C., G. L. Van Hoosier, Jr., Jacqueline Shields, Kristina Stephens and W. A. Stenback. *Lab. Animal Care* **16,** 109–118 (1966).
5. McDougall, P. T., N. S. Wolf, W. A. Stenback and J. S. Trentin. *Lab. Animal Care* **17,** 204–214 (1967).
6. Wensinck, F., D. W. Van Bekkum, and H. Renaud. *Radiat. Res.* **7,** 491–499 (1957).
7. Brennan, P. C. and R. C. Simkins. Argonne National Laboratory Biological and Medical Research Division Annual Report, 1969. ANL-7635, pp. 65–66.
8. Brennan, P. C. and R. C. Simkins. *Proc. Soc. Exptl. Biol. Med.* **134,** 566–570 (1970).
9. Wharton, G. W. *Science* **167,** 1382–1383 (1970).
10. Humphreys, W. J., P. E. Hunter, and H. E. Barke. Cambridge Proceedings Third Annual Stereoscan Scanning Electron Microscope Colloquium, April 27, 1970, Chicago, Illinois. Kent Cambridge Scientific, Inc., Morton Grove, Illinois, 1970, pp. 177–187.

LABORATORY ANIMAL MEDICINE. III. LABORATORY ANIMAL MANAGEMENT

Proper care of laboratory animals is both a humane and scientific requirement. Unfortunately, objective, experimentally-obtained information is often lacking on what constitutes proper care. It is for this reason that the Division's animal facilities' group studies laboratory animal management.

A. Frequency of Cage Cleaning and the Survival of Mice

Robert J. Flynn and Calvin M. Poole

This study was initiated to establish whether the frequency of cage cleaning influences the health and survival of laboratory mice.[1, 2]

CF#1/Anl[Anl 66] female mice were divided, at weaning, into four groups of 245 mice each and two groups of 210 mice each. The cages of the first four groups were cleaned three times a week, twice a week, once a week, or once every 2 weeks. Cages of the other two groups were cleaned once every 4 weeks or were never cleaned. Spontaneous deaths were recorded daily.

Several problems were encountered in the never-cleaned cages. One problem was that the cages had to be at least partially cleaned about every month, either because food cut down into the cage left little room for the mice, or, because the cages became wet when food and feces were pushed against the water bottle nipple and the bottle contents was leaked into the cage. The cages were scraped but no bedding was added.

Another problem was that "vinegar" gnats and larvae were first observed when the mice were about 8 months of age. An attempt to eradicate them by moving the mice from affected cages to clean cages and then spraying the room with an insecticide that contained pyrethrins and piperonyl butoxide was unsuccessful; the gnats persisted throughout the experiment.

The ears of mice in the infrequently-changed cages

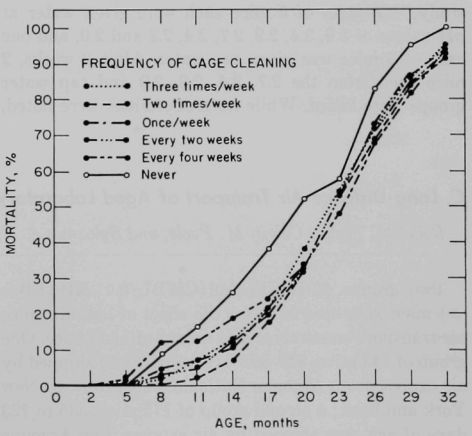

FIG. 4.—Mortality of CF#1/Anl[Anl 66] mice from 0 to 32 months of age related to frequency of cage cleaning.

were reddened, a condition apparently caused by the high ammonia content of the air in the cages. Within seconds after the cage cover was removed, the redness disappeared.

Only two differences in mortality were observed (Fig. 4). The first occurred when the mice were about 8 months of age. At this time, several deaths occurred, particularly in the cages cleaned least frequently. These deaths appeared to be caused by *Pasteurella pneumotropica* but this was not confirmed.[3]

The other difference was noted in the *never-cleaned* cages. Mortality became highest in these cages when the mice were about 8 months of age, when the apparent *P. pneumotropica* epizootic occurred, and persisted unchanged throughout the experiment.

A frequency of cage cleaning ranging from three times a week to as seldom as once every 4 weeks, had no noticeable effect on the long-term survival of laboratory mice. Only when cages were never cleaned was a life-shortening effect noted, and even then it is remarkable to us how well the mice survived, in spite of being crowded into less than 10% of their original cage space, being constantly wet from leaking water bottles, being surrounded by larvae and adult vinegar gnats, and forced to live in an environment high in ammonia content.

B. Effects of Acidified Water on Health of Mice

Calvin M. Poole, Thomas E. Fritz, and Robert J. Flynn

Acidification of water with 0.1 N HCl to pH 2.5 has been reported by several investigators to control *Pseudomonas aeruginosa.*[4-6] Unfortunately, little is known of the effects of this treatment on the health of the mice, other than that there are no apparent ill effects. Because such acidification of the drinking water is planned for our rodent breeding colonies and the JANUS experimental animals, 45, 5-month-old female CF♀1/Anl[Anl 66] mice were given pH 2.5 water for 90 days and 45 mice of the same age, sex and strain were given tap water for the same period. No difference in water consumption, body weight or general health was noted and the mice were discarded. In another study,[7] 7 cages of 5 mice each were given water at pH values of 3.9, 3.4, 2.9, 2.7, 2.4, 2.2 and 2.0, and one cage of 5 mice was given tap water. After 2 weeks, 2 mice each from the 2.7, 2.4, 2.2, 2.0 and tap water groups were killed. While no gross lesions were noted, one mouse that had been given pH 2.4 water was found, on histologic examination, to have an acute gastritis. For this reason a more extensive study was initiated.

Sixty female and 60 male $B6CF_1$/Anl[Anl 66] weanling mice were grouped 5 per cage. Half of the cages are receiving pH 2.4 water; the other half receives tap water. All the mice are weighed every 2 weeks and 10 mice that receive acid water and 10 that receive tap water are to be killed after 2, 4, 6, 10 weeks, 5 months, and 1 year. Gross lesions are recorded and tissues are taken for histologic examination. Should any mice die before their scheduled sacrifice date, they are to be examined for gross and histologic lesions.

The 2-, 4-, 6- and 10-week groups have been killed. None showed significant gross lesions; tissues taken for histologic study have not yet been examined. There have been no spontaneous deaths.

C. Long-Distance Air Transport of Aged Laboratory Mice*

Robert J. Flynn, Calvin M. Poole, and Sylvanus A. Tyler

Two groups of $B6CF_1$/Anl(C57BL/6♀ XBALB/c♂) mice were used to assess the effect of long-distance air transport on survival and weight of aged mice. One group of 143 mice, 529–895 days of age, was shipped by air express from Argonne National Laboratory to New York and back; a second group of 175 mice, 535 to 723 days of age, was shipped by air express from Argonne to Los Angeles and back. The time in transit for each shipment was about 30 hours. The transported mice experienced a severe weight loss (about 3 g/mouse), but this loss was only temporary (48 hours) and appeared to be from dehydration. Only one mouse died in each group during transit and the subsequent mortality was low, except among mice over 800 days of age, and even in this age group most survived at least 30 days after shipment. From these results it

* Abstract of a paper accepted by *J. Gerontology.*

is concluded that old mice can be shipped long distances by air express with little effect on their health other than a transient dehydration.

REFERENCES

1. Flynn, R. J. Argonne National Laboratory Biological and Medical Research Division Annual Report, 1968. ANL-7535, p. 194.
2. Flynn, R. J., and C. M. Poole. Argonne National Laboratory Biological and Medical Research Division Annual Report, 1969. ANL-7635, p. 64.
3. Flynn, R. J., T. E. Fritz, C. M. Poole, R. W. Camden, and Patricia C. Brennan. Argonne National Laboratory Biological and Medical Research Division Annual Report, 1968. ANL-7535, p. 180.
4. McPherson, C. W. *Lab. Animal Care* **13**, 737–744 (1963).
5. Trentin, J. C., G. L. Van Hoosier, Jr., Jacqueline Shields, Kristina Stephens, and W. A. Stenback. *Lab. Animal Care* **16**, 109–118 (1966).
6. McDougall, P. T., N. S. Wolf, W. A. Stenback, and J. S. Trentin. *Lab. Animal Care* **17**, 204–214 (1967).
7. Brennan, P. C. Survival of *Pseudomonas aeruginosa* in acidified water. This report.

Theoretical Biology

DO BAND CELLS FOLLOW "FIRST IN-FIRST OUT" KINETICS?

*Ernesto Trucco**

PURPOSE AND METHODS

Measurements on granulocyte kinetics in the dog were performed by H. M. Patt and M. A. Maloney.[1] These authors (personal communication) believe that, at least approximately, the metamyelocytes and the band cells in the marrow follow "first in-first out" kinetics. If this is true, there should be very little spread in cellular transit times through each of the two stages in question.

For simplicity, the folowing investigation is limited to the band cells in the marrow. It is assumed that the metamyelocytes behave as a "first in-first out" deme† with a fixed transit time of $D_1 = 20$ hr. Let $P_1(t)$ be the fraction of the input flow into the metamyelocytes that is labeled, after a single injection of tritiated thymidine administered at time $t = 0$. (For example, if at some time 100 cells per hour become metamyelocytes and 10 of them are labeled, then $P_1(t) = 0.1$). Denote by $P_2(t)$ a similar function for the band cells. From the assumption that the metamyelocytes are "first in-first out" we have

$$P_2(t) = P_1(t - D_1). \tag{1}$$

Let $\phi_2(a)$ be the survivorship function for the band cells; i.e., if a sample of cells is observed, all of which become band cells at time $t = 0$, then $\phi_2(a)$ indicates what fraction of them is still present as band cells at time $t = a$. Thus, $\phi_2(a)$ must be a decreasing function of a which varies from 1 to 0 as a increases from 0 to ∞. The negative derivative of $\phi_2(a)$,

$$\delta_2(a) = -\frac{d\phi_2(a)}{da}, \tag{2}$$

describes the distribution of sojourn times for band cells; $\delta_2(a)\,da$ is the probability that a cell will die or emigrate when it has age between a and $a + da$. The mean sojourn time in the band cell deme, D_2, is equal to

$$D_2 = \int_{a=0}^{\infty} a\phi_2(a)\,da, \tag{3}$$

and the labeling index, Z_2, for the band cells is given by

$$\begin{aligned} Z_2(t) &= \frac{1}{D_2}\int_{a=0}^{\infty} P_2(t-a)\phi_2(a)\,da \\ &= \frac{1}{D_2}\int_{a=0}^{\infty} P_1(t-D_1-a)\phi_2(a)\,da \\ &= \frac{1}{D_2}\int_{\mu=-\infty}^{t-D_1} P_1(\mu)\phi(t-D_1-\mu)\,d\mu \end{aligned} \tag{4}$$

Since $P_1(\mu) = 0$ for $\mu < 0$, this becomes

$$Z_2(t) = \begin{cases} 0 & \text{if } t \le D_1 \\ \dfrac{1}{D_2}\displaystyle\int_{\mu=0}^{t-D_2} P_1(\mu)\phi_2(t-D_1-\mu)\,d\mu \end{cases} \tag{5}$$

The quantity $P_1(t)$ is unknown and not easily obtained experimentally. It depends on the uptake of label and on the laws governing cell division in precursor demes (myelocytes, myeloblasts, etc.). Purely empirically, by trial and error, the function shown graphically in Figure 5 and tabulated in Table 10 was obtained as the $P_1(t)$ that corresponds to the available labeling data.

PROGRESS REPORT

As a test case for the subsequent calculations, the expression (5) for $Z_2(t)$ was evaluated first with a step

* Deceased.

† A "deme" is the same as that usually called a "compartment". There are, however, good reasons for preferring the word deme (see Ref. 2, p. 286).

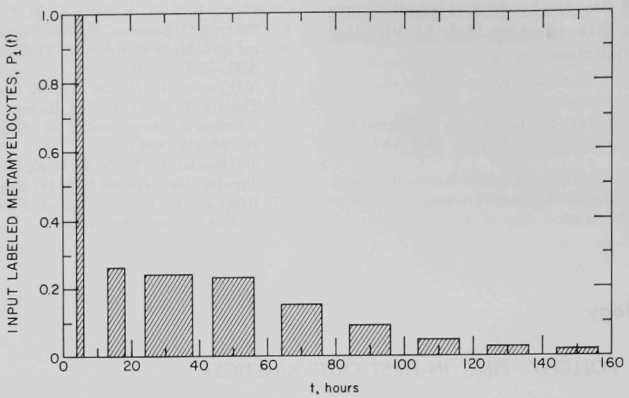

FIG. 5.—Assumed metamyelocyte input after spike label with tritiated thymidine at $t = 0$, $P_1(t)$ vs t (see text, Table 10).

TABLE 10. ASSUMED METAMYELOCYTE INPUT

t, hr	$P_1(t)$
$0 \leq t < 4$	0
$4 \leq t < 6$	1.00
$6 \leq t < 13$	0
$13 \leq t < 18$	0.26
$18 \leq t < 24$	0
$24 \leq t < 38$	0.24
$38 \leq t < 44$	0
$44 \leq t < 56$	0.23
$56 \leq t < 64$	0
$64 \leq t < 76$	0.15
$76 \leq t < 84$	0
$84 \leq t < 96$	0.09
$96 \leq t < 104$	0
$104 \leq t < 116$	0.045
$116 \leq t < 124$	0
$124 \leq t < 136$	0.025
$136 \leq t < 144$	0
$144 \leq t < 156$	0.017
$t \geq 156$	0

function input, i.e.,

$$P_1(t) = \begin{cases} 0 & \text{for } t < 0 \\ 0.2 & \text{for } t \geq 0. \end{cases} \tag{6}$$

Seven different functions were chosen for $\phi_2(a)$, ranging from "first in-first out" to "random exit." In all cases, D_2 was taken equal to 27 hours, as indicated by Patt and Maloney.[1]

The choices are $\phi_2(a)$ are as follows:

1) "First in-First out,"

$$\phi_2(a) = \begin{cases} 1 & \text{for } 0 \leq a < D_2 \\ 0 & \text{for } a \geq D_2; \end{cases} \tag{7}$$

2), 3), and 4),

$$\phi_2(a) = \begin{cases} 1 & \text{for } \leq a \leq D_2 - \sigma \\ \cos^2 \dfrac{\pi(a + \sigma - D_2}{4\sigma} & \text{for } D_2 - \sigma \leq a \leq D_2 + \sigma \\ 0 & \text{for } a \geq D_2 + \sigma\,, \end{cases} \tag{8}$$

with $\sigma = 8$ hours, $\sigma = 16$ hours, or $\sigma = 27$ hours.

5), 6), and 7),

$$\phi_2(a) = \frac{\Gamma(k,x)}{\Gamma(k)} \tag{9}$$

where

$$x = \frac{ka}{D_2} \tag{10}$$

$$\Gamma(k, x) = \int_{\mu=x}^{\infty} \mu^{k-1} e^{-\mu} d\mu, \tag{11}$$

and

$$\Gamma(k) \equiv \Gamma(k, 0); \tag{12}$$

three different values were assigned to the parameter k, namely, $k = 3$, $k = 2$, and $k = 1$. The last of these is the same as "random exit," since $\phi_2(a)$, equation 9, becomes a simple exponential function for $k = 1$.

The seven functions $\phi_2(a)$ are shown in Figure 6, and the probability density functions $\sigma_2(a)$ derived from them are plotted in Figure 7.

Figure 8 shows the result of computing $Z_2(t)$ from equation (5) with the input function $P_1(t)$ given by equation (6); each graph corresponds to 1 of the 7 choices for $\phi_2(a)$. The same curves were obtained using a computer program to find $Z_2(t)$.

Next, $Z_2(t)$ was evaluated by means of computer

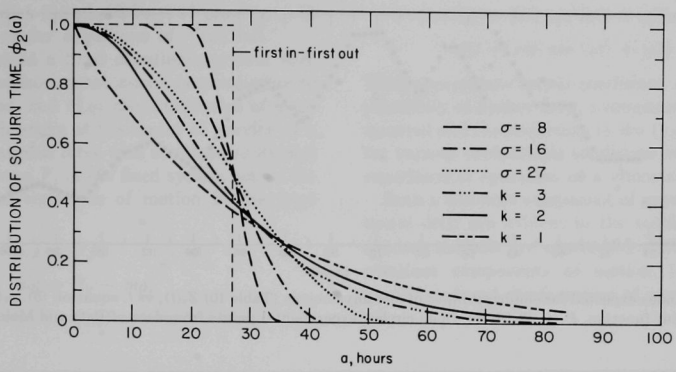

FIG. 6.—The 7 choices of the distribution function for sojourn times, $\phi_2(a)$; see text for details.

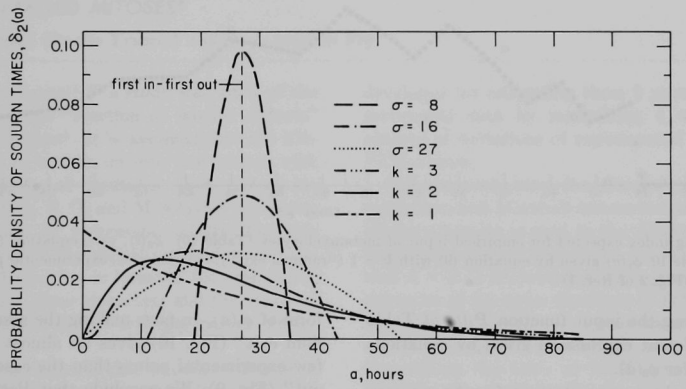

FIG. 7.—The probability densities $\delta_2(a)$ obtained from the functions $\phi_2(a)$ of Figure 6.

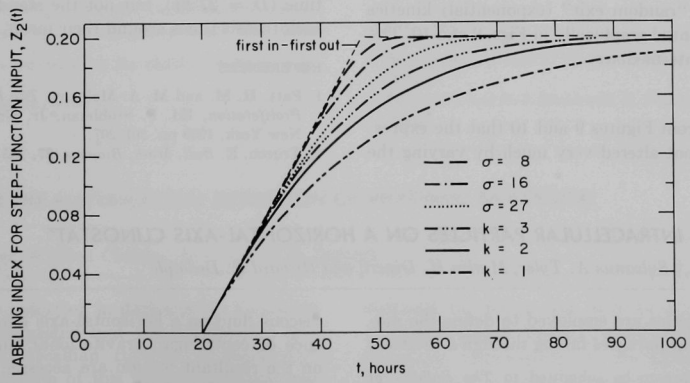

FIG. 8.—$Z_2(t)$, equation (5), for a step-function input of metamyelocytes, $P_1(t)$, as in equation (6).

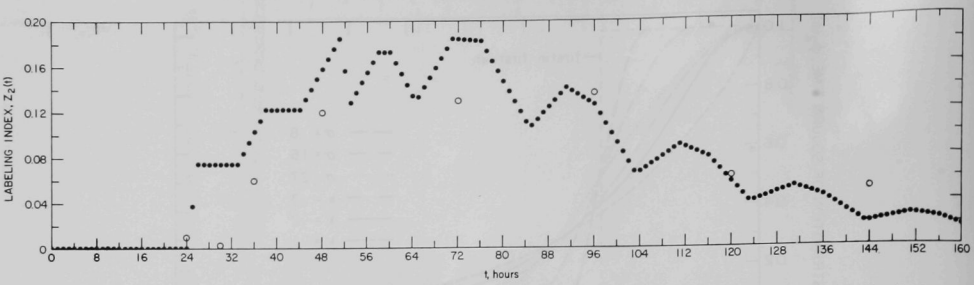

FIG. 9.—Labeling index expected for empirical input of metamyelocytes (Table 10) $Z_2(t)$, vs t, equation (5). $\phi_2(a)$: first in-first out kinetics [Eq. (7)]; input function, $P_1(t)$, Table 10. Open circles, experimental points from data of Patt and Maloney (Fig. 2 of Ref. 1).

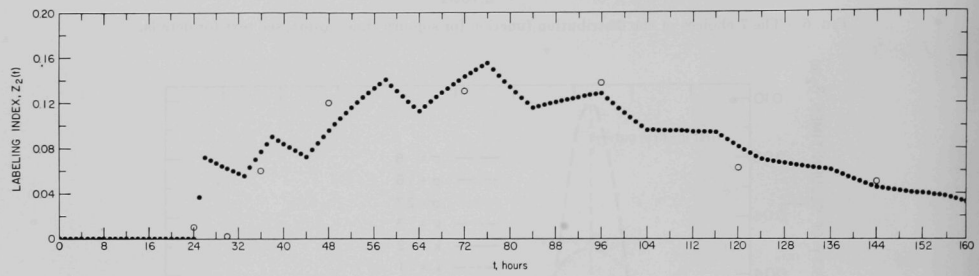

FIG. 10.—Labeling index expected for empirical input of metamyelocytes (Table 10). $Z_2(t)$, vs t, equation (5); input function, $P_1(t)$, given by Table 10. $\phi_2(a)$ given by equation (9) with $k = 1$ ("random exit"). Open circles, experimental points from data of Patt and Maloney (Fig. 2 of Ref. 1).

calculations, taking the input function $P_1(t)$ of Table 10 and the 7 different expressions given by equations (7), (8), and (9) for $\phi_2(a)$.

The results of these computations for the two extreme cases; a) first in-first out (rectangular) kinetics (Fig. 6) and b) "random exit" (exponential) kinetics (Fig. 6) are presented graphically in Figs. 9 and 10. The other cases are intermediate.

CONCLUSIONS

It is evident from Figures 9 and 10 that the expression for $Z_2(t)$ is not altered very much by varying the form of $\phi_2(a)$. In fact, making the assumption of "random exit" (Fig. 10) gives an almost better fit to the few experimental points than the case of "first in-first out" (Fig. 9). We conclude that Patt and Maloney's data are barely sufficient to estimate the mean transit time (D = 27 hr), but not the standard deviation of such transit times around their mean.

REFERENCES

1. Patt, H. M. and M. A. Maloney. *The Kinetics of Cellular Proliferation*, Ed. F. Stohlman, Jr. Grune and Stratton, New York, 1959 pp. 201–207.
2. Trucco, E. *Bull. Math. Biophys.* **27**, 285–304 (1965).

THE "FALL" OF INTRACELLULAR PARTICLES ON A HORIZONTAL-AXIS CLINOSTAT*

Ernesto Trucco,† Sylvanus A. Tyler, Merlin H. Dipert, and Richard R. Dedolph

Newtonian kinetics are employed to define the motion of intracellular particles falling through a rotating, viscous fluid on a horizontal-axis clinostat. The influence of centrifugal, gravitational, and coriolis forces on the resultant motion are accessed and criteria for the nullification of gravitational displacement of particles in cytoplasm are examined. Results may be used

* Abstract of paper to be submitted to *The Bulletin of Mathematical Biophysics.*

† Deceased.

to study and predict the physiology of plant growth and development under conditions of "free fall."

Let (x,y) represent a fixed coordinate system with vertical y-axis and horizontal x-axis perpendicular to the axis of rotation, and (ξ,η) the coordinates of a rotating system with origin at the center of gravity of a particle. A gravitational force with components $[0,-mg]$ and a frictional force, F, in the fixed system act on the particle. From the equations of motion in the fixed system,

$$m\ddot{x} = F_x$$

$$m\ddot{y} = F_y - mg,$$

the motion relative to the (ξ,η)-system is found,

$$\xi(t) = x(t) \cos(\omega t) + y(t) \sin(\omega t)$$

$$\eta(t) = x(t) \sin(\omega t) + y(t) \cos(\omega t)$$

With appropriate initial conditions and assuming applicability of Stokes' Law, a computer algorithm is constructed and the trajectory in the (ξ,η)-plane is plotted for various controllable conditions consistent with the experimental operation of a clinostat.

Both a non-zero component of gravity and a translational drift are evident in the motion. Compensating counter motions are considered which minimize these resultant components of motion, i.e., minimize the gravity-induced displacement of particles in the cytoplasm.

THE DETERMINATION OF CELL-CYCLE PARAMETERS FROM MEASUREMENTS OF THE FRACTION OF LABELED MITOSES*

Peter J. Brockwell,† Ernesto Trucco,‡ and R. J. Michael Fry

In two previous papers[1, 2] a study was made of the theoretical form of the "fraction of labeled mitoses" function (FLM-function). It is assumed that the lifetime of a cell can be broken up into four phases with independently distributed durations; these phases are usually denoted by G_1, S, G_2 and M, where S represents DNA synthesis and M represents mitosis. For this mathematical model a theoretical expression was derived for the FLM-function in terms of the probability densities of the four phase durations and the expected number of recycling daughter cells per parent, designated A.

Assuming that the mitotic time and the value of A are known and that the durations of G_1, S and G_2 have gamma distributions, then the theoretical FLM-function is a function of the means and coefficients of variation of G_1, S and G_2. A computer code has been developed for estimating these 6 parameters from experimental data by minimizing a weighted sum of squares of deviations of experimental from theoretical FLM-values.

Experimental data for the hair follicle, corneal epithelium and Marshall tumors are analyzed and particular attention is paid to the difference in the fitted parameters when it is assumed (a) that $A = 1$ and (b) that $A = 2$. It is found that for a given set of data the estimates of the mean durations of DNA synthesis and the mean cycle time are slightly larger if it is assumed that $A = 2$ rather than $A = 1$. It does not seem possible however on the basis of FLM-data alone to obtain reliable estimates for either the value of A or the mean duration of mitosis.

* Abstract of paper submitted to the *Bulletin of Mathematical Biophysics*.

† Applied Mathematics Division.

‡ Deceased.

REFERENCES

1. Brockwell, P. J. and E. Trucco. *J. Theoret. Biol.* **26**, 149–179 (1970).
2. Trucco, E. and P. J. Brockwell. *J. Theoret. Biol.* **20**, 321–327 (1968).

A METHOD FOR THE MATHEMATICAL DEFINITION OF RHYTHMIC BIOLOGICAL RESPONSES*

Merlin H. Dipert, William Chorney, and Richard R. Dedolph

Data on flower induction in darkness by *Xanthium pennsylvanicum* suggested that the phenomenon displayed showed a circadian rhythm. A meaningful quantitative description of this periodic response was obtained by fitting the data to a two-dimensional damped harmonic model. The effect of an interacting treatment (interruption of the flower-inducing dark period at various times after its initiation) on the two-dimensional model was assessed and quantified by ex-

* Abstract of paper to be submitted to *Biometrics*.

tension of the two-dimensional model into a third dimension by fitting data from all curves to this more comprehensive system.

The methods provided not only enabled the quantitative definition of rhythmic responses and a quantitative description of the changes in this primary rhythmic response resulting from an interacting treatment, but also the means by which marked discontinuities in the resulting surface can be discerned and delineated.

BINOMIAL-SEQUENTIAL MODEL OF PHOTOREACTIVATION

*Sylvanus A. Tyler and David J. G. Davies**

PURPOSE AND METHODS

Bacteria repair some of the damage produced by UV irradiation. Part of the repair (in strains of interest here) is accomplished by photoreactivation—recovery induced by visible light (360 to 440 nm.). Michaelis-Menton kinetics are accepted generally as descriptive of this recovery process:[1, 2]

$$S + E \underset{k_2}{\overset{k_1}{\rightleftharpoons}} SE \xrightarrow{k_3} P + E,$$

where the enzyme molecule, E, complexes reversibly with the substrate, S, in a light-independent reaction which, in response to visible light, repairs the lesion, giving rise, in turn, to the repaired product, P, with the release of the enzyme molecule. The accumulated experimental evidence suggests that the substrate is the UV-induced *lesion*—a pyrimidine dimer. Pyrimidine dimers formed along the DNA molecule, are split, restoring the pyrimidine base to its original state. From *"in vitro"* studies,[3, 4] H. Harm and C. S. Rupert conclude that the reaction scheme obeys first-order kinetics. This implies that photoreactivable, UV-induced lesions are repaired at random. This conclusion is not supported by studies,[5] which show that sequential rather than a random repair of lesions is more compatible with data for *E. coli* WP2 hcr$^-$.

The Poisson-Sequential Model,[5] proposed previously by us, only permits postulation of a single enzyme molecule in the cell as active in the repair of UV lesions, and does not provide for the possibility that several enzyme molecules may operate in unison or in "sequential" order to effect repair. For this reason, the original model was modified and tested with data from different strains of bacteria known to vary greatly in UV sensitivity. The modification, called "the Binomial-Sequential Model" and the theoretical derivations by S. Tyler and M. Dipert are summarized in ANL-7635.[6] An interim report of the experiments is given here.

* School of Pharmacy, Bath University of Technology, Bath, England.

PROGRESS REPORT

E. coli, WP2 hcr$^-$, K12AB1886, and K12AB2480, were used in this study. Sensitivity of the first two strains is similar, and the number of pyrimidine dimers formed per lethal event presumably is also similar. K12AB2480 is about 40 times more sensitive, and the number of pyrimidine dimers per lethal event is 2 or 3, instead of 100, as in the other two strains. The experimental procedure is described in reference 5.

Preliminary experiments with each strain established the minimum photo-reactivating dose rate required for a constant rate of repair. This reaction rate, which is independent of the rate of photon absorption, is dependent only on the light-independent complexing process. Photoreactivation was at irradiances significantly above this level (4,000, 1,356, and 385.5 ergs mm^{-2} sec^{-1} for WP2 hcr$^-$, AB1886, and AB2480, respectively). Results and theoretical curves for AB1886 and AB2480, based on the Binomial-Sequential Model, are presented in Figures 11 and 12.

Minimum and maximum photoreactivation curves were fitted to the expression

$$S = 1 - (1 - e^{-kD})^n,$$

where S is the fraction of cells surviving a dose, D, and k and n are constants. Least squares estimate of k and the photoreactivable proportion of total damage (column 4) are shown in Table 11.

CONCLUSIONS

The following stem from this study.

1. Size of the photoreactivable sector is independent of dimers split.
2. Period of exposure to visible light for maximum photoreactivation is independent of dimers split.
3. Period of exposure is a function of the rate of movement of enzymes along the DNA molecule.
4. The Binomial-Sequential Model sets a low limit to the number of steps, N, required for maximum photoreactivation (column 6 of table). In contradiction, a large number of pyrimidine dimers are formed

in DNA in proportion to UV dose.[7] Thus, we are led to recognize that the *inactivating event* (lesion) and the *reactivating event* (repair) are separate and distinct entities in the photoreactivation process.

5. The number, N, represents the number of enzyme molecules present in the cell and active in the photorepair process. This process is illustrated in Figure 13.

A consequence of this interpretation is that the lim-

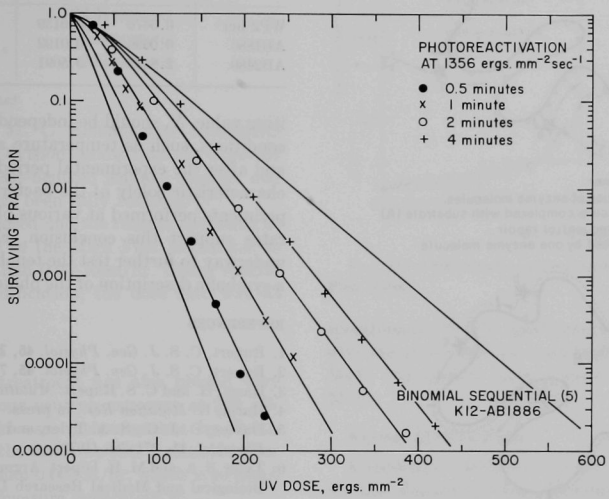

FIG. 11.—Survival of *E. coli* K12AB1886 after selected periods of photoreactivation.

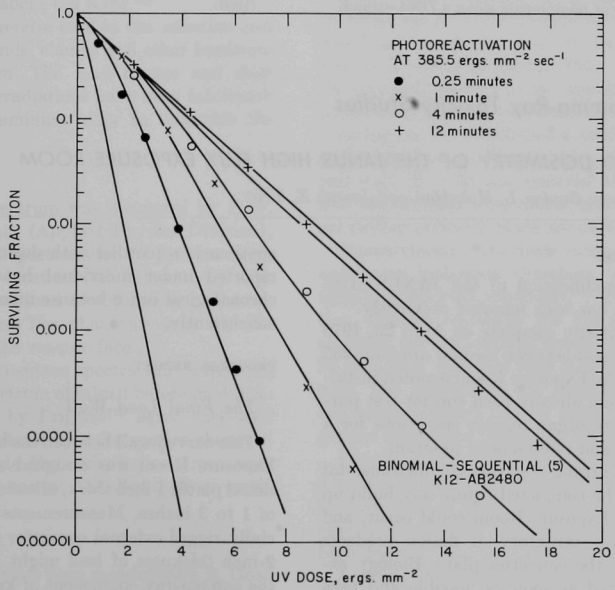

FIG. 12.—Survival of *E. coli* K12AB2480 after selected periods of photoreactivation.

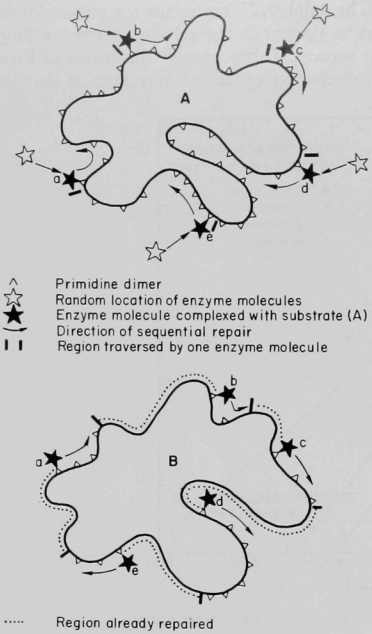

FIG. 13.—Conception of photorepair along a DNA strand.

TABLE 11. PHOTOREACTIVATION CONSTANTS

E. coli strain	*k* min., (ergs. mm^{-2})$^{-1}$	*k* max., (ergs. mm^{-2})$^{-1}$	$\frac{(k \text{ min.} - k \text{ max.})}{k \text{ min.}}$	Time to max. photoreactivation, min	*N*
WP2 her$^-$	0.0470	0.0139	0.70	8	11
AB1886	0.0596	0.0192	0.68	12	5
AB2480	2.8437	0.5091	0.82	12	5

iting value, *N*, should be independent of environmental conditions, such as temperature and dose rate, during and after the experimental period; and, therefore, is a characteristic solely of the bacterial strain. Recent experiments performed at various photoreactivating dose rates support this conclusion. Experiments are now underway to further test the tenability of this model as a symbolic description of the photoreactivation process.

REFERENCES

1. Rupert, C. S. *J. Gen. Physiol.* **45,** 703–724 (1962).
2. Rupert, C. S. *J. Gen. Physiol.* **45,** 725–741 (1962).
3. Harm, H. and C. S. Rupert. *Mutation Res.* **6,** 355–370 (1968).
4. Harm, H. *Mutation Res.*, in press.
5. Davies, D. J. G., S. A. Tyler, and R. B. Webb. *Photochem. Photobiol.* **11,** 371–386 (1970).
6. Tyler, S. A. and M. H. Dipert. Argonne National Laboratory Biological and Medical Research Division Annual Report, 1969. ANL-7635, pp. 86–88.
7. Swenson, P. A. and R. B. Setlow. *J. Mol. Biol.* **15,** 201–219 (1966).

Neutron and Gamma-Ray Toxicity Studies

COMPLETION AND DOSIMETRY OF THE JANUS HIGH FLUX EXPOSURE ROOM

Frank S. Williamson, Gordon L. Holmblad and Joseph E. Trier

PURPOSE AND METHODS

Progress in the modification of the JANUS High Flux Exposure room has been reported previously.[1-3] This work was essentially complete on April 23, 1970 when the final lead shield between the new uranium-235 converter plate and the Exposure Room awaited installation. The reactor had already been run for test purposes and on this date began regular operations for a combined dosimetry and radiobiology program.

This program was arranged so that the instrumental spectrometry would be completed before any build up of activation in the Exposure Room could occur, and before any significant inventory of fission products could accumulate in the converter plate. Biology experiments were started as soon as possible and then continued in parallel with dosimetry. Results will be reported under individual headings rather than in chronological order because many activities proceeded concurrently.

PROGRESS REPORT

The Final Lead Wall

This curved wall between the converter plate and the Exposure Room was designed and fabricated in sectional plates 1 inch thick, allowing optional thicknesses of 1 to 3 inches. Measurements in 1966, using a specially-rigged external converter plate, indicated that a 2-inch thickness of lead might be sufficient to reduce the gamma-ray component of kerma to about 3.9 per-

cent of the neutron kerma rate; consequently this option was chosen.[1]

As each of the two layers was added, gamma-to-neutron kerma-rate ratios were measured as follows:

no lead	22.7 percent
1 inch	5.8 percent
2 inches	2.6 percent

Shutter Effectiveness

Measurements by M. C. Schumacher (Industrial Hygiene and Safety Division) show that the expected improvement in the fast-neutron leakage through and around the shutters has been fully realized.[4]

With the shutters closed and the reactor operating at 200 kW the dose rate in the High Flux Room due to fast neutrons is less than 0.05 Rem/hr. Under similar conditions before modification, the dose rate was 33 Rem/hr.[5]

Neutron Activation

The unusual wall treatment has also proved very effective. After a 1-hour neutron exposure at 200 kW with the converter in use, measurements by Schumacher indicate that the exposure rate 2 minutes after reactor scram is less than 0.003 R/hr, which is so small that it is difficult to measure accurately.[4]

Prior to modification, the corresponding exposure rate would have been about 0.6 R/hr.[5]

It is necessary to exercise care in the selection and use of material for stands, clamps and other hardware in the Exposure Room. The load frames and shelf units used for mouse irradiations have been fabricated from a magnesium-aluminum alloy to minimize the activation problem.

Neutron Spectrum

The fast-neutron spectrum was measured by E. F. Bennett and T. J. Yule (Applied Physics Division), using a proton-recoil spectrometer.[6] Spectra were taken at the reference location (see below) both with and without a simulated load of 456 mouse phantoms in polyethylene cartons. The phantoms were distributed in an arc across the reactor face.

Figure 14 shows the neutron spectra thus measured, with a replot of the spectrum obtained before modification.[1] Measurements by Frigerio[7] agree very well with these data and indicate that the spectra shown in Figure 14 underestimate the contribution from neutrons above 1.5 MeV in energy. Detailed findings await further data reduction.

Gamma Spectra

Gamma-ray spectra have been measured by R. Gold (Applied Physics Division) using a Compton-recoil

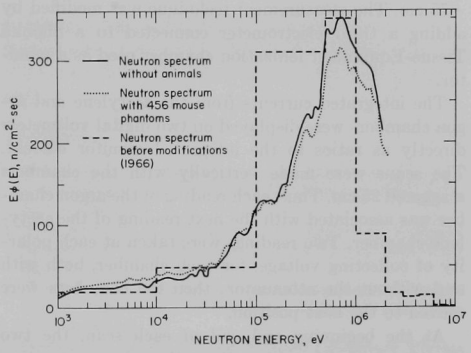

FIG. 14.—Preliminary neutron spectra in the JANUS High Flux Room.

spectrometer.[8] The spectrometer gives fine detail but with the small detector used tends to cut off above 2.2 MeV. The spectra show a large contribution above 2 MeV.

Kerma Distributions

A cartesian-coordinate system has been established for the Exposure Room. Because the reactor face is curved, the opposing wall was chosen as the base plane. The line which is normal to the reactor face at its center forms the Z-axis and intersects the wall at (0, 0, 0). The Y-axis is vertical, with the floor at $Y = -96$ cm., and the X-axis is horizontal. Thus a person standing at the rear wall, looking at the reactor face, sees the face as he would a graph with vertical Y and horizontal X.

Initial studies established a small volume for the irradiation of up to 20 mice, in a plane parallel to the real wall ($Z = 0$) and centered at $X = -3$, $Y = 0$, $Z = 100$ cm. Like most rooms, this one has walls which are neither perfectly plane nor orthogonal.

Measurements were made using a pair of acetylene and argon ionization chambers, with an integrating technique reported previously.[9] At the reference location, with the reactor at 200 kW and without the attenuator, the fast-neutron kerma rate is approximately 23 rads/min, with less than 3 percent gamma component. The addition of 456 phantom mice reduces the fast-neutron kerma rate by about 2 percent, while the gamma component maintains the same ratio.

For the *in vitro* cell exposures reported by Sinclair, a variety of locations were used and individually measured. Several of these locations were chosen to be as close as practicable to locations at which spectra had been taken.

A scan of the room was made at 50-cm intervals in X and Z, and 25-cm intervals in Y from -75 cm to

+75 cm. The measurement technique was modified by adding a third electrometer connected to a Shonka Tissue-Equivalent ionization chamber used as a monitor.

The integrated currents from the acetylene and argon chambers were displayed on two digital voltmeters directly as ratios to the integrated monitor current. The scans were made vertically with the chambers staggered 25 cm. Thus, each reading of the argon chamber was associated with the next reading of the acetylene chamber. Two readings were taken at each polarity of collecting voltage, for each chamber, both with and without the attenuator; then the chambers were moved to the next position.

At the beginning and end of each scan, the two chambers were placed in a jig at the reference location ($X = 0$, $Y = 0$, $Z = 100$) and measurements were taken. In this way, data were obtained for 275 locations. An interactive computer terminal adjacent to the JANUS Biology Control Console was used to enter the instrument readings and compute the kerma ratios as percentages of kerma at the reference location, at the same time, storing these data in the IBM 360/50-75 System in the ANL Computing Center.

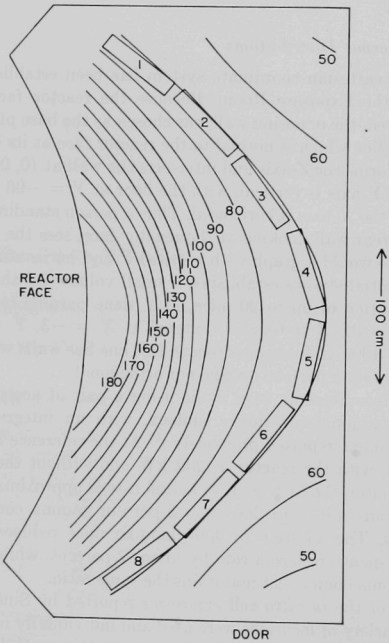

FIG. 15.—Plan view of the JANUS High Flux Room showing isodose contours expressed as percentages of kerma at location ($X = 0$, $Y = 0$, $Z = 100$ cm), with the graded attenuator in use. A trial layout of 8 load frames (400 mice) is shown as computer-fitted to the 70% isodose contour.

A series of computer programs has been developed and used on the 360/75 in addition to those used interactively.

Program 1 processes the observational data, again, taking the appropriate pair of reference measurements for each scan, and stores the data for the room in binary form. It is intended that an audit trail of dosimetry data shall be established, leading from these instrument readings to the final animal absorbed doses, so that refinements, such as recalculation of chamber characteristics in the light of later spectral data, can be reprocessed with trivial effort. Furthermore, when measurements are made with phantoms and depth doses determined, these data can be introduced at an appropriate level for reprocessing to yield the absorbed doses to the experimental animals.

Irradiation Planning

Mice are irradiated in 1-pint polyethylene cartons, snapped into a shelf holding 5 cartons (there are 5 mice to a cage). These shelves fit into a loading frame with a capacity of up to 12 shelves. The frames hang from light aluminum supports fastened to the ceiling of the Exposure Room.

Advanced planning aids are needed to assist in deciding optimum room loadings for various experiments. The second and third computer programs in our series develop isodose contour plots of the room in sets of parallel planes, either Y- or X-planes. Program 2 produces output directly on 35-mm film for 2- × 2-inch slides, and Program 3 produces Calcomp output.

Program 4 uses the same stored data base and calculates the neutron and gamma kerma ratios (as a percentage of that at the reference location) for each mouse in a load frame at a specified room location and angle to the X-axis. This information is printed in a detailed table and also stored on a direct-access storage device as a further step in the audit trail. A range of shelf positions which are to be used may be specified, and then the average kerma ratio is calculated over this range of shelves and the individual deviations from average are printed in the table.

The program also allows automatic planning. If desired, it will slew the frame so that its right and left halves receive the same average kerma ratio, and then position the frame so that the overall average lies on a specified isodose contour. A further option allows a number of frames to be laid out automatically with a suitable separation between the frame edges to facilitate handling.

A typical trial layout of 8 frames takes about 1.2 minutes of computer time at a cost of less than 4 dollars. Programs 2 and 3 can use the data stored by Program 4 to draw the frame layouts on an isodose contour plot.

CONCLUSIONS

Figure 15 shows a possible layout with isodose contours obtained in this way for the plane $Y = +2.6$, corresponding to the height of mice in shelf number 6. The contours are in percentages of kerma at the reference location with the attenuator in use.

The attenuator has the effect of pushing the ends of the contour lines away from the reactor face. In the Y-planes (plan view, as in Fig. 15) no greater effect could be tolerated or it would reduce the number of frames which could be exposed at one time at the same kerma rate. Greater flattening in the vertical direction would be desirable, but this would be difficult to achieve even with a uniform flux across the converter plate.

The loading layout shown, using 10 shelves per frame, has a worst-case deviation from average of -9.7 percent in the top and bottom shelves of frames 1 and 8, for the individual animal locations closest to the reactor face (1 percent of the animal loading). The use of only 8 shelves per frame greatly improves this situation.

REFERENCES

1. Williamson, F. S. Argonne National Laboratory Biological and Medical Research Division Annual Report, 1966. ANL-7278, pp. 63–69.
2. Williamson, F. S. Argonne National Laboratory Biological and Medical Research Division Annual Report, 1968. ANL-7535, p. 130.
3. Williamson, F. S. Argonne National Laboratory Biological and Medical Research Division Annual Report, 1969. ANL-7635, pp. 89–90.
4. Schumacher, M. C., Argonne National Laboratory. Private communication.
5. Williamson, F. S. and M. C. Schumacher. Argonne National Laboratory Biological and Medical Research Division Annual Report, 1965. ANL-7136, pp. 5–6.
6. Bennett, E. F. and T. J. Yule. To be published.
7. Frigerio, N. A., Argonne National Laboratory. Private communication.
8. Gold, R. *Nucl. Instr. Methods* **84**, 173–194 (1970).
9. Williamson, F. S., L. B. Hubbard, and D. L. Jordan. Argonne National Laboratory Biological and Medical Research Division Annual Report, 1968. ANL-7535, pp. 153–156.

THE EFFECT OF FISSION NEUTRONS FROM THE JANUS REACTOR UPON CHINESE HAMSTER CELLS IN CULTURE

Warren K. Sinclair

PURPOSE AND METHODS

The several aims of these studies include (1) the use of the highly quantitative assay method of colony formation in cultured cells as a measure of lethal damage to describe certain features of the dosimetry at various locations in the exposure region, including the potential effects of spectrum variations and dose rate changes; (2) the response of Chinese hamster cells to JANUS neutrons may be used to describe the nature of the JANUS fission neutron spectrum, compared with X and γ rays, or compared with the past premodification JANUS spectrum, etc. These responses include the parameters of the asynchronous survival curve, the variation in response throughout the cell cycle, and recovery from sublethal damage, as determined by the two-dose method. This information may enable some predictions to be made concerning whole animal responses; (3) JANUS neutrons may provide a suitable source of high LET radiation for radiobiological investigations in cultured cells.

The method is to irradiate single asynchronous or synchronous Chinese hamster cells in culture dishes at different dose levels, in different locations, or circumstances in the exposure room and determine survival curves by scoring colony formation after 10 days of incubation. X rays, 250 kVp HVL 0.9 mm Cu, ~150 rads/min are used as a standard of comparison.

PROGRESS REPORT

Asynchronous cell survival at various room locations. Survival was measured over 3 decades at five room locations identified as P(23 rads/min), Q(44 rads/min), R(16 rads/min), S(12.5 rads/min), and T(12 rads/min), with the results shown in Figure 16. All the survival curves have about the same shoulder or extrapolation number, ~1.7 to 1.8, but P and Q have a D_0 of 92 rads and S and T ~87 rads, while R is intermediate. The difference is not large but the curves are distinct. If there were any dose rate effect S and T might be expected to be less, not more, effective than P and Q. Since S and T are near the walls, at the side, there is the possibility of a spectrum change producing a small effect. [Note: These data (May 1970) agree well but not exactly with the effects of JANUS neutrons on Chi-

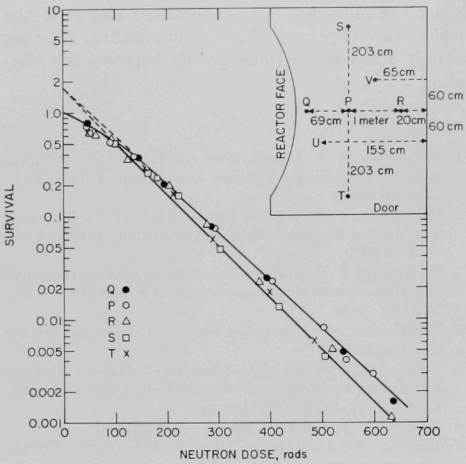

FIG. 16.—Survival of Chinese hamster cells (as measured by colony formation) after exposure to JANUS neutrons at different exposure room locations.

Location	Coordinates	Dose rate, rad/min	Symbol	Survival, n	Curve, D_0
P	0, 0, 100	23	○	1.75	92
Q	0, 0, 169	44	●	1.75	92
R	0, 0, 20	16	△	1.75	87–92
S	203, 0, 100	12.5	□	1.75	87
T	−203, 0, 100	12	×	1.75	87
U	−60, 0, 155	35.5	—	—	—
V	60, 0, 65	16.8	—	—	—

nese hamster cells before modification of the exposure room (March 1966), for which $n \sim 2$ to 3, D_0 82 rads was found. The subline used at that time, V79-285B, had X-ray survival parameters exhibiting a larger shoulder and lower D_0 ($n \sim 8$ to 10, D_0 190 to 200 rads for synchronous S cells[1]) than the present subline V79-S171 ($n \sim 3$ to 4, $D_0 \sim 230$ rads for synchronous S cells[2]), and thus the small difference here may be due only to the change in sublines and not to the spectrum or dosimetry.]

Because the parameters of the survival curves in Figure 16 differ from those for X rays taken in the same population on the same day, the Relative Biological Effectiveness (RBE) is a function of dose, as shown in Figure 17. At high doses the RBE is ~2.4.

The effects of dose rate and spectrum were investigated by obtaining survival data at P and at S at two power levels, full (200 kW) and half (100 kW) power. The dose rate at P was ~23 and ~11.5 rads/min respectively, and at S ~12.5 and ~6.25 rads/min. The results are shown in Figure 18.

The differences between the two sets of data at position P on the one hand and position S on the other are within the various experimental errors involved. Thus, there would appear to be no significant dose rate effect between ~6 rads/min and 44 rads/min (position Q in Figure 16). The difference between position P, half power, and position S, half or full power (i.e. at the

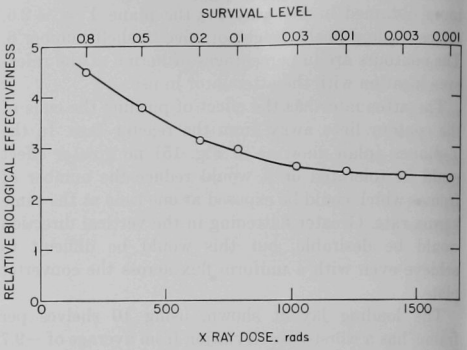

FIG. 17.—RBE of JANUS neutrons (at location P and Q) versus 250 kVp X rays for Chinese hamster cells as a function of X ray dose [determined for same population on same day].

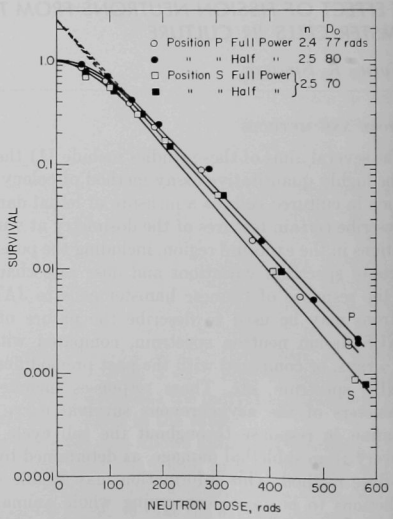

FIG. 18.—Survival of asynchronous Chinese hamster cells at positions P and S (as indicated in Figure 16) at full and half power. At position P, the parameters of the survival curves are: full power $n \sim 2.4$, $D_0 \sim 77$ rads; half power $n \sim 2.5$, $D_0 \sim 70$ rads.

same dose rate) is about 10 rads (70 to 80 rads) in D_0. This probably is significant although note that some of the experimental points on Figure 18 differ by only small amounts. Computer analysis[3] of the data indicates that the two curves at P are well within one standard error of each other in both "n" and "D_0," and likewise for the two curves at S. However, the curves at P and at S differ in D_0 by almost two standard errors. Thus, there may be a change between P and S. We know from the spectral studies that these spectrum changes exist and apparently are reflected in the response of Chinese hamster cells. The difference in spectrum is small, however, and may not have much effect on the response of mice.

Synchronous cells: Cell cycle variation and recovery. The results of an experiment in which cells synchronized by mitotic selection were exposed as a function of time (after synchronization) during the first generation cycle at different room locations are shown in Figure 19. The different room locations were chosen at appropriate dose rates so that 10-min exposures at all points yielded a range of neutron doses.

The results show, first, that the exposure to JANUS neutrons varies through the cell cycle, but to a lesser extent than for 250 kVp X rays at about the same survival level [cf. peak/trough ratio for curve P ~2.3 and for X (710 rads) ~4.2].

Second, from the limited survival data available in the experiment of Figure 19, it appears that the parameters of the survival curve for late S cells [n ~1.3, D_0 ~102 rads] differ from those of G_1 cells [n ~1.3, D_0 ~72 rads] mainly in the slope rather than the shoulder. However, more extensive data are needed on this point. These compare with published values for X rays for this subline of n ~3.3, D_0 230 rads for late S cells and n ~1.9, D_0 ~160 rads for G_1 cells.[2] Thus, shoulders are clearly smaller for JANUS neutrons than for X rays at all stages of the cell cycle.

Third, recovery was examined in a single "two-dose" experiment using late S cells, shown in Figure 19, in which the survival of cells exposed to ~235 rads followed by an interval t of time, and then a second 235 rads was compared with that of cells given ~470 rads. It is evident that survival is greater as t increases between fractions, indicating recovery from sublethal damage. The magnitude of recovery is difficult to assess because of the cellular multiplicity changes, but this experiment is consistent with full recovery of the shoulder by about the time of division (~12+ hours after synchronization). Further investigation is required before full quantitative details can be supplied.

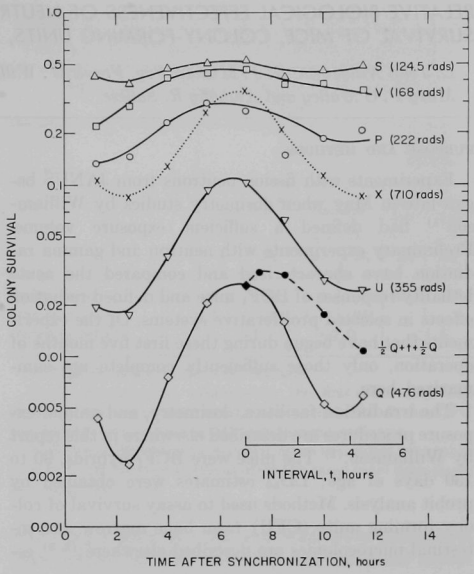

FIG. 19.—Survival of synchronous Chinese hamster cells after different JANUS neutron doses at different times during the cell cycle. Data for one X ray dose (710 rads) are included also. Curve $\frac{1}{2}Q + t + \frac{1}{2}Q$, is for a two dose experiment in which the dose was given in two equal halves separated by various intervals of time, t. (Note P, Q, R, U, V, are the points identified in Figure 16, insert.)

REFERENCES

1. Sinclair, W. K. and R. A. Morton. *Radiat. Res.* **29,** 450 (1966).
2. Sinclair, W. K. *Radiat. Res.* **39,** 135 (1969).
3. Tyler, S. A. and M. H. Dipert. *Physics in Medicine and Biology* **7,** 201 (1962).

RELATIVE BIOLOGICAL EFFECTIVENESS OF NEUTRONS FROM THE JANUS REACTOR: SURVIVAL OF MICE, COLONY-FORMING UNITS, AND INTESTINAL MICROCOLONIES

E. John Ainsworth, R. J. Michael Fry, Frank W. Williamson, Donn L. Jordan, Mary P. O'Malley and Anthony R. Sallese

PURPOSE AND METHODS

Experiments with fission neutrons from JANUS began late in May when dosimetry studies by Williamson[1] had defined a sufficient exposure volume. Preliminary experiments with neutron and gamma radiation have characterized and compared the acute lethality responses of BCF_1 mice and defined radiation effects in selected proliferative systems. Of the experiments that have begun during these first five months of operation, only those sufficiently complete are summarized here.

The irradiation facilities, dosimetry, and animal exposure procedures are described elsewhere in this report by Williamson.[1] The mice were BCF_1 hybrids, 90 to 130 days of age; LD_{50} estimates were obtained by probit analysis. Methods used to assay survival of colony-forming units (CFU) from bone marrow and intestinal microcolonies are described elsewhere;[2, 3] estimates of D_0, the reciprocal of the slope on the exponential portion of the survival curve and n, the extrapolation number, were obtained by routine methods.

PROGRESS REPORT

The $LD_{50/30}$'s determined for gamma- or neutron-irradiated mice before and after modification of the JANUS High Flux Room are shown in Table 12. These results show: (1) no effect of sex on $LD_{50/30}$; (2) a significant increase in neutron $LD_{50/30}$ for both sexes after modification; and (3) no significant change in the gamma $LD_{50/30}$ between 1968 and 1970. The Relative Biological Effectiveness (RBE) of the neutrons decreased from 2.5 to 2.2 after modification. The change in RBE is underestimated by these values, because no adjustment has been made for the decreased gamma contribution to total dose after modification. The decrease in RBE after modification of the High

TABLE 12. $LD_{50/30}$ AND $LD_{50/6}$ IN NEUTRON- AND GAMMA-IRRADIATED BCF_1 MICE. A COMPARISON OF RBE OF NEUTRONS BEFORE AND AFTER MODIFICATION OF THE JANUS HIGH FLUX ROOM

	Males		Females	
	Neutron	Gamma	Neutron	Gamma
Before modification				
$LD_{50/30}$, rads	386	959	387	959
(range)	(374–398)[a]	(943–974)	(373–401)	(926–992)
No. animals	401	213	288	120
No. dose-levels	7	7	6	5
Slope[b] of dose-response curve	0.027 ± 0.004	0.018 ± 0.003	0.031 ± 0.005	0.012 ± 0.001
RBE	2.48		2.48	
After modification				
$LD_{50/30}$, rads	459	969	443	976
(range)	(451–467)	(949–980)	(427–459)	(959–994)
No. animals	160	283	155	298
No. dose levels	9	19	9	20
Slope of dose-response curve	0.033 ± 0.004	0.012 ± 0.002	0.029 ± 0.007	0.014 ± 0.002
RBE	2.11		2.20	
$LD_{50/6}$, rads	656	1557	571	1416
(range)	(612–701)	(1407–1705)	(458–685)	(1244–1588)
No. animals	100	164	60	165
No. dose levels	5	11	3	11
Slope of dose-response curve	0.02 ± 0.005	0.005 ± 0.002	0.02 ± .004	0.005 ± 0.002
RBE	2.37		2.48	

[a] 95% confidence limit of the $LD_{50/30}$.

[b] Coordinates are probit of mortality and radiation dose in rads.

Flux Room could be related to hardening of the neutron spectrum.[1] Neutron energy is known to influence $LD_{50/30}$.[4, 5]

The $LD_{50/5}$, a time endpoint for assessment of intestinal damage, may also have shifted after modification. Although a determination of the $LD_{50/5}$ for neutrons was not completed before modification, 475 rads, a dose approximately 90 rads above the $LD_{50/30}$, produced 85% death within 5 days in the 1968 experiments. In the 1970 experiments, 562 rads, a dose approximately 110 rads higher than the $LD_{50/30}$, produced only 8% mortality within 5 days. Even doses of 888 to 891 neutron rads produced only 13% mortality in 1970. Because the highest dose of neutrons explored to date, 2000 rads, has not produced a significant number of 5-day deaths, the present preliminary estimates of RBE for intestinal damage are based on a 6-day endpoint. The $LD_{50/6}$ estimates in Table 12 yield RBE's of 2.4 or 2.5.

Survival results on proliferative cells, bone marrow CFU and intestinal microcolonies are summarized in Table 13. The RBE values based on a single exposure to neutron or gamma radiation are approximately 2.2 and 2.0 for CFU and intestinal microcolonies, respectively (the estimate of D_0 for the microcolonies exposed to gamma irradiation was obtained by Dr. R. Withers).

Initial studies of cellular repair of radiation injury involve only a 6-hr fractionation interval (Table 13). No significant fractionation effect that indicated repair was detected for CFU or intestinal microcolonies after neutron irradiation. After gamma irradiation the survival ratio was 2.0 for CFU, indicating repair, and even a higher survival ratio for microcolonies has been obtained by Dr. R. Withers on BCF_1 mice from ANL.

TABLE 13. ESTIMATES OF EXTRAPOLATION NUMBER (n) AND/OR D_0 FOR MARROW CFU AND INTESTINAL MICROCOLONIES AFTER SINGLE OR FRACTIONATED EXPOSURE TO NEUTRON OR GAMMA RADIATION. DOSES EXPRESSED IN RADS

	CFU				Microcolonies	
	Neutron		Gamma		Neutron	Gamma
	n	D_0	n	D_0	D_0	D_0
Single dose	1.0	36	1.4	78	55	107[a]
6-hr fraction[b]	1.1	34	1.7	84		
Survival ratio[c]	~1.0		~2.0		<1.5	

[a] This D_0 estimate from R. Withers.

[b] In fractionation experiments the first dose (D_1) was constant, the second dose at 6 hr was varied. The D_1 for CFU was 50 rads of neutrons or 145 rads gamma radiation.

[c] Ratio of the percent survival after two doses separated by 6 hr to the percent survival after the same total dose given to a single exposure.

CONCLUSIONS

Modification of the JANUS High Flux Room resulted in a shift in the neutron spectrum which decreased the neutron RBE from ~2.5 to ~2.2 based on $LD_{50/30}$. After modification, the RBE for $LD_{50/6}$ is ~2.5, and RBE's of ~2.2 and ~2.0 were determined from survival studies with CFU and intestinal microcolonies, respectively. No significant cellular repair of neutron radiation injury was detected at 6 hr in CFU and intestinal microcolonies.

REFERENCES

1. Williamson, F. S.,G. L. Holmblad, and J. E. Trier. This report.
2. Ainsworth, E. J., R. M. Larsen *Radiat. Res.* **40**, 149–176 (1969).
3. Withers, H. R. and M.M. Elkind. *Int. J. Radiat. Biol.* **17**, 261–267 (1970).
4. Frigerio, N. A. and D. L. Jordan. *Biological Effects of Neutron and Proton Irradiations;* IAEA, Vienna, 1964, Vol. I, pp. 117–128.
5. Ainsworth, E. J., R. M. Larsen, K. Kendall, G. F. Leong, J. S. Krebs and F. A. Mitchell. *Proc. Symposium on Neutrons in Radiobiology.* USAEC Report CONF-691106 (1969), pp. 435–450.

STRAIN DIFFERENCES OF GUT AND BONE MARROW AND THEIR RELATION TO RADIOSENSITIVITY

R. J. Michael Fry, Walter E. Kisieleski, E. John Ainsworth, and Anthony R. Sallese

PURPOSE AND METHODS

Strain differences in response to irradiation are not understood completely.[1] For example, it is not clear why BALB/c mice (one of the parent strains of the BCF_1) has a lower $LD_{50/6}$ than BCF_1 mice. Theoretically, the sensitivity for gut death after irradiation should be related to the number of crypt clonogenic cells. As previous observations we made apparently were not consistent with a direct relationship of $LD_{50/6}$ and the estimated number of crypt proliferative cells, we have begun an investigation into the factors determining strain differences in radiosensitivity.

TABLE 14. QUANTITATION OF PROLIFERATIVE CELL POPULATIONS

Strain	Sex	Labeled cells/crypt Mean ± S D	Mitoses/ crypt Mean	dpm/crypt Mean ± SD	Crypts/ section Mean ± SD	Villi/ section Mean	dpm/ section Mean	dpm/cell
BALB/c	♂	90 ± 7.0	4.4	4.93 ± 0.6	102 ± 10	45.0	120.0	0.055
BALB/c	♀	85.0 ± 5.0	5.1	4.08 ± 0.4	98.0 ± 7.0	39.0	110.0	0.048
C57BL/6	♂	71.0 ± 11.0	4.0	3.64 ± 0.7	79.0 ± 6.0	38.0	94.0	0.051
C57L	♂	121.0 ± 10.0	9.9	6.0 ± 1.1	84.0 ± 5	40.0	110.0	0.050
BCF_1	♂	55.4	3.9		89.0	41.0		

This report is concerned with the parent strains of the BCF_1 (the strain selected for the neutron-gamma toxicity experiments) namely, BALB/c and C57BL/6, some data for BCF_1 and C57L. The number of labeled nuclei, the dpm/crypt and dpm/section one hour after injection of ^{3}HTdR (0.5 μCi/g S.A. 0.36 Ci/mM) were determined as were mitoses per crypt and crypts and villi per circumference. The same region of the jejunun has been sampled in each case.

PROGRESS REPORT

The results are shown in Table 14. It can be seen that the numbers of labeled nuclei per crypt is strain dependent. As there is little strain difference in the cell cycle durations, the number of labeled nuclei per crypt reflects the strain differences in the number of cells in cycle. The differences in dpm/crypt and mitoses per crypt substantiate these findings. It is of interest to note that there were fewer proliferative cells per crypt in BCF_1 than in either of the parent strains. The differences in the number of crypts per circumference is not as great. If the product of the number of crypts per circumference and the number of labeled cells is used for comparison purposes the number of labeled cells per circumference in C57L is about twice that in BCF_1. The $LD_{50/6}$ is not concomitantly higher.

CONCLUSIONS

It is clear even at this stage of the investigation, that a number of unresolved factors are of importance in the strain differences in the radiosensitivity of the gut. Further studies both on the gut, (e.g., transit times), and on the marrow, (e.g., estimates of CFU's), should elucidate underlying factors involved in differences in radiosensitivity.

REFERENCE

1. Yuhas, J. M. and J. B. Storer. *Radiat. Res.* **39**, 608–622 (1969).

PROPERTIES OF COLONY-FORMING UNITS—STUDIES IN PROGRESS

E. John Ainsworth and Mary P. O'Malley

PURPOSE AND METHODS

Colony-forming units (CFU) or colony-forming cells (CFC) exhibit pluripotent properties attributed to the hematopoietic stem cell.[1, 2] CFU have been used extensively as a model system in radiobiology and experimental hematology.[3-5] Sensitivity of CFU to neutrons from JANUS and preliminary hematology studies, relating to CFU, are described elsewhere.[6, 7] Induced proliferation of CFU is one way to quantitate the adaptive potential of hematopoietic stem cells in mice exposed to protracted neutron or gamma radiation and also in aged controls. Responsiveness of the stem cell compartment to protracted irradiation may be a sensitive indicator of injury. Pursuant to future studies of CFU proliferation, baseline experiments were conducted to determine the reproducibility of femur CFU content. Different marrow isolation procedures are compared to establish their effect on estimates of CFU content in reference to their radiation sensitivity.

Procedures used in CFU studies are described elsewhere.[4] CFU were obtained by two methods: (1) by aspirating marrow by flushing Hanks solution through the femur; or (2) by grinding the femurs in Hanks solution in a mortar and pestle, after which bone fragments are removed from marrow by filtration.[4] Marrow diluted with Hanks solution is injected intravenously into supralethally irradiated recipients (1068 rads ^{60}Co γ or 873 rads 250 kVp X rays), and spleen colonies (0.5 mm or larger) were counted after 8 days' growth in recipients. Mice used were BCF_1 100 to 140 days old; marrow from male donors was injected into female recipients.

TABLE 15. EXPERIMENTS COMPARING THE YIELD OF NUCLEATED CELLS AND COLONY-FORMING UNITS AFTER ASPIRATION OF MARROW AND AFTER GRINDING FEMURS. MARROW FROM 10–16 FEMURS WAS POOLED AND INJECTED INTO 25 to 40 RECIPIENTS

Aspirated marrow			Ground femur		
Nucleated cells/femur × 10^7	CFU/femur	CFU/10^5 N.C.[a]	Nucleated cells/femur × 10^7	CFU/femur	CFU/10^5 N.C.
3.3 (2.8–3.8)[b]	6346 (5293–7399)	19.3 (16.1–22.4)	4.4 (3.3–5.6)	9139 (7852–10,426)	20.3 (17.4–23.2)
3.0 (2.0–4.0)	7148 (6131–8166)	24.0 (20.6–27.4)	4.3 (4.0–4.6)	7132 (5990–8273)	16.6 (14.0–19.3)
2.3 (1.5–3.0)	7276 (6259–8293)	31.9 (27.5–36.4)	4.6 (4.0–5.2)	9478 (8488–10,468)	20.6 (18.4–22.7)
2.9 (1.7–4.1)	6194 (4979–7410)	21.4 (17.2–26.0)	4.6	7795 (6450–9141)	17.1 (14.2–20.1)
			3.9 (2.2–5.7)	6782 (5859–7707)	17.2 (14.9–19.5)
			4.4 (4.2–4.5)	8143 (6567–9718)	18.7 (15.1–22.3)
			4.5	7619 (6564–8674)	17.0 (14.7–19.4)
Pooled values[c]					
2.9 (2.6–3.2)	6805 (6286–7324)	24.6 (22.5–26.7)	4.5 (4.3–4.7)	7980 (7565–8394)	18.0 (17.1–18.9)

[a] Nucleated cells.
[b] 95% confidence limits.
[c] Pooled values based on nodule counts in 100 and 171 spleens, respectively, for aspiration and grinding of marrow.

TABLE 16. CFU IN ASPIRATED MARROW, IN ASPIRATED MARROW AFTER GRINDING WITH BONE FRAGMENTS AND THE RESIDUAL POPULATION IN BONE AFTER MARROW EXPRESSION IN TWO EXPERIMENTS

	Nucleated cells × 10^7		CFU/10^5		CFU/femur	
Aspirated	2.9	2.9	20.6 (18.5–22.6)[a]	23.5 (20.5–26.5)	5972 (5378–6566)	7056 (6141–7970)
Aspirated ground	3.4	3.2	15.4 (12.5–18.2)	19.0 (15.3–22.6)	5222 (4253–6129)	6063 (4896–7229)
Residual in femur	1.9	2.3	14.3 (11.3–17.3)	16.4 (13.1–19.6)	1395 (1005–1685)	1883 (1507–2260)

[a] 95% confidence limits.

PROGRESS REPORT

CFU and nucleated cell counts in the femur after marrow had been aspirated or femurs were ground and filtered are summarized in Table 15. In an experiment, in which aspirated marrow was used, the ratio of CFU/10^5 nucleated cells was 50% higher, 30/10^5, than in other groups receiving the same treatment. Significant variability in CFU/femur also was noted within groups treated with marrow obtained from femurs that were ground. Time of vaccination against ectromelia before marrow was obtained may explain this variability; mice vaccinated within 30 days before the experiment had a significant increase in CFU/10^5 nucleated cells. Vaccination of young mice had been temporarily suspended owing to other exigencies; when vaccination was reinstituted, mice approaching experimental age were innoculated with vaccinia virus. This variable has been eliminated, but complicates these comparisons. Based on pooled results, marrow obtained by grinding increases the yield of both nucleated cells and CFU/femur, although not proportionately. Results of an experiment (Table 16), in which an aliquot of marrow was aspirated from the femur, show a significantly lower ratio of CFU/10^5 nucleated cells after they were ground with bone fragments. These data show the magnitude of the residual CFU population after marrow has been aspirated from the femur. Important hematopoietic and osteoblastic roles attributed to mesenchymal cells in the interstices of bone[8] indicate that the properties of residual CFU should be investigated. Although the way marrow is harvested affects both the number and ratio of CFU, radiation sensitivity of CFU in marrow obtained by grinding the femur does not differ significantly from CFU in marrow obtained by aspiration (Table 17) which is not surprising, because the CFU assay procedure is based on proliferation and differentiation, processes that are seldom accomplished by traumatized cells.

TABLE 17. ESTIMATES OF D_0 AND n FOR CFU HARVESTED BY ASPIRATION AND BY GRINDING. DOSES IN RADS OF ^{60}Co GAMMA RADIATION

	D_0	n	No points
Expression	79	1.2	12
Grinding	76	1.3	10

CONCLUSIONS

Grinding is one way to obtain bone marrow from femurs for the study of cell population changes after irradiation. The marrow yield of CFU/femur is increased in ground femur, but the ratio of CFU/10^5 nucleated marrow cells is decreased, relative to their number in marrow aspirated from the femur by the routine procedure of forcing Hanks solution through the bone shaft. Significant numbers of CFU, amounting

to 20 to 25% of the number expressed, remain in the femur after aspiration of the marrow. Estimates of CFU content may be influenced by a recent immunization of the mice with vaccinia virus. The radiation sensitivity of CFU that survive either type of isolation trauma (aspiration or grinding the femur) is similar.

REFERENCES

1. Lewis, J. P. and F. E. Trobaugh. *Nature* **201**, 589–590 (1964).
2. Siminovitch, L., E. A. McCulloch, and J. E. Till. *J. Cell. Comp. Physiol.* **62**, 327–336 (1963).
3. Till, J. E. and E. A. McCulloch. *Ann. N. Y. Acad. Sci.* **114**, 115–125 (1964).
4. Ainsworth, E. J. and R. M. Larsen. *Radiat. Res.* **40**, 149–176 (1969).
5. Smith, W. W., G. Brecher, S. Fred, and R. A. Budd. *Radiat. Res.* **27**, 710–717 (1966).
6. Ainsworth, E. J., R. J. M. Fry, F. S. Williamson, D. L. Jordan, M. P. O'Malley, and A. R. Sallese. This report.
7. Ainsworth, E. J., E. M. Cooke, M. Miller, and M. P. O'Malley. This report.
8. Patt, H. M. and M. A. Maloney. *Radiat. Res.* **41**, 500–506 (1970).

HEMATOPOIETIC INJURY AND RECOVERY: EVALUATION BY GRANULOCYTE MOBILIZATION

E. John Ainsworth, Eugenia M. Cooke, Marietta Miller, and Mary P. O'Malley

PURPOSE AND METHODS

Many more mature granulocytes are stored in bone marrow than are found in peripheral circulation.[1] This large population constitutes the "granulocyte reserve", and the size of this population, estimated by experimentally-induced mobilization, has been used as an index of hematopoiesis in various disease states in humans[2] and after radiation injury in experimental animals.[3, 4] Hematopoietic recovery after irradiation is detected earlier and more precisely by changes in the granulocyte reserve than by changes in circulating granulocytes. In mice, an abortive rise[5] in circulating granulocytes, which is of considerable prognostic significance, is rarely detected; whereas, abortive granulopoiesis is quite evident in the marrow granulocyte reserve.[4] The granulocyte reserve is one of several indices of hematopoiesis to be used in the JANUS program to detect injury after single or protracted exposures to neutron or gamma radiation and to measure age-related changes.[6] Baseline experiments summarized here are prerequisite for evaluating the granulocyte reserve in irradiated mice.

The mice were BCF_1 males 95 to 110 days old, weighing 30 to 33 g; they were held 5 per cage under routine laboratory conditions. A 0.5 μCi dose of ^{59}Fe, in the form of ferrous citrate diluted in 0.9% NaCl, was injected intraperitoneally. Granulocyte mobilization was induced by i.p. injection of 5 μg endotoxin from *Pseudomonas*.[7] Blood samples were taken from the brachial artery under ether anesthesia. The anticoagulent used was EDTA. A Coulter Counter Model B was used for total leukocyte counts. The counts were made within 30 minutes after addition of saponin (ZAP-ISOTON). Differential leukocyte counts were made by standard method. Monocytes and eosinophils were not included in the lymphocyte and granulocyte counts. Granulocyte production by transplanted marrow cells was evaluated in one experiment; femoral marrow was obtained from normal donors, using techniques described elsewhere[8] and injected intravenously within 6 hr after the recipient mice had received 1068 rads of ^{60}Co radiation.

PROGRESS REPORT

Diurnal change in circulating leukocytes during the work day is a commonly ignored variable which contributes to heterogeneity of hematology studies in mice. Results in Table 18 show that two of three groups bled between 1300 and 1600 had lymphocyte counts significantly higher than at 0900. Afternoon counts of total leukocytes were predictably higher, because, in mice, lymphocytes constitute 80 to 95% of all leukocytes; granulocytes did not change significantly during this period. Results in Table 19 show that saline injection (0.9% NaCl-pyrogen free) produced no significant change in granulocyte count, but in two of three groups lymphocyte counts were significantly lower than the afternoon samples (1300–1600) shown in Table 18. This effect is probably attributable to the trauma of capture and injection rather than to saline *per se*. Whatever the cause and however mediated physiologically (presumably hormonally), the pattern of diurnal change is altered. This effect was also observed in controls of a separate series of experiments (Table 20) in which mice were injected with endotoxin. A control group injected with saline and ^{59}Fe had a significantly lower lymphocyte count than the 1300 and 1600 groups in Table 18. Another saline control group shown in Table 20 did not have a significant drop. Although this effect of "stress" on lymphocytes is not completely re-

TABLE 18. DIURNAL CHANGES IN CIRCULATING LEUKOCYTES IN BCF_1 MICE. MEAN VALUES ARE BASED ON 10 ANIMALS/GROUP. BLOOD SAMPLES WERE TAKEN FROM THE BRACHIAL ARTERY

Time	Mean cell counts/mm³		
	Total leukocytes	Granulocytes	Lymphocytes
0900 hours	5462 (4775–6149)[a]	1012 (665–1359)	4102 (3189–5014)
1300 hours	7387[b] (6477–8296)	937 (709–1165)	6023[b] (5017–7030)
1500 hours	6328 (5168–7488)	628 (443–812)	5571 (4543–6600)
1600 hours	7194[b] (6262–7925)	960 (728–1193)	5863[b] (5217–6508)
2100 hours	6185 (4495–7874)	1050 (732–1368)	4714 (3090–6338)

[a] 95% confidence limits.
[b] Differs significantly from the count at 0900.

TABLE 19. INFLUENCE OF SALINE INJECTION ON CIRCULATING LEUKOCYTES IN BCF_1 MICE. BLOOD SAMPLES WERE TAKEN FROM THE BRACHIAL ARTERY 6 HOURS (1500) AFTER INJECTION

Volume injected, ml	Mean cell counts/mm³			*N*
	Total leukocytes	Granulocytes	Lymphocytes	
0.05	4007 (3264–4750)[a]	935 (682–1187)	2952 (2346–3554)	10
0.10	3750 (2913–4388)	735 (455–1004)	2839 (2285–3393)	10
0.20	6213 (5359–7067)	924 (649–1199)	4900 (4188–5612)	15

[a] 95% confidence limits.

producible at statistically significant levels, it appears as a real variable that must be considered in mobilization studies.

Future studies of hematopoiesis will involve clearance and incorporation of ^{59}Fe into erythrocytes, making it necessary to establish that the ^{59}Fe vehicle is free of endotoxin and will not, in any way, interfere with mobilization responses elicited by endotoxin. Results in Table 20 show that endotoxin-induced mobilization of granulocytes was not diminished by concomitant injection of ^{59}Fe, and no mobilizing effect could be attributed to ^{59}Fe.

Hematopoietic injury sustained during fractionated neutron or gamma irradiation produced changes in cell populations and in functional indices of hematopoiesis. One means of evaluating injury and adaptative phenomena involves transplantation of hematopoietic stem cells and quantitation of their functional capacity, as measured by production of differentiated progeny, i.e., granulocytes or erythrocytes.[9, 10] It may be possible to distinguish changes in the number of stem cells from changes in the functional integrity of stem cells and

TABLE 20. INFLUENCE OF ^{59}Fe AND ENDOTOXIN ON GRANULOCYTE MOBILIZATION IN BCF_1 MICE. ALL INJECTIONS WERE AT 0900 AND BLOOD SAMPLES FROM THE BRACHIAL ARTERY WERE TAKEN 6 HOURS LATER. THE INJECTION VOLUME WAS 0.2 ML.

Treatment	Mean cell count/mm³			*N*
	Total leukocytes	Granulocytes	Lymphocytes	
Saline	6213 (5359–7069)	924 (649–1199)	4900 (4188–5612)	15
Saline + ^{59}Fe[a]	5208 (4522–5895)	852 (664–1040)	4051 (3383–4720)	15
Endotoxin[b]	5498 (5278–6717)	1566 (1180–1953)	4256 (3721–4791)	15
Endotoxin + ^{59}Fe	7213 (6713–7712)	1731 (1486–1976)	5157 (4622–5652)	13

[a] 0.5 μCi/mouse, i.p.
[b] 5 μg, i.p.

TABLE 21. GRANULOCYTE MOBILIZATION AT 10 DAYS AFTER INJECTION OF 2.55×10^6 NUCLEATED MARROW CELLS. SAMPLES FROM THE BRACHIAL ARTERY WERE TAKEN FROM ONE GROUP AT 0800, THE TIME THAT EITHER ENDOTOXIN (5 μg) OR SALINE WAS INJECTED INTO OTHER GROUPS

Treatment	Mean cell count/mm³			*N*
	Total leukocytes	Granulocytes	Lymphocytes	
Marrow[a] only (0800)	1396 (901–1891)	502 (399–605)	842 (405–1278)	13
Marrow injected, 6-hr samples (1400)				
Saline	1417 (1198–1636)	543 (428–648)	831 (701–961)	13
Endotoxin[b]	1706 (1456–1957)	198 (971–1425)	464 (391–537)	15

[a] All animals were injected with femoral marrow, suspended in Hanks solution, in a volume of 0.2 ml. The content of CFU in the injected marrow was ~673.
[b] 5 μg, i.p.

their progeny. Also, responsiveness to exogenous erythropoietin or endotoxin may provide insight into hematopoietic control systems in irradiated animals.

Preliminary results on production of granulocytes and lymphocytes after transplantation of bone marrow cells are summarized in Table 21. Before initiating studies with irradiated marrow, quantal relationship must be established between number of nucleated cells or colony-forming units injected and production of differentiated cells. These results show a significant mobilization of granulocytes can be elicited 10 days after transplantation. A comparison of the lymphocyte counts in the saline- and endotoxin-injected groups indicates that endotoxin produced a significant lymphocytopenia in these supralethally irradiated recipients of bone marrow. This did not occur when the same dose of endotoxin was given unirradiated mice (Table 20). Studies in progress will evaluate mobilization response over a range of nucleated cell doses; planned extensions of these experiments include incorporation of ^{59}Fe and ^{125}IUDR.

CONCLUSIONS

Studies of granulocytopoiesis involving endotoxin-induced mobilization must consider diurnal or artifactual changes produced by experimental variables other than injection of endotoxin. Although no significant diurnal change was found in the number of circulating granulocytes between 0900 and 1600, some significant increases in lymphocyte count were observed. Injection of saline at 0900, or more likely the stress attendant to injection, influenced the diurnal change in lymphocytes. Mobilization of granulocytes was demonstrated in non-irradiated BCF_1 mice injected with 5 μg of endotoxin and in supralethally irradiated mice (1068 rads ^{60}Co γ) injected with normal bone marrow. The aqueous vehicle for ^{59}Fe is not contaminated with an amount of endotoxin sufficient to produce granulocyte mobilization.

REFERENCES

1. Patt, H. M. *Blood* **12**, 777–787 (1957).
2. Craddock, C. G., Jr., S. Perry, L. E. Ventzke, and J. S. Lawrence. *Blood* **15**, 840–855 (1960).
3. Smith, W. W., I. A., Alderman, and J. Cornfield. *Am. J. Physiol.* **201**, 396–403 (1961).
4. Ainsworth, E. J., K. Kendall, F. A. Mitchell, and T. L. Phillips. U. S. Naval Radiological Defense Laboratory Report USNRDL-TR-1023 (1966).
5. Bond, V. P., T. M. Fliedner, and J. O. Archambeau. *Mammalian Radiation Lethality.* Academic Press. New York, 1963, pp. 159–230.
6. Ainsworth, E. J. and R. L. Straube. Argonne National Laboratory Biological and Medical Research Division Semiannual Report, 1961. ANL-6464, pp. 16–18.
7. Ainsworth, E. J. and P. D. Forbes. *Radiat. Res.* **14**, 767–774 (1961).
8. Ainsworth, E. J. and R. M.Larsen.*Radiat. Res.* **40**, 149–176 (1969).
9. Hellman, S., and H. E. Grate. *Blood* **30**, 103–111 (1967).
10. Blackett, N. M., P. J. Roylance, and K. Adams. *Brit. J. Hematol.* **10**, 453–457 (1964).

NEUTRON AND GAMMA-RAY TOXICITY STUDIES: FURTHER ANALYSIS OF SURVIVAL AND CAUSE OF DEATH STATISTICS FOR MICE UNDER DURATION-OF-LIFE GAMMA IRRADIATION

Douglas Grahn, Ruth Ann Lea, Katherine Allen, R. J. Michael Fry, John Rust, and George Sacher

PURPOSE AND METHODS

The late effects of protracted, lifetime exposures to external radiation sources continue to be a matter of operational concern to the nuclear energy industry. Recent challenge of existing standards of operational safety, increased concern over environmental pollution from the burning of fossil fuels, and the continuing concern over the control of radiation hazards attendant with the use of nuclear powered generating systems have all created a renewed interest in the field of radiation toxicity and epidemiology. In recognition of these factors, and while long-term studies employing the JANUS reactor are being initiated, the analysis of existing data from earlier studies continues.

Most of the data are from the irradiation of inbred mouse strains A/JGh, BALB/cJGh, C57BL/6JGh and the F_1 hybrid derived from the C57BL/6:BALB/c cross (BCF_1). The animals were exposed to ^{60}Co γ-radition from a starting age of about 100 days for the duration of their life. Nine daily exposure levels ranging from 0.3 R/day to 56 R/day plus a control were used. The basic survival and tumor death rate statistics have been reported.[1, 2]

For two reasons particular emphasis is being given to the use of actuarial statistical techniques. One, the data under analysis are the most complete available at low daily exposure levels, i.e., those that produce only 2% to 20% life shortening. The basic survival statistics are also well supported by pathology data on at least

an 80% sample. Second, the data are being used to develop and test a series of statistical procedures that will be used for the analysis of data obtained in the JANUS studies.

PROGRESS REPORT

The efforts of the past year have been principally in three areas.

1. Extension of the analysis for selected causes of death to additional endpoints at the lower dose levels (below 12 R/day) to identify radiation-related responses that may occur at various ages after exposure is initiated.

2. Extension of the analysis for the major causes of death in the individual strains and sexes.

3. Development of more precise isolation of radiation related changes in death rate and identification of dose-response relationships.

The following endpoints are being utilized or studied for their usefulness and sensitivity to radiation exposure:

1) All causes of death.
2) All causes—populations decremented for leukemia deaths.
3) Leukemia (reticular tissue tumors).
4) All tumors—including and excluding leukemia.
5) Pulmonary tumors.
6) Ovarian tumors and cysts.
7) Miscellaneous tumors—population decremented for leukemia deaths.
8) Renal lesions.

Items 1, 3, and 4 are particularly important as typical of the data employed for the analysis of human hazards.

The full range of endpoints has been exploited for the data on the combined strains and sexes. Sample sizes are over 800 at 0 R and 1.3 R/day and about 500 at 0.3 R/day, 2.6 R/day and 6 R/day for the combined data, which permits even some low probability events to be detected. For example, evidence of radiation injury is detectable at 0.3 R/day beyond 800 days of age (>200 R accumulated) for ovarian tumor and miscellaneous tumor endpoints. A slight, but not significant, elevation of the death rate from all causes is also seen at this dose late in life.

For the individual strains, the analysis must be restricted to a few of the predominant endpoints. More attention is given here to the estimation of the 100-days of age death-rate intercept from which the separate exposure groups diverge within each strain. This is a genetic parameter and it varies among the genotypes by a factor of ten. The control regressions of death rate on age are not significantly different among strains, however. Thus, genetic differences in normal life expectancy, in this study, are not a product of differences in the rate of change of mortality with age, but are a function of differences in the initial probability of death. Strain differences in radiation-induced changes in life expectancy have not been completely analyzed.

One of the analytical objectives is to isolate, as precisely as possible, the time and dose specific responses to the cumulative radiation. Tumor or death incidence, daily exposure level, and age all interact non-linearly, but the death rate statistic emerges as a clear measure of radiation damage. The measurement of differences between irradiated and control death rates is the obvious approach, and the procedure being explored is simply to derive the differential and integral death rates, with respect to the control, for selected causes of death and daily exposure levels. The differential death rates are derived in 25 to 100 day increments of age and plotted against the age variable. Integral death rates are sequentially derived in 25 to 100 day steps and plotted against accumulated dose to the age at derivation.

The evaluation of integral death rates has been especially fruitful in establishing dose-response relationships, in comparing exposure patterns, and in identifying the existence of a basic long-term injury parameter that appears to be constant for all exposures below 24 R/day. At 24 R/day and above, there is an acceleration of injury with dose, while at 12 R/day and below, injury is linearly related to accumulating dose along a common dose-response line for all the low rates of exposure. This has also been derived through a slightly different approach by Sacher in a recent report.[3] The all-causes-of-death doubling dose for the chronic injury term, strains combined, is about 6000 R for males and 4000 R for females. Doubling doses for other endpoints vary from about 300 R for leukemia induced by single doses, 2200 R for leukemia after protracted exposure, 2800 R for pulmonary tumors, and 5200 R for all tumors.

CONCLUSIONS

Actuarial statistical techniques are used to define the responses of populations of mice to protracted gamma irradiation. This analysis of age-specific death rates provides a clear presentation of a variety of responses to irradiation. The integral death rates, derived with respect to the control, offer a direct measure of dose response relations that can be used to compare different endpoints, radiation exposure factors, radiation quality factors, or other experimental differentials.

REFERENCES

1. Grahn, D., G. A. Sacher, J. H. Rust, and R. J. M. Fry. Argonne National Laboratory Biological and Medical Resaerch Division Annual Report, 1969. ANL-7635, pp. 1–9.
2. Grahn, D. *Late Effects of Radiation*, Ed. R. J. M. Fry, D. Grahn, M. Griem and J. H. Rust. Taylor & Francis Ltd., London, 1970, pp. 101–136.
3. Sacher, G. A. Proc. 4th Intl. Congress of Radiation Research, Evian, France, June 29–July 4, 1970, in press.

PATHOLOGICAL FINDINGS AFTER SINGLE DOSE NEUTRON IRRADIATION

R. J. Michael Fry, John H. Rust, Janet E. Newlin and Everett Staffeldt

PURPOSE AND METHODS

This investigation had two purposes: (1) to determine whether increased proliferative activity in the biliary tract and hepatocytes altered the incidence of tumors arising from these cells after irradiation, (2) to obtain information for a sacrifice series on the incidence of tumors and lens abnormalities after exposure to a single dose of neutron irradiation in the BCF_1 mouse, the strain chosen for the JANUS program.

Male and female BCF_1 mice, 155–180 days of age, were used. Mice were exposed at CP-5* to approximately half the $LD_{50/30}$ dose (170 rads). Apart from those sacrificed at about 250 days of age for serological examination for viral antibodies and of course those dying, the mice were sacrificed at 699 to 723 days of age, about 550 days after irradiation. The choice of time of sacrifice is a compromise; it is early enough that a reasonable sized sample was obtained and sufficiently long after the irradiation to include the latent period of most tumors.

Increased proliferative activity of the biliary tract, hepatocytes and littoral cells was stimulated by giving a diet containing 2% deoxycholic acid[1] for 48 hours prior to irradiation.

PROGRESS REPORT

The pathological findings for the pooled data of the irradiated groups are compared to those of pooled data for the control group of this experiment and data for BCF_1 mice of a similar age group and are shown in Table 22.

TABLE 22. PATHOLOGICAL FINDINGS: PERCENT INCIDENCE

No. of BCF_1 mice 650–750 days old	Tumors of the reticular tissue				Tumors				
	Thymic lymphoma	Lymphosarcoma[a]	Myelogenous leukemia	Unclassified	Pulmonary	Hepatic	Ovarian[b]	Miscellaneous	Lens[c] abnormalities
0.0 rads									
♂ 47	0.0	8.5	0.0	0.0	17.0	8.5		0.0	15.0
♀ 42	2.4	16.7	0.0	0.0	11.9	0.0	2.4	4.8	56.5
Total 89	1.1	12.4	0.0	0.0	14.6	4.5			34.8
	Pooled: 13.5								
170 rads neutrons									
♂ 63	0.0	4.8	7.9	0.0	27.0	14.3		11.1	100.0
♀ 66	0.0	7.6	1.5	3.0	9.1	6.1	31.8	18.1	100.0
Total 129	0.0	6.2	4.7	1.5	17.8	10.1		14.7	100.0
	Pooled: 12.4								

(a) Includes all tumors, for example reticulum cell sarcoma, arising in lymphoid tissue other than the thymus.
(b) The data for ovarian tumors and cysts have been pooled.
(c) The degree of abnormality is markedly less in the control mice, and the incidence is based on the presence of any deviation from normal microscopic appearance.

The points of interest are the following: (1) There was no change in the incidence of tumors of the reticular tissue, but six cases of myelogenous leukemia were found. We have not found this condition in any of the large number of unirradiated BCF_1 examined, nor in those exposed to chronic gamma irradiation, but have diagnosed it after single exposures to X rays (100 R and 395 R). An increased incidence of myelogenous leukemia with single dose neutron irradiation compared to protracted exposures has been reported.[2] (2) There was an increase in the incidence of ovarian tumors and

* We are grateful to Dr. H. Vogel and R. Barhorst for exposing the mice.

cysts and miscellaneous tumors, which included two in the area of the gastroduodenal junction. This latter type of tumor has not been found in this age group of unirradiated or chronically irradiated mice. (3) Abnormalities of the lens were found in all of the eyes examined in the irradiated group, including those sacrificed about 100 days after irradiation. Slight abnormalities were found in 35% of the control animals at about 700 days of age. (4) There were 10% hepatomas in the irradiated groups compared to 4.5% in the control mice. The incidence of hepatomas was 18% in the mice given the diet 48 hr prior to irradiation compared to 6% in the mice receiving only irradiation. (5) One tumor of the gall bladder was found, and it is perhaps of interest that it was in one of the mice in the groups given the diet after irradiation. Accelerated induction of hepatomas after neutron irradiation and carbon tetrachloride, which results in proliferation secondary to liver degeneration, has been reported.[3] Significant titres for antibodies to PVM, GDVII, Sendai, and mouse hepatitis were found in both irradiated and control mice.

CONCLUSIONS

The induction of myelogenous leukemia with the single exposures to neutron irradiation and X rays in a strain which shows no such disease either in the unirradiated or in mice exposed to protracted gamma irradiation raises some interesting questions about the etiology of the disease that can be investigated in the JANUS program. The results for the incidence of tumors of the liver and of the single tumor of the gall bladder after irradiation and induced proliferation suggest that this method of altering proliferation in these cell systems will be useful for investigating the interrelationship of proliferative activity and radiation induction of tumors.

REFERENCES

1. Fry, R. J. M. and E. Staffeldt. *Nature*, **203**, 1396–1398 (1964).
2. Upton, A. C., M. L. Randolph, and J. W. Conklin. *Radiat. Res.* **41**, 467–491 (1970).
3. Cole, L. J. and P. C. Nowell. *Biological Effects of Proton Irradiation*. Int. Atomic Energy Agency, IAEA, Vienna, 1964, Vol. II, pp. 129–141.

STUDIES OF LONG-TERM IRRADIATED SURVIVORS AND AGED MICE

E. John Ainsworth, R. J. Michael Fry, Patricia C. Brennan, Donn L. Jordan, and Mary P. O'Malley

PURPOSE AND METHODS

An objective of the JANUS program is to elucidate the late effects of radiation that involve changes in cell populations and functional integrity of physiological systems. Comparisons are made between irradiated survivors and comparably aged controls so results contribute to the understanding of aging as well as to the late effects of radiation. Although operation of the JANUS reactor resumed only recently, baseline studies have been conducted on survivors and aged controls from 1968 JANUS experiments. This report summarizes results on the femur and spleen content of colony-forming units (CFU) and their radiation sensitivity in these animals and young BCF_1 mice. The terms "young" and "aged" are used throughout in reference to animals 90 to 130 days old and those ranging from 800 to 1100 days, respectively; ages ±50 days of aged animals are shown in the tables. Survivors had received neutron doses of 300 to 380 rads or X-ray doses of 670 to 730 rads; exposures were given in ~30 minutes. In lethality and survival time experiments, mice were exposed to ^{60}Co gamma radiation, or fission neutron radiation in facilities described by Williamson.[1] Methodology for CFU and data reduction are described elsewhere.[2]

PROGRESS REPORT

The CFU and nucleated cell content in spleen and/or femur was determined in aged mice, in aged survivors, and in young unirradiated animals. Only these three classes are included in this report. Aged survivors differed significantly from aged controls in both femur and spleen CFU content (Table 23). The femur CFU content in survivors ranged from only 33 to 63% of the content in aged controls. Survivors also showed a lower ratio of CFU/10^5 nucleated marrow cells, and in one survivor group the difference from aged controls was statistically significant. The spleen CFU content and CFU ratio were significantly depressed in that survivor group in which measurements were made. Cell population changes in these survivors may indicate a significant deficit in hematopoietic capability which is related to non-recuperable injury[3] and an increased probability of death.[4]

There was no age-related reduction in the CFU population in femur or spleen. Indeed, the nucleated cell and CFU content in the femur of aged mice was higher in the young. Although no comparable measurements were made on spleens of aged and young mice, data are available on the spleen CFU content of young LAF_1

TABLE 23. NUCLEATED CELL AND CFU CONTENT IN FEMUR AND SPLEEN OF AGED, AGED-IRRADIATED, AND YOUNG MICE

Group	Nucleated cells × 10^7		CFU/10^6 Nucleated cells		CFU/organ × 10^3	
	Marrow	Spleen	Marrow	Spleen	Marrow	Spleen
Aged[a] (1000 days)	6.6 (6.3–7.4)[c]	27.3 (26.1–28.4)	18.8 (17.4–20.1)	1.4 (1.2–1.5)	12.8 (11.9–13.7)	3.7 (3.3–4.1)
Young[a]	4.4 (3.3–5.5)		20.3 (17.4–23.2)	—	9.1 (7.9–10.4)	—
Aged[b] (1100 days)	4.3	39.7 (22.5–56.8)	17.3 (14.1–20.5)	1.2 (0.9–1.4)	7.2 (5.8–8.5)	4.7 (3.6–5.7)
Young[b]	3.3 (2.8–3.8)	—	19.3 (16.1–22.4)	—	6.4 (5.3–7.4)	—
Aged neutron[b] survivors (~700 days)	3.3 (3.2–3.4)	29.7	11.9 (6.8–17.0)	0.9 (0.7–1.1)	4.0 (2.3–5.7)	2.6 (1.9–3.2)
Aged neutron survivors (~1000 days)	2.8 (2.1–3.3)	—	16.0 (13.2–18.7)	—	4.5 (3.7–5.2)	—
Aged X-ray[b] survivors (~700 days)	2.7 (2.0–3.5)	—	8.5 (6.8–10.2)	—	2.3 (1.9–2.8)	—

[a] Marrow obtained by grinding femurs.
[b] Marrow obtained by aspiration.
[c] 95% confidence limits.

TABLE 24. PRELIMINARY ESTIMATES OF D_0 AND EXTRAPOLATION NUMBER (n) FOR MARROW CFU FROM AGED ANIMALS AND IRRADIATED SURVIVORS

Donors	Age, days	n	D_0	Number of doses	Radiation
Neutron survivors	900	1.7	58	5	250 kVp X rays
X-radiation survivors	800	1.7	50	4	" " " "
Unirradiated controls	100	1.4	64	10	" " " "
Unirradiated controls	1100	1.6	74	5	^{60}Co gamma rays
Unirradiated controls	100	1.4	81	9	" " "

TABLE 25. MEAN SURVIVAL TIMES AFTER SUPRALETHAL EXPOSURE TO GAMMA RADIATION FOR ANIMALS OF DIFFERENT AGES. DEATHS WERE RECORDED EVERY 6 HOURS. ANIMALS FOUND DEAD WERE ASSIGNED A SURVIVAL TIME CORRESPONDING TO THE MIDPOINT OF THE 6 HR INTERVAL. EACH DOSE GROUP CONTAINED 15 MICE

Dose, rads	Mean survival time, hours		
	Animals' age, days		
	100	1000	1100
3880	133 (128–138)[a]	123 (113–133)	115 (106–124)
1940	126 (122–130)	130 (113–147)	
1455	183 (170–196)	132 (119–145)	

[a] 95% confidence limits.

hybrid mice:[2] 17 × 10^7 nucleated cells and 1800 CFU/spleen. The aged BCF_1 mice, therefore, may show increased nucleated cell and CFU content in the spleen. The increased femur and spleen CFU content in aged mice is related to increased cellularity which may be correlated, at least partially, with increased body weight.[5]

Preliminary results on radiation sensitivity of marrow CFU from aged survivors, aged and young animals are summarized in Table 24. The marrow response of all aged animals, including survivors, is characterized by a slightly lower D_0 and a slightly higher n than was observed in young animals. Although preliminary, these results do not approach the 25% reduction in D_0 reported for aged mice.[6] Additional survival results and definition of the functional types of spleen colonies, must be in hand before the significance of these small changes in radiation response can be evaluated.

Increased radiation sensitivity of aged mice, based on lethality endpoints, has been attributed to an age-dependent increase in the intestinal component of injury.[7] One means of comparing radiosensitivity of the gut in aged and young mice is based on the animals survival time after a radiation dose sufficient to kill dividing crypt cells. This assumes that survival time is primarily related to life-span of the epithelial cells. A short life span, resulting in rapid depopulation of villi, should produce a short survival time.[8] Other studies of survival of intestinal microcolonies indicate no difference in the radiation sensitivity of stem cells in animals over an age range similar to that used here. The survival times in aged and young animals, summarized in Table 25, show no significant differences at 3880 or 1940 rads. At 1455 rads, survival of aged animals was significantly shorter than for young. At 3880 rads, mean survival times ranged from 115 to 133, and it is assumed that death results from an intestinal syndrome which, for the most part, is not related to interactions with microbial flora. At the lower dose of 1455 rads, the survival time for aged animals was similar to that at 3880 rads, but the cause of death could be quite different. Interactions with microbial flora or septicemia may contribute to death at the lower dose. It

TABLE 26. $LD_{50/30}$ ESTIMATES FOR AGED AND YOUNG MICE EXPOSED TO GAMMA OR NEUTRON RADIATION

Radiation quality	Age group	$LD_{50/30}$ (rads)			Mean survival time, days
		Males	Females	Sexes combined	
Gamma	young	1039 ± 66[a] β 0.005 ± 0.003[d] Doses 10 N = 170	951 ± 19 β 0.015 ± 0.005 Doses 6 N = 88	988 ± 30 β 0.008 ± 0.003	15.3 ± 0.5 N = 53
	aged	951 ± 64 β 0.003 ± 0.002 Doses 8 N = 119	832 ± 13 β 0.008 ± 0.0009 Doses 5 N = 67	878 ± 29 β 0.005 ± 0.002	12.0 ± 0.5 N = 99
Neutron	young	—	477 ± 11 β 0.016 ± 0.003 Doses 4 N = 60	—	13.3 ± 0.98[b] N = 8 12.2 ± 0.7[c] N = 17
	aged	—	371 ± 9 β 0.023 ± 0.006 Doses 4 N = 60	—	11.1 ± 0.5 N = 42

[a] Standard error.
[b] Based on decedents from one experiment.
[c] Based on pooled results from other experiments[9].
[d] Slope of dose-response curve.

does not necessarily follow that similar survival times after 1455 to 3880 rads are *prima facie* evidence for similar mechanism of tissue injury and death in aged animals. Before accepting a hypothesis of enhanced gut sensitivity in aged mice[6] as an explanation for the survival time difference at 1455 rads, reasonable alternatives based on interactions including pre-existing neoplasia, infection and a change in the discreteness of the contributing syndromes must be established. Such studies are in progress.

Thirty-day lethality experiments with aged and young animals are summarized in Table 26. Aged mice show an increased sensitivity to either gamma or neutron radiation. The gamma radiation $LD_{50/30}$ for aged animals was approximately 12% lower than for young, whereas the neutron $LD_{50/30}$ from a single experiment shows a 22% reduction. Use of a pooled $LD_{50/30}$ for neutron-irradiated females[9] gives an estimated LD_{50} reduction of 14%. The "natural" mortality among 77 unirradiated, aged control animals during the 30-day observation period was 18%; no deaths were observed among 90 young animals. No correction for "natural" mortality was applied to the radiation lethality data from aged animals. Results of neutron exposures are insufficient for comparison of survival times, but the survival time of aged decedents after the gamma irradiation was significantly shorter than for young. In aged animals, 10% had died before 7 days, whereas among the young, mortality in the same period was nil. Since death before 7 days after irradiation may indicate changes other than increased intestinal sensitivity, effort was devoted to postmortem studies including pathology and bacteriology. Although these data are not yet completely analyzed, certain generalizations are clear. Pure cultures of *Pseudomonas aeruginosa* which were obtained from the heart blood of some aged animals were not recovered among the young. *Pasturella pneumotropica* contributed to mixed septicemias in aged but not in young animals. Mixed septicemias including α streptococci and/or micrococci were more frequent among the aged, whereas *E. coli* was most prevalent in the young. In some aged animals, gross pathology was found which may have contributed to death and to time of death after irradiation. In the comparison of the sensitivity of gut and marrow death in young and old animal, a way must be found to discount the contribution of latent or apparent disease processes to the lethality of the old.

CONCLUSIONS

The CFU content in femur and/or spleen was lower in neutron- or X-irradiated survivors than in aged unirradiated animals. Based on CFU content in the femur, aging alone did not produce a hematopoietic deficit. Aged animals had greater numbers of CFU and nucleated cells in the femur than did the young. Sensitivity in aged animal to intestinal injury was not enhanced, based on survival time after 3880 or 1940

rads of ^{60}Co gamma radiation. At 1455 rads, the survival time of aged animals was shorter than that of young; at this dose, interactions with microbial flora and pre-existing disease processes may influence survival time in aged animals. The neutron or gamma radiation $LD_{50/30}$ was lower in aged than in young animals. Preliminary bacteriology and pathology indicate the importance of complex interactions distinct from enhanced sensitivity to radiation injury *per se*.

REFERENCES

1. Williamson, F. S. This report.
2. Ainsworth, E. J. and R. M. Larsen, *Radiat. Res.* **40**, 149–176 (1969).
3. Krebs, J. S., R. W. Brauer, and H. Kalbach, *Radiat. Res.* **10**, 80–88 (1959).
4. Grahn, D. and G. A. Sacher, Proc. Symp. on Dose Rate in Mammalian Biology, Oak Ridge, Tennessee. U. S. Atomic Energy Commission Report CONF-680410 (1968).
5. Coggle, J. E. and C. Proukakis, *Gerontologia*. **16**, 25–29 (1970).
6. Proukakis, C. and P. J. Lindop. *Nature* **215**, 655–656 (1967).
7. Yuhas, J. M., D. Huang, and J. B. Storer, *Radiat. Res.* **38**, 501–512 (1969).
8. Fry, R. J. M., A. B. Reiskin, W. Kisieleski, A. Sallese, and E. Staffeldt, *Comparative Cellular and Species Radiosensitivity*, Ed. V. P. Bond and T. Sugahara. Igaku Skoin, Tokyo, 1969, pp. 255–270.
9. Ainsworth, E. J., R. J. M. Fry, F. S. Williamson, D. L. Jordan, M. P. O'Malley, and A. R. Sallese, This report.

BACTERIOLOGY ON IRRADIATED MICE IN THE JANUS PROGRAM

E. John Ainsworth, Patricia C. Brennan, Donn L. Jordan, Mary P. O'Malley, Richard C. Simkins, and Calvin M. Poole

PURPOSE AND METHODS

Non-random variables which interfere with short- or long-term radiation studies in the JANUS program must be defined and hopefully eliminated. Such variables can often be ascribed to bacterial or viral flora in experimental animals. *Pseudomonas aeruginosa* is perhaps the best known source of interference in short-term experiments since both $LD_{50/30}$ and mean survival time are affected, but other problematic organisms are known.[1, 2] In comparative radiation studies conducted over months or years, it is imperative that the stability of microbial flora at least be monitored, especially in an animal facility that houses many species of trapped feral rodents and commercially produced experimental animals.

Recent studies in viral oncology[3] and late effects of radiation[4] stress the requirement for defining and monitoring microbial flora, even where current understanding of epidemiology precludes complete microbial control.[5] When an anomaly that can be attributed to microorganisms occurs in radiation experiments, the cause of this anomaly must be sought in the hope that institution of microbial screening procedures may eliminate future problems. Identification of bacteria contributing to postirradiation septicemia is an important means of monitoring microbial flora in the experimental animals used in the JANUS program. The following report summarizes part of our experience with the relationship of bacterial flora to radiation responses.

The mice were BCF_1 ($B6CF_1$/Anl[Anl 66]) of both sexes, 90 to 120 days old. Exposure to gamma radiation was at 50 R/min. Wensinck's glycerol medium was used to detect *P. aeruginosa* in either drinking water or heart blood.[2] Identification of other bacteria in heart blood was accomplished by routine methods.

PROGRESS REPORT

Pseudomonas aeruginosa *and Radiation Mortality*

The complicating role of *P. aeruginosa* in short-term studies of radiation lethality is well known.[1, 2] The importance of this organism in long-term or late effects experiments is undefined, but most of the anticipated consequences are undesirable. We have, therefore, chosen to attempt to exclude animals carrying *P. aeruginosa* from all JANUS experiments, and screening of drinking water for this organism is done routinely. In February and March of 1970 *P. aeruginosa* was detected in some water bottles from breeding stock, holding stock, and experimental animals. Routine culture of drinking water was expanded to repeated culture on a large number of cages. Three cultures, one week apart, indicated that the cages could be classified in three categories: (I) those from which water bottles were positive for *P. aeruginosa;* (II) those from which *P. aeruginosa* was not recovered; and (III) those from which cultures initially were positive but thereafter were not.

The third group, the temporarily positive animals, posed the problem as to their suitability for future radiation experiments. Had the organism been shed or was it simply undetected? If the organism were shed, it would be unnecessary as well as uneconomical to cull temporarily positive animals. Pursuant to defining the

experimental suitability of the temporarily positive animals, mice from all three categories were irradiated to compare $LD_{50/30}$ and the frequency of Pseudomonas septicemia. The mortality results (males and females pooled) are summarized in Table 27.

Postmortem bacteriology (Table 27) showed that the 51 animals cultured from Group I had *P. aeruginosa* septicemia, whereas in the other groups this organism was detected in only one of 136 heart blood cultures. The probability of postirradiation septicemia with *P. aeruginosa* is thus predictable from water bottle culture. Mice from which two consecutive negative cultures were obtained after an initial positive did not die with *P. aeruginosa* septicemia, but their $LD_{50/30}$ was significantly lower than that for animals in Group II with no history of *P. aeruginosa*. As no other determinative bacteriology was done on animals in these experiments, we have no explanation for the increased radiosensitivity of mice in Group III. While this experiment with temporarily positive animals should be repeated, until additional results are available, no animals with a history of *P. aeruginosa* will be used in short- or long-term JANUS experiments.

Variability of radiation response precludes computation of an $LD_{50/30}$ for mice consistently positive for *P. aeruginosa*. Non-uniformity of "infection," qualitatively or quantitatively could contribute to this heterogeniety. Although *P. aeruginosa* is classically associated with "early death", i.e., before 8 to 10 days, the present results show that most cases of septicemia were detected after that time, the latest at 26 days (Table 28). A surge of early death only signals *P. aeruginosa* septicemia in populations of irradiated mice, and a point not generally appreciated is the contribution of this organism to radiation death during the second postirradiation week. Time of onset of septicemia may be influenced by the time of cross infection among animals within a cage and by the numbers of *P. aeruginosa* harbored in the nasopharynx or intestinal tract. We anticipate that acidification of drinking water, a practice to be instituted in the near future for mice in JANUS experiments will decrease cross infection and ameliorate our problems with *P. aeruginosa*.

TABLE 27. ^{60}Co Gamma $LD_{50/30}$ for BCF_1 Mice According to Status of *P. aeruginosa* Cultured from Drinking Water

	I Positive	II Negative	III Positive-negative
$LD_{50/30}$, rads	<755	983 (957–1008)[a]	910 (900–919)
Number of animals in LD_{50} experiment	155	238	195
Mean survival time of decedents, days	14.2 (12.8–15.6)	15.6 (14.9–16.3)[a]	16.1 (15.3–16.9)
Heart blood cultures: *P. aeruginosa* positive/total cultures	51/51	1/57	0/79

The comparisons involve "positive" mice the drinking water from which was contaminated with *P. aeruginosa* on three consecutive weekly cultures, "negative" mice from which *P. aeruginosa* was not detected on the same culture routine, and "temporarily positive" animals, which showed two negative cultures after an initial positive. Animals were irradiated within 7 days of completion of bacteriology. Results obtained with the sexes are pooled.

[a] 95% confidence limits.

TABLE 28. Radiation Dose-Response and *P. aeruginosa* Positive Blood Cultures in Mice from Group I in which *P. aeruginosa* Was Detected in the Drinking Water

Sex	Dose, rads	Dead/total	Day of death[a]	Day *P. aeruginosa* septicemia detected[a]
Females	874	4/12	(2)19, 20, 26	(2)19, 20, 26
	734	8/13	(3)9, (2)14, 15, (2)19	14, (2)19
	824	6/15	14, 15, (2)24, (2)27	14, 15, (2)24
	752	17/30	(6)7, (2)8, 9, (4)10, 12, 14, 15	(4)7, (2)8, 9, (4)10, 15
	679	10/15	7, 11, (2)14, (2)16, (3)21, 22	7, 16, (3)21, 22
	631	8/15	11, 16, 17, 18, 20, 21, 22, 27	11, 17, 18, 21, 22
	606	0/15	—	—
Males	824	8/15	(2)6, (4)7, 8, 9	6, (4)7, 8, 9
	752	13/15	11, (7)14, (3)15, 16, 21	(7)14, (2)15, 21

[a] Number of animals (if more than one) is in parentheses.

Survival Anomaly in Irradiated Mice

A split-dose lethality experiment with BCF_1 male mice exposed to neutrons began in September, 1970. Three hundred mice received a conditioning dose of 300 rads, and subgroups were subjected to graded challenge doses to determine the $LD_{50/30}$ at 5 hr, 1, 2 and 3 days. The single dose $LD_{50/30}$ for males, based on three experiments conducted during the preceding four months, is 460 rads.[6] Part of the split-dose lethality results are shown in Table 29. When total doses that approach the single dose $LD_{50/30}$ of 460 rads were given in two fractions, at times indicated above, mortality was unexpectedly high (95 to 100%). Recovery after neutron irradiation, based on $LD_{50/30}$, has been reported in mice,[7-9] so that even the doses of 498 to 534 rads sustained at an interval of 3 days should not kill all exposed animals. Mean survival time of decedents as short as 3 days after the challenge dose is without precedent. Even the longest survival time (5.6 days) is

TABLE 29. MORTALITY AND SURVIVAL TIME OF NEUTRON-IRRADIATED MALE BCF_1 MICE. GRADED CHALLENGE DOSES WERE GIVEN BETWEEN 5 HOURS AND 3 DAYS AFTER A CONDITIONING DOSE OF 300 RADS

Interval	Total dose, rads[a]	30-day mortality, dead/total	Mean survival time of decedents, days[b]
5 hr	375–456	43/45	5.3 (4.5–6.1)[c]
1 day	444–484	30/30	3.1 (3.0–3.2)
2 days	476–516	30/30	3.0 (2.7–3.3)
3 days	498–534	30/30	4.6 (3.7–5.5)

[a] Conditioning plus challenge doses.

[b] Computed from the time of the challenge dose. After single doses of neutrons, the mean survival times and 95% confidence limits are from 12.1 (10.6–13.6) to 9.7 (8.8–10.6) over the dose range from 420 to 530 rads.

[c] 95% to confidence limits.

about half the mean survival time (10.8 days) for all decedents in the single-dose $LD_{50/30}$ experiments.[6]

The anomaly was not unique to neutron-irradiated animals. High mortality before 8 days, 47% of 468 mice, was observed in BCF_1 mice of both sexes given 1068 rads of ^{60}Co gamma radiation during the same month. This dose was delivered in two exposures, separated by approximately 18 hr, or as a single exposure. Although some mice were injected with bone marrow after this exposure, others that died early had not received marrow.

In earlier marrow transplantation studies, mortality by 8 days was well below 47% after gamma doses of 1068 or 1164 rads or a 250 kVp X-ray dose of 874 rads. These total doses were delivered either in two fractions, separated by 18 hr, or as a single exposure. The mortality was 2.1% in 1230 animals irradiated January through June, and was 6.9% in 1460 irradiated July through August. In $LD_{50/30}$ gamma-radiation experiments conducted before July, the mean survival time after 1050 to 1090 rads is 12.9 (12.4 to 13.4) days in which only 1 of 58 animals died before 8 days.

Heart blood cultures and tissue samples from some of these mice indicated no *P. aeruginosa* septicemia. Species identification of other enteric bacteria and evaluations of histopathology are in progress. We hope to learn whether this is a recognized problem or a new one. Subsequent single dose $LD_{50/30}$ experiments show no abundance of early deaths after a gamma dose of 1068 rads and "normal" survival times of 10 to 12 days after neutron irradiation. Thus, this anomaly may have been transient. This episode points to the requirement for extensive microbiology and other testing of representative animals in each replicate population which enters the JANUS late effects experiment.

A Shift from Gram Positive to Gram Negative Septicemia

These preliminary findings include the identification of bacteria responsible for septicemia in two single-exposure $LD_{50/30}$ experiments with ^{60}Co gamma radiation. These experiments, conducted approximately one year apart, are designated 1969 and 1970, respectively. Other results were obtained from a split-dose LD_{50} series in 1969 that was not completed because of an outbreak of *Pseudomonas aeruginosa*. Heart blood cultures were made from irradiated decedents that were either sacrificed while moribund or were found dead. In either case, heart blood was cultured by routine methods within 4 to 6 hours after the animals' demise.

TABLE 30. BACTERIA DETECTED IN BLOOD CULTURES OF BCF_1 MICE FROM SINGLE-DOSE $LD_{50/30}$ EXPERIMENTS IN 1969 AND 1970

1969		1970	
$LD_{50/30}$ 966 (946–988)[a] rads Number of animals = 110 M.S.T., days = 14.3 (13.3–15.3) N[b] = 45		$LD_{50/30}$ 973 (938–1009) rads Number of animals = 58 M.S.T., days = 15.6 (14.2–17.0) N = 26	
Organism	Number of animals	Organism	Number of animals
α hemolytic streptococci	6	*E. coli*	19
Micrococci	1	Enterococci	2
Pasteurella pneumotropica	1	*Bacillus* sp.	1
Mixed:		Mixed:	
α hemolytic streptococci + micrococci	2	*E. coli* + enterococci	3
α hemolytic streptococci + coliforms	2	Micrococci + *Hemophillus* sp.	1
α hemolytic streptococci + *P. pneumotropica*	2		
	N = 14		N = 26

[a] 95% confidence limits of rad dose.

[b] Number of decedents.

Portmortem invasion that may have occurred was similar in both experiments.

The bacterial recovery from the two single-exposure $LD_{50/30}$ experiments is presented in Table 30, along with estimates of the $LD_{50/30}$ and mean survival time of decedents. Bacteriological results from the split-dose experiments are shown in Table 31. The major difference between the 1969 and 1970 experiments is related to organisms recovered from septicemic animals. In 1969, pure cultures of coliforms were detected in only 2 (6%) animals with septicemia, and α hemolytic streptococci were the organisms most frequently recovered. In 1970 coliforms accounted for 73% of the septicemia. More extensive bacteriology conducted recently on neutron-irradiated mice also shows a predominance of coliforms. Although the spectrum of organisms associated with septicemia appears to have shifted from Gram positive to Gram negative, we have as yet detected no significant effect on $LD_{50/30}$ or on mean survival time of decedents. The shift in microorganisms contributing to bacteremia may indicate a different primary route of invasion.

TABLE 31. BACTERIA DETECTED IN BLOOD CULTURES OF BCF_1 MICE FROM SPLIT-DOSE $LD_{50/30}$ EXPERIMENTS IN 1969

Organism	Number of animals
α hemolytic streptococci	10
Micrococci	3
Coliforms	2
P. pneumotropica	1
Mixed:	
α hemolytic streptococci and coliforms	2
α hemolytic streptococci, micrococci, and coliforms	1
α hemolytic streptococci and diptheroid	1
α hemolytic streptococci and *P. pneumotropica*	1
P. pneumotropica and coliforms	1
	$N = 22$

CONCLUSIONS

The $LD_{50/30}$ was decreased in BCF_1 mice from which *P. aeruginosa* was initially cultured from drinking water then two subsequent weekly cultures were negative for this organism. This alteration in $LD_{50/30}$ occurred in the absence of *P. aeruginosa* septicemia. Mice with any history of *P. aeruginosa* should not be used in radiation experiments.

A survival anomaly, characterized by "early death," occurred in mice given fractionated neutron irradiation or a single dose of gamma radiation. *P. aeruginosa* was not detected, and species identification of enteric organisms is in progress. Although survival results from more recent studies indicate this anomaly may have been transient, this episode points to the necessity for further routine testing of animals allocated to late effects studies.

Over a period of one year a shift occurred in the spectrum of organisms contributing to septicemia in gamma-irradiated mice. In 1969 heart blood cultures showed a predominance of α hemolytic streptococci and micrococci, whereas in 1970 coliforms were most frequently recovered. Although an unwelcome variable, which may indicate a changing microbial flora in the experimental animals, has appeared, no effect on $LD_{50/30}$ or mean survival time has yet been detected.

REFERENCES

1. Flynn, R. J., E. J. Ainsworth, and I. Greco. Argonne National Laboratory Biological and Medical Research Division Annual Report, 1960. ANL-6368, pp. 35–37.
2. Flynn, R. J. *Lab. Animal Care* **13**, 25–35 (1963).
3. Haran-Ghera, N. and A. Peled. *Brit. J. Canc.* **21**, 730–738 (1967).
4. Walburg, H. E., G. E. Cosgrove, and A. C. Upton. *Int. J. Cancer* **3**, 150–154 (1968).
5. Serrano, L. J., R. C. Allen, R. C. Brown, N. K. Clapp, G. E. Cosgrove, E. B. Darden, Jr., T. T. Odell, Jr., R. L. Tyndall, A. C. Upton, and H. E. Walburg, Jr. Proc. Symposium on Defining the Laboratory Animal in the Search for Health, Washington, D.C. 1969. Int. Committee on Laboratory Animals. Nat. Acad. Sci., Washington, D.C., in press.
6. Ainsworth, E. J., R. J. M. Fry, F. W. Williamson, D. L. Jordan, M. P. O'Malley, and A. R. Sallese. This report.
7. Melville, G. S., F. P. Conte, M. Slater and A. C. Upton *Brit. J. Radiol.* **30**, 196–199 (1957).
8. Vogel Jr., H. H., D. L. Jordan and S. Lesher. *Radiation Biology*, Ed. J. H. Martin. Butterworths, London, pp. 1959, 221–235.
9. Ainsworth, E. J., R. M. Larsen, K. Kendall, G. F. Leong, J. S. Krebs, and F. A. Mitchell. Proc. Symp. on Neutrons in Radiobiology, Oak Ridge National Laboratory, 1969. U.S. Atomic Energy Commission Report CONF 691106, pp. 435–450.

MECHANISMS OF CARCINOGENESIS

*Austin M. Brues, Donald D. Grube, and Harry Auerbach**

PURPOSE AND METHODS

These studies center around the problem of carcinogenesis from localized irradiation. This is one of the most difficult matters to analyze or to investigate experimentally, from the standpoint of developing radiation protection criteria and standards. For example, a microgram of ^{239}Pu, which is approximately equal to the occupational permissible total-body burden in man,[1] has produced sarcomas readily after injection into local sites in small rodents,[2, 3] yet there has been no explicit recognition of the differences in cell susceptibility that are implied by obviously large species differences in responses when calculations are made on a volume dose basis. Examples of this have been given[4] and are tabulated here.

Among the subjects that we have investigated are: skin carcinogenesis from external beta irradiation and its cellular basis; conditions determining carcinogenesis by implanted plastics; chronic action of radioactive implants; skin and bone carcinogenesis by locally injected plutonium; development of benign and malignant breast tumors in rats; and effect of chemical promoters on radiation carcinogenesis.

In this report we present data on the effect of croton oil resins on superficial beta-ray carcinogenesis, and relations between tissue distribution of plutonium and tumor production. Due to depletion of the staff, some other areas of research, notably on the mechanism of tumor production by plastics, are not active at present. Various details of experimental procedures were given in earlier reports.[5, 6]

PROGRESS REPORT

1. Hairless (hrhr) mice and their haired (heterozygous) siblings were given 5000 rads of external beta irradiation to the lower two-thirds of the body, and groups of these were then painted 3 times weekly for one year with a mixture of phorbol esters A and C, a derivative of croton oil which is a potent promoter of carcinogenesis initiated by hydrocarbon carcinogens.[5] Treatment was started at six months of age and the experiment is almost completed at this time, 24 months later. Control mice have been followed to 30 months of age. Malignant tumors have been tabulated and examined histologically, and data are presented in Table 32. Benign papillomas, which are not shown, appeared in all treated groups but were almost all transitory. In the hairless mice, two bone tumors (not included in the sarcomas scored) occurred in the 185 mice irradiated, and one bone tumor in the 79 controls.

It appears from this that treatment by phorbol esters increases the tumor incidence in both groups of mice and this increase is significant in the sarcomas as well as in the skin carcinomas. It also appears that tumors are more frequent following irradiation in the hairless than in the haired mice, in contrast to the relationship reported after treatment of mice of the same strain with DMBA.[8] Examination of the location of tumors in our mice shows that 75% of those in mice treated with phorbol esters were in the painted area, while only 12% appeared in the corresponding area of the unpainted animals; for sarcomas alone, there is also a highly significant difference (54% as compared with 14%). It is also of interest that there is no evidence that the promoter shortens the appearance time of tumors of either type.

2. An earlier report[3] suggested that castration of female rats influences the distribution of bone tumors after subcutaneous injection of plutonium. We have now nearly completed a second experiment which was designed to test this observation and to provide further data on the production of local and osteogenic sarcomas. In this experiment, the injections were made at four subcutaneous sites in the anterior abdominal wall, using polymeric ^{239}Pu of which about 1% was ultrafilterable. Analyses were made of the plutonium content of one femur and the skeletal content was assumed to be 25 times that value. Tabulation of the results to date (Table 33) fails to show the difference in bone tumor incidence that was reported earlier between intact and castrated rats.

Linear regression analysis of the amounts of ^{239}Pu found in bone shows a small negative slope with time (between 4 and 10% of mean values per 100 days) which is not significant in individual groups but is seen in all groups. Because of the spread of individual values, we have expressed the relation of tumor incidence to burden (last column in the table) in terms of the mean of analytical results in each group. The apparent relation of retained percent to injected dose and of tumor yield to retained amount cannot be considered significant at this stage of the analysis. It is apparent

* Present address: Illinois Regional Medical Program.

TABLE 32. EFFECT OF HAIRLESS PHENOTYPE AND OF PHORBOL ESTER TREATMENT ON EXTERNAL BETA RAY EFFECTS

	Original No. of mice	Median survival, months[a]	Mean time of tumor appearance[a]		Total No. of tumors		Tumor death rate at 24 months[a,b]	
			Carcinoma	Sarcoma	Skin carcinoma	Sarcoma	Carcinoma	Sarcoma
No promoter; hairless	136	17	13.6	15.4	10	16	0.18	0.20
No promoter; haired	95	18	16.0	20.0	2	2	0.04	0.05
Phorbol ester treated; hairless	49	16	19.2	14.2	8	8	0.48	0.34
Phorbol ester treated; haired	45	18	17.8	21.0	7	3	0.35	0.17
Untreated;[c] hairless	79	21	—	21.5	0	2	—	0.07
Untreated; haired	55	17	—	—	0	0	—	—

[a] Months after treatment; in controls, after 6 months of age.
[b] Rates attributed to tumor alone, i.e., corrected for deaths from other causes.[7]
[c] Unirradiated and untreated by promoter.

TABLE 33. TUMOR PRODUCTION FOLLOWING SUBCUTANEOUS INJECTION OF ^{239}Pu IN PARTICULATE FORM

Pre-treatment	Amount injected, μg	No. of rats	Bone sarcomas		No. of local tumors	Mean skeletal[a] burden, μg	% in skeleton	Bone tumors/μg
			No.	%				
Intact	5.1	47	22	47	1	1.05 ± 0.33	20.5	0.45
Castrate	5.1	49	24	49	3	0.77 ± 0.21	15.1	0.64
Intact	3.2	49	9	18	1	0.58 ± 0.23	18.0	0.31
Castrate	3.2	37	9	24	3	0.62 ± 0.19	19.3	0.39
Intact	1.7	43	1	2	0	0.37 ± 0.09	22.0	0.05
Castrate	1.7	48	4	8	2	0.44 ± 0.12	26.0	0.18
Intact	0.87	48	4	8	0	0.23 ± 0.07	26.2	0.35
Castrate	0.87	47	3	6	0	0.23 ± 0.08	26.8	0.26

[a] Mean values in animals sacrificed after one year following injection, estimated as 20 times femoral assay ± S.D. of individual values.

TABLE 34. RELATION OF TUMOR PRODUCTION BY ^{90}Sr AND ^{239}Pu TO SKELETAL IRRADIATION, IN MICE AND DOGS

	Administered		Estimated mean skeletal rads	Tumor yield, %	Kg rads (skeleton)	Kg rads/tumor	Ratio dog:mouse
	μCi	μCi/kg					
Plutonium							
Mouse (500–700 days)	0.017	0.7	600	30	1.5	5.0	
	0.009	0.35	300	16	0.75	4.7	
							80
Dog (2000–2500 days)	0.5	0.05	200	46	200	435	
	0.16	0.016	90	29	90	320	
Strontium							
Mouse (500–600 days)	11	440	10,000	71	25	35	
	5	200	4,500	13	11.5	88	
	2.2	88	2,000	2	5.0	(250)	
							320
Dog (900–1700 days)	1000	100	8,000	73	8,000	11,000	
	600	60	5,000	17	5,000	29,000	
	100	10	3,000	(0/12)	3,000	—	

that the number of bone tumors exceeds the number of locally induced sarcomas at all levels of injection.

3. As shown in previous reports[4, 6] the adult dog fails to respond to embedded beta sources which induce subcutaneous tumors in a much shorter period in almost 100% of rats. Mole[9] has indicated, similarly, that data on the response of skin of small animals to beta irradiation show a response, per unit area of surface, that would imply a much greater carcinogenicity of sublethal whole-body irradiations to man than is actually observed. We have made calculations from published data on bone sarcoma induction in mice[10] and dogs,[11] with estimates of the mean accumulated skeletal dosages and of the volume doses (Table 34).

While these calculations are imprecise, they leave no doubt that on the basis of radiation exposure to individual cells, those of the dog are much less sensitive to the carcinogenic stimulus. It is tempting to suggest that the ratio of effectiveness per volume dose unit is about equal to the ratio of body mass in the case of strontium, and of surface in the case of plutonium. The roles played by differences in duration of exposure and biological age can hardly be evaluated.

REFERENCES

1. International Commission on Radiological Protection, Publication #2, Pergamon Press, Oxford, 1959, p. 82.
2. Brues, A. M., H. Auerbach, and G. DeRoche. Argonne National Laboratory Biological and Medical Research Division Semiannual Report, 1963. ANL-6823, pp. 81–85.
3. Brues, A. M., H. Auerbach, G. DeRoche, and D. D. Grube. Argonne National Laboratory Biological and Medical Research Division Annual Report, 1966. ANL-7278, pp. 132–134.
4. Brues, A. M. and H. Auerbach. Abstracts, Fourth International Congress of Radiation Research, 1970, p. 35.
5. Brues, A. M. H. Auerbach, G. DeRoche, and D. D. Grube. Argonne National Laboratory Biological and Medical Research Division Annual Report, 1968. ANL-7535, pp. 28–31.
6. Brues, A. M., H. Auerbach, G. DeRoche, and D. D. Grube. Argonne National Laboratory Biological and Medical Research Division Annual Report, 1969. ANL-7655, pp. 115–119.
7. Spicer, C. C. *Brit. J. Cancer* **1**, 298–310 (1947).
8. Giovanella, B. C., J. Liegel, and C. Heidelberger. *Cancer Res.* **30**, 2590–2597 (1970).
9. Mole, R. H. *Ann. Rev. Nucl. Sci.* **15**, 207–240 (1965).
10. Finkel, M. P. and B. O. Biskis. *Prog. Exp. Tumor Res.* **10**, 72–111 (1968).
11. Univ. of Utah Radiobiology Division Annual Report, 1969. COO-119-240.

RETENTION OF RADIOSTRONTIUM IN SOFT TISSUES

*Austin M. Brues, Donald D. Grube, and Harry Auerbach**

PURPOSE AND METHODS

Our previous report[1] summarized experiments on the retention of radiostrontium in soft tissues and blood. It was shown that radiation exposures to these tissues from ^{90}Sr are strongly dependent on species, age, and physiological factors influencing removal of the nuclide by the rapidly exchanging calcium pool in bone and by excretory pathways. These studies indicated the suitability of the adult dog for studies bearing on human exposure. Preliminary results were presented, in which fixation in sperm was determined at very low levels. During the past year we have been studying methods for the extraction of ^{90}Sr from its yttrium daughter and for increasing the sensitivity of analytical methods in order to investigate the translocation of endogenous ^{90}Y to soft tissues and to determine its fixation in sperm.

In our previous work, strontium free of yttrium was obtained by solvent extraction. We find it more satisfactory to prepare injection solutions by ion exchange separation. A solution containing ^{90}Sr and ^{90}Y is treated with citrate at pH 5.5 to complex the yttrium, and is passed through a small column of anion exchange resin that has been converted to the hydroxyl form.[2] Using about one gram of resin in a column made from a plastic syringe barrel, a 1-ml sample of the mixture is drawn through the column under gentle negative pressure, followed by two washings to a final volume of 5 ml containing about 95% of the strontium. This can be prepared for injection within a few minutes after beginning the separation.

^{90}Y can be counted directly, at about one percent efficiency, in fluid or homogeneous tissue samples in a well-type gamma counter, and double tracer measurements of ^{90}Y and ^{85}Sr are feasible; ^{90}Sr is estimated by ingrowth of yttrium daughter after allowing the material to approach equilibrium. Variations in container wall thickness introduce an error of ±10% in absolute measurement of ^{90}Y beta particles, but estimation of the ^{90}Sr:^{90}Y ratio is independent of this source of error. In order to handle material of low activity, conditions for the simultaneous measurement of ^{90}Sr and ^{90}Y in low amounts by liquid scintillation counting of ashed tissues have been worked out, and it appears that it

* Present address: Illinois Regional Medical Program.

may be feasible to measure ^{85}Sr at the same time. This method gives very much higher counting efficiency but involves considerable loss of time in preparation of samples for counting. Preliminary trials using tissues of mice injected with ^{90}Sr three months previously have shown the possibility of carrying out detailed studies on dogs.

PROGRESS REPORT

A few mice were injected intraperitoneally with ^{90}Sr containing less than 1% ^{90}Y in amounts between 3 and 12 μCi/g. The 30-day LD_{50} appears to be between 6 and 8 μCi/g. Spleen weights of those dying between 9 and 14 days after injection were 15 to 30% of control weights. Ratios of $^{90}Y:^{90}Sr$ of certain tissues are shown in Table 35; absolute measurements are not available.

Two additional studies have been made on plasma and sperm concentrations of ^{85}Sr in dogs, which confirm the conclusions given in the last report.[1] By means of the techniques described above, experiments on dogs injected with sublethal amounts of ^{90}Sr are planned.

TABLE 35. RATIOS OF ^{90}Y: ^{90}Sr IN TISSUES OF MICE INJECTED WITH ^{90}Sr

Days after injection	Spleen	Liver	Kidney	μCi/g injected
10	2.2	2.4	1.8	10
13	2.3	1.5	1.9	10
14	1.8	1.6	1.9	8
34	1.3	1.8	1.4	6

REFERENCES

1. Brues, A. M., H. Auerbach, D. D. Grube, and G. DeRoche. Argonne National Laboratory Biological and Medical Research Division Annual Report, 1969. ANL-7655, pp. 119–120.
2. Doering, R. F., W. D. Tucker and L. G. Strang, *J. Inorg. Nucl. Chem.* **15**, 215–221 (1960).

PROMOTION BY PHENOBARBITAL OF HEPATOCARCINOGENESIS INDUCED BY ACETYLAMINOFLUORENE IN RATS

Carl Peraino, R. J. Michael Fry, and Everett Staffeldt

PURPOSE AND METHODS

In previous studies the hepatocarcinogenic action of dietary acetylaminofluorene (AAF) was reported to be substantially reduced if phenobarbital also was included in the diet.[1] This protective effect of phenobarbital results from its stimulation of AAF-degrading enzymes in the liver.[2] Subsequent preliminary studies of the sequential, rather than simultaneous, feeding of AAF and phenobarbital suggested that the feeding of phenobarbital to these rats after their exposure to AAF stimulates the production of liver tumors.[3, 4] The potential importance of this observation required that it be subjected to rigorous further testing.

The general experimental procedure is as described previously,[4] except that more rats were used, and changes in the exposure and test intervals were made. In addition, the overall experiment was divided into three replicates, offset by one-week intervals.

PROGRESS REPORT

Table 36 shows the tumor incidence in rats fed a diet containing 0.02% AAF for various time intervals followed by a control diet or one containing 0.05% phenobarbital. The table also shows the cumulative results at the end of 260 days. Data from the three replicate experiments were pooled in all AAF-treatment periods. Subsequent exposure to phenobarbital increased the incidence of hepatomas, clearly demonstrating that phenobarbital, when given after AAF, promotes hepatocarcinogenesis.

Table 37 shows the proliferative activity of liver cells in rats fed phenobarbital for 72 hours before they were killed. In both age groups, phenobarbital increased the labeling index in both the parenchymal and

TABLE 36. TOTAL INCIDENCE OF HEPATOMAS AFTER 260 DAYS IN RATS FED A DIET CONTAINING 0.02% AAF FOR VARIOUS PERIODS FOLLOWED BY THE FEEDING OF A CONTROL DIET OR ONE CONTAINING 0.05% PHENOBARBITAL

Days on AAF	Total No. of rats with hepatomas/total No. of rats in group	
	AAF followed by control diet	AAF followed by phenobarbital diet
11	2/105	17/106
16	7/101	42/104
21	18/103	64/102
26	27/103	86/108
Totals	54/412	209/420
Deaths	20/432	12/432

TABLE 37. EFFECTS OF DIETARY PHENOBARBITAL AND AGE ON PROLIFERATIVE ACTIVITY IN HEPATOCYTES AND LITTORAL CELLS[a]

Treatment	Age, days	Labeling index, mean ± S.D. (4 rats/group)	
		Hepatocytes	Littoral cells
Control	43	0.83 ± 0.1	3.6 ± 0.6
Phenobarbital	43	1.95 ± 0.4	6.5 ± 1.2
Control	56	0.57 ± 0.2	1.9 ± 0.4
Phenobarbital	56	2.00 ± 0.4	3.0 ± 0.7

The rats were fed a diet containing 0.05% phenobarbital for 3 days.

littoral cells, suggesting that phenobarbital stimulates cellular proliferation in the liver. Further study is required to determine whether or not the increase in the number of cells synthesizing DNA is related to the promoting effect of phenobarbital on liver carcinogenesis.

CONCLUSION

Phenobarbital, an agent that is not, itself, hepatocarcinogenic, can promote liver carcinogenesis. Combined with previous observations,[1, 3, 4] results in this report suggest that phenobarbital enhances the expression of the neoplastic lesion previously produced by the carcinogen and not by sensitizing the target to the action of the carcinogen. Future experiments will investigate the mechanism of the carcinogenesis-promoting effect of phenobarbital.

REFERENCES

1. Peraino, C. Argonne National Laboratory Biological and Medical Research Division Annual Report, 1967. ANL-7409, p. 165.
2. Kato, R., M. Shoji, and A. Takunata. *Gann* **58**, 467–469 (1967).
3. Peraino, C. and R. J. M. Fry. Argonne National Laboratory Biological and Medical Research Division Annual Report, 1968. ANL-7535, p. 39.
4. Peraino, C., R. J. M. Fry, and E. Staffeldt. Argonne National Laboratory Biological and Medical Research Division Annual Report, 1969. ANL-7635, p. 131.

DIETARY AND HORMONAL INTERPLAY IN THE REGULATION OF RAT-LIVER ORNITHINE AMINOTRANSFERASE

Carl Peraino

PURPOSE AND METHODS

Forced feeding of casein hydrolysate to rats pre-fed a protein-free diet resulted in an elevated production of liver ornithine aminotransferase. This elevation was blocked by simultaneous forced feeding of glucose.[1] The injection of cortisone into rats force-fed both casein hydrolysate and glucose prevented the blocking effect of glucose and permitted the casein hydrolysate-stimulated increase in ornithine aminotransferase.[2] In contrast the elevation of ornithine aminotransferase produced by the *ad libitum* feeding of a high protein diet was blocked by the injection of cortisone or triamcinolone.[3, 4] These paradoxical effects of glucocorticoids observed under different experimental conditions led to an investigation of the interactions of dietary protein, carbohydrate, and injected glucocorticoid in the regulation of ornithine aminotransferase under a single set of experimental conditions.

Male albino rats (Charles River) with an average weight of 150 g were fed diets containing 0, 15, 30, or 60% protein. The usable carbohydrate content in one set of diets was adjusted to compensate for changes in protein content and in the other set the usable carbohydrate was limited to 20%, with the remaining bulk consisting of powdered cellulose. Beginning on the fourth day after initiation of feeding and continuing for the next five days, each rat received a single daily intramuscular injection of 5 mg of triamcinolone. The livers from five rats killed each day from each group were assayed for ornithine aminotransferase activity.[3]

PROGRESS REPORT

Feeding a diet containing 60% protein (carbohydrate 25%) resulted in a high level of liver ornithine aminotransferase activity; this activity was reduced substantially by treating the rats with triamcinolone. When the 30% protein (55% carbohydrate) diet was fed the level of ornithine aminotransferase was approximately ⅓ that observed in rats on the 60% protein diet, and the depressive effect of triamcinolone was much less pronounced. With 15% and 0% protein (70% and 85% carbohydrate, respectively) in the diet the enzyme was reduced to still lower levels; treatment of these rats with triamcinolone produced a marked *increase* in the enzyme.

By restricting the dietary carbohydrate to 20%, the ornithine aminotransferase activity in rats on the 15% protein diet was increased four-fold above that observed when the diet contained the same protein concentration but a carbohydrate content of 70%. This result indicates that dietary carbohydrate exerts a repressive effect on ornithine aminotransferase that, under *ad libitum* feeding conditions, is similar to that observed when the protein and carbohydrate are force-fed.[1] Treatment of the rats on the 15% protein-20% carbohydrate diet with triamcinolone produced a decrease in ornithine aminotransferase, in contrast to the increase obtained in rats on the 15% protein-70% carbohydrate diet. The increase produced by triamcinolone treatment is, therefore, in part the manifestation of the protective effect of glucocorticoid against the repressive effect of the high dietary carbohydrate. When carbohydrate was restricted and the enzyme consequently rose to high levels owing to the absence of carbohydrate repression, the negative effect of triamcinolone became apparent.

CONCLUSION

The present results reconcile the apparently conflicting regulatory effects of glucocorticoids on ornithine aminotransferase observed under differing experimental conditions, and help lay the groundwork for further studies of the mechanism by which this enzyme responds to dietary and hormonal stimuli.

REFERENCES

1. Peraino, C. and H. C. Pitot. *J. Biol. Chem.* **239,** 4308–4313 (1964).
2. Peraino, C., C. Lamar, Jr., and H. C. Pitot. *J. Biol. Chem.* **241,** 2944–2948 (1966).
3. Peraino, C. *J. Biol. Chem.* **242,** 3860–3867 (1967).
4. Peraino, C. *Biochim. Biophys. Acta* **165,** 108–112 (1968).

FUNCTIONAL PROPERTIES OF THE ORNITHINE AMINOTRANSFERASE MOLECULE

Carl Peraino

PURPOSE AND METHODS

An approach to the study of the ornithine aminotransferase molecule involved the separation of the overall enzyme reaction into its half-reactions and the investigation of each half-reaction under a variety of conditions.[1] The observation that the half-reactions responded differently to pH changes was interpreted as evidence that the active sites on the enzyme were different for each substrate. Stoichiometric measurements of the half-reactions showed that one mole of ornithine aminotransferase reacts with two moles of ornithine but only 1.5 moles of alphaketoglutarate. This lower value for alphaketoglutarate suggested a partial loss in the functional capacity of the enzyme after its conversion to the pyridoxamine form. Further studies of the half-reactions were conducted to investigate this possibility as well as to disclose additional properties of the enzyme molecule.

PROGRESS REPORT

When the enzyme was converted to the pyridoxamine form and its capacity to perform in each half-reaction was tested as a function of time, the enzyme rapidly lost the capacity to participate in the second half-reaction while regaining the capacity to perform in the first half-reaction. This means that the enzyme spontaneously reverted from the pyridoxamine form to the pyridoxal form and explains the lower value obtained for the reaction with alphaketoglutarate in the stoichiometry experiment.

Later studies have shown that the enzyme is partially inactivated by exposing it to excess pyridoxal phosphate, which binds relatively weakly to the enzyme. This binding and inactivation does not occur if the exposure is carried out in the presence of tris(hydroxymethyl) aminoethane which forms a Schiff base with pyridoxal phosphate. Further studies on the interaction of pyridoxal phosphate with the enzyme suggest that there are three modes of binding of pyridoxal phosphate to the enzyme. One is the weak binding of several pyridoxal phosphate moieties associated with enzyme inactivation. The second is the binding of two such moieties at the active site; these moieties are released by heat denaturation in tris or phosphate buffer. The third is the binding of a single pyridoxal phosphate at a site other than the active site; this bound pyridoxal phosphate can accept an amino group from the active site, producing spontaneous "reversion" of the enzyme from the pyridoxamine to the pyridoxal form. This moiety is released from the enzyme by heat denaturation in tris but not in phosphate.

CONCLUSION

Analysis of the half-reactions of ornithine aminotransferase is a highly productive method for determining the functional properties of the molecule. This

will help to clarify the nature of aminotransferase reactions in general and will also aid in the understanding of the role that ornithine aminotransferase plays in amino acid metabolism.

REFERENCE

1. Peraino, C. Argonne National Laboratory Biological and Medical Research Division Annual Report, 1969. ANL-7635, pp. 131–133.

CERENKOV RADIATION AND LIQUID SCINTILLATION COUNTING*

Walter E. Kisieleski

The measurement of Cerenkov radiation in combination with conventional liquid scintillation counting procedures offers a new dimension in liquid scintillation methodology. The detection and measurement of Cerenkov radiation, produced in an aqueous media by β-emitting radionuclides of energies greater than 260 keV, has found increasing application in biological and medical research for the counting of ^{32}P, ^{42}K, ^{40}K, ^{90}Sr, ^{90}Y, ^{137}Cs, and ^{47}Ca. Our present investigations are aimed toward the possible detection and measurement of ^{32}P (1.72 MeV) in the presence of ^{33}P (0.25 MeV) and ^{3}H (0.018 MeV). Measurements were made to determine and compare, in various solvent systems, the counting efficiency of ^{32}P, ^{33}P, and ^{3}H by Cerenkov counting and liquid scintillation counting with organic fluors. Similar measurements were made of ^{32}P and ^{33}P in the presence of varying amounts of dried biological materials (e.g., blood and liver) utilizing a vacuum-line combustion technique for sample preparation. The results indicate that in dual-labeled experiments this combined method of assay allows quantitative measurement of energetic β emitters in the presence of low energy β emitters. Furthermore, the method can be used when combustion techniques are required to eliminate problems of sample solubility and "quenching" limitations. The advantages of this method of analysis for problems in biology and medicine are discussed.

* Abstract of a paper submitted to the *Journal of the American Chemical Society*.

CONCERNING THE UPTAKE OF LIPID BY THE NUCLEUS*

Ambrose D. Barton, Walter E. Kisieleski, and Friedrich Wassermann†

Our previous radioautographic experiments, suggesting absorption of lipid by the nucleus, have been followed by direct examination of liver cell nuclei isolated from the animals at various times after oral administration of palmitic acid-9, 10-^{3}H. Twenty-four hours post-administration, the tritium activity in the isolated nuclei was still present in lipid. At this time and at all subsequent times examined, the total radioactivity in the nuclei never exceeded 1% of that in the liver. Treatment of the nuclei with Triton X 100 to remove the nuclear membrane removed most of the radioactivity; that remaining was associated primarily with chromatin with very little found in the nucleolar fraction.

* Abstract of paper submitted to *Z. Zellforsch.*
† Deceased.

EXPERIMENTAL MODIFICATION OF STRUCTURES AT THE PERIPHERY OF THE LIVER CELL NUCLEUS*

Ambrose D. Barton, Walter E. Kisieleski, Friedrich Wassermann,† *and Faustina Mackevicius*

Morphological effects of various experimental treatments on structures at the periphery of isolated liver cell nuclei demonstrate that the outer and inner nuclei membranes, the pre-annulus complex, the fibrous laminae, and the perinuclear chromatin layer are interconnected and, together, constitute an integrated cortex surrounding the nucleus in these interphase cells.

* Abstract of paper submitted for publication to *Z. Zellforsch.*
† Deceased.

Biochemistry

EFFECTS OF RADIOPROTECTIVE THIOLS IN VIVO ON THE SEDIMENTABILITY OF MITOCHONDRIA*

John F. Thomson, Sharron L. Nance, and Sandra L. Tollaksen

The sedimentation characteristics of mitochondria from livers of mice treated with various radioprotective aminothiols were measured by techniques of density-gradient and zonal centrifugation. Treatment with cysteine, mercaptoethylamine (MEA), or the phosphorothioate of MEA caused the mitochondria to sediment more slowly; S-(2-aminoethyl)-isothiouronium bromide hydrobromide (AET) caused them to sediment more rapidly. Other compounds had no significant effect. These changes are interpreted as the result of either swelling or contraction of the mitochondrial outer membranes.

None of the compounds that affected liver mitochondria had any effect on the sedimentability of mitochondria isolated from Ehrlich ascites tumor cells that had been incubated with those compounds.

* Abstract of a manuscript to be published in *Radiation Research.*

STABLE ISOTOPE ANALYSIS OF ORGANIC MOLECULES USING COMBINED GAS CHROMATOGRAPHY-MASS SPECTROSCOPY: APPLICATION TO CLINICAL MEASUREMENTS OF BILE ACID POOL SIZE

Peter D. Klein, Otto W. Berngruber, Patricia A. Szczepanik, Rudy G. Danziger, Alan F. Hofmann,* and Leslie J. Schoenfield**

PURPOSE AND METHODS

The replacement of radioactive tracers with stable isotopes in clinical measurements offers a unique opportunity to reduce radiation exposure as well as to conduct metabolic studies in children or pregnant women. Acceptance of this concept requires the confluence of three factors: instrumentation of the required sensitivity and accuracy; availability of the appropriately labeled material; and demonstration of the equivalence of the two procedures in a clinically meaningful measurement. Measurements of bile acid pool size appear to be a particularly attractive area for such a demonstration: pool size determined by radioisotope dilution has been reported to be significantly decreased despite normal synthesis rates in patients with cholesterol cholelithiasis.[1] Early detection of susceptible individuals, particularly among high risk groups, prior to the development of gall stones, would facilitate evaluation of preventive therapy. From the analytical standpoint, bile acid pool size measurements involve low dilution factors of 10 to 100. The technology for production of the deuterium labeled form already exists and follows that of the tritium form[2] and a direct comparison between ^{2}H and ^{3}H labeling is possible. Thus these measurements appear to offer the opportunity to establish the utility of stable isotope labeling in clinical measurements.

PROGRESS REPORT

One subject with cholelithiasis and two normal subjects were given ^{3}H-chenodeoxycholic acid and ^{2}H-chenodeoxycholic acid (40 mg d_4) intravenously. Bile samples were obtained by duodenal intubation 1, 2, 3, 5, and 7 days later and the bile acids were isolated by saponification of the conjugates and chromatographic separation into dihydroxy and trihydroxy fractions. At the Mayo Clinic, the ^{3}H specific activity was determined by liquid scintillation counting and gas chromatography. At Argonne, the ^{2}H specific activity was

* Gastroenterology Unit, Mayo Clinic and Mayo Foundation, Rochester, Minnesota.

determined by combined gas chromatography-mass spectrometry with accelerating voltage alternation (GC/MS/AVA).[3] The decrease in ^3H specific activity or in isotope abundance of ^2H of the isolated chenodeoxycholic acid over the time intervals studied reflects two parameters of bile acid metabolism: the initial pool size and the synthesis rate per day. A semilogarithmic plot of the data for the patient with cholelithiasis is shown in Figure 20; from the intercept and slope the two parameters can be determined. The values obtained from these three patients are compared in Table 38. Results obtained by the two methods were similar, indicating that ^2H-labeled bile acids may be used to define bile acid pool size and synthesis rate in man.

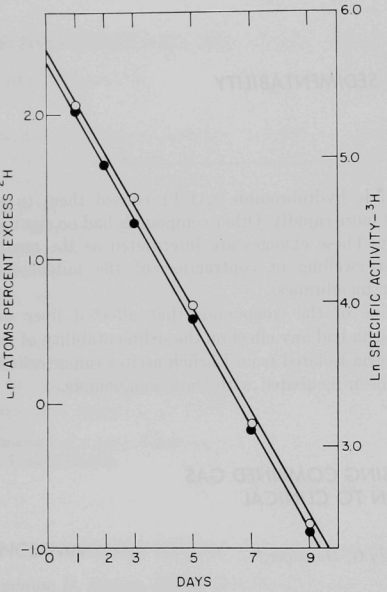

FIG. 20.—Comparison of ^3H and ^2H specific activities in chenodeoxycholic acid in man following administration of radioactive and stable isotopically labeled bile acid. Open circles, ^3H; solid circles, ^2H.

TABLE 38. COMPARISON OF RADIOACTIVE AND STABLE ISOTOPE LABELED BILE ACIDS IN THE DETERMINATION OF BILE ACID POOL SIZE

Patient	Diagnosis	Pool, g		Synthesis, g/day	
		^3H	^2H	^3H	^2H
1	Cholelithiasis	0.3	0.3	0.12	0.12
2	Normal	1.0	1.3	0.07	0.08
3	Normal	0.9	1.2	0.23	0.20

CONCLUSIONS

The technique of stable isotope analysis by the GC/MS/AVA system appears to have broad applicability to studies of intermediary or drug metabolism in man, especially when administration of radioactivity is contraindicated.

REFERENCES

1. Vlahcevic, Z. R., C. C. Bell, Jr., I. Buhac, J. T. Farrar, and L. Swell. *Gastroenterology* **59**, 165–173 (1970).
2. Hofmann, A. F., P. A. Szczepanik, and P. D. Klein. *J. Lipid Res.* **9**, 707–713 (1968).
3. Klein, P. D., J. Haumann, O. W. Berngruber, and W. J. Eisler. This report.

ANALYSIS OF DEUTERIUM-LABELED COMPOUNDS BY GAS CHROMATOGRAPHY-MASS SPECTROSCOPY: INSTRUMENT MODIFICATIONS AND ANALYSIS OF TEST MIXTURES

Peter D. Klein, Joseph Haumann, Otto W. Berngruber, and William J. Eisler

PURPOSE AND METHODS

The development of a combined gas chromatograph-mass spectrometer system for the analysis of compounds labeled with stable isotopes[1] progressed this year to the point where initial measurements on model compounds could be carried out. A substantial portion of this progress was achieved by three instrument modifications: a peak-switching chassis, a digital gaussmeter and an improved analogue-to-digital conversion system (ADC). Although the third modification is still under construction, it became possible to measure deuterium atom percent excesses as low as 1% with acceptable accuracy and reproducibility. This report described these modifications and some of the calibration results, using d_4-chenodeoxycholic acid.

PROGRESS REPORT

Instrument Modifications

Measurement of the isotope ratio in an organic molecule during its passage, as a gas chromatographic peak,

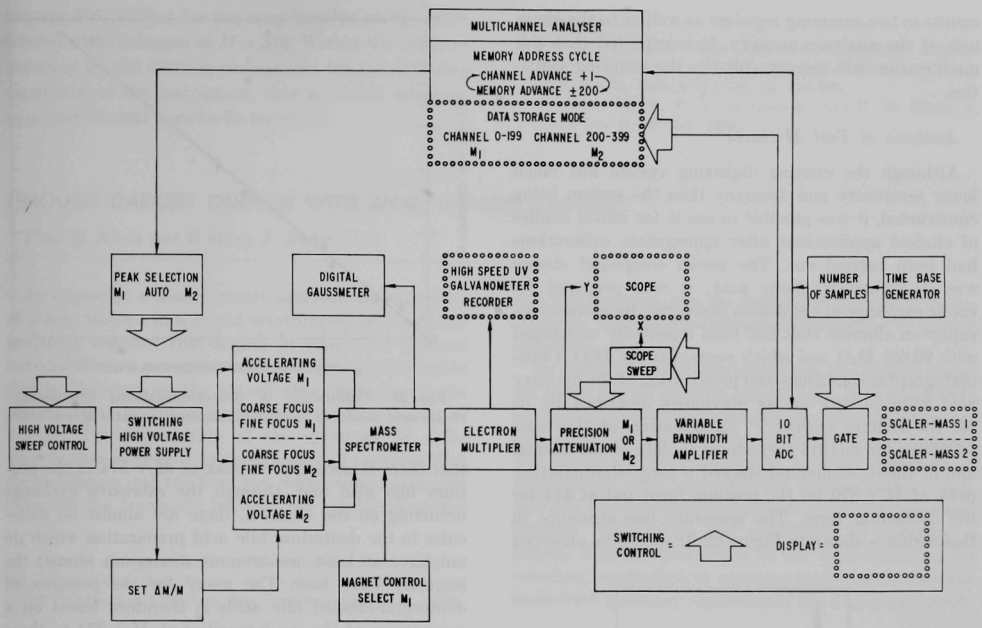

FIG. 21—Block diagram of gas chromatograph-mass spectrometer system for determination of stable isotope ratios.

through the mass spectrometer requires a rapid alternation of spectrometer focus between a characteristic light and heavy ion peak. The modifications suggested by the manufacturer, described previously,[1] proved to be unworkable and an alternative design was provided and constructed in the Electronics Division. These components are shown in the overall system block diagram of Figure 21. It consists of an independent ultrastable high voltage supply that replaces the accelerating voltage power supply of the mass spectrometer. From this supply are provided two sets of focussing controls for the coarse focus, fine focus, and lenses 1 and 2 (not shown) for the lower mass and for the upper mass. These enable the focus to be switched between two ion peaks of widely different mass without degrading the ion optics and losing spectral resolution. The initial focus on the lower mass is set by reference to the digital gaussmeter which has been calibrated to give the relationship between magnetic field and mass number. The selected peak can be viewed in the associated scope, and the magnetic field is adjusted to center the focus on the peak maximum. Next, the upper peak is focussed by decreasing an increment of the accelerating voltage until the proper value of $\Delta M/M$ is reached and the second peak is centered on the electron multiplier detector. When the incremental change in the accelerating voltage is removed, the focus reverts to the lower peak. Peak switching thus consists of adding and subtracting this increment of accelerating voltage. From the electron multiplier detector, the signal passes to a precision attenuation system that permits the intensity of the more abundant ion peak to be reduced to that of the less abundant ion before passing the signal to the ADC for conversion. The precision of this attenuation is ten parts per million, or the ability to reduce the abundance to 0.010 ± 0.001% of its original intensity. The use of this attenuation system permits the less abundant ion peak to be amplified to the same precision of A/D conversion as the more abundant peak without overloading the ADC range. The attenuation of the signal is coordinated to the peak-switching cycle.

At present, the time base generator is used to digitize the electron multiplier signal: it has a limited 7-volt range, or the capability of measuring the signal voltage to one part in 128. Moreover, it samples the voltage only once in each time interval. The replacement modification under construction, shown in Figure 21, will sample the voltage up to 100 times per time interval, digitize the value to one part in 1028 and pass the

counts to two summing registers as well as to the channels of the analyser memory. It is expected that this modification will greatly enhance the counting statistics.

Analysis of Test Mixtures

Although the existing digitizing system has much lower sensitivity and accuracy than the system being constructed, it was possible to use it for initial studies of clinical applications after appropriate calibrations had been carried out. The model compound chosen was d_4-chenodeoxycholic acid; it was prepared by enolic exchange of the 3-keto derivative by chromatography on alumina that had been repeatedly exchanged with 99.6% D_2O and which contained 3% D_2O. Chromatographic conditions and preparation of the hydroxy acid were carried out as previously described by us for the tritium variety.[2] Examination of the mass spectrum for methyl chenodeoxycholate of the normal and of the d_4 compound showed a large characteristic peak at M/e 370 for the protium form and at 374 for the deuterium form. The spectrum fine structure in this region is shown in Figure 22. It should be observed

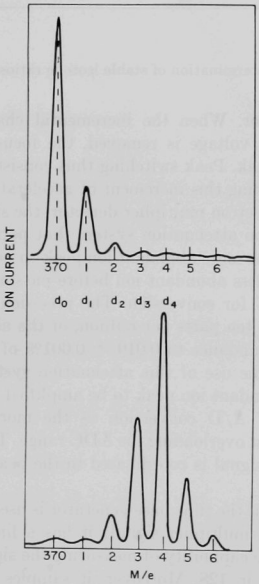

FIG. 22.—Fine structure of mass spectrum for methyl chenodeoxycholate in the vicinity of M/e 370. Upper figure, protium form; lower figure, deuterium form.

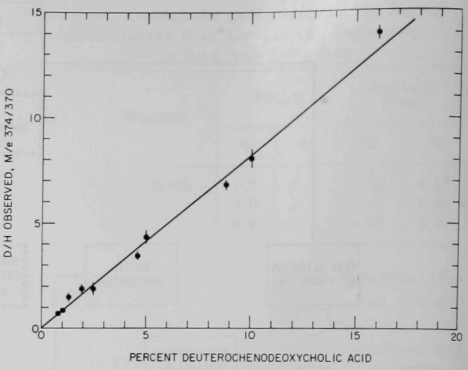

FIG. 23.—Calibration of deuterium-labeled chenodeoxycholic acid mixtures against ion intensities ratio M/e 374/370.

that there is normally no peak at M/e 374 in the protium bile acid and, through the extensive exchange occurring on the alumina, there are almost no molecules in the deuterium bile acid preparation which do not have at least one or more deuterium atoms; the majority have four. The assay for the presence of deuterium-labeled bile acids is therefore based on a comparison of the ion intensities at M/e 374 to those at M/e 370; as in a dual beta isotope measurement by liquid scintillation counting, the ratio of these two isotopes is related to the ratio of these counts or intensities. Because not *all* of the deuterium-labeled molecules have four deuterium atoms, the yield of ions at M/e 374 per mole is not as high as the M/e 370 ion yield for the protium form. The deuterium preparations must be assayed to obtain the correlation between ion yield and percent deuterium-labeled bile acid. Figure 23 shows such a calibration run in which dilutions ranging from 20% to less than 1% atoms percent excess were prepared and assayed. In the assay procedure, the mixtures of protium- and deuterium-chenodeoxycholate (as the diacetates of the methyl esters) were injected into the gas chromatographic column and the areas of the gas chromatographic peaks measured at M/e 370 and 374 were recorded and integrated in the multichannel analyser. Appropriate background corrections were made by counting at the same attenuation and amplification for equivalent times and subtracting these values. The resulting ratios were plotted against the percent deuterium-chenodeoxycholate in the mixture. The standard errors of the observations were between 1 and 10% of the actual value and as expected were larger at lower concentrations. The slope of the line indicated that the yield of ions at M/e 374 was approx-

imately 80% of that for the same number of molecules labeled with hydrogen at M/e 370. Within the limits of accuracy for the dilution process and for the digitizing capability of the instrument, this appeared adequate to permit clinical tests to be initiated.

REFERENCES

1. Klein, P. D., W. J. Eisler, and P. A. Szczepanik. Argonne National Laboratory Biological and Medical Division Annual Report, 1969. ANL-7635, pp. 214–216.
2. Hofmann, A. F., P. A. Szczepanik, and P. D. Klein. *J. Lipid Res.* **9**, 707–713 (1968).

THROUGH DARKEST QUENCH WITH ANALYSER AND CAMERA*

Peter D. Klein and William J. Eisler

As viewed in a multichannel analyser, the spectrum of a beta isotope in a liquid scintillation spectrometer has three regions: that region in which the photons have insufficient energy to be detected; a middle region that is distorted by the cut-off characteristics of the pulse height discrimination circuit; and a region of fidelity. The degradation of the spectrum by color quenching corresponds to the transfer of photons from the last region into the first, but conventional detection measures the transition between the combined second and third regions into the first. This appears to be responsible for many curvilinear relationships in quench correction.

By integrating the spectrum from the highest channel to the lowest (reverse integration), it is possible to distinguish the region of fidelity and the distortion occurring in the region of pulse height discrimination. The region of fidelity exhibits a linear reduction in pulse height with quenching for tritium, radiocarbon, and the cesium external standard spectra in the same solution. This offers the possibility of selecting a known, constant proportion of the total spectrum for counting; equivalent to counting each sample with the same fixed efficiency regardless of the degree of quench.

* Abstract of a paper to be published in the Proceedings of the International Symposium on Organic Scintillators and Liquid Scintillation Counting, San Francisco, California, 1970.

BIOLOGICAL ASSAY OF BILE SALT PURITY*

Roger Lester,† Otto W. Berngruber, Joanna M. Little,† and Peter D. Klein

An alternate method for assaying the purity of radiolabeled bile salt is described. ^{14}C-labeled test material and a ^{3}H-labeled standard are administered intravenously to an animal prepared with a biliary fistula. The relative rates of isotope excretion are analysed and compared by double isotope techniques. Using this method, it was shown that a commercial preparation of ^{14}C-taurocholate was grossly contaminated and that this contaminant partially persisted after preparative chromatography in three solvent systems.

* Abstract of a paper submitted for publication to the *Journal of Lipid Research.*

† Department of Medicine, Boston University School of Medicine.

FATTY ACID COMPOSITION OF PSEUDOMONAS ANGULATA, PSEUDOMONAS PHASEOLICA, AND PSEUDOMONAS TABACI*

Paul Sacco,† James J. McNeill,‡ Patricia A. Szczepanik, and Peter D. Klein

The fatty acid spectra of three heretofore unreported Gram negative phytopathogenic bacteria, cultured in a defined liquid medium were compared. The data indicated the uniform presence of $C_{12:0}$, $C_{14:0}$, $C_{16:0}$, and $C_{18:0}$ saturated fatty acids, $C_{16:1}$, $C_{18:1}$ unsaturated

* Abstract of a paper submitted for publication in the *Journal of the American Oil Chemists Society.*

† Xavier University College of Pharmacy, New Orleans, Louisiana 70125.

‡ Department of Animal Science, North Carolina State University, Raleigh, North Carolina 27607.

fatty acids and 2-hydroxylauric acid. C_{17}-cyclopropane acid was present in all cultures and seemingly was produced at the expense of $C_{16:1}$. C_{19}-cyclopropane occurred in the old cultures of *phaseolica* and *tabaci* but in significantly smaller amounts. While differences exist in the fatty acid spectra of these organisms, they do not appear to be sufficient to differentiate these species on a taxonomic basis.

IDENTIFICATION AND CHARACTERIZATION OF FULLY DEUTERATED FATTY ACIDS ISOLATED FROM SCENEDESMUS OBLIQUUS CULTURED IN DEUTERIUM OXIDE*

Gustav Graff,† Patricia A. Szczepanik, Peter D. Klein, and Ralph T. Holman

The algae *Scenedesmus obliquus,* cultured in deuterated water, yielded fully deuterated long-chain fatty acids of saturated and unsaturated character during their biosynthesis. The long-chain fatty acids were purified, identified and characterized by mass spectroscopy, infrared and near-infrared spectroscopy, nuclear magnetic resonance spectroscopy and the equivalent chain lengths were determined by gas-liquid chromatography. A new hexadeca-3,6-dienoic acid was identified. The fatty acid compositions of the total lipid and of individual lipid classes were analysed. The melting point of methyl perdeutero palmitate is lower than for its hydrogen containing counterpart. Methyl esters of perdeutero fatty acids have lower retention times in gas-liquid chromatography of polar and nonpolar phases.

* Abstract of a paper to be published in *Lipids.*

† The Hormel Institute, University of Minnesota, Austin, Minnesota 55912.

PREPARATION OF TRITIUM-LABELED STEROLS AND THE SYNTHESIS OF LABELED 24-AZACHOLESTEROL*

Malcolm J. Thompson,† Otto W. Berngruber, and Peter D. Klein

A method is presented for the preparation of 2,4-^{3}H sterols (stigmasterol, β-sitosterol, campesterol, fucosterol, and 7-dehydrocholesterol) via the technique of exchange-labeling of keto steroids and their subsequent conversion to sterols. The preparation of tritium-labeled 3 β-hydroxyl-24-norchol-5-en-23-oic acid and the synthesis of 2,4-^{3}H-24-azacholesterol are reported. Some advantages of the exchange labeling method over the conventional catalytic exchange method are discussed.

* Abstract of paper to be published in *Lipids.*

† Entomology Research Division, ARS, USDA, Beltsville, Maryland.

MEMBRANE-BOUND ENZYMES IN MAMMALIAN CELLS: INTRODUCTION

Yueh-Erh Rahman, Elizabeth A. Cerny, Carl Peraino, Faustina Mackevicius, Betty Jean Wright, Theodore N. Tahmisian, Sarmukh S. Brar, and Donald M. Nelson**

Cellular and intracellular membranes regulate transport between cells and their environment and between the intracellular particles and their surrounding cytoplasm. This program seeks information on mechanisms operating in these cellular and intracellular membranes by studying membrane-bound enzymes involved either with the permeability of the membranes or related to some metabolic properties of a given type of biological membrane.

Tissues of control rats, and animals under various metabolic conditions (*in vivo* or *in vitro*) are investigated by methods that include purifications of cellular and intracellular membranes (i.e., plasma membranes, inner and outer membranes of mitochondria, mem-

* Radiological Physics Division.

branes of lysosomes and membranous fragments of endoplasmic reticulum) by 1) sucrose gradient and zonal gradient centrifugations; 2) biochemical determination of various enzymes in the purified membranes; 3) purification of enzymes by column chromatography, electrophoresis and electrofocusing system; 4) morphological examination of these purified membranes by electron microscopy; and 5) chemical analysis of some principal constituents of these purified membranes (e.g., lipids, carbohydrates, trace metals, etc.).

MEMBRANE-BOUND ENZYMES IN MAMMALIAN CELLS.

I. STUDIES OF PHOSPHOLIPASES A

Yueh-Erh Rahman, Elizabeth A. Cerny, Carl Peraino, Faustina Mackevicius, Betty Jean Wright, Theodore N. Tahmisian, Sarmukh S. Brar, and Donald M. Nelson

A. Phospholipases A in Cellular and Intracellular Membranes of Rat Liver*

Intracellular distributions of phospholipases A in rat liver were investigated with emphasis on purified cellular and intracellular membranes. Phospholipase A_2, reported to be located in the outer membranes of mitochondria, was demonstrated to be in the lysosomal membranes; this finding led to the conclusion that phospholipase A_2 can be used as a marker enzyme for lysosomal membranes.

Subfractionation of endoplasmic reticulum into smooth membranes, rough membranes and polysomes showed the polysome fraction to have the highest specific activity of phospholipase A_1.

Two phospholipases A were found in purified plasma membranes, one has a pH optimum at 6.5, specific for the fatty acid at the 2-position, and another has a pH optimum at 8.0, specific for the fatty acid at the 1-position; both enzymes are activated by Ca^{2+}.

The possible biological functions of these membrane-bound phospholipases are discussed.

* Abstract of a paper to be submitted for publication in the *Journal of Membrane Biology*.

B. Studies of Phospholipase A in Rat Spleen Endoplasmic Reticulum

PURPOSE AND METHODS

In experiments on the specificity of phospholipase, 1-palmitoyl-2-^{14}C-linoleoyl-glyceryl-3 phosphorylethanolamine was used as the substrate; it was synthesized according to van den Bosch et al.[1]

Subfractionation of spleen endoplasmic reticulum was by the method of Bloemendal et al.[2]

Whole-body X radiation was delivered at a rate of 100 R/min with a single dose of 1000 R/rat.

PROGRESS REPORT

Table 39 shows the level of phospholipase A in the spleen endoplasmic reticulum as compared to other tissues. The spleen has the highest phospholipase A activity.

Spleen phospholipase activity was found to be moderately activated by Ca^{2+}, whereas Mg^{2+} and Zn^{2+} inhibited it. The enzyme is stable in acidic medium and heat treatment.

Spleen phospholipase hydrolyzed the fatty acid specifically at the 2-position.

TABLE 39. PHOSPHOLIPASE A ACTIVITIES IN ENDOPLASMIC RETICULUM OF VARIOUS TISSUES

Tissues	% Substrate hydrolyzed/100 μg protein/30 min
Spleen	58.1
Liver	18.6
Thymus	19.0
Heart	26.5
Brain	27.4
Kidney	5.1

Averages of 4 to 8 separate experiments. The enzymes were determined in the presence of 8mM $CaCl_2$ at pH 7.5 with 100 μg of protein from endoplasmic reticulum preparations of indicated rat tissues. The incubation time was 30 minutes.

Subfractionation studies showed that the polysomes have the lowest specific activity, while the smooth and the rough membranes have comparable levels of enzyme activity.

Whole-body X irradiation resulted in a slight increase of phospholipase A activity between 2 and 24 hours after radiation.

Bilirubin (10 μmoles) and *p*-chloromercuribenzoate (100 nmoles) did not significantly inhibit the spleen phospholipase A activity.

CONCLUSIONS

1. The spleen has an unusually high phospholipase A activity, as compared to other tissues.

2. Spleen phospholipase was found to be: a) specific for the fatty acid at the 2-position, b) acid and heat stable, and c) not to be inhibited by *p*-chloromercuribenzoate. These characteristics are similar to those of phospholipase A in snake venom and porcine pancreas, but different from the phospholipases in rat liver or brain.

3. Spleen phospholipase was significantly activated after it was heated to 50° and 60° for 10 minutes in acidic medium. This finding was reproducible, but no explanation for this result can be offered at present.

4. Results obtained with X-irradiated rats suggested that the phospholipase A in the spleen is probably located in the population of macrophages and reticular cells rather than the population of lymphocytes, although further work is needed to prove this point.

5. Purification of spleen phospholipase is under way; with the purified enzyme, it will be possible to explore its biological function in relation to the lysis of aged erythrocytes in the spleen.

C. *Purification of Phospholipase A from Rat Spleen*

A summary of the purification procedure follows:

1. SD/Anl rats were used, and the spleen homogenate, prepared in 0.15 M NaCl, was acidified with HCl to pH 4.0, then sonicated twice for 5 minutes.

2. This sonicated homogenate was centrifuged in the International Centrifuge Model PR-2, at 2,000 rpm for 15 minutes.

3. The supernatant from the centrifugation was heated to 70°C for 10 minutes.

4. The heated supernatant was centrifuged in the Spinco Centrifuge with the 30 rotor at 30,000 rpm for 30 minutes.

5. The supernatant was then filtered through a Sephadex G_{50} column, with distilled water as the solvent. This column yielded two major protein peaks.

6. These two protein peaks were used for further purification by the electrofocusing system; preparation of this system was the same as that previously described.[3]

7. Phospholipase A was determined with uniformly labeled ^{14}C-phosphatidyl ethanolamine as the substrate; the method used has been described elsewhere.[4]

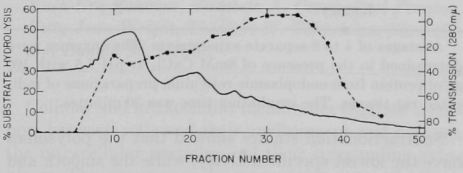

FIG. 24.—Purification of spleen phospholipase A in an electro-focusing system. The pH gradient ranged from 3.0–10.0. Two-ml fractions were collected. Each enzyme determination was done with 0.4 ml sample, in the presence of 8 mM $CaCl_2$, the incubation time was 30 minutes.

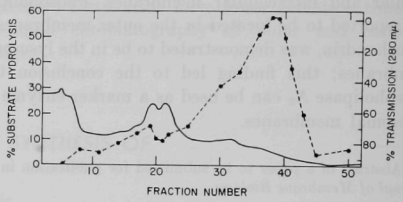

FIG. 25.—Purification of spleen phospholipase A in an electro-focusing system. The pH gradient ranged from 5.0–9.0. The enzyme determinations were the same as those described in figure 24.

PROGRESS REPORT

Both protein peaks obtained from Sephadex G_{50} column had phospholipase A activities; after they were further purified by the electrofocusing system, only peak #1 had active phospholipase activity.

Figure 24 shows the distribution of phospholipase A in the fractions obtained from an electrofocusing system with the pH gradient ranging from 3.0 to 10.0.

Figure 25 shows results from a similar experiment in which the pH gradient ranged from 5.0 to 9.0.

Results of both experiments (Figs. 24 and 25) indicate that the phospholipase A from rat spleen has an isoelectric point between 7.60 and 7.70.

Fractions #35 to #40 from the experiment in Figure 25 were pooled, and exhaustively dialyzed against distilled water to remove the ampholines; the dialyzed sample was then subjected to polyacrylamide gel electrophoresis.[5] A single band of protein was observed about 1 cm from the origin.

CONCLUSIONS

Purification of phospholipase A from rat spleen was successful after completion of three simple steps: 1) acid and heat treatment, 2) Sephadex G_{50} filtration, 3) electrofocusing.

The remaining problem is to obtain significant quantities of purified phospholipase protein in order to carry out further experiments, including chemical characterization, tests for its biological functions, and the regulatory mechanism of the enzyme.

D. Biological Regulation(s) of Membrane-Bound Phospholipases A

Two biological membranes, (the plasma membranes and the lysosomal membranes) play an important role in self-protection; hence, the interest in studying their regulatory mechanism(s).

Various cations, metabolites, hormones, and some drugs are being tested to establish their effects on the activity of these membrane-bound phospholipases.

Figure 26 shows the effect of Triton X-100, EDTA, bilirubin and deoxycholate on the activity of membrane-bound phospholipase A. All compounds inhibited phospholipase activity.

Table 40 presents results obtained with various cations on membrane-bound phospholipase A activity from rat liver, spleen, and brain. There is a strict specificity for Ca^{2+} in the brain enzyme, while Mg^{2+} and Zn^{2+} also inhibited the activity of the enzyme from liver and spleen.

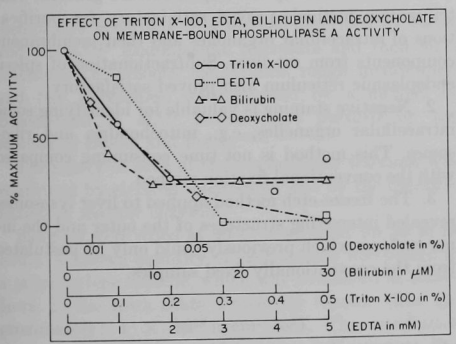

FIG. 26.—Effect of Triton X-100, EDTA, Bilirubin and Deoxycholate on Membrane-bound Phospholipase A Activity. The indicated concentration of each compound was added to the incubation medium, all enzyme determinations were done in the presence of 8 mM $CaCl_2$, at pH 7.5, with 100 μg of protein. The incubation time was 30 minutes.

TABLE 40. EFFECT OF VARIOUS DIVALENT CATIONS ON MEMBRANE-BOUND PHOSPHOLIPASE A IN ENDOPLASMIC RETICULUM OF LIVER, SPLEEN AND BRAIN

	Relative specific activity		
	Liver	Spleen	Brain
None	28.1	75.0	0.0
$CaCl_2$ (8 mM)	100.0	100.0	100.0
$MgCl_2$ (8 mM)	68.6	5.1	0.0
$ZnCl_2$ (1 mM)	5.2	0.0	0.0

The enzyme determinations were done with 100 μg of protein, at pH 7.5, and the incubation time was 30 minutes.

ATP also was found to inhibit the membrane-bound enzyme in the liver.

CONCLUSIONS

1. Triton X-100, EDTA, bilirubin, and deoxycholate inhibited membrane-bound phospholipase A. These results indicated that the membrane-bound enzymes required the integrity of biological membranes to be active.
2. Membrane-bound phospholipases A from liver, spleen, and brain required Ca^{2+} for their activity, while Mg^{2+} and Zn^{2+} inhibited these enzymes.
3. ATP inhibited the liver enzyme. This may be due to the affinity of ATP to Ca^{2+} ions; further work is needed to clear up this point. The effect of ATP also will be tested for phospholipases of other tissues.
4. The effect of various hormones (some known to protect liver lysosomal membranes) will be studied.

MEMBRANE-BOUND ENZYMES IN MAMMALIAN CELLS

II. STUDIES OF MEMBRANE COMPONENTS

Yueh-Erh Rahman, Elizabeth A. Cerny, Carl Peraino, Faustina Mackevicius, Betty Jean Wright, Theodore N. Tahmisian, Sarmukh S. Brar, and Donald M. Nelson

A. Electron Microscopic Studies of Isolated Intracellular Organelles and Their Purified Membranous Components

PURPOSE AND METHODS

Purified fractions, including nuclei, mitochondria, lysosomes, and polysomes, were either fixed according to Karnovsky's method[6] before they were examined in the electron microscope, or were examined directly after they were negatively stained with 2% phosphotungstate at pH 5.8.

Membranous components isolated from purified organelles were fixed and sectioned by the conventional method.

Some fractions of lysosomes isolated from rat liver also were examined by the freeze-etch method.[7, 8]

PROGRESS REPORT

Preparations from rat liver and spleen were examined. Purified fractions from rat liver (nuclei, mitochondria, lysosomes, as well as smooth and rough membranes, and free polysomes from the endoplasmic reticulum) were examined. Purity of these fractions was most satisfactory although few free polysomes were found still attached to membranous material.

Lysosomal membranes from rat liver prepared by sonication had small vesicles, whereas those prepared by dialysis gave the appearance of open fragments.

Free polysomes isolated from the spleen endoplasmic reticulum, examined after negative staining, showed very clear thin threads of *m*RNA between some clusters or strings of ribosomes. Lysosomes from rat liver examined by the freeze-etch method revealed that the fractured face is relatively smooth without visible particles attached; there was no patchwork-like pattern as that described on mitochondrial surface. The inner face of the lysosomal particles was covered with a number of particles of different sizes; some lysosomes had fewer of these particles than others, however. The structure of the outer and the inner surfaces revealed by this unfixed freeze-etch method correlates with that seen in conventionally prepared samples.

CONCLUSIONS

1. Various recently developed sucrose gradient centrifugation methods proved satisfactory for purifications of intracellular organelles and their membranous components from rat liver. Subfractionation of spleen endoplasmic reticulum also proved satisfactory.
2. Negative staining is valuable for identifying some intracellular organelles, e.g., mitochondria and ribosomes. This method is not time consuming compared with the conventional fixation method.
3. The freeze-etch method applied to liver lysosomes revealed interesting structures of the outer and the inner surfaces which previously could only be postulated from the conventionally fixed samples.

B. Thermal Neutral Activation Analysis of Purified Biological Membranes*

PURPOSE AND METHODS

Biological functions of some trace elements have been extensively studied in recent years. These elements play essential roles in many intracellular catalytic reactions, and a few are essential components of many enzyme molecules.[9]

Although trace elements are widespread in animal and plant tissues, their intracellular distributions are poorly known because subfractionation of tissues usually yields amounts inadequate for chemical analyses. Because neutron activation analysis has proved valuable in quantitative determinations of minute samples, experiments were initiated to apply this method to analyze subcellular fractions, with emphasis on purified intracellular membranes. Although we used rat liver in this preliminary study, we intend to extend the study to other tissues as the technical aspect of the program becomes well established.

Female rats of SD/Anl [Anl 66] strain were used throughout these experiments. Lysosomes were prepared by the flotation method described by Trouet;[10] membranes were further isolated from these particles by the method described previously.[3] Mitochondria also were purified by a previously described method.[3] They were further subfractionated into inner and outer

* This report will also appear in the Argonne National Laboratory Radiological Physics Division Annual Report, ANL-7760-III.

TABLE 41. GAMMA-RAY EMITTING NUCLIDES FOUND IN VARIOUS BIOLOGICAL MEMBRANES

Sample*	Dry sample weight, mg	Half-life, days							
		45.00	245.0	19.21	27.80	60.20	18.66	120.0	1.667
		Nuclide, counts/100 min/10 mg dry sample							
		^{59}Fe	^{65}Zn	^{60}Co	^{51}Cr	^{124}Sb	^{86}Rb	^{75}Se	^{140}La
Lysosomal membranes #1	14.2	1,700	42,000	260	1,100	3	—	180	—
Lysosomal membranes #2	20.0	1,900	6,000	110	350	8	33	180	16
Lysosomal membranes #3	16.7	1,300	1,400	71	3,500	4	130	55	—
Lysosomal membranes #4	13.3	1,300	790	220	2,000	—	46	89	21
Unfractionated mitochondria	80.7	110	700	38	160	5	120	140	14
Mitochondrial inner membranes	155.2	53	670	33	41	5	6	86	—
Unfractionated endoplasmic recticulum #1	146.5	540	290	5	46	—	32	17	—
Unfractionated endoplasmic reticulum #2	85.4	1,500	450	7	120	1	98	38	—
Smooth membranes of endoplasmic reticulum #1	51.4	140	57	1	37	12	19	6	10
Smooth membranes of endoplasmic reticulum #2	112.0	180	160	2	18	3	120	27	7
Nuclei	142.4	22	140	2	63	1	3	—	—

* The numbers 1, 2, etc. represent separate preparations from different groups of animals.

membranes according to a method described by Jones and Jones.[11] Endoplasmic reticulum and their subfractions, i.e., smooth membranes, rough membranes, and free polysomes, were purified by a method of Bloemendal et al.[2] Nuclei were purified by the method of Blobel and Potter.[12]

The purity of each of these subcellular fractions was confirmed by electron microscopy and by the determination of marker enzymes.

Samples were dried at 90°C in an oven for 24 to 36 hours. A known quantity of each sample was placed in a polyethylene capsule, which was irradiated at Ames, Iowa, in the Iowa State University reactor (flux approximately: 1×10^{13} n/cm^2/sec). The irradiation time for all samples was 13 hours and 35 minutes. Except for ^{140}La, this analysis was restricted to "long-lived" nuclides. Gamma-ray spectrometry was done, in conjunction with a 35-cc Ge(Li) detector and a 4096 channel analyzer. The first analysis began about 10 days after irradiation, with each sample counted for 20,000 seconds. The analysis was repeated (except for ^{140}La) approximately 53 days after irradiation, with each sample counted for 60,000 seconds (1000 minutes). Gamma-ray analysis was by a peak integration method furnished by Henry Lucas of Radiological Physics Division.

PROGRESS REPORT

Table 41 is a summary of gamma-ray emitting nuclides in various samples under study. Results are presented in counts per 100 minutes per 10 mg of dried sample weight.

As the concentrations of these elements have not been quantitated, results should be read as relative values, and compared from one category of preparations against the others.

CONCLUSIONS

1. Iron, zinc, cobalt, chromium, antimony, rubidium, selenium, and lanthanum were found in the samples tested. The first 5 elements were found in all samples, while the last 4 elements are absent from some.

2. Lysosomal membranes have the highest content of iron, zinc, cobalt, and chromium per unit dried weight. The content of zinc and chromium varied widely from one preparation to the other; this might be due to a difference in food intake and absorption.

3. Mitochondria have a relatively high content of zinc, and this element seems mainly to be localized in the inner membranes. The inner membranes, however, had only a small fraction of the iron, chromium, and rubidium, compared with the concentrations of these elements in the whole mitochondria.

4. Endoplasmic reticulum has a high concentration of iron and zinc, and a very low concentration of cobalt. Concentrations of these first two elements, however, were much lower in the smooth membranes, compared with the whole endoplasmic reticulum fraction.

5. Purified nuclei have few trace elements, and their concentrations are low; the concentration of zinc is highest among elements.

6. The above results indicate that neutron activation analysis is valuable for the studies of purified biological membranes. Work is in progress to quantitate these elements, and it is intended to apply this method to other biological membranes, including those from normal and pathological human tissues. Other biologically important elements, including arsenic, mercury, calcium, magnesium, vanadium, manganese, copper, nickel, will also be included in this study.

REFERENCES

1. Van den Bosch, H., L. M. G. van Golde, A. J. Slotboom, and L. L. M. van Deenen. *Biochim. Biophys. Acta* **152,** 694–703 (1968).
2. Bloemendal, H., W. S. Bont, M. de Vries, and E. Benedetti. *Biochem. J.* **103,** 177–182 (1967).
3. Haglund, H. *Science Tools* **14,** 17–23 (1967).
4. Rahman, Y. E., J. Verhagen, and D. F. M. v.d. Wiel. *Biochem. Biophys. Res. Commun.* **38,** 670–677 (1970).
5. Rahman, Y. E., C. Peraino, and E. A. Cerny. Argonne National Laboratory Biological and Medical Research Division Annual Report, 1969. ANL-7635, pp. 220–224.
6. Karnovsky, M. J. *J. Cell Biol.* **27,** 137 A (1965).
7. Steere, R. L. *J. Biophys. Biochem. Cytol.* **3,** 45–60 (1957).
8. Wrigglesworth, J. M., L. Packer, and D. Branton. *Biochim. Biophys. Acta* **205,** 125–135 (1970).
9. Bowen, H. J. M. Trace Elements in Biochemistry. Academic Press, 1966.
10. Trouet, A. *Arch. Int. Physiol. Biochim.* **72,** 698–700 (1964).
11. Jones, M. S. and O. T. G. Jones. *Biochem. J.* **113,** 507–514 (1969).
12. Blobel, B. and V. R. Potter. *Science* **154,** 1662–1665 (1966).

THE SPECIFICITY OF DEAMINATION OF ADENOSINE SULFUR COMPOUNDS

Fritz Schlenk, Cynthia R. Zydek-Cwick and Nancy K. Hutson

PURPOSE AND METHODS

The deamination of adenosine-5′-thioethers by an enzyme from *Aspergillus oryzae*[1] has been studied in some detail to provide a firm foundation for the numerous analytical applications of this enzyme.[2, 3] The relative rate of deamination of adenosine derivatives is illustrated in Figure 27. 5′-Methylthioadenosine is the most reactive of all adenosine derivatives studied to this date. As in the case of the thioethers, the deamination of 5′-methylthioadenosine (±) sulfoxide and of S-adenosyl-L-homocysteine (±) sulfoxide was found to proceed to completion. This shows that the enzyme reacts with both sulfoxide stereoisomers.

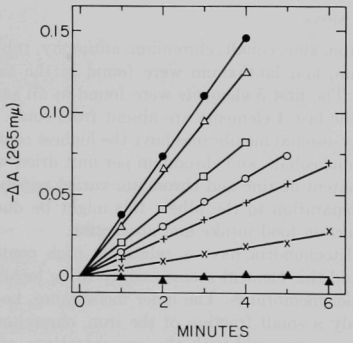

FIG. 27.—Initial rate of deamination of adenosine 5′-sulfur derivatives by deaminase from *Aspergillus oryzae*. The concentration of the substrates was 0.067 mM in 0.1 M potassium phosphate buffer, pH 6.8. Purified deaminase (1.5 μg/ml) was added, and the decrease in absorbance (265 mμ) was measured at 25°. 5′-Methylthioadenosine, (●); 5′-ethylthioadenosine, (△); adenosine, (□); 5′-methylthioadenosine (±) sulfoxide, (○); S-adenosyl-L-homocysteine, (+); S-adenosyl-L-homocysteine (±) sulfoxide, (×); (−)S-adenosyl-L-methionine, with a tenfold concentration of enzyme, (▲).

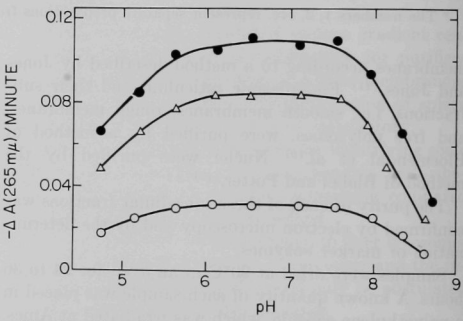

FIG. 28.—The pH activity relation of deamination by the *Aspergillus oryzae* deaminase. The substrates (0.10 mM) in 0.1 M potassium phosphate were treated with purified enzyme (1.2 μg protein per ml) at 25°; the pH values were determined after the reaction. 5′-Methylthioadenosine, (●); adenosine, (△); S-adenosyl-L-homocysteine, (○).

PROGRESS REPORT

None of the adenosine sulfonium compounds was affected by the deaminase. Examined were, (−)S-adenosyl-L-methionine, (−)S-adenosyl-L-ethionine, (−)S-adenosyl-L-(2-hydroxy-4-methylthio)butyric

acid, (±)S-adenosyl-L-methionine, and 5′-S-dimethylthioadenosine. The inactivity of the latter two compounds as substrates indicates that steric factors are not involved in their failure to be bound by the deaminase. In the (+)stereoisomer, the amino acid part is oriented differently, and the small size of the substituents in the 5′-dimethylsulfonium compound should permit interaction with the enzyme. The positive charge of the sulfonium pole apparently precludes the approach to the deaminase.

Of the reactive compounds, the adenosine thioethers are most important in nature, because they are the residual products after enzymatic group transfer from the sulfonium donor, (−)S-adenosyl-L-methionine. Their reaction was studied, therefore, in more detail. Figure 28 shows the pH-activity relationship. The binding constants are illustrated in Figure 29. Experiments with adenosine were included for reference.

In other experiments, it was found that a threefold excess of the deaminated reaction products, 5′-methylthioinosine and S-inosyl-L-homocysteine did not inhibit the rate of deamination of the corresponding adenosine compounds by more than 15%. The presence of twice the amount of (−)S-adenosyl-L-methionine, from which the adenosine thioethers are formed in biological processes, did not inhibit the deamination in a measurable way.

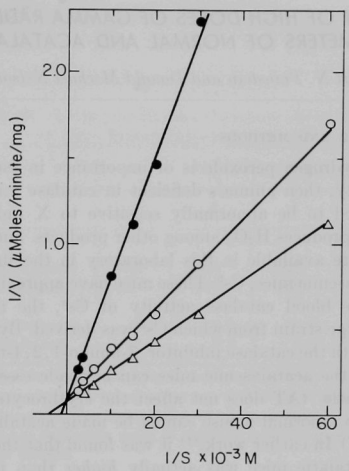

FIG. 29.—The substrate dependence of the rate of deamination of S-adenosyl-L-homocysteine, (●); adenosine, (○); and 5′-methylthioadenosine, (△). The rate of deamination was measured by spectrophotometry at 265 mμ.

CONCLUSIONS

All prerequisites for spectrophotometric assay of transmethylation[1] are fulfilled, provided that the absorbance of the substrate and reaction product does not cause major interference with the measurements at 265 nm. The deamination of the demethylated donor is very fast compared with most of the known transmethylations; hence, kinetic measurements of transmethylation by continuous spectrophotometry is possible.

REFERENCES

1. Schlenk, F. and C. R. Zydek-Cwick. Argonne National Laboratory Biological and Medical Research Division Annual Report, 1968. ANL-7535, pp. 250–251.
2. Zappia, V. and F. Schlenk. Argonne National Laboratory Biological and Medical Research Division Annual Report, 1968. ANL-7535, pp. 251–253.
3. Schlenk, F. and C. R. Zydek-Cwick. Argonne National Laboratory Biological and Medical Research Division Annual Report, 1969. ANL-7635, pp. 201–203.

STABILIZATION OF MUTANT CATALASE BY COMPLEX FORMATION WITH ANTIBODY TO NORMAL CATALASE*

Robert N. Feinstein, Bernard N. Jaroslow, Judith B. Howard, and Joann T. Faulhaber

This study concerns a mouse strain which is mutant with respect to blood and tissue catalase. The mutant catalase is abnormally sensitive to heat and extraordinarily sensitive to mild alkalinity. Antisera prepared by immunizing rabbits to the blood of normal mice stabilize the mutant catalases against the effect of heat and alkaline pH. As a result of this stabilization, the antigen-antibody complex exhibits a greater catalatic activity than was originally added, i.e., an apparent activation.

* Abstract of paper to be published in *J. Immunology*.

EFFECT OF HIGH DOSES OF GAMMA RADIATION ON SURVIVAL AND CERTAIN BLOOD PARAMETERS OF NORMAL AND ACATALASEMIC MICE

*Robert N. Feinstein and Donald Michael Nelson**

PURPOSE AND METHODS

If hydrogen peroxide is of importance in radiation lethality, then animals deficient in catalase might be expected to be abnormally sensitive to X radiation, which produces H_2O_2 among other products. Such animals are available in this laboratory in the shape of acatalasemic mice, Cs^b. These mice have approximately 1% the blood catalase activity of Cs^a, the normal, wild type strain from which Cs^b was derived. By injection with the catalase inhibitor, 3-amino-1,2,4-triazole (AT), the acatalasemic mice can be made essentially acatalatic. (AT does not affect the erythrocyte catalase, so a normal mouse cannot be made acatalatic by its use.) In earlier work,[1] it was found that the LD_{50} of acatalatic mice was actually *higher* than that of normal mice, rather than lower, as expected. Because H_2O_2 might be of greater significance after a very large dose, we have irradiated normal and acatalasemic mice, with and without preliminary injections of AT, with 25 to 75 kR of gamma radiation and have measured the survival time. In addition, because of fortuitous observations of apparent strain differences in certain blood parameters after these high doses, we have also done some systematic, though preliminary, studies of heme pigments, serum proteins, and hematocrit.

PROGRESS REPORT

Data from this study have been analyzed according to mouse strain and sex, treatment with AT (vs. control with saline), dose of radiation, and, in the case of the various blood parameters, time after irradiation at which blood was sampled. Results are far too voluminous to detail in this brief report, but the following are tentative statements of results observed:

a) Cs^b (acatalasemic) mice survive for significantly shorter periods of time after 25 to 75 kR than do Cs^a (normal) mice.

b) Generally, more methemoglobin is found in the blood of Cs^b mice than Cs^a after irradiation.

c) The postradiation hematocrit tends to be higher in Cs^b than in Cs^a mice.

d) As might be expected in mice with increased hematocrit values, the total heme pigment of the blood of Cs^b mice post-radiation tends to be higher than that of Cs^a mice.

e) The serum protein level of Cs^b mice post-radiation is generally lower than that of comparably treated Cs^a animals.

It must be emphasized that (1) these are preliminary results only, and (2) the interstrain differences noted are statistically significant only in some of the groups. Much more work is needed to establish these findings with certainty. In particular, it is expected that when the Cs^b locus is established in a highly inbred mouse line—a procedure now in progress—data will be more consistent and definitive.

CONCLUSIONS

The presence or absence of catalase, particularly in the blood, has important consequences on the response of mice to high doses (25 to 75 kR) of gamma radiation. It is tentatively concluded that animals with and without blood catalase respond to these high doses differently with respect to survival time, hematocrit, total heme pigment of blood, percent of methemoglobin, and serum protein levels.

REFERENCE

1. Feinstein, R. N., J. T. Faulhaber, and J. B. Howard. *Radiat. Res.* **35**, 341 (1968).

* Associated Colleges of the Midwest semester student from Cornell College.

BIOCHEMISTRY OF CATALASE: INTRODUCTION

Robert N. Feinstein

Our studies on the chemistry, reactions, and functions of the enzyme catalase have led into a variety of areas. The overall purpose of these studies is to assess the role of this enzyme in mammalian physiology and pathology. Subsidiary to this basic purpose are investigations on modification of catalatic levels *in vivo;* properties and activity levels of the enzyme in various sources; and attempts at purification of the enzyme from hitherto unused sources.

BIOCHEMISTRY OF CATALASE. I. CATALASE DECREASE IN LIVER AFTER SUBCUTANEOUS INJECTION OF TALC

Robert N. Feinstein and Judith B. Howard

PURPOSE AND METHODS

It has been widely reported that the level of catalase activity in the liver is considerably decreased as the result of a far-ranging gamut of diseases and other traumata. Best known and most studied is the effect of the presence of a malignancy. However, liver catalase will also be decreased as a result of such traumata as partial hepatectomy or even sham partial hepatectomy (laparotomy without hepatectomy),[1] the subcutaneous implantation of talc,[2] and others. Although liver catalase decreases, its disposition has not yet been determined. Using Nishimura's[2] technique of talc implantation, we wished to confirm his observation, and to see whether or not the decreased liver catalatic activity ever appears in the blood. To this end, a series of normal mice were injected subcutaneously either with sterile distilled water, or with a suspension of talc in sterile distilled water. Mice were sacrificed daily, and the catalase activity of the liver and of the plasma was assayed.

PROGRESS REPORT

Table 42 substantiates the decrease in liver catalase reported by Nishimura after talc injection.[2] It also indicates that catalatic activity does not increase in the plasma.

TABLE 42. LIVER AND PLASMA CATALASE AFTER INJECTION OF TALC SUBCUTANEOUSLY INTO MICE

	Days post-injection			
	1	2	3	4
Liver				
Water-injected	990	1010	1120	1000
Talc-injected	991	533	460	630
Plasma				
Water-injected	0.7	0.8	0.9	0.6
Talc-injected	0.8	0.6	0.5	0.7

Mice were injected subcutaneously either with one gram of talc suspended in 2 ml of water, or with 2 ml of water alone. Each datum is the mean value of three individual animals. Figures are perborate units of catalase activity/gram of liver or/ml of plasma.

CONCLUSIONS

The amount of catalatic activity lost from the liver after talc injection should have been readily detected in the plasma *if* it appeared in the circulation as active catalase. Because an increase in plasma catalatic activity was not detected, we conclude that liver catalase undergoes some sort of transformation after animal exposure to this sort of trauma. The most probable mechanisms would seem to be conversion to an inactive form, proteolytic degradation, or dissociation into subunits.

BIOCHEMISTRY OF CATALASE. II. EFFECT OF COMPOUNDS RELATED TO AMINOTRIAZOLE ON BLOOD AND LIVER CATALASE

Robert N. Feinstein, Judith B. Howard, and Rosanne Savol

PURPOSE AND METHODS

This continues a series of reports of a search for compounds capable of inhibiting the catalase activity of mouse liver and blood *in vivo*. These tests are conducted in two steps: a) Intraperitoneal toxicity is tested, generally starting with a maximum of 1000 mg/kg and serially diluting by a factor of two until a nonlethal level is reached. If the compound is strongly acid or alkaline, it is brought to within the range of pH 6 to 8 by addition of NaOH or HCl immediately before use; if the compound is insufficiently soluble, it is suspended in neutralized 5% gum arabic. b) The compound is injected intraperitoneally at the highest nonlethal level, and one hour later blood and liver are sampled and assayed for catalatic activity. Enzyme activities are compared (Table 43) with those of mice injected with saline.

TABLE 43. COMPOUNDS TESTED

Compound	Dose tested, mg/kg	Effect on catalase of	
		Liver, %	Blood, %
Cyanamide	100	−73	+25
Dimethyldithiocarbamic acid	500	−17	+2
3-Amino-3-pyrazoline	500	−4	+18
Thiazole	1000	−16	+3
5-Amino-4-pyrazolecarboxamide	1000	−18	+12
2-Thiophene carbonitrile	1000	−4	+21
Pyrazole	600	−43	+15
5-Amino-4-pyrazole carbonitrile	1000	−10	−6
5-Amino-3-methylisothiazole	500	+19	+8
1H-Tetrazole	100	+9	+12
Isothiazole	25	+11	+8

PROGRESS REPORT

Since the last report,[3] compounds (Table 43), all purchased from Aldrich Chemical Company, Milwaukee, Wisconsin, have been tested.

CONCLUSIONS

No compound has yet been tested, either in previous work or in the present report, which inhibits blood catalase significantly *in vivo*. In those instances where blood catalase appears to *increase* somewhat, the mechanism is probably a mild hemoconcentration, although this possibility has not been specifically tested. Among the present compounds, pyrazole inhibits liver catalase somewhat, and cyanamide inhibits appreciably. Neither of these compounds, however, is as efficient an inhibitor as some reported earlier.[4]

BIOCHEMISTRY OF CATALASE. III. HEAT STABILITY AND UREA STABILITY OF CATALATIC ACTIVITY IN BLOOD AND VARIOUS TISSUES

Robert N. Feinstein and Judith B. Howard

PURPOSE AND METHODS

Stability to heat and to urea have proven to be fairly sensitive and very reproducible parameters which describe the behavior of catalatic activity in a variety of bloods.[5, 6] We were interested in extending these observations to tissue extracts. The ultimate aims are twofold: a) the possibility of distinguishing between the catalase of tissue cells and that of blood contaminating the tissue, and b) the possibility of distinguishing between the catalase of normal tissues and those exposed to such influences as infections, etc., where an exogenous catalase might be introduced. Methods have been described in earlier papers.[5, 6] Although the shape of temperature- and urea-sensitivity curves is also of interest, the single point taken as characteristic of the preparation tested is the T_{50} or the U_{50}, defined as the temperature (in degrees C) or the urea concentration (in molarity) at which 50% of the catalatic activity is lost under the conditions of the test.

TABLE 44. STABILITY TO HEAT AND UREA OF THE CATALATIC ACTIVITY OF VARIOUS MOUSE BLOODS AND TISSUES

Catalase source	T_{50}, °C	U_{50}, M
Cs^a (normal, wild type) blood	47.7	1.70
Cs^c (hypocatalasemic homozygote) blood	44.2	0.75
Cs^aCs^c (hypocat. heterozygote) blood	46.3	1.26
Cs^a liver (treated as 0.1% homogenate)	52.4	1.28
Cs^a liver (treated as 2% homogenate)	48.6	not done
Cs^a kidney (treated as 0.2% homogenate)	49.5	1.53
Cs^a brain (treated as 10% homogenate)	48.1	1.75

T_{50} and U_{50} are defined, respectively, as the temperature (in degrees C) or the urea concentration (in molarity) at which 50% of the catalatic activity is lost under the conditions of the test.

PROGRESS REPORT

Table 44 lists the T_{50} and the U_{50} values for the variety of mouse bloods and tissues thus far tested. For the sake of completeness, some values are also included from the earlier studies.[5, 6]

CONCLUSIONS

Several conclusions seem permissible from the data of Table 44:

1. The sensitivity of brain catalase and blood catalase to both heat and urea is so similar as to suggest the possibility that much or all of the small catalatic activity of brain is actually blood contaminant.

2. As earlier indicated,[2] differences in sensitivity to urea tend to be greater than differences in sensitivity to heat.

3. Exact sensitivity to heat is dependent on the concentration of tissue tested. Surprisingly, in the one instance tested, the more concentrated liver homogenate was significantly *more* sensitive to heat than was a less concentrated homogenate. This is in contrast to the usual biochemical dictum that in concentration there lies stability.

BIOCHEMISTRY OF CATALASE. IV. AGE VARIATION IN CATALATIC ACTIVITY OF LEG AND BREAST MUSCLE OF MALLARD DUCKS

*Robert N. Feinstein and Charles W. Dane**

PURPOSE AND METHODS

We earlier found[7] that in three species of wild duck (*Anas clypeata, A. discors,* and *A. crecca*), catalase of leg muscle was lower in activity than was catalase of breast muscle, whereas the ratio was reversed in the case of the common chicken (*G. domesticus*). This was interpreted as suggesting that muscle catalase activity may be a reflection of functional usage. To gain further evidence on this point, the breast and leg muscles of mallard ducks (*Anas platyrchynchos*) were assayed for catalase activity at various ages, before and after flight capability. Birds were sampled at 3, 21, 37, and 87 days of age. Only the 87-day-old birds had full flight capability, but the breast muscle of 37-day-old birds may have received some increased use because the weight of primaries may have begun to require additional effort in holding wings up in place. Birds were sacrificed, and muscles dissected, in North Dakota. Muscles were then shipped frozen in dry ice to Argonne, where they were assayed.

PROGRESS REPORT

Table 45 lists mean and standard error of the mean, of catalase activity of breast and leg muscles of birds of various ages. The ratio of catalatic activity of breast muscle to that of leg muscle is also given.

CONCLUSION

The data shown do not bolster the earlier suggestion that muscle catalase reflects functional usage. Results of breast muscle assays are particularly conclusive: whereas the above suggestion would predict an increase in catalatic activity as the birds attain flight capability, the data show a definite decrease with age, covering both flight and pre-flight periods.

TABLE 45. BREAST AND LEG MUSCLE CATALASE

Age, days	Catalase activity, perborate units /gram		Ratio breast/leg
	Breast	Leg	
3	15.5 ± 0.7	13.6 ± 0.9	1.15
21	11.6 ± 0.6	7.9 ± 0.8	1.51
87	9.5 ± 0.7	6.7 ± 0.8	1.49
87	7.9 ± 1.0	6.7 ± 0.6	1.18

Each group consists of five male birds. Data given are mean and standard error of the mean.

* Northern Prairie Wildlife Research Center, Jamestown, North Dakota.

BIOCHEMISTRY OF CATALASE. V. ATTEMPTS AT DIRECT SEPARATION OF CATALASE FROM MOUSE BLOOD

Robert N. Feinstein, Rosanne Savol, Judith B. Howard, and Carl Peraino

PURPOSE AND METHODS

For a variety of reasons, it would be very desirable to have a preparation of pure mouse blood catalase. Many methods are available for the preparation of pure catalase from the liver and blood of many mammalian species, including the catalase of mouse liver, but none for obtaining catalase from mouse blood. Part of this is due to the obvious difficulty of obtaining large quantities of mouse blood, but this is not an insurmountable obstacle. Exsanguination of one adult mouse, via the orbital sinus, will yield 0.5 to 0.8 ml of whole blood, and a skilled operator can exsanguinate almost 100 mice per hour. Far more important than this consideration is the fact that mouse blood catalase is extremely labile. Even if all work is carefully performed in an ice bath or a cold room, loss of catalatic activity is prohibitive over a prolonged period. We have therefore considered several techniques for a possible single-pass purification, or at least a technique with minimal manipulation. The techniques that have been tested are the following:

1. Isoelectric focusing
2. Separation by Sephadex gel filtration
3. Separation by $Ca_3(PO_4)_2$ or hydroxylapatite gel adsorption
4. Separation by filtration through Diaflo membranes.

PROGRESS REPORT

None of the above have proven satisfactory, for the following reasons:

1. Isoelectric focusing, with apparatus at present available, can accept only small samples, a maximum of perhaps 2 ml of concentrated blood lysate. Special large-scale columns can approximately quadruple this volume, but even such amounts are quite inadequate. Isoelectric separation requires approximately 48 hours, and in this time 50 to 80% of the catalatic activity will have been lost. Furthermore, because of isoelectric heterogeneity, the original volume of blood is manyfold expanded in catalase fractions, and a considerable concentration, with unavoidable further loss, would be required. Finally, there is still appreciable overlap between catalase bands and hemoglobin bands.

2. Sephadex gel filtration is perhaps the most promising of the techniques tested. There is only a slight overlap of catalase and hemoglobin peaks, and with recycling techniques, the separation could probably be made quite sharp. This technique also does not lend itself to large-scale preparations, 0.5 to 1.0 ml of blood lysate being the maximum usable on laboratory size columns; large scale equipment is available, however, on which many times this amount could be filtered. Time required is perhaps a quarter of that needed for isoelectric focusing, or even less, but the problem remains that volumes expand enormously in the process of elution, so that considerable concentration again becomes essential.

3. Although differential adsorption on, and elution from, $Ca_3(PO_4)_2$ gel is a common step in many catalase purifications, it is not satisfactory for the initial separation of catalase from the bulk of blood proteins, especially hemoglobin. We have tested a wide variety of pH's, ionic strengths, etc., for the adsorption on, and elution from, both $Ca_3(PO_4)_2$ and the related hydroxylapatite gels. In no case have we achieved a satisfactory separation of catalase.

4. The use of Diaflo membranes (Amicon Corporation) once appeared to be the answer to our problem. These membranes are available in graded pore size, including some that theoretically should pass hemoglobin but not catalase. An additional advantage is that equipment is available for large scale, even continuous process, preparations. Unfortunately, the membranes do not live up to their advance billing; separation of catalase and hemoglobin is extremely poor.

CONCLUSIONS

Although the preparation of pure mouse blood catalase remains a highly desirable goal, we have made essentially no progress toward it, other than the testing and eliminating of several unsatisfactory techniques.

REFERENCES

1. Feinstein, R. N., J. B. Howard, and H. Suter. Argonne National Laboratory Biological and Medical Research Division Annual Report, 1967. ANL-7409, p. 128.
2. Nishimura, E. T., S. Rosenheim, and L. Klein. Lab. Investigation **12**, 415(1963).
3. Feinstein, R. N., J. T. Faulhaber, and J. B. Howard. Argonne National Laboratory Biological and Medical Research Division Annual Report, 1968. ANL-7535, p. 96.
4. Feinstein, R. N., J. E. Seaholm, and L. B. Ballonoff. *Enzymologia* **27**, 30 (1964).
5. Feinstein, R. N., G. A. Sacher, J. B. Howard, and J. T. Braun. *Arch. Biochem. Biophys.* **122**, 338 (1967).
6. Feinstein, R. N., J. T. Braun, and J. B. Howard. *Biochem. Gen.* **1**, 277 (1968).
7. Feinstein, R. N., J. B. Howard, and J. T. Faulhaber. *Int. J. Radiation Biol.* **15**, 341 (1969).

CYTOLOGICAL EFFECTS OF LETHAL X IRRADIATION ON YEAST CELLS

George Svihla, Julia L. Dainko, and Fritz Schlenk

PURPOSE AND METHODS

The inability to form colonies has been used in most X-irradiation studies of yeast as a criterion of the radiation effect. Although colonies are not formed after large doses of radiation, the cells may produce one or two deformed buds. Few cytological details of this process have been reported.

When yeast cells (e.g., *Candida utilis*) are cultivated in a medium supplemented with L-methionine, chemical analysis reveals that the cells contain S-adenosyl-L-methionine, and ultraviolet micrography reveals that most of the material is confined to the vacuole.[1]

Lethal X radiation (400 kR) and gamma radiation (1.0 Mrad) do not impair the ability of the cells to synthesize ATP and S-adenosylmethionine, or to accumulate the S-adenosylmethionine in the vacuole.[2]

Therefore, it appeared possible to study the continued biosynthetic function of the cell after lethal doses of X radiation by utilizing ultraviolet micrographs of the process of bud formation under these conditions.

PROGRESS REPORT

Yeast cells (*Candida utilis*) cultivated in L-methionine supplemented medium contained 20 to 25 μmoles of S-adenosyl-L-methionine per gram of cells. When the cells were X irradiated (100 kR), the viability, as judged by plate counts, was reduced to less than 0.1%.

After transfer of the cells into non-supplemented ammonium salt and glucose medium, an ultraviolet micrographic record of bud formation was made. Unirradiated cells produced normal buds. Most irradiated cells produced greatly elongated buds that did not separate from the parent cells. In the early stages of bud formation, when the bud was smaller than the parent, the concentrations of S-adenosylmethionine in the vacuoles of parent and bud were about equal. As the buds became larger, more S-adenosylmethionine appeared to be located in the bud than in the parent cell (5 hr at 30°C). After prolonged cultivation, 24, and 72 hours, some of the elongated buds produced structures that resembled spores of *Sporobolomyces;* in fact, the complex of parent cell, elongated bud, and sporelike bud strongly resembled structures formed when a *Sporobolomyces* spore germinates under poor nutritional conditions, produces a short mycelium, and then produces a spore at the end of the mycelium.

Candida utilis cells may produce elongated buds under nutritional stress. Our irradiated cells produced elongated cells in a medium provided with more than ample nutrients to support normal budding of unirradiated cells.

CONCLUSIONS

The change in shape of newly synthesized cell walls after lethal X irradiation in yeast cells, suggests a change in the enzyme systems responsible for the determination of the structure and shape of the cell wall. The reason for the presence of more S-adenosylmethionine in the vacuoles of the elongated buds than in the parent cells cannot be established from existing information. Further investigation of the characteristics of the cell wall is to be carried on by the use of enzymes to digest the cell wall. Hopefully, the response of the cell walls and protoplasts of both bud and parent cell will provide some clue to the observed irradiation effects.

REFERENCES

1. Janicek, L. E. and G. Svihla. *J. Biol. Photographic Assoc.* **36,** 59–66 (1968).
2. Schlenk, F. and J. L. Dainko. *Radiat. Research* **16,** 327–335 (1962).

CRYOSTAT CUT, FREEZE-DRIED TISSUES FOR MICROSCOPIC INVESTIGATIONS*

Per Freitag,† Milton B. Engel,† and George Svihla

Employing the cryostat and freeze-dry techniques we have prepared tissues with minimal artifacts for interferometry, ultraviolet micrography, and light microscopy. Pieces of tissue, measuring 2 to 3 mm in diameter, are attached to aluminum nails with blood, frozen quickly at −150°C in isopentane chilled in liquid nitrogen, and sections 2 micra or thicker are cut in a cryostat. The sections are freeze-dried under vacuum inside the cryostat at −40°C. When dry, the sections are brought to room temperature in a desiccator and used directly (for interferometry or enzyme histochemistry), vapor fixed (for UV micrography), or fixed in conventional fixatives (for histological staining). The technique has the advantage of leaving extractable tissue components *in situ.*

* Abstract of a paper presented at INTER/MICRO-70, an international conference on microscopy in Chicago, June 29–July 2, 1970 and to be published in the *Microscope.*

† Temporary appointees, Center for Educational Affairs and Division of Biological and Medical Research. Present addresses: P.F.—Dept. of Anatomy, University of Minnesota; M.B.E.—University of Illinois at the Medical Center.

THE BIOCHEMISTRY OF DEVELOPMENT

Richard E. Ecker

This is an extension of work that, in prior years, has been collaboratively reported by L. D. Smith and me. No report was submitted in 1969, as Dr. Smith had terminated and I was on leave as Distinguished Visiting Professor of Biology at Morehouse College in Atlanta, Georgia. It has been, and will continue to be, the purpose of this program to investigate the biochemical mechanisms involved in the control of developmental processes. The methods we used for these studies have been outlined in previous reports.

The following five abstracts represent work completed in this program since the publication of our last report in 1968.

As I have only recently returned to the Laboratory, there are no current results to report. However, the work now in progress will concentrate primarily on the biochemical basis of hormone action.

THE BIOCHEMISTRY OF DEVELOPMENT. I. UTERINE SUPPRESSION OF BIOCHEMICAL AND MORPHOGENETIC EVENTS IN RANA PIPIENS*

L. Dennis Smith and Richard E. Ecker

The induction of maturation in *R. pipiens* oocytes, either *in vivo* or *in vitro*, stimulates events which occur at the same rate in both beyond the time of ovulation (first meiotic metaphase). When oocytes are maintained *in vitro*, they proceed to the second meiotic metaphase and beyond, uninterrupted, to the limits of their potential. Given the proper *in vitro* environment, this potential includes gastrulalike morphogenetic movements (pseudo-gastrulation) and a characteristic decreasing rate of protein synthesis. When maturing oocytes are maintained *in vivo*, however, the pattern is interrupted at some point after the oocytes enter the oviductal-uterine environment. This interruption includes a change in environment sufficient to halt pseudo-gastrulation and may also include a marked decrease in the rate of protein synthesis to a level sufficient to maintain mature eggs for several days in storage. At some point soon after expulsion from the uterine environment, protein synthesis increases to an elevated level. We have suggested that this "second" stimulation is brought about by the environmental change, not by fertilization or artificial activation as such.

* Abstract of paper published in *Develop. Biol.* **22**, 622–637 (1970).

THE BIOCHEMISTRY OF DEVELOPMENT. II. INFLUENCE OF EXOGENOUS IONS ON THE EVENTS OF MATURATION IN RANA PIPIENS OOCYTES*

Richard E. Ecker and L. Dennis Smith

Full-grown ovarian oocytes removed from non-hormone-treated *Rana pipiens* females exhibit a low level of protein synthesis, the rate of which is dependent upon the ionic environment. The highest rates of protein synthesis in these oocytes are obtained in media containing either a divalent cation (Ca^{++} or Mg^{++}) or high levels of K^+. The dependence of protein synthesis on ionic environment persists through about the first 18–24 hours of maturation (at 18°C). Normal maturation of oocytes *in vitro* also has specific ionic requirements for the first 24 hours. In this case, the process requires high ionic strength ($\Gamma/2 = 0.10 - 0.12$) and divalent cations. The kinetics of K^+ exchange suggest that K^+ exists in the ovarian oocyte in two compartments; one in equilibrium with the exogenous medium and freely exchangeable; the other in equilibrium with the first internal compartment and only very slowly exchangeable. The slowly exchangeable (bound) compartment contains about 95% of all endogenous K^+. In hormone-stimulated oocytes, the kinetics of K^+ exchange are essentially the same. Oocyte adaptation to ionic environment is discussed as a possible regulatory mechanism during maturation.

* Abstract of paper to be published in *Journal of Cellular Physiology*.

THE BIOCHEMISTRY OF DEVELOPMENT. III. THE NATURE AND FATE OF RANA PIPIENS PROTEINS SYNTHESIZED DURING MATURATION AND EARLY CLEAVAGE*

Richard E. Ecker and L. Dennis Smith

Electrophoretic analysis of proteins synthesized during maturation, cleavage, and gastrulation indicates that patterns of protein synthesis are characteristic for each stage studied. Oocytes induced to mature *in vitro* markedly alter their pattern of protein synthesis during the period between 24 and 48 hours after hormone exposure. The same alteration occurs in oocytes from which the germinal vesicles were removed prior to hormone exposure, indicating that the oocyte cytoplasm during maturation is capable of regulating the nature of protein synthesis.

Proteins are synthesized by full-grown oocytes which have not been induced to mature. These proteins accumulate in the germinal vesicle to a concentration about 6 to 7 times that in the cytoplasm. If such oocytes are subsequently induced to mature and to

* Abstract of paper to be published in *Developmental Biology*.

continue development, the nuclei of the resulting blastulas also accumulate these proteins to about 6 to 7 times the cytoplasmic concentration, with 20 to 25% of the total amount in the blastula nuclei. Similar results are obtained with proteins synthesized at first meiotic metaphase or in cleavage embryos.

Transplanted blastula nuclei accumulate, from the cytoplasm of activated eggs, proteins that were made during maturation. Blastula nuclei, which have accumulated proteins made at earlier stages, retain these proteins when the nuclei are transplanted back into enucleated eggs and appear to apportion the protein to daughter nuclei as cell division occurs.

It is suggested that the concentration of these early proteins in the nuclei constitutes a mechanism for cytoplasmic control of nuclear function.

THE BIOCHEMISTRY OF DEVELOPMENT. IV. THE ACTION OF STEROID HORMONES ON ISOLATED OOCYTES OF RANA PIPIENS*

L. Dennis Smith and Richard E. Ecker

A variety of steroid hormones are taken up from the incubation medium by isolated *Rana pipiens* oocytes, and of those tried, eight were capable of inducing maturation *in vitro*. However, the amount of uptake varied greatly among the hormones tested, as did effectiveness in inducing maturation, and there was no clear correlation between amount of uptake and induction effectiveness. Uptake of progesterone from the medium was linear with time and proportional to the concentration of hormone in the medium. Once bound, about 50%, or more, of the hormone remained permanently associated with the oocyte.

Primary interaction of the hormone with the oocyte must occur at the oocyte surface, as injection of the hormone into the oocyte does not effect the maturation response. Injection of cytoplasm from maturing eggs, however will effect maturation in oocytes not treated with hormone. We suggest that the steroid acts at or near the surface to cause the production of a second effector which, when accumulated to a sufficient level in the oocyte, induces the observable events associated with maturation.

* Abstract of paper submitted to *Developmental Biology*.

THE BIOCHEMISTRY OF DEVELOPMENT. V. RNA SYNTHESIS DURING THE DEVELOPMENT OF THE LARGE MILKWEED BUG, ONCOPELTUS FASCIATUS*

Richard E. McDowell

RNA synthesis was studied during postembryonic and adult life of the large milkweed bug, *Oncopeltus fasciatus* (Dallas). Total RNA was synthesized at an increased rate early in each immature stage beginning immediately after nymphal ecdysis. The rate of synthesis slowed toward the end of each stage. Low molecular weight RNA (<12S) was also synthesized in a cyclic fashion, but in contrast to total RNA, synthesis peaked prior to ecdysis and then declined after ecdysis. An elevation in the synthesis of RNA with sedimentation properties characteristic of m-RNA was not observed until the second day of the fifth stadium and continued until the metamorphic ecdysis when the tritiated uridine labeling pattern was indistinguishable from that found in the early nymphal stages. The synthesis of "m-RNA" resumed later in adult life. In contrast to nymphal ecdyses, the metamorphic ecdysis resulted in only a limited increase in the rate of total RNA synthesis. The rate of synthesis in adult female insects increased later in the adult stage while a decrease in RNA content characterized the adult male. Although no differences were detected in the types of RNA synthesized by adult males and females, different species of RNA were synthesized at different rates in the two sexes.

* Abstracted from the Ph.D. thesis of Richard E. McDowell (AUA-ANL Fellowship Appointee), submitted to the faculty of St. Louis University, 1970.

Biophysics

STUDIES WITH MAMMALIAN CELLS IN CULTURE

The objectives of this program are to use mammalian cells *in vitro* (1) to examine various responses to stresses such as ionizing and ultraviolet radiation, (2) to determine basic properties of mammalian cells, particularly those relating to their growth and regulatory mechanisms. In general, these investigations embrace studies that are either difficult or impossible to conduct in mammalian cells *in vivo,* and an additional important aspect of such a program is to examine the extent to which measured responses *in vitro* can be expected to occur also *in vivo.*

In most of the investigations carried out during the past year populations of cells synchronized by various methods, but especially by mitotic selection, have been used to examine cell cycle dependent responses and phenomena. Apart from some studies of the effects of radiation on cell division and its relation to biochemical processes, the main emphasis has been on studies relating to the biochemical mechanisms underlying the dependence of cell survival upon cell cycle stage. In this regard, studies with protective agents and with sensitizers have been especially useful. Cytological studies on these cells also form an important part of the program.

In most of the investigations reported below a subline (V79-S171) of a single line of Chinese hamster cells (the V79 line derived from female lung tissue) was used. Synchronized populations of these cells were obtained by mitotic selection either with or without the addition of colcemid and the cells were subsequently treated or examined at different stages of the cell cycle. In studies involving survival, cells were allowed to grow out into colonies (after ~10 days of incubation); in population studies, cells were followed by Coulter counting and in cytological studies, cells were usually examined at the next, and in some cases additional, mitoses after treatment.

X rays were obtained from a Maxitron (G.E.) X ray machine operated at 250 kVp, 30 mA at a half value layer of 0.9 mm Cu and the cells were generally exposed to about 100 or 160 rads/min (0.945 rads/R).

Ultraviolet radiation was obtained from a G.E. germicidal lamp delivering 8.7 ergs/mm^2/sec to the exposure level of the cells.

The principal areas of investigation during the past year were (1) basic studies on the cell generation cycle, (2) radiation effects on cell division, (3) effects of protective agents and sensitizers on Chinese hamster cells, and (4) cytological studies. Summaries of these studies follow.

STUDIES WITH MAMMALIAN CELLS IN CULTURE. I. BASIC STUDIES ON CELL GENERATION CYCLES

A. Cell Cycle Compartment Analysis of Chinese Hamster Cells in Stationary Phase Cultures*

Dennis W. Ross and Warren K. Sinclair

The distribution of Chinese hamster cells with respect to the compartments of the cell generation cycle was studied in cultures in the stationary phase of growth in two different media. A measure of the state of depletion of the nutrient medium was formulated by defining a quantity termed the "nutritive capacity" of the medium. This quantity was used to verify that the cessation of cell proliferation was due to nutrient deficiencies and not to density dependent growth inhibition. Cell cultures in stationary phase were diluted into fresh medium and as growth resumed, mitotic index, cumulative mitotic index, label index and viability were measured as a function of time. The distribution of cells with respect to compartments of the cell generation cycle in stationary phase populations was reconstructed from these data. Stationary phase populations of Chinese hamster cells were found to be arrested in the G_1 and G_2 portions of the cycle, the relative proportion of cells in G_1 increasing with time in the stationary phase. In one cell medium, a fraction of the population in S was observed during stationary phase, but this fraction was not stimulated to renewed growth by dilution into fresh medium.

* Abstract of paper to be submitted to *Cell & Tissue Kinetics.*

B. Synchrony by Mitotic Selection Alone or with Colcemid in Chinese Hamster Cells

Warren K. Sinclair

The mitotic selection method of obtaining synchronous mammalian cells, first employed successfully by Terasima and Tolmach,[1] has been widely useful in many studies using Chinese hamster cells in this laboratory.[2, 3] It is the method of choice in circumstances where relatively few cells are adequate.[4] However, yield of cells is a problem in many applications and it can be increased if the culture is first treated with colcemid[5] for a period of hours and then mitotic cells are selected by shaking.[2] Since colcemid is known to have cytological and possibly other deleterious effects upon mammalian cells, it is necessary to compare responses in synchronous cells obtained with or without colcemid treatment prior to mitotic selection.

The results of pulse labeling synchronous V79-S171 cells with ^{3}HTdR as a function of time are shown in Figure 30. Evidently, although the patterns are quite similar, the colcemid-treated cells show improved synchrony but the entry of these cells into S is delayed, i.e., G_1 is prolonged and the over all length of the cell cycle is increased by this prolongation, the S period itself being of about normal duration. This is further demonstrated by the data of Figure 31 on the response of

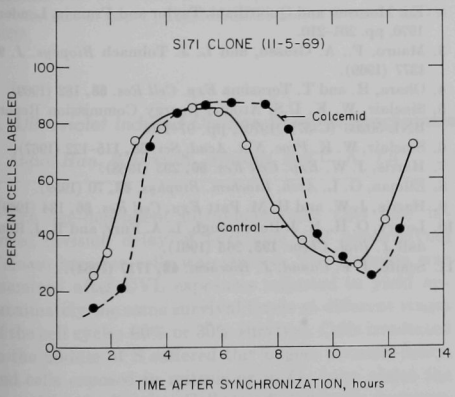

FIG. 30.—The percentage of cells labeled with ^{3}HTdR (14 Ci/mmole, 0.2 μCi/ml after a pulse label of 15 minutes at different times during the cell cycle of mitotically selected synchronous Chinese hamster cells. ○, Control. ●, Treated with 0.1 μg/ml colcemid for 2 hours prior to selection.

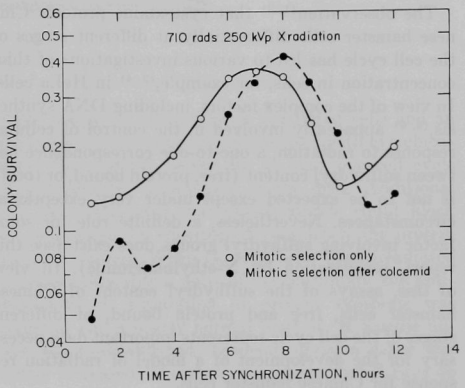

FIG. 31.—Survival of cells after 710 rads of 250 kVp X radiation given at different times during the cell cycle of mitotically selected synchronous Chinese hamster cells. ○, Control. ●, Treated with 0.1 μg/ml colcemid for 2 hours prior to selection.

these cells to X rays. Again, it is evident that the over all pattern of response is quite similar but synchrony is markedly improved with colcemid, the cell cycle is delayed by an hour or more at its end and in the prolonged G_1 period a small period of resistance, characteristic usually of longer G_1 cell lines,[3] is evident. Thus, while no major differences are evident, it is clear that the G_1 period is prolonged by approximately an hour after this treatment with colcemid and more structure may then appear in the X-ray response for G_1 cells. The plating efficiency of the colcemid-treated cells was not affected and the yield was increased by a factor of two. The improvement in synchrony is a useful property, especially as the synchrony properties of individual sublines tend to deteriorate with time and reselection is usually necessary ultimately.

REFERENCES

1. Terasima, T. and L. J. Tolmach. *Nature* **190,** 1210 (1961).
2. Sinclair, W. K. and R. A. Morton. *Nature* **199,** 1158 (1963).
3. Sinclair, W. K. *Radiation Research* **33,** 620 (1968).
4. Sinclair, W. K. *Normal and Malignant Cell Growth.* Springer Verlag, New York, pp. 90–103, 1969.
5. Stubblefield, E. and R. Klevecz. *Exp. Cell Res.* **40,** 660 (1965).

C. Variation in Sulfhydryl Content of Chinese Hamster Cells during the Cell Cycle

Warren K. Sinclair and Melvin D. Long

The observation[1, 2] that cysteamine protects Chinese hamster cells differentially at different stages of the cell cycle has led to various investigations of thiol concentration in cells, for example,[3, 4] in HeLa cells. In view of the complex factors, including DNA synthesis,[5, 6] apparently involved in the control of cellular response to radiation, a one-to-one correspondence between sulfhydryl content (free, protein bound, or total) is not to be expected except under very exceptional circumstances. Nevertheless, a definite role for some factor involving sulfhydryl groups does exist (see this report, sensitization by N-ethylmaleimide). In view of this, assays of the sulfhydryl content of Chinese hamster cells, free and protein bound, at different stages of the cell cycle represents important data necessary for the development of a model of radiation response for Chinese hamster cells.

The method is to obtain as large a quantity as possible of synchronous cells by mitotic selection (aided by colcemid treatment) and assay these cells at different times after synchronization during the subsequent cell cycle for non-protein bound (free) sulfhydryl (NPSH), protein bound sulfhydryl (PSH) and total cellular protein (P). Assays of NPSH were performed as described by Harris[7] to whom we are also indebted for advice and assistance. The method involves extraction by sulfosalicylic acid in the cold followed by assay with the Ellman dye reagent[8] 5,5′-dithiobis-(2 nitrobenzoic acid) (DTNB) and absorbance read at 412 mμ. Total protein is assayed by a modification of Lowry's procedure[9, 10] and total sulfhydryl is assayed by sonication of cells in nitrogen, in phosphate buffer containing DTNB, similar to the method described by Scaife.[11] Separate cell samples were needed for the latter. Control X-ray survival data (after 750 R) were obtained in the cell samples assayed.

The method outlined above for NPSH yields satisfactory reproducible results in Chinese hamster cells when large quantities of asynchronous cells are available for assay, provided homogenization of cells is complete so that total extraction of NPSH by the sulfosalicylic acid is achieved. EDTA may also be added to the acid to reduce oxidation of SH groups.

In experiments involving synchronous cells when only 0.5–1.0 $\times$ 10^6 cells/sample are available, optical density readings are small, cell loss and chemical assay factors become serious, and reproducibility is a much greater problem. Nevertheless, replicate samples often yield results within ~2% of each other. The results of several experiments on the NPSH content and protein content of Chinese hamster cells indicate that these compounds fluctuate during the cell cycle in a regular manner. However, at this point additional experiments and greater reproducibility are needed in order to describe the nature of these fluctuations adequately.

REFERENCES

1. Sinclair, W. K. *Radiation Research* **33,** 620–643 (1968).
2. Sinclair, W. K. *Radiation Protection and Sensitization,* Ed. Moroson and Quintiliani. Taylor and Francis, London, 1970, pp. 201–210.
3. Mauro, F., A. Grasso, and L. J. Tolmach *Biophys. J.* **9,** 1377 (1969).
4. Ohara, H. and T. Terasima *Exp. Cell Res.* **58,** 182 (1969).
5. Sinclair, W. K. U.S. Atomic Energy Commission Report BNL-50203 (C-57) (1970), pp. 97–116.
6. Sinclair, W. K. *Proc. Nat. Acad. Sci.* **58,** 115–122 (1967).
7. Harris, J. W. *Exp. Cell Res.* **50,** 293 (1968).
8. Ellman, G. L. *Arch. Biochem. Biophys.* **82,** 70 (1959).
9. Harris, J. W. and H. M. Patt *Exp. Cell Res.* **56,** 134 (1969).
10. Lowry, O. H., N. J. Rosebrough, L. A. Furr, and R. J. Randall *J. Biol. Chem.* **193,** 265 (1961).
11. Scaife, J. F. *Canad. J. Biochem.* **42,** 1717 (1964).

STUDIES WITH MAMMALIAN CELLS IN CULTURE. II. RADIATION EFFECTS ON CELL DIVISION

A. Cycloheximide and Radiation Induced Division Delay in Synchronized Chinese Hamster Cells*

Silvia Bacchetti and Warren K. Sinclair

We have studied the effects of X rays on the progression toward division and on the synthesis of proteins in Chinese hamster cells in G_2 phase, with the aim of clarifying the role played by protein synthesis in radiation-induced division delay. The results have been compared with those obtained in similar experiments with cycloheximide, an inhibitor of protein synthesis. We have observed that the terminal point of action of X rays in arresting the progression of G_2 cells occurs at 90 to 60 minutes before division and is dose-independent over the range 200 to 710 rads. However, the terminal point of action of cycloheximide is concentration-dependent and occurs at 120 to 90 minutes before division for concentrations of 2 and 5 μg/ml, and at 90 to 60 minutes before division for 50 μg/ml. Therefore, only at the higher concentration is there coincidence with X rays in the time of the terminal points of action. The two agents, moreover, have opposite effects on the synthesis of proteins. We have observed a stimulation of the uptake of ^{3}H-leucine in irradiated cells and an inhibition of this uptake in cells treated with cycloheximide. These effects persist for at least one cell cycle after irradiation or removal of the drug. Additional data have suggested that cycloheximide could block cell progression by shutting off completely the protein synthetic process. When G_2 cells have been irradiated and then exposed to a pulse of cycloheximide, the radiation-induced stimulation of protein synthesis was abolished and a nearly normal level of ^{3}H-leucine uptake was re-established; however, division delay was further increased. Therefore, it appears that X rays do not cause division delay by inhibiting the synthesis of specific proteins or the synthetic process *per se*. It also appears that the extra synthesis of proteins is not responsible for the delay, since controlling it by addition of cycloheximide prevents cell division for even a longer time. The significance of the observed extra synthesis of proteins and a possible mechanism of action of X rays in inducing division delay are discussed.

* Abstract of paper published in *Radiation Research* **44**, 788 (1970).

B. Ultraviolet Induced Division Delay in Synchronized Chinese Hamster Cells*

Antun Han, Warren K. Sinclair, and C. K. Yu

The age-dependent ultraviolet light (254 nm) induced division delay of surviving and nonsurviving Chinese hamster cells was studied. The response was examined after UVL exposures adjusted to yield approximately the same survival levels at different stages of the cell cycle: 60% or 30% survival. Cells irradiated in the middle of S suffered the longest division delay, and cells exposed in mitosis or in G_1 have about the same delay in division. Cells irradiated in G_2, however, were not delayed, at either survival level. It was further established, after exposures that yielded about 30% survivors at various stages of the cycle, that surviving cells have shorter delays than nonsurvivors. This difference was not observed for cells in G_2 at the time of exposure, i.e., both surviving and nonsurviving G_2 cells were equally delayed in division. The examination of mitotic index versus time revealed that most cells reach mitosis, but all of the increase in the number of cells in the population can be accounted for by the increase of the viable cell fraction. These observations suggest strongly that nonsurviving cells, although present during most of the experiment, are stopped at mitosis and do not divide. Cells in mitosis at the time of irradiation complete their division, and in the same length of time as unirradiated controls. Division and mitotic delays after UVL are relatively much larger than after X-ray doses that reduce survival to about the same level.

* Abstract of paper submitted to *Biophysical Journal*.

C. Effect of X Rays on DNA, RNA and Protein Synthesis in Synchronized Chinese Hamster Cells*

Silvia Bacchetti and Warren K. Sinclair

The effect of X rays on DNA, RNA and protein synthesis have been studied, using radioactive precursors, during one or two consecutive synchronous cycles of Chinese hamster cells irradiated at different stages. The results obtained for DNA synthesis have shown that maximum effects are induced when the cells are irradiated in S phase. When cells are irradiated in G_1 or G_2 phase, DNA synthesis is essentially unaffected in subsequent cycles except for division delay. These observations confirm other data in the literature. Irradiated cells were stimulated to synthesize RNA and proteins at a higher rate than the control. The stimulation was more pronounced for protein than for RNA synthesis and greatest for cells irradiated in G_1 phase. The extent of the stimulation in irradiated G_2 cells, however, was difficult to determine due to decay of synchrony and division delay. Addition of 50 μg/ml of cycloheximide for 3 hours after irradiation of G_1 and G_2 cells protected the cells to some extent against the loss of colony forming ability and inhibited the overall synthesis of DNA, RNA and proteins. After removal of the drug, the cells recovered only partially their normal level of synthesis and no indication of unscheduled metabolic activity was observed during the subsequent cycle. These observations are discussed together with other data obtained on the effects of X rays and cycloheximide on division delay.

* Abstract of paper submitted to *Radiation Research.*

STUDIES WITH MAMMALIAN CELLS IN CULTURE. III. EFFECTS OF PROTECTIVE AGENTS AND SENSITIZERS ON CHINESE HAMSTER CELLS

A. Sensitization of Chinese Hamster Cells to X Rays by N-Ethylmaleimide

Warren K. Sinclair

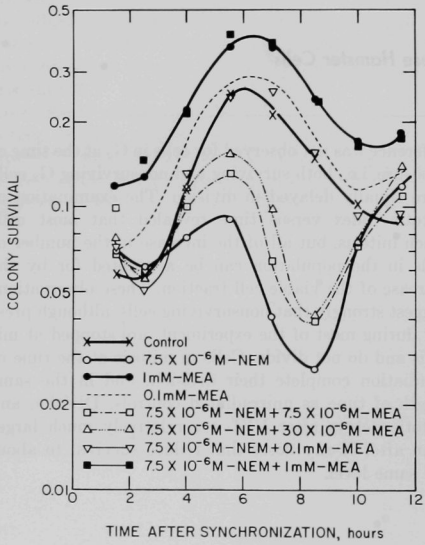

FIG. 32.—The survival of synchronous Chinese hamster cells after X rays (710 rads) at different times during the cell cycle with either no agent, N-ethylmaleimide (NEM) or cysteamine (MEA) or both in the concentrations indicated, present during irradiation.

The initial sensitization produced by 0.0075 mM NEM during the late S period, reported last year,[1] has been extended to a more complete range of doses. These data show that not only does NEM erase the resistance which normally develops during S but cells are actually maximally sensitive at about 8 to 9 hours in the cell cycle. The timing does not coincide exactly with the peak resistance (~7 hours) but occurs 1 to 2 hours later. The sensitization factor is ~1.5 to 1.6.

Cysteamine may release a protective factor (such as free non-protein sulfhydryl, NPSH) when added to the culture medium and NEM may bind to this factor. If so, it should be possible to "titrate" cysteamine (MEA) against NEM, using the sensitive Chinese hamster cells as the indicator.[2] This has been done in the data of Figure 32, in which it is clear that 0.0075 mM NEM is exactly counterbalanced by 0.1 mM MEA. The fact that the molar equivalents differ may be due to the products in the culture medium which include many

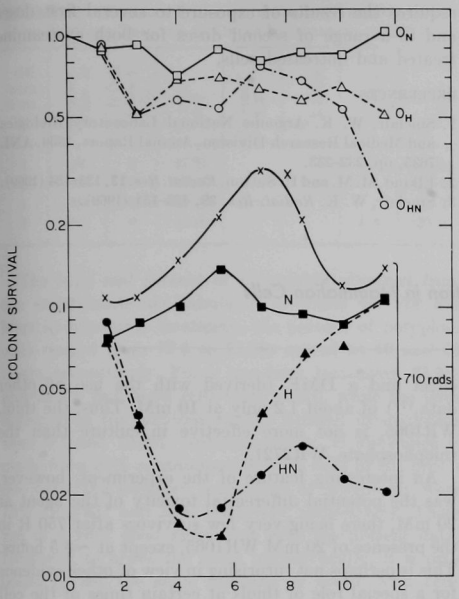

FIG. 33.—The effect of N-ethylmaleimide NEM, 0.0075 mM present during the irradiation of synchronous Chinese hamster cells with 710 rads of 250 kVp X irradiation. Curve X, 710 rads only; curve N, 710 rads given in the presence of 0.0075 mM NEM; curve H, 710 rads given to cells in which 1 mM hydroxyurea was added at 1 hour (G_1) and removed at the time of irradiation; curve HN, 710 rads given to cells in which 1 mM hydroxyurea was added at 1 hour (G_1) and 0.0075 mM NEM was present during irradiation; curves O_N, O_H, and O_{HN} indicate survival of unirradiated cells after the addition of NEM, HU, or NSM + HU, under the same conditions as for irradiated cells. The data for irradiated cells were correlated accordingly.

sulfhydryl containing reagents. This experiment suggests that whatever MEA releases, which affects radiation survival, NEM can bind and neutralize that factor completely.

In earlier studies[3, 4] it had been shown that DNA synthesis influences cell survival greatly but that when DNA synthesis was completely arrested with agents such as hydroxyurea (HU) changes in survival still took place. This seemed to suggest that another factor (? sulfhydryl or sulfhydryl-related), in addition to DNA synthesis, controlled response. An experiment in which the survival of HU-inhibited cells was examined in the presence of NEM is shown in Figure 33. NEM has no effect early in the cycle but later, when survival normally rises, only a small increase occurs and most of the rise is suppressed. It would appear that NEM can bind and, therefore, suppress whatever factor normally causes survival to rise in DNA inhibited cells.

REFERENCES

1. Sinclair, W. K. Argonne National Laboratory Biological and Medical Research Division, Annual Report, 1969. ANL-7635, p. 236.
2. Sinclair, W. K. Proc. 4th Int. Congr. of Radiation Research, Evian, France, in press.
3. Sinclair, W. K. *Proc. Nat. Acad. Sci.* **58**, 115 (1967).
4. Sinclair, W. K. U.S. Atomic Energy Commission Report BNL-50203 (C-57) (1970), pp. 97–116.

B. Recovery from Sublethal Damage Induced by X Irradiation in Cysteamine Protected Chinese Hamster Cells

Warren K. Sinclair

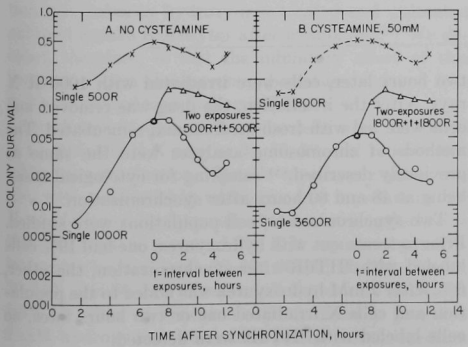

In a previous report,[1] I indicated that recovery from sublethal damage occurred in cysteamine-protected S phase cells. Current studies, by the two-dose method,[2] have been concerned with the magnitude of this recovery compared with cells not treated with MEA, at about the same survival level. (Cells with and without MEA have been shown to have a similar magnitude of shoulder in the single dose survival curve.[3])

FIG. 34.—Recovery in cysteamine treated and untreated Chinese hamster cells. A. No cysteamine. Survival of cells after exposure to 500 R, 1000 R, or two doses of 500 R separated by intervals of time, *t*, as shown. B. 50 mM cysteamine (present during irradiation only). Survival of cells after exposure to 1800 R, 3600 R, or two doses of 1800 R separated by intervals of time, *t*, as shown.

In Figure 34 are shown two sets of data, (A) for controls irradiated with 500 R, 1000 R, or 500 R + interval t + 500 R, (B) for cells with 50 mM MEA present during irradiation with 1800 R, 3600 R, or 1800 R + interval t, + 1800 R. In both cases the two-exposure survival data vs. time peaks at about 1½ to 2 hours with a recovery factor of ~2 to 3. Recovery is clearly not less in MEA treated cells and to a first approximation it is about the same. A more complete statement requires the results of exposure to several first doses and to a range of second doses for both cysteamine treated and untreated cells.

REFERENCES

1. Sinclair, W. K. Argonne National Laboratory Biological and Medical Research Division, Annual Report, 1969. ANL-7635, pp. 232–233.
2. Elkind, M. M. and H. Sutton. *Radiat. Res.* **13**, 135–154 (1969).
3. Sinclair, W. K. *Radiat. Res.* **39**, 135–154 (1969).

C. Protective Effect of Certain Agents against X Irradiation in Mammalian Cells

Warren K. Sinclair

An earlier report[1] described the effects and DMF's of 6 protective agents on synchronous Chinese hamster cells. One agent, a thiophosphate, identified as WR2721, which has been shown to be very effective in animals,[2] had a DMF of only ~1.2 in Chinese hamster cells. This poor result in Chinese hamster cells may be due to the inability of the culture system to liberate thiols in these cells, in which case the thiol counterpart WR1065* may be more effective in culture. This possibility was tested when a supply of WR1065 became available [WR1065 is $H_2N\ (CH_2)_3 \cdot HN \cdot CH_2\ CH_2\ SH \cdot 2HCl$]. The results showed only modest protection at 750 R (710 rads), with no detectable differential effect and a DMF (derived with the use of other data,[1]) of about 1.2 only at 10 mM. Thus, the thiol, WR1065, is not more effective in culture than the thiophosphate, WR2721.

An interesting feature of the experiment, however, was the potential differential toxicity of the agent at 20 mM, there being very few survivors after 750 R in the presence of 20 mM WR1065, except at ~8.5 hours. This is perhaps not surprising in view of other evidence for a special role of thiols at certain times of the cell cycle.

REFERENCES

1. Sinclair, W. K. Argonne National Laboratory Biological and Medical Research Division, Annual Report, 1969. ANL-7635, p. 234.
2. Yuhas, J. M. and J. B. Storer. *J. Nat. Cancer Inst.* **42**, 331–336 (1969).

* I am indebted to Col. W. Rothe, Walter Reed Army Institute of Research, for making a sample of WR1065 available to me.

STUDIES WITH MAMMALIAN CELLS IN CULTURE. IV. CYTOLOGICAL EFFECTS

A. Polyploidy Induced by X Rays in G_1 Cells of Chinese Hamster in Vitro

C. K. Yu and Warren K. Sinclair

Our previous report suggested that polyploid cells can only be induced by X rays when cells are irradiated in the G_1 phase of the cell cycle.[1] However, when large numbers of cells are required as in these assays, the synchrony technique is less satisfactory, and there are often 10 to 40% S cells contaminating the G_1 population. Further work was therefore undertaken on the induction of polyploid cells, using an improved synchronous G_1 population free of contamination by S cells.

2 mM hydroxyurea was added to a G_1 population synchronized by the usual selection method. One or two hours later, cells were irradiated with 1000 R X rays. After the irradiation, the drug was removed and cells were fed with fresh medium and reincubated. The methods of chromosome analyses were the same as previously described,[1] sampling for cytological assay being at 48 and 60 hours after synchronization.

Two synchronized G_1 cell populations were studied. Prior to treatment with hydroxyurea, one had 19% cells labeled with ^{3}HTdR after synchronization, the other, 6%. After 2 mM hydroxyurea was added to the population and cells X irradiated one or two hours later, no cells labeled with ^{3}HTdR were detected.

TABLE 46. PERCENT POLYPOLOID CELLS OBTAINED IN HYDROXYUREA TREATED G_1 CELLS IRRADIATED AT 1000 R

HU treatment, hr	Sampling time, hr	% ^{3}HTdR labeled cells	% true 4 *N*	% true 8 *N*	% 2 EDR	% 4 EDR	% total
1	48	0	17.6				17.6
2	48	0	19.0		4.8		23.8
1	60	0	19.7	1.6			21.3
2	60	0	14.8			7.4	22.2

The type and percent of polyploidy obtained from the experiments are tabulated in Table 46. For one hour hydroxyurea treatment, the percent of polyploid cells ranged from 17.6 to 21.3% scored at 48 and 60 hours, respectively. For a two-hour treatment, 23.8% and 22.2% polyploid cells were scored, while the data obtained in the previous studies without hydroxyurea were 9.3 and 13.9%, correspondingly. If allowance is made for a 37% contamination by S cells in the previous data, the adjusted percentage of polyploidy were 15% (9.3/63) and 22% (13.9/63), respectively. These are in a very good agreement with the present data. However, to prove the point unequivocally, it is proposed to use the same protocol as above with cells irradiated one or two hours after release from hydroxyurea which are therefore all in S. These experiments are in progress.

Two types of polyploidy were induced in hydroxyurea treated cells. The "true" tetraploid (double the stem number of chromosomes for a near-diploid cell) and endoreduplication polyploidy. The endoreduplication configuration is frequently in double form (4 chromosomes of each type) (4.8%) and quadruple form (8 chromosomes of each type) (7.4%), especially in those cells that were scored 60 hours after synchronization. The endoreduplicated cells with double form were found only once in non-hydroxyurea treated populations.

The high incidence of endoreduplication in multiple form is probably the result of hydroxyurea treatment. Hydroxyurea inhibits DNA synthesis, but RNA and protein syntheses continue unimpaired. Cells inhibited by hydroxyurea possess increased RNA and protein and these cells apparently are more likely to become multiple endoreduplication cells when irradiated.

REFERENCE

1. Yu, C. K. and W. K. Sinclair. Argonne National Laboratory Biological and Medical Research Division Annual Report, 1969. ANL-7635, p. 247.

B. Effect of Hydroxyurea on the Chromosome Repair Process

C. K. Yu and Warren K. Sinclair

It has been demonstrated autoradiographically that hydroxyurea, an inhibitor of DNA synthesis, has no effect upon unscheduled DNA synthesis in HeLa cells and that unscheduled DNA synthesis appears to be essential for chromosome repair.[1, 2] In another study, however, an inhibitory effect of hydroxyurea has been demonstrated by the difference in chromosome aberration rate between hydroxyurea-treated and untreated cultured human leukocytes after irradiation.[3] We decided, therefore, to test the inhibitory effect of this compound upon chromosome aberrations induced in a well-established mammalian cell line.

Synchronized Chinese hamster cells were irradiated in G_1 with 250 R X rays at 20, 50, 80, and 110 minutes after synchronization. Double-exposure experiments also were conducted in which the first exposure to 250 R was followed by intervals of different lengths before the cells received a second 250 R X ray exposure. The interval schedules were 20–50; 20–80; 20–110; 50–80; 50–110; and 80–110 minutes (all times were measured from the time of synchronization). Freshly prepared 2 mM hydroxyurea was added to the culture medium before the cells were irradiated, and remained there until after the second X ray exposure. For single exposures, hydroxyurea was removed shortly after irradiation. G_1 cells, 90 minutes after synchronization, also were irradiated with 500 R X ray exposure (single dose) in the absence of hydroxyurea.

The percent chromosome aberrations, i.e., dicentric and ring chromosomes, were studied at the next mitosis, i.e., at the end of the first cycle. The technique of synchronization, the preparation of hydroxyurea, and the method for chromosome studies are the same as those previously described.[5, 6]

The percent of chromosome aberrations obtained from several experiments are given in Table 47. The chromosome aberration rate (5.4 to 6.0%) after irradiation with 250 R at various times was similar. Similar data (5.1 to 6.0%) also were obtained when cells were irradiated while they were being treated with 2 mM hydroxyurea. These results indicate that the effectiveness of X rays in inducing chromosome aberrations remains the same at any part of G_1 and that hydroxyurea does not affect the chromosome aberration rate. The

TABLE 47. CHROMOSOME ABERRATIONS INDUCED BY X RAYS IN CHINESE HAMSTER CELLS SYNCHRONIZED IN G_1

Exposure, R	Exposure time after synchrony, min	Percent of chromosome aberrations, dicentric and ring chromosomes			
		X ray only		X ray + hydroxyurea	
		No. of mitoses scored	% aberrations	No. of mitoses scored	% aberration
250	20	178	6.1	122	5.1
	50	175	5.6	252	5.1
	80	186	5.4	236	6.0
	110	157	5.7	107	5.6
250 + 250	20 — 50	285	11.2	191	11.0
	20 — 80	338	10.7	139	10.0
	20 — 110	257	10.0	310	9.3
	50 — 80	359	10.0	293	10.2
	50 — 110	132	10.0	175	8.6
	80 — 110	165	10.0	126	8.7
500	90	421	25.0		
	60[a]	200	38.0		
	90[b]	100	29.0		

[a] See Reference 5.
[b] See Reference 6.

latter result already had been determined for cell lethality.[4]

Irradiation with two exposures of 250 R resulted in 10.0 to 11.2% chromosome aberrations, depending upon the interval, the average being 10.3%; this is approximately twice the number of aberrations induced by a single exposure of 250 R. This indicates that when the interval was between 30 and 90 minutes, the effect of X rays upon the chromosome aberration rate is additive. A single exposure to twice this dose, 500 R, produces an aberration rate of 25% (see Table 47), the rate obtained after this dose is about four times greater than the rate after 250 R. (This is the expected value when the dose is *doubled*, because dicentric and ring chromosomes increase as the square of the dose.) Chromosome restitution, therefore, must have taken place after exposure, with the process complete within the shortest time used in this study, i.e., 30 minutes.

When 2 mM hydroxyurea remained in the medium between two exposures of the cells to 250 R, the percent aberrations ranged from 8.6 to 11.0%, averaging 9.6%. This rate is similar to that induced by X rays in the absence of hydroxyurea. Thus, whether hydroxyurea is present or not, chromosome restitution takes place after exposure.

Restitution is complete within a short time, certainly in less than 30 minutes. Had this repair process been inhibited by hydroxyurea, a visible *open* chromosome lesion would have been expected. Because the aberration rate did not increase, we conclude that in the presence of hydroxyurea, repair of chromosome damage in G_1 after exposure often is not inhibited by the agent. Thus, unscheduled DNA synthesis may be responsible for the repair process in this strain of Chinese hamster cells as it apparently is in HeLa cells.[1, 2]

REFERENCES

1. Cleaver, J. E. *Radiation Research* **37**, 334 (1969).
2. Painter, R. B. and J. E. Cleaver, *Nature* **216**, 369 (1967).
3. Prempree, T. and T. Merz, *Nature* **224**, 603 (1969).
4. Sinclair, W. K. *Cancer Research* **28**, 198 (1968).
5. Yu, C. K. and W. K. Sinclair, *J. Nat. Cancer Inst.* **39**, 619–632 (1967).
6. Yu, C. K. and W. K. Sinclair, *Radiat. Res.* **43**, 357–371 (1970).

MAGNETIC RESONANCE STUDIES OF THE STRUCTURES AND INTERACTIONS OF BIOLOGICALLY ACTIVE MOLECULES

Steven S. Danyluk, David B. Davies, George E. Chapman, and William A. Bernhard

The objectives of this program have been outlined in previous annual reports and, briefly stated, are twofold: (1) We wish to determine as precisely as possible the structures and conformations of important biological molecules in solution; (2) having the conformational information in hand we then wish to show what unique structural features are involved in interactions of these molecules in aqueous media.

The ultimate goal is to provide a sound and detailed structural interpretation for inter- and intramolecular interactions of biological molecules.

In order to achieve these objectives we have undertaken extensive and systematic nuclear magnetic resonance (NMR) and electron paramagnetic resonance (EPR) measurements on various families of biomolecules including nucleic acids, proteins, oligopeptides, and antibiotics. Our attention has been focused not only upon the naturally occurring macromolecules but also upon smaller monomeric and oligomeric constituents which can serve as model systems. Various phases of this work have been reported in the literature and in earlier annual reports.

In the past year NMR studies were continued in three principal areas: nucleic acid constituents, oligopeptides, and chromopeptide antibiotics. A new NMR study dealing with the hydration structure of oriented biopolymers was also initiated. Brief summaries of several aspects of these studies follow.

MAGNETIC RESONANCE STUDIES OF THE STRUCTURES AND INTERACTIONS OF BIOLOGICALLY ACTIVE MOLECULES. I. NUCLEIC ACIDS: STRUCTURE AND CONFORMATION

A. Assignment and Conformational Properties of the Sugar-Ring Hydroxyl Protons of the Common Nucleosides*

David B. Davies and Steven S. Danyluk

A 60 MHz proton magnetic resonance study has been made of the hydroxyl protons of the ribose and deoxyribose rings for the common nucleosides dissolved in mixtures of dry DMSO-d_6 and C_6D_6. Use of this solvent system permitted the detection and assignment of the exchange-free spin-coupled multiplets for the hydroxyl protons. The assignment was confirmed by spin-decoupling experiments.

Based on the magnitudes of the observed coupling constants, it is concluded that the O—$H_{5'}$ group is freely rotating around the $C_{5'}$—$O_{5'}$ bond. It is calculated that the O—$H_{3'}$ bond favors a *gauche* conformation found in the solid state for the $H_{3'}$—$C_{3'}$—$O_{3'}$—P bonds of the nucleoside 3′-phosphates. The conformation of the O—$H_{2'}$ bond relative to the $C_{2'}$—$H_{2'}$ bond demonstrates no preference for the *gauche* rotamer. Such a rotamer might be expected if a hydrogen bond between the 2′-OH and the purine base exists in this solvent system, as well as in aqueous solutions where such an interaction has been postulated as a stabilizing influence for ribosides.

* Abstract of paper published in *Canadian Journal of Chemistry* **48**, 3112–3115 (1970).

B. A Complete Conformational Model for Uridine-5′-Monophosphate in Aqueous Solution*

David B. Davies and Steven S. Danyluk

A complete assignment has been made of the high-resolution proton NMR spectrum of uridine-5′-monophosphate (UMP-5′) in D_2O. Spectra for UMP-5′ were measured at 220 MHz and the assignment was made with the aid of ^1H-^1H and ^1H-^{31}P decoupling experiments. The final chemical shift and coupling constants were obtained by computer simulation of the complete proton spectrum.

Based upon the magnitudes of the derived coupling constants and using well-established correlations between vicinal ^1H-^1H and ^1H-^{31}P coupling constants and dihedral angles it has been possible to construct a complete conformational model for UMP-5′. Among the more important conformational features deduced from the NMR data are (1) the *anti* orientation of the uri-

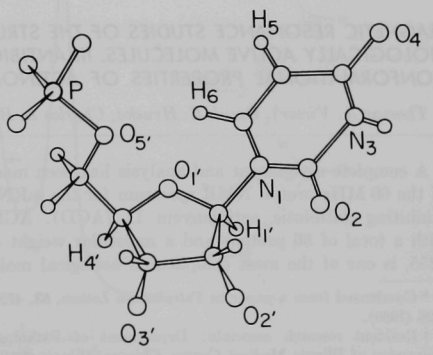

FIG. 35.—Conformational model of uridine-5′-monophosphate deduced from the NMR data.

* Condensation of a paper submitted to *Canadian Journal of Chemistry*.

dine and ribose groups about ϕ_{CN}; (2) an all *trans* orientation for the bonds along $H_{4'}$—$C_{4'}$—$C_{5'}$—$O_{5'}$—P; (3) a favoring of the C-2′ endo conformation of the ribose ring. An illustration of a conformational model incorporating all the features established by the NMR measurements is given in Figure 35.

C. Complete Analysis of the Proton Spectrum of Uridylyl-(3′ → 5′)-Adenosine: Conformational Structure*

David B. Davies and Steven S. Danyluk

As the next step in our systematic NMR study of nucleic acid conformations in solution we now report the first complete assignment and analysis of the proton spectrum of a dinucleoside monophosphate, uridylyl-(3′ → 5′)-adenosine (UpA). An assignment of the 220 MHz proton spectrum for UpA was made with the aid of ^{1}H-^{1}H and ^{1}H-^{31}P decoupling and spin-tickling experiments combined with a correlation of chemical shifts with those for corresponding monomers. The final parameters for the spectrum were obtained by computer simulation of the spectrum.

A number of interesting deductions concerning the UpA conformation can be made from the NMR data: Summarizing briefly these are: (1) Both ribose rings are interconverting rapidly between different conformers with the C-2′ endo form being favored at 18°C. (2) All of the bonds along the ribose-phosphate backbone ($C_{3'}$—$O_{3'}$—P—$O_{5'}$—$C_{5'}$—$C_{4'}$, 3′ → 5′) are in *trans* orientations with respect to each other. (3) The uridine and adenine rings are partially stacked over each other.

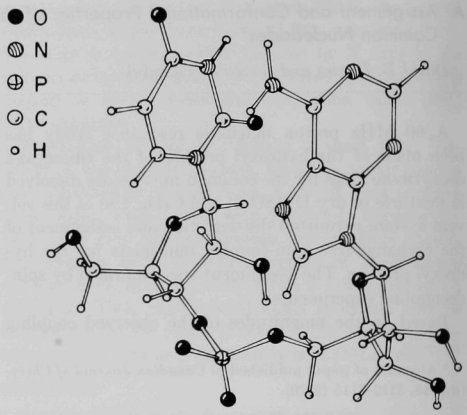

FIG. 36.—Conformational model of uridylyl-(3′ → 5′)-adenosine.

When these conformational features are combined it is possible to construct the conformational model for UpA shown in Figure 36.

* Condensation of a paper submitted to *Journal of the American Chemical Society*.

MAGNETIC RESONANCE STUDIES OF THE STRUCTURES AND INTERACTIONS OF BIOLOGICALLY ACTIVE MOLECULES. II. ANTIBIOTIC STRUCTURE: ANALYSIS AND CONFORMATIONAL PROPERTIES OF ACTINOMYCIN D*

Thomas A. Victor†, Frank E. Hruska, Charles L. Bell‡ and Steven S. Danyluk

A complete assignment and analysis has been made of the 60 MHz proton NMR spectrum for the *m*RNA inhibiting antibiotic actinomycin D (ACD). ACD, with a total of 86 protons and a molecular weight of 1255, is one of the most complicated biological molecules analyzed completely thus far. Because of the complexity of the ACD proton spectrum, the detailed assignment required the use of extensive supplementary experiments including deuterium exchange, spin-decoupling, and solvent perturbation.

Based upon the chemical shifts and coupling constants determined from the analysis, it is possible to make a number of tentative conclusions about the conformation of ACD in solution: (1) *trans* orientations are indicated for the HC—NH groups of the two valyl

* Condensed from a paper in *Tetrahedron Letters*, **53**, 4721–4726 (1969).

† Resident research associate; Department of Pathology, University of Illinois Medical Center, Chicago, Illinois 60612.

‡ Visiting summer scientist, 1968. Permanent address: University of Illinois Medical Center, Chicago, Illinois 60612.

and two threonyl residues; (2) *gauche* orientations are indicated from HC^{α}-$C^{\beta}H$ protons on the threonyl and valyl residues while a *trans* orientation is likely for the corresponding protons on the methylvalyl residues; (3) the absence of any solvent or temperature dependence for the sarcosyl N—CH_3 group is consistent with a combined screening of these protons by the prolyl ring and by a side-by-side orientation of the two pentapeptide rings in ACD; (4) temperature measurements support an out-of-plane orientation of the pentapeptide rings with respect to the plane of the actinocyl chromophore; (5) the valyl N—H protons are strongly hydrogen bonded to the sarcosyl C=O group.

All of these NMR deduced conformational results can be accomodated satisfactorly in a conformational model of ACD proposed by[1] us recently.

REFERENCE

1. Danyluk, S. S. and T. A. Victor. *Quantum Aspects of Heterocyclic Compounds*, Ed. E. D. Bergmann and B. Pullman. Israel Academy of Sciences, Jerusalem, 1970, pp. 394–412.

MAGNETIC RESONANCE STUDIES OF THE STRUCTURES AND INTERACTIONS OF BIOLOGICALLY ACTIVE MOLECULES. III. THE HYDRATION STRUCTURE OF COLLAGEN

George E. Chapman and Steven S. Danyluk

PURPOSE AND METHODS

Speculation about the role that water might play in the stabilization of biological macromolecules has been widespread for many years. The first evidence in favor of a definite hydration structure for a protein was obtained by nuclear magnetic resonance (NMR) studies of water adsorbed on oriented fibres of collagen.[1] In this work the signal for water was found to be split into a doublet (Fig. 37a and b). The doublet arises from an incomplete averaging of interproton dipolar interactions in water molecules undergoing anisotropic motion on the collagen.

In a more recent study, this anisotropic motion has been analyzed in terms of spherical harmonic probability series, using data obtained from proton and deuteron NMR spectra, and from dielectric constant measurements.[2] This study suggested that a dynamically reforming chain structure of the water molecules (Fig. 37c) oriented along the collagen was in accord with the analysis.

The present work was undertaken in order to provide additional confirmation of the chain structure for hydration water in collagen, to obtain a complete structural and kinetic description of the hydration phase, and to assess the contribution of the hydration structure to the stability of the native protein.

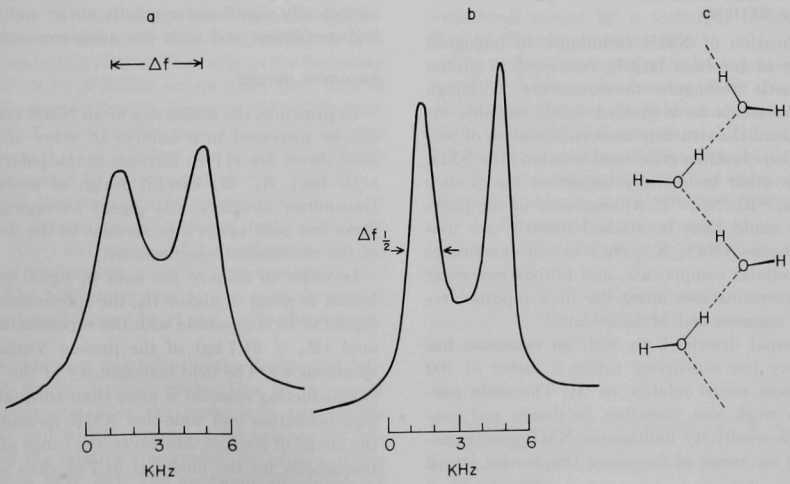

FIG. 37.—a. Proton spectrum of 32% H_2O on collagen at −23°C. b. As (a) but at 0°C. c. The water chain model.

PROGRESS REPORT

The refinement of the water chain model involves the calculation of expected proton and deuteron spectral splittings of H_2O and D_2O in a completely oriented but dynamically reforming chain structure,[2] with the water molecules in a tetrahedral configuration. On this model the calculated proton splitting is +10.4 kHz and deuteron splitting is −35 kHz. The observed ratio of $^2H/^1H$ is approximately 3.20 and is in good agreement with the calculated ratio of 3.40. Also, the signs of the splittings agree with those observed.[2] Thus, the water chain model must be regarded as well established.

Several other features of the spectra of H_2O adsorbed on collagen fibers are worthy of note, (1) the splitting of the doublet Δf and the linewidths, $\Delta f_{1/2}$, of each component of the doublet both decrease with an increase in water content, (2) the doublet splittings and linewidths both increase with a decrease in temperature, (3) at room temperature the water doublet shows signs of collapse due to proton exchange.

An attempt was made to interpret the kinetic process indicated by (2) in terms of a statistical model in which the hydrate water molecules are rotating in a cylindrically symmetric potential energy well. Comparison of the observed and theoretically predicted temperature dependence of Δf showed that the best fit of the data was obtained for the case where the hydrate water is assumed to be present in two phases. The two-phase structure appears to be made up of a highly ordered inner hydration structure whose water molecules are exchanging very rapidly (on an NMR time scale) with molecules in a less ordered outer hydration shell.

Furthermore, an analysis of the $\Delta f_{1/2}$ variation with temperature indicates that there are two motional processes in the hydration shell. One form of motion appears to be cooperative with an activation energy of ~4 kcal/mole and is tentatively ascribed to rotation of the water molecules. The other process is noncooperative with an activation energy of ~7 kcal/mole. The latter process is highly dependent upon the water content, as would be expected for a diffusion process.

REFERENCES

1. Berendsen, H. J. C. *J. Chem. Phys.* **36**, 3297–3308 (1962).
2. Chapman, G. E. and K. A. McLauchlan. *Proc. Roy. Soc.* **B173**, 223–234 (1969).

MAGNETIC RESONANCE STUDIES OF THE STRUCTURES AND INTERACTIONS OF BIOLOGICALLY ACTIVE MOLECULES. IV. A SUPERCONDUCTING MULTINUCLEI NUCLEAR MAGNETIC RESONANCE SPECTROMETER SYSTEM

George E. Chapman, Steven S. Danyluk, Joseph R. Haumann, and Bruno S. Kotula*

PURPOSE AND METHODS

The application of NMR techniques to biological systems has so far been largely restricted to proton (^1H) magnetic resonance measurements. Although these measurements have yielded much valuable information about the structure and conformation of biomolecules, there is still a great need to extend the NMR technique to other biologically important nuclei such as ^{13}C, ^{23}Na, ^{39}K, ^{35}Cl, ^{31}P. Among some of the problems which could then be studied directly are ion-binding processes (Na^+, K^+, etc.) in cell membranes and other cellular components, and fibrous molecular structure determinations along the lines reported recently by Chapman and McLauchlan.[1]

The principal drawback to such an extension has been the very low sensitivity (often a factor of 100 lower) of most nuclei relative to ^1H. The main purpose of this work was, therefore, to design and construct a high-sensitivity multinuclei NMR spectrometer covering the range of resonance frequencies for all biologically significant magnetic nuclei and capable of high-resolution and wide-line measurements.

PROGRESS REPORT

In principle, the sensitivity of an NMR spectrometer can be increased in a number of ways of which the most direct are (1) an increase in the polarizing magnetic field, H_0, (2) careful design of probe-receiver-transmitter circuitry, (3) signal averaging. Each of these has been taken into account in the development of the multinuclei spectrometer.

In order to achieve the gain in signal to noise inherent in going to higher H_0, the spectrometer was designed to be compatible with the superconducting solenoid (H_0 = 51.7 kg) of the present Varian HR-220 spectrometer. The field homogeneity of the Varian superconducting solenoid is more than adequate for both high-resolution and wide-line NMR measurements on the nuclei of interest. Moreover, the range of resonance frequencies for the nuclei at 51.7 kg does not present any major rf circuit design problems.

* Electronics Division.

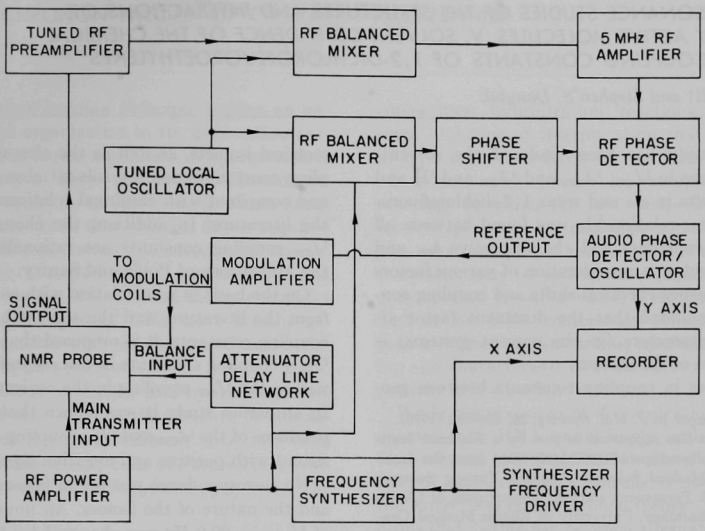

FIG. 38.—Spectrometer system block diagram.

A block diagram of the components used in the receiver-transmitter-recorder section of the spectrometer is given in Figure 38. The spectrometer is of the crossed-coil nuclear induction type[2] and is designed to operate in the frequency-sweep mode. This mode of operation has a number of advantages over the field-sweep mode of the Varian HR-220 spectrometer. A novel feature of the transmitter section is the use of a high stability fast-switching-time frequency synthesizer (Rohde and Schwartz Model ND100M) to generate the irradiating rf field. The range of the frequency synthesizer (9 to 90 MHz) covers more than 90% of the known magnetic nuclei. Sweep of the synthesizer, the recorder X axis (and the time-averaging computer where necessary) are initiated and synchronized with a signal generated by a frequency driver (Fig. 38).

Additional electronic design features in the receiver-transmitter section include a tuned high impedance low-noise (ca. 1 db) preamplifier enabling impedance matching of the receiver coil over a wide range of frequencies. The receiver system proper is of the superheterodyne type followed by rf and audio phase detection.

Considerable care was taken in the design and fabrication of the multinuclei probe. One of the novel features incorporated in the probe is a two-section transmitter coil which permits probe balance by adjustment of the relative amplitudes and phases of the two rf inputs (Fig. 38). The electronic simulation of receiver coil rotation and rf paddle adjustment eliminates the microphonic problems associated with the latter. Another probe innovation is the use of extremely low capacitance receiver leads, enabling direct tuning of the receiver coil over wide frequency ranges thereby eliminating the need of separate probes for different rf ranges. A third probe feature is the high precision Faraday screen machined onto a rigid epoxy cylindrical mount by a technique developed in the Biology Division machine shop.

The probe is equipped with homogeneity shim coils mounted on the probe housing. With these shim coils and sample spinning, the field homogeneity at the sample is expected to be more than satisfactory for high-resolution measurements. The probe is designed to accept 10-mm spinning sample tubes (twice the diameter of tubes used in the present Varian HR-220 spectrometer) or 12-mm static tubes and is equipped with an evacuated dewar assembly to permit variable temperature studies.

Finally, the overall spectrometer system is readily adaptable to non-CW modes of operation, i.e., Fourier transform method.

REFERENCES

1. Chapman, G. E., I. D. Campbell, and K. A. McLauchlan. *Nature* **225**, 639–642 (1970).
2. Block, F., W. W. Hansen, and M. E. Packard. *Phys. Rev.* **69** 127–135 (1946).

MAGNETIC RESONANCE STUDIES OF THE STRUCTURES AND INTERACTIONS OF BIOLOGICALLY ACTIVE MOLECULES. V. SOLVENT DEPENDENCE OF THE CHEMICAL SHIFTS AND COUPLING CONSTANTS OF 1,2-DICHLOROFLUOROETHYLENES*

Charles L. Bell† and Stephen S. Danyluk

A detailed study has been made of the solvent-induced variations in $^1J_{CH}$, $^1J_{CF}$, and $^3J_{HF}$ and ^1H and ^{19}F chemical shifts in *cis* and *trans* 1,2-dichlorofluoroethylene. A linear relationship was found between all three coupling constants and the respective δ_{1H} and ϕ_{19F} values. Based on a consideration of various factors expected to influence chemical shifts and coupling constants, it is concluded that the dominant factor affecting these parameters (in the present systems) is the reaction field of the solvent.

The differences in coupling constants between geometrical isomers, as well as the alteration of the coupling constant caused by solvent change, are discussed and compared with empirical relationships reported in the literature. In addition, the changes in $^1J_{CH}$ and $^1J_{CF}$ coupling constants are rationalized in terms of the MO theory of Pople and Santry.

On the basis of a correlation with coupling constants from the literature, and the solvent behavior of these coupling constants, it is proposed that the signs of the $^2J_{CCH}$ coupling constants in the *cis* and *trans* isomers as well as the $^3J_{HF}$ coupling in the *cis* isomer are positive. In an earlier study it was shown that the solvent dependence of the $^1J_{CH}$ and $^1J_{CF}$ coupling constants is consistent with positive and negative signs respectively.

No correspondence was noted between the ^2J values and the nature of the isomer. An unusually low value of $^2J_{CCF}$ = 20.0 Hz was observed for the *trans* isomer.

* Abstract of paper in *J. Mol. Spectry.* **35**, 376–392 (1970).

† This work was also supported in part by a National Institutes of Health Fellowship (1FO3GM45084-01) from the Institute for General Medical Sciences. Argonne Visiting Summer Scientist 1965–1969. Permanent address: Department of Chemistry, College of Pharmacy, University of Illinois Medical Center, Chicago, 60612.

THE PHOTOBIOLOGY OF CIRCADIAN RHYTHMS IN PROTOZOA AND OTHER EUKARYOTIC MICROORGANISMS*

Charles F. Ehret and John J. Wille, Jr.

A review of the literature and of our own data on daily rhythms and biological clocks focuses on several parameters of formerly unrecognized general significance. Specifically in *Gonyaulax, Euglena,* and *Tetrahymena,* population growth is more correctly described as consisting of an ultradian (or *fast* exponential) mode of growth and an infradian (or *slow* exponential) mode of growth (rather than as the formerly used less correct terms "exponential" and "stationary" phases); circadian rhythms are seen in the infradian mode. This "G.E.T. effect" can be extended from similar studies on other higher cells into the Circadian-Infradian Rule: circadian outputs can be induced in eukaryotic cells by light signals given in the infradian mode. From these and other observations the phenomena are regarded as biologically fundamental, and are generalized as the *Eukaryotic-Circadian Principle:* that circadian clocks are limited to eukaryotes, that all eukaryotes have regulatory capacities for circadian time-keeping, that these regulatory capacities are invariably turned on in the infradian mode, and that they can be set by light.

* Abstract of paper published in *Photobiology of Microorganisms,* ed. Per Halldal. John Wiley, New York, 1970, pp. 369–416.

TESTING THE CHRONON THEORY OF CIRCADIAN TIMEKEEPING*

Audrey Barnett, Charles F. Ehret, and John J. Wille, Jr.

The *Eukaryotic-Circadian Principle* implies an underlying temporal organization in the gene-action systems of the cells of higher organisms. A special case is the chronon theory of Ehret and Trucco. The chronon is a long linear sequence of DNA along which linear transcription proceeds so that about a day is required from beginning to end, cistron by cistron, until one arrives again after a recycling and reinitiating round back at the first cistron. The chronon theory postulates that such optimal lengths of DNA have become genetically indispensable and are the rate limiting elements common to all eukaryotes.

Using the methods of nucleic acid hybridization we present evidence that suggests the presence of characteristic species of RNA's in different time cuts from synchronized populations of cells of *Paramecium multimicronucleatum* and of *Tetrahymena pyriformis*. The competition hybridization reactions, however, pose some problems of interpretation that we consider to be typical of whole RNA derived from a large eukaryotic genome: these include, for example, some expected orderings in which the best competitor for a pulse-labeled species is its unlabeled homolog-in-time; but also some unexpected rankings occur in which a good competitor may be best against a temporally heterologous species. In other cases, a competitor may rank high at low RNA competition concentration, but be poor at higher concentrations, resulting in curve crossing also characteristic of eukaryotic whole-RNA competition hybridization reactions.

While the unequivocal demonstration of temporally characteristic RNA would imply ordinality of genetic transcription and would narrow down considerably the field of gene-action mechanisms, it does not yet prove the correctness of the chronon theory. Testable mechanisms that distinguish between alternatives have therefore been carefully considered, and the ground work is being prepared to make the critical experiments.

* Abstract of paper to be published in the *Symposium on Biochronometry*, Ed. M. Menaker. Submitted to *Proc. Acad. of Science*, Washington, D. C.

MOLECULAR BIOLOGY OF CIRCADIAN RHYTHMS IN EUKARYOTIC CELLS

Charles F. Ehret and Audrey Barnett

PURPOSE AND METHODS

Circadian rhythms occur in all higher plants and animals, including man, whose well known daily biological clock appears sometimes as his master. There is good evidence convergent from many fields of study that the biological time sense is an inevitable feature of the gene-action systems of eukaryotic organisms. The Chronon Theory of Ehret and Trucco[1] further asserts that extremely long polygenic replicons (chronons) are the sequential transcription components of the circadian clock-escapements.

Our purpose is to find the underlying physical basis for the biological clock. An initial goal has been to identify by means of molecular hybridization the presence of temporally characteristic RNA's in the circadian cycle.[2, 3] These studies continue to require research and development of large scale continuous culture methods yielding kilogram quantities of synchronously grown cells.

Our earlier studies have also revealed some problematic features of eukaryotic molecular hybridization reactions that suggest the interplay of multiple RNA components during annealing. The presence of such components, and some attendant properties are given below. Annealing was in 33% formamide, 0.2 × SSC (standard saline citrate) at 25°C.

PROGRESS REPORT

In Figure 39, reaction kinetics are shown for the hybridization of *Tetrahymena* DNA with whole RNA derived from pulse-labeled (1 hr) *Tetrahymena* synchronized in the Circadian-Infradian Mode, and given ^{3}HUr 18 hours after "dawn" (stock TC18 ^{3}HUr 1 hr). Just as the annealing reactions appear about to plateau around 12 to 18 hours after the start of annealing, a break in each curve appears, and each curve shows a renewed positive slope for days thereafter.

That the reaction kinetics reflect a mixture of components in the pulse-labeled RNA is shown by the following experiment. We reasoned that a fast reaction resulted from a relatively long-lived, highly redundant RNA component, transcribed from relatively rare DNA template sites; and that a slow reaction resulted from relatively short-lived rarer RNA species, tran-

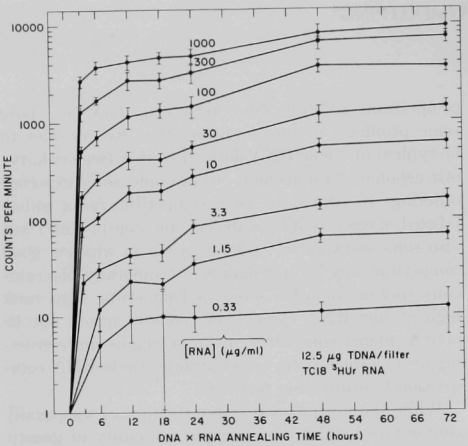

FIG. 39.—A family of curves showing the reaction kinetics of whole DNA and whole pulse-labeled RNA from *Tetrahymena*. Annealing occurred in 2.5 ml of 2 × SSC and 33% formamide at about 27 C. Counts on blank filters have been subtracted and the mean of 10 filters with 2 × S.E. are shown.

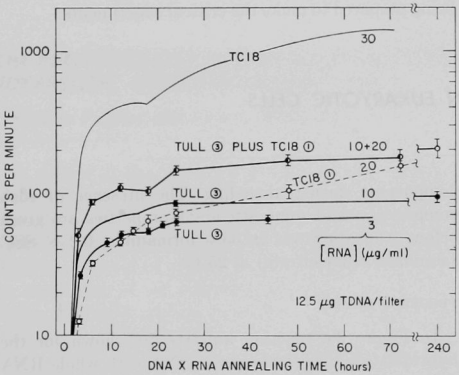

FIG. 40.—Kinetic curves of whole *Tetrahymena* DNA with partial RNA stocks and a stock constructed from the partial stocks. Annealing occurred in 3 ml of 2 × SSC and 33% formamide at about 27 C. Counts on blank filters have been subtracted and the mean of 10 filters with 2 × S.E. are shown.

scribed from unique DNA template sites, but present in groups and families of related genes in the genome. Sucrose gradient cuts of a 15-minute pulse-labeled RNA circadian stock (TC18 ^{3}HUr 0.25 hr) provided the necessary short-lived RNA species; similar cuts of RNA derived from a population of ultradian cells that had gone through over 6 fissions in the presence of ^{3}HUr for 31 hours and a fission post-label were also prepared (stock TULL ^{3}HUr 31 hr). For the short-lived species, the sucrose cut [cut (1)] used in Figure 40 was from the heavier-than-ribosomal zones (<30S). For the long-lived RNA species, we used a sucrose cut [cut (3)] from the mid-ribosomal zone (~20–28 S). The reaction kinetics of these components taken separately are just as predicted [Figure 40, TULL (3) cf TC 18 (1)]. Furthermore, the reconstruction stock [TULL (3) + TC 18 (1)] gives reaction kinetics similar to those observed initially in an intact RNA (whole TC 18, top curve Fig. 40).

The interplay of components is similarly seen in a number of experiments not shown here but of particular importance not only in presaturation competition experiments in which rare DNA sites are first saturated with unlabeled redundant RNA's before the interesting labeled stocks and unlabeled competitors are introduced; but also in the interpretation of competition-hybridization reactions employing whole or intact RNA's and showing steps and cross-overs in their otherwise generally smooth and hyperbolic forms.

CONCLUSION

Molecular approaches to the circadian clock are complex, technically difficult and challenging, but remarkably promising. The circadian oscillation *does* appear to be an output of the gene-action system; the chronon remains the best testable model. Further studies on this central aspect of eukaryotic regulation will focus on the following questions: (1) How do rates of replication compare with transcription rates during ultradian as against circadian-infradian growth? (2) Do interspecies hybrids show temporally homologous RNA's? (3) What is the influence of drugs, hormones, and radiations as Zeitgebers or effective synchronizers? (4) Can we extrapolate our results to man?

REFERENCES

1. Ehret, C. and E. Trucco. *J. Theoret. Biol.* **15**, 240–242 (1967).
2. Ehret, C., J. Wille, and E. Trucco. Proceedings of the Symposium on Oscillations, Ed. B. Chance and K. Pye. Academic Press, New York, in press.
3. Barnett, A., C. F. Ehret, and J. Wille. *Symposium on Biochronometry*, Ed. M. Menaker, Natl. Acad. Sci., Washington, D.C., in press.

TWO CLASSES OF POSTIRRADIATION OXYGEN EFFECT IN STAPHYLOCOCCUS AUREUS

Robert B. Webb

PURPOSE AND METHODS

Oxygen-dependent and -independent processes have been studied extensively in irradiated bacterial spores.[1] More recently it was possible to study a vegetative cell, *Staphylococcus aureus*, under conditions similar to those used with the bacterial spore.[2]

The purpose of this study is the elucidation of the different kinds of oxygen enhancement of X-ray lethality in the vegetative cell *S. aureus* with reference to the bacterial spore *Bacillus megaterium*.

Procedures and techniques have been described.[2] X irradiation was provided by an OEG-60 tube with a beryllium window, operating at 50 kVp and 45 mA. The dose rates were approximately 17 kR/min.

Dose-survival curves were fitted with the equation

$$S = ne^{-kD},$$

where S is the surviving fraction, D is the X-ray dose in kR, k is the inactivation constant (events kR^{-1}), and n is the extrapolation number. In most cases the survival response was a simple exponential ($n = 1$). All curves were fitted by a digital computer method.

PROGRESS REPORT

The overall X ray response of *S. aureus* equilibrated to water vapor from 23 to less than 10^{-5} torr in the presence and absence of oxygen and nitric oxide is given in Figure 41. The response is qualitatively like that of the bacterial spore at equilibrium water vapor pressures (EVP) below 5 torr.[1] However, the sensitivity is 3 to 6 times greater than in the spore under the conditions studied. Above 5 torr EVP the response of *S. aureus* is markedly different from that of the spore.

In the bacterial spore, it has been possible to partition the oxygen-dependent component of X-ray damage into two components.[1] As previously described,[1] recognition of the values of the components of the radiation damage is possible because the dose-survival response remains exponential for the various conditions tested. The inactivation constant k can be separated into parts k_{I}, k_{II}, and k_{III} which are components of the total damage associated with different experimental treatments. Values of k can be obtained from the following relationships:

$$k_{O_2 \to O_2} = k_{\mathrm{I}} + k_{\mathrm{II}} + k_{\mathrm{III}}$$

(irradiated in O_2, then exposed to O_2)

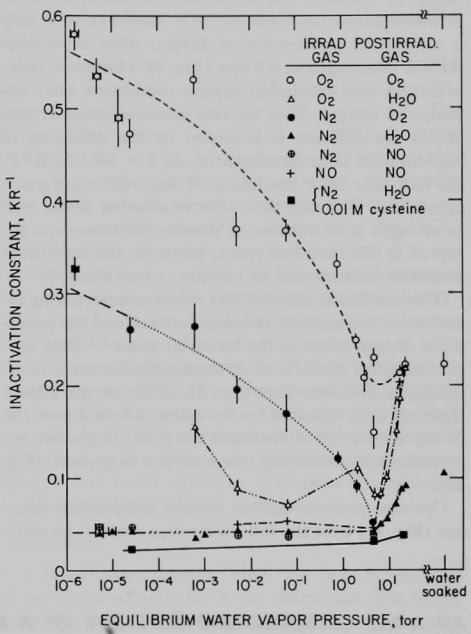

FIG. 41.—X-ray sensitivity (k) of *S. aureaus* in the presence of oxygen, nitrogen, nitric oxide, and cysteine at equilibrium water vapor pressures from 10^{-5} to 23 torr.

$$k_{N_2 \to O_2} = k_{\mathrm{I}} + k_{\mathrm{III}}$$

(irradiated in N_2, then exposed to O_2)

$$k_{N_2 \to H_2O} = k_{N_2 \to NO} = k_{\mathrm{I}}$$

(irradiated in N_2, then exposed to H_2O or NO)

That the k_{II} component of damage is not an "immediate" oxygen effect, although the presence of oxygen is required *during* irradiation, is evident from Figure 41. The open triangles represent the sensitivity of cells irradiated in oxygen then exposed to 23 torr water vapor immediately after the irradiation was completed, about 15 minutes after the beginning of the X-ray exposure. At EVP values of 4.7 torr and below, k_{II} based on a minimum exposure of oxygen after irradiation, is much smaller than k_{II} based on subtracting $k_{N_2 \to O_2}$ from $k_{O_2 \to O_2}$. Most of the k_{II} oxygen component that has been considered the "immediate" oxygen effect[1]

is actually a postirradiation oxygen effect that develops in *S. aureus* only if oxygen is present during irradiation. Such a postirradiation component of damage in k_{II} was recognized in the spore at levels of EVP below 10^{-3} torr,[1] but not at EVP levels of 5 torr as is here reported for *S. aureus*. In *S. aureus* there is only a very small postirradiation oxygen effect after irradiation in nitrogen at 4.7 torr (Fig. 41); however, there is a large postirradiation oxygen component after exposure in oxygen. That the two postirradiation oxygen effects are different is indicated by the difference in half-time for their development. At 5×10^4 torr EVP, the half-time after irradiation of the cells in oxygen is 65 minutes. The half-time after irradiation of the cells in nitrogen is 30 minutes. A similar difference was observed in the bacterial spore; however, the half-times were 480 minutes and 84 minutes, respectively.[3]

The sensitizing effect of NO, when present during irradiation, is suggested as being indicative of the immediate oxygen effect in the bacterial spore.[1] This sensitizing effect of nitric oxide during irradiation is much smaller in *S. aureus* (less than 5% of the oxygen effect) than has been reported for the spore. Above 5 torr, the X-ray sensitivity of *S. aureus* when NO is present approaches the sensitivity when oxygen is present (Fig. 41).

Cysteine protects against oxygen independent damage (Fig. 41) over the full EVP range studied. In addition, even trace amounts of cysteine prevent the expression of the three oxygen-dependent components.

CONCLUSIONS

1. The "immediate" oxygen effect (k_{II}) in *S. aureus* actually develops over a period of several hours, with a half-time of approximately 65 minutes. However, oxygen must be present at the time of irradiation.

2. The postirradiation oxygen effect (k_{III}) develops with a half-time of approximately 35 minutes in *S. aureus*. The full enhancing effect is obtained if oxygen is added after anoxic irradiation. These species are stable for many hours at 25°C; however, they can be readily effectively removed by NO, 23-torr H_2O, and cysteine.

3. The effect of NO during irradiation is less than 5% of the total oxygen effect in *S. aureus*, whereas in the bacterial spore, the sensitizing effect of NO is 35% as large as the total oxygen effect.

REFERENCES

1. Powers, E. L. and A. Tallentire. *Actions Chimiques et Biologiques des Radiations*, Ed. M. Haissinsky. pp. 1–67 (1968).
2. Webb, R. B. in *Physical Processes in Radiation Biology*, Ed. L. Augenstein. pp. 267–285 (1964).
3. Davies, D. J. G. Ph.D. thesis, University of Manchester, 1964.

AN X-RAY CRYSTALLOGRAPHIC STUDY OF A BENCE-JONES PROTEIN

Allen B. Edmundson, Marianne Schiffer, Mical K. Wood, Karl D. Hardman, and Kathryn R. Ely

PURPOSE AND METHODS

Both the serum IgG immunoglobulin and the urinary Bence-Jones protein from a patient (Mcg) with multiple myeloma have been crystallized in forms suitable for X-ray diffraction experiments. IgG immunoglobulins in both myelomatous and normal sera consist of two light chains (MW 22,000 to 23,000) and two heavy chains (MW 50,000 to 55,000) linked by interchain disulfide bonds. Bence-Jones proteins represent excreted light chains and their presence in urine is pathognomonic of multiple myeloma. The isolation of crystalline IgG and Bence-Jones proteins from one patient is particularly significant, because the amino acid sequence of the IgG light chain constituent is identical with that of the Bence-Jones protein only when the proteins are obtained from the same individual. This provides a unique system for the determination of the three-dimensional structure of an antibody molecule. The high resolution study possible with the Bence-Jones protein can complement and extend the low resolution study attainable with the myeloma protein.

Preliminary results of the crystallographic studies of the myeloma protein have been reported.[1] The Bence-Jones protein has been crystallized in two forms. The first[2] was crystallized from distilled water in the orthorhombic space group $P2_12_12$. The second, with the trigonal space group $P3_121$, was obtained by crystallization in ammonium sulfate. Both crystal forms have been used in diffraction studies at Argonne and at the University of Bristol, where one of us (A.E.) has been working with Dr. H. C. Watson since July 1970.

Isomorphous derivatives with heavy atoms including platinum, mercury, and uranium are required to solve the "phase problem" in protein crystallography. Both crystal forms were treated with potassium chloroplatinite ($PtCl_4^{=}$), "mersalyl" (a mercurial), and

uranyl nitrate. "Double" derivatives of the orthorhombic form were obtained by soaking the $PtCl_4^{=}$ derivative in uranyl nitrate. Precession photographs were taken of the treated crystals to determine the optimum conditions for producing isomorphous derivatives. Three-dimensional data were collected with an automated diffractometer for the native protein and the $PtCl_4^{=}$ and mersalyl derivatives of the trigonal form and for the native protein and the $PtCl_4^{=}$ derivative of the orthorhombic form. Attempts were made to define the heavy atom positions by the "difference Patterson" method.

PROGRESS REPORT

The crystallization and symmetry of the orthorhombic form of the Bence-Jones protein were described previously.[2] The unit cell dimensions were $a = 72.6$; $b = 81.9$; and $c = 71.0$ A. A second crystalline form was obtained by dissolving the protein in 0.02 M phosphate buffer, pH = 7.4 (O.D. of the solution was 20 to 30 units) and adding an approximately equal volume of 3 M ammonium sulfate. On addition of ammonium sulfate to the protein solution a gel formed. Well-separated prismatic crystals grew out of this gel. The crystals were elongated along the c axis and had 32 symmetry. They were up to 3 mm in length with a diameter of 1 mm.

The symmetry of the three-dimensional diffraction pattern indicated a trigonal unit cell. From the systematic absences and the symmetry of the diffraction pattern, the space group was identified as $P3_121$ (No. 152 in Ref. 3) or its enantiomorph $P3_221$ (No. 154 in Ref. 3). The dimensions of the unit cell were $a = 72.3 \pm 0.2$; and $c = 185.9 \pm 0.6$ A and the calculated volume was 841,000 A^3. Assuming that the dimer[2] (M—S—S—M,* MW = 46,000) was the crystallographic asymmetric unit, the fractional volume of the solvent was estimated to be 60%. Precession photographs contained reflections with 2θ values corresponding to interplanar spacings of 2.3 A.

The two crystal forms were examined in parallel because each offered advantages and disadvantages in the quest for a structure. The trigonal form crystallized easily, was amenable to the preparation of suitable isomorphous derivatives, and was relatively stable in the X-ray beam. Unfortunately, one of the crystallographic axes (c) was 186 A, over twice the length of any axis in the orthorhombic form. This property had the effect of making certain groups of reflections closely spaced and difficult to resolve either with precession methods or with a diffractometer.

In comparison the crystallographic problems arising from the use of the orthorhombic form were straightforward, but the solubility problems were not. The Bence-Jones protein has a finite solubility in water and may take as long as two months to form suitable crystals in water at 22°. Heavy atoms are usually salts which tend to dissolve these crystals during attempts to prepare isomorphous derivatives. The $PtCl_4^{=}$ is an exception. It appears to enter the crystal in one principal site and to make the protein in the crystal less soluble in water. The success in locating the heavy-atom position in the $PtCl_4^{=}$ derivative makes the orthorhombic form our first choice in attempting to solve the structure of this protein. At Watson's suggestion, we now use the $PtCl_4^{=}$ derivative as our starting point in the search for second and third derivatives. Both mersalyl and uranyl nitrate dissolve the orthorhombic crystals of native protein in concentrations as low as 10^{-4} M, but do *not* significantly increase the solubility of the crystals of the $PtCl_4^{=}$ derivative.

CONCLUSIONS

A Bence-Jones protein (Mcg) has been crystallized in two forms suitable for X-ray diffraction. The heavy atom site in the $PtCl_4^{=}$ derivative of the orthorhombic form has been located. The $PtCl_4^{=}$ lowers the solubility of the crystals in water and thereby makes possible the addition of heavy-atom salts that normally dissolve the crystals of native protein, to form "double" derivatives.

REFERENCES

1. Edmundson, A. B., M. K. Wood, M. Schiffer, K. D. Hardman, C. F. Ainsworth, K. R. Ely, and H. F. Deutsch. *J. Biol. Chem.* **245**(10), 2763–2764 (1970).
2. Schiffer, M., K. D. Hardman, M. K. Wood, A. B. Edmundson, M. E. Hook, K. R. Ely and H. F. Deutsch. *J. Biol. Chem.* **245**(4), 728–730 (1970).
3. *International Tables for X-ray Crystallography*, Vol. I, Ed. N. F. M. Henry and K. Lonsdale. The Kynoch Press, Birmingham, England, 1965, pp. 465–466.

* Two identical polypeptide chains (M) linked by a disulfide bond.

CHEMICAL STUDIES OF CONCANAVALIN A

Allen B. Edmundson, Kathryn R. Ely, Dayle A. Sly, Florence A. Westholm, and Dennis A. Powers

PURPOSE AND METHODS

In a program designed to complement crystallographic studies of concanavalin A (Con A), a phytohemagglutinin isolated from jack beans (*Canavalia ensiformis*), initial attempts to study the amino acid sequence in a conventional manner proved difficult. Resistance to trypsin and inaccessibility of sites for cleavage with papain, chymotrypsin, and thermolysin were found as major obstacles in sequence studies. Peptides released from unique regions of tetrameric Con A during enzymatic studies did not indicate four identical subunits. Crystallographic results indicated an asymmetric unit of one-half the tetrameric molecule.[1] New chemical studies of the subunits in the asymmetric unit began when we found that the protein could be dissociated in acidic solutions of urea. The chromatographic methods used for the separation of the α and β chains of hemoglobin on Amberlite CG-50 in such solvents were applied to Con A.

Subunits were prepared from the following types of samples which have been used at one time or another in the chemical and crystallographic studies: (1) Con A isolated after double passage through Sephadex columns; (2) Con A crystallized once after initial purification as in type (1); (3) twice-crystallized Con A after initial purification; and (4) commercial samples of twice-crystallized Con A. The purities of the samples of parent protein and its subunits were evaluated by disc electrophoresis and end-group analysis with an Illitron sequenator.

PROGRESS REPORT

Con A was shown to consist of two types of subunits, which we have called α and β. These subunits could be prepared in quantities of 100 to 200 mg in a single chromatographic separation.

Samples of Con A (types 1 and 2 as listed above) contained impurities for chemical studies (although single crystals generally provide sufficiently pure samples for diffraction work). Fortunately, high levels of purity were attained by recrystallization. Electrophoretically homogeneous subunits were obtained from samples of twice-crystallized Con A (types 3 and 4). The sequence for the amino-terminal segment of each subunit indicated the presence of a single polypeptide chain.

The sequence of the first 11 residues in the α chain is: Ala–Asp–Pro–Ile–Val–Ala–Val–Glu–Ile–Asp–Pro. The corresponding sequence in the β chain is not certain at this time.

The α and β chains can now be degraded singly with enzymes and chemical reagents such as cyanogen bromide. The results will be correlated with the large volume of information we accumulated during work on tetrameric Con A before we could separate the chains.

CONCLUSIONS

For the first time, concanavalin A was shown to consist of two types of subunits, α and β, which can be obtained in highly purified form in quantities sufficient for sequential analysis.

REFERENCE

1. Hardman, K. D., M. K. Wood, M. Schiffer, and C. F. Ainsworth. An X-ray Crystallographic Study of the Structure of Concanavalin A. This report.

AN X-RAY CRYSTALLOGRAPHIC STUDY OF THE STRUCTURE OF CONCANAVALIN A

Karl D. Hardman, Mical K. Wood, Marianne Schiffer, and Clinton F. Ainsworth

PURPOSE AND METHODS

Concanavalin A (Con A), a phytohemagglutinin from jack beans, has several properties that make it an excellent protein for structural study. The molecule is a tetramer and has three distinct pairs of binding sites for carbohydrate, calcium ions, and transition metal ions. A more detailed description of these properties and preliminary crystallographic information have been summarized previously.[1]

PROGRESS REPORT

Recent studies indicate that the molecular weight of Con A is in the range of 50,000 to 55,000. Earlier literature values ranged from 55,000 to 71,000.[2, 3] An ul-

TABLE 48. HEAVY ATOM SITES FOR CONCANAVALIN A

	$PtCl_4$	$PtCl_6$
Site 1		
X	0.045	0.042
Y	0.010	0.013
Z	0.060	0.058
Occupancy	0.75	0.85
Site 2		
X	0.050	0.052
Y	0.001	0.001
Z	0.124	0.122
Occupancy	0.30	0.30
Site 3		
X	0.156	0.148
Y	0.226	0.220
Z	0.316	0.314
Occupancy	0.15	0.65

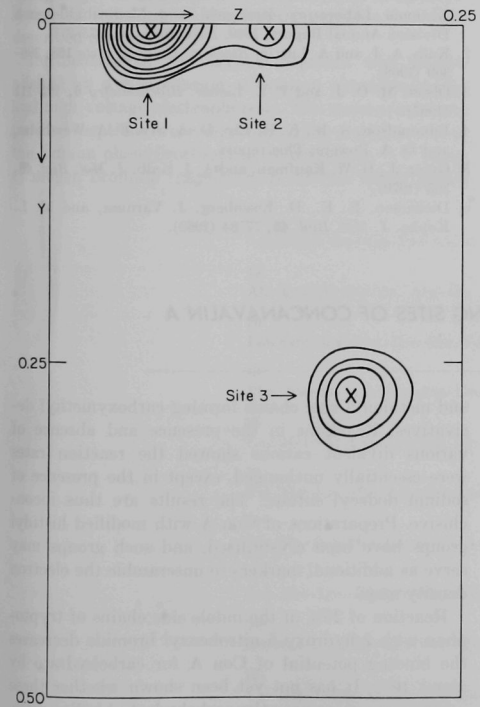

FIG. 42.—An electron density map of the 0*kl* 2-dimensional projection obtained by a Fourier synthesis using heavy atom data from the $PtCl_6^{=}$ derivative. The heavy atom data necessary for this calculation are obtained by subtracting the protein data from the protein + heavy atom data. These sites are prob-

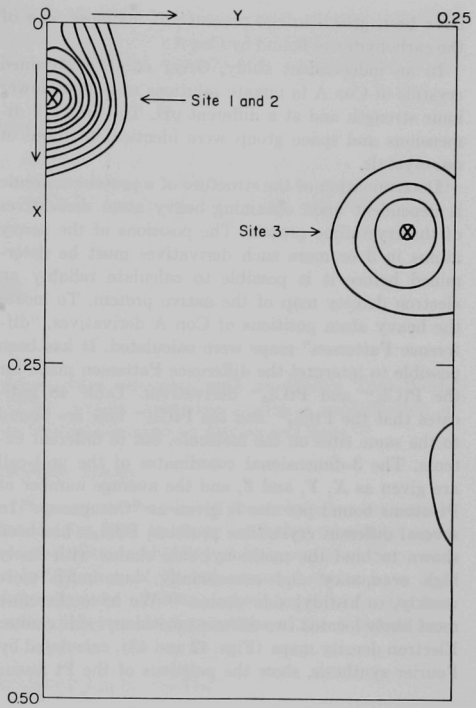

FIG. 43.—The same derivative as Fig. 42, showing the *hk*0 2-dimensional projection. In this projection, sites 1 and 2 are superimposed on each other.

tracentrifuge study by one of us (C.F.A.) indicates a molecular weight of 48,000. Chemical studies of Con A[4] support a molecular weight in the range of 50,000 to 55,000 and also indicate that the tetramer has two different types of subunits. The crystallographic unit cell contains four protein molecules (eight asymmetric units). Therefore, the asymmetric unit is a dimer made up of one chain of each type. The crystal contains 45% to 50% solvent.

Crystals were obtained at pH 5.9 with 2.0 M phosphate containing calcium and manganese ions. Crystals grown with nickel replacing manganese ions show no significant differences in unit-cell dimensions or in measured intensities at low resolution. Con A also has been crystallized in solutions free of divalent cations, but these crystals have a different space group, and the unit-cell dimensions are much larger. Crystals

ably adjacent to methionyl side chains in the Con A molecule. These maps show only one asymmetric unit (½ of the total molecule).

have been grown in the presence of mannose, one of the carbohydrates bound by Con A.

In an independent study, Greer et al.[5] obtained crystals of Con A in nitrate solutions at a much lower ionic strength and at a different pH. The unit-cell dimensions and space group were identical to those of our crystals.

Determination of the structure of a protein molecule is dependent upon obtaining heavy atom derivatives of the crystalline protein. The positions of the heavy atoms in 3 or more such derivatives must be determined before it is possible to calculate reliably an electron density map of the native protein. To locate the heavy atom positions of Con A derivatives, "difference Patterson" maps were calculated. It has been possible to interpret the difference Patterson maps for the $PtCl_6^=$ and $PtCl_4^=$ derivatives. Table 48 indicates that the $PtCl_4^=$ and the $PtCl_6^=$ ions are bound to the same sites on the molecule, but to different extents. The 3-dimensional coordinates of the unit-cell are given as X, Y, and Z, and the average number of Pt atoms bound per site is given as "Occupancy." In several different crystalline proteins, $PtCl_4^=$ has been shown to bind the methionyl side chains with fairly high occupancy and occasionally, but much more weakly, to histidyl side chains.[6] We have therefore most likely located two different methionyl side chains. Electron density maps (Figs. 42 and 43), calculated by Fourier synthesis, show the positions of the Pt atoms in the $PtCl_6^=$ derivative. Work is in progress to obtain additional heavy atom derivatives, for example with U, Hg, Ir, or Au compounds, which will bind at different sites from those shown above. It will then be possible to calculate an electron density map of the Con A molecule.

CONCLUSION

The space group of Con A has been shown to be *I*222 by solution of difference Patterson maps. The positions of two heavy atom derivatives, $PtCl_4^=$ and $PtCl_6^=$, have been located and refined by crystallographic least squares computations in preparation for calculation of a low resolution electron density map.

REFERENCES

1. Hardman, K. D., M. K. Wood, M. Schiffer, A. B. Edmundson, M. E. Hook, C. F. Ainsworth, and K. R. Ely. Argonne National Laboratory Biological and Medical Research Division Annual Report, 1969. ANL-7635, pp. 275–277.
2. Kalb, A. J. and A. Lustig. *Biochim. Biophys. Acta* **168**, 366–369 (1968).
3. Olson, M. O. J. and I. E. Liener. *Biochemistry* **6**, 105–111 (1967).
4. Edmundson, A. B., K. R. Ely, D. A. Sly, F. A. Westholm, and D. A. Powers. This report.
5. Greer, J., H. W. Kaufman, and A. J. Kalb. *J. Mol. Biol.* **48**, 365 (1970).
6. Dickerson, R. E., D. Eisenberg, J. Varnum, and M. L. Kopka. *J. Mol. Biol.* **45**, 77–84 (1969).

A CHEMICAL STUDY OF THE CARBOHYDRATE BINDING SITES OF CONCANAVALIN A

Karl D. Hardman and Clinton F. Ainsworth

PURPOSE AND METHODS

This study, which has been directed toward determination of the amino acid side chains involved in the carbohydrate binding sites,[1] has been terminated as a separate project and incorporated into the crystallographic study of concanavalian A (Con A). This has been done because of the lack of both time and personnel. Identification of specific amino acids in a protein by chemical modification is useful for the interpretation of an electron density map. Once a map is obtained, the known amino acids can be located, providing an important initial key to fitting the rest of the amino acid sequence to the map.

PROGRESS REPORT

Chemical modification of Con A with bromoacetate, was studied briefly to determine whether the imidazole rings were involved in the binding of carbohydrate or divalent cations. This compound reacts with histidyl and methionyl side chains forming carboxymethyl derivatives. Reactions in the presence and absence of various divalent cations showed the reaction rates were essentially unchanged, except in the presence of sodium dodecyl sulfate. The results are thus inconclusive. Preparations of Con A with modified histidyl groups have been crystallized, and such groups may serve as additional markers to unscramble the electron density map.

Reaction of 25% of the indole side chains of tryptophan with 2-hydroxy-5-nitrobenzyl bromide decreases the binding potential of Con A for carbohydrate by about 10%. It has not yet been shown whether these residues are in or near the carbohydrate binding sites. If this derivative can be crystallized, the "tagged" tryptophans could also prove useful in the interpretation of the electron density map.

Crystals of Con A complexed with mannose have been obtained. Mannose, which binds more readily

than other hexoses, hopefully can be located in the crystalline complex by a difference Fourier synthesis. This, if possible, will be the most satisfactory method for identifying the structural features of the carbohydrate binding site.

CONCLUSION

The two crystalline derivatives of Con A obtained from this study, carboxymethylated Con A and the Con A-mannose complex, should provide excellent markers for identifying modified histidyl residues and the carbohydrate binding sites, respectively, in the Con A molecule.

REFERENCE

1. Hardman, K. D., C. F. Ainsworth, and D. A. Eppstein. Argonne National Laboratory, Biological and Medical Research Division Annual Report, 1969. ANL-7635, p. 277.

THE PRIMARY STRUCTURE OF SUCKER HEMOGLOBINS

Dennis A. Powers and Allen B. Edmundson

PURPOSE AND METHODS

The general purpose of this investigation, the separation of the polypeptide subunits and the preliminary fractionation of the tryptic peptides, has been described previously.[1]

Purification of the tryptic peptides was accomplished by a combination of column chromatography and high voltage electrophoresis. The sequences of the purified peptides were determined by modification of the Edman phenylisothiocyanate procedure.[2, 3] Large cyanogen bromide fragments, as well as whole globin chains, were sequenced with an Illinois Tool Works (ITW) protein sequenator, using a modification of the method described by Edman and Begg.[2]

PROGRESS REPORT

The sequence for most of the α chain has been established (Fig. 44). Its "core" is being sequenced again because of the ambiguity of four positions. Sequences of half of each of the two major β chains have been determined. In addition, tryptic peptides for the majority of the remaining portions of the β chains have

1 14
*-Ser-Leu-Ser-Asp-Lys-Asp-Lys-Ala-Asp-Val-Lys-Ile-Ala-Trp-

15 28
Ala-Lys-Ile-Ser-Pro-Arg-Ala-Asp-Glu-Ile-Gly-Ala-Glu-Ala-

29 42
Leu-Gly-Arg-Met-Leu-Thr-Val-Tyr-Pro-Gln-Thr-Lys-Thr-Tyr-

43 55
Phe-Ala-His-Trp-Ala-Asp-Leu-Ser-Pro-Gly-Ser-Gly-Pro-Val-

56 71
Lys-His-Gly-Lys-Lys-Val-Ile-Met-Gly-Ala-Ile-Gly-Asp-Ala

70 83
Val-Thr-Lys-Phe-Asp-Asp-Leu-Leu-Gly-Gly-Leu-Ala-Ser-Leu-

84 96
Ser-Glu-Leu-His-Ala-Ser-Lys-Leu-Arg-Val-Asp-Pro-Ser

97 108
Asn-Phe-Lys-Ile-Leu-Ala-Asn-X-Ile-Val-Val-Gly-

109 120
Ile-Met-Phe-Tyr-Leu-Pro-Gly-Asp-Phe-Pro-Glu-

121 133
Val-His-X-Ser-X-Asp-Lys-Phe-X-Gln-Asn-Leu-Ala-

134 141
Leu-Ala-Leu-Ser-Glu-Lys-Tyr-Arg

FIG. 44.—The sequence of *C. clarkii* α chain from the fish's hemoglobins. $\times$ = unidentified. Dashes connect residues related by sequence, commas separate residues whose sequence is uncertain but aligned by homology with other hemoglobins. * = 80% blocked N-terminus.

TABLE 49. HEME CONTACTS IN THE ALPHA CHAINS FROM FOUR SPECIES[a]

Position (horse)	α chain			
	Horse	Human	Sucker	Carp
B 13	Met	Met	Met	Met
C 4	Thr	Thr	Thr	Thr
C 7	Tyr	Tyr	Tyr	Tyr
CD 1	Phe	Phe	Phe	Phe
CD 3	His	His	His	His
CD 4	Phe	Phe	Trp	Trp
E 7	His	His	His	His
E 11	Val	Val	Val	Val
F 4	Leu	Leu	Leu	Leu
F 7	Leu	Leu	Leu	Leu
F 8	His	His	His	His
FG 3	Leu	Leu	Leu	Leu
FG 5	Val	Val	Val	Val
G 4	Asn	Asn	Asn	Asn
G 5	Phe	Phe	Phe	Phe
G 8	Leu	Leu	Leu	Leu
H 12	Leu	Leu	Phe	Phe
H 15	Val	Val	Leu	Leu
H 19	Leu	Leu	Leu	Leu

[a] Homology with horse hemoglobin (see Ref. 4).

been isolated and purified. Partial sequences and some purified peptides from two minor chains also have been isolated.

These are the first fish hemoglobin β chains ever sequenced; and these results should help explain teleost multiple hemoglobin patterns (11 in the case of *Catostomus clarkii*). A correlation is sought between the physiological activity of the various hemoglobin components, their protein structure and various environmental parameters (e.g., temperature).

CONCLUSION

The sequence for the alpha chain of *Catostomus clarkii* hemoglobin is proposed in Figure 44. Using structural homology, most "substitutions" are on the exterior of the molecule and differences between closely related animals are usually isopolar interchanges. Furthermore, important heme contacts for animals as diverse as the horse (*Equus caballus*), man (*Homo sapiens*), sucker (*Catostomus clarkii*), and carp (*Cyprinus carpio*) are virtually the same (two isopolar differences) despite variation in total sequences as great as 50 percent (see Table 49).

REFERENCES

1. Powers, D. A. Argonne National Laboratory Biological and Medical Research Division Annual Report, 1969. ANL-7635, pp. 287–288.
2. Edman, P. and G. Begg. *Eur. J. Biochem.* **1**, 80 (1967).
3. Gray, W. R. and B. S. Hartley. *Biochem. J.* **89**, 59 (1963).
4. Perutz, M. F. *Proc. Roy. Soc.*, **B173**, 113–140 (1969).

Cellular Fine Structure and Related Function

MORPHOLOGICAL CHANGES IN CELLULAR ORGANELLES OF X-IRRADIATED BACTERIA-FREE GRASSHOPPER DIAPAUSE EMBRYOS*

Theodore N. Tahmisian and Betty Jean Wright

The grasshopper (*Melanoplus differentialis*) embryo during diapause was used to study the effect of X irradiation on the ultrastructure of cells in a basal metabolic condition. The gross effect of 25 kR on the embryo is a diminution in size. Ultrastructurally the cells exhibit injury earlier than can be detected by gross morphology. The nucleolus shows radiation injury first, and ultimately the whole nucleus becomes pyknotic. The cytoplasm of irradiated cells contains an abundance of rough endoplasmic reticulum, an organelle rarely found in the control cells. There also is an increase in free ribosomes in the treated cells. Cytoplasmic myelination and the presence of cytolysomes is common in the X-irradiated cells. The mitochondria, for the most part, remain undamaged although their overall shape is modified and a few do become myelinated. The centriole remains unchanged throughout the entire postirradiation period. Organelles are differentially susceptible to irradiation; some exhibit no change, some are duplicated, some undergo degradation and at times structures never seen in normal cells are newly synthesized. The irradiation syndrome in biological material is dependent upon the level of organelle differentiation as well as on the metabolic state of the organism.

* Abstract of paper submitted for publication in *Radiation Research*.

THE STRUCTURE OF PARAMECIUM AS VIEWED FROM ITS CONSTITUENT LEVELS OF ORGANIZATION*

Charles F. Ehret and Eugene W. McArdle

An anthology of original and classical electron micrographs is presented, in which the cell is built up, level by level, from its constituent building-blocks: macromolecular and suborganellar levels (trichynin, axonemal fiber protein), organelles (kinetosomes, trichocysts), organelle complexes and systems (pellicle system of organelles, gullet system of organelles), and finally the whole cell. Particular attention is given to the central role of such archetypically interesting organelles as kinetosomes and trichocysts, their origins, development, multiplication, and comparative ultrastructure.

* Abstract of Chapter 9 in the *Biology of* Paramecium aurelia, Ed. Wilhelm van Wagtendonk, Ronald Press, in press.

Plant Radiobiology

CORRELATIVE DETERMINANTS OF RNA METABOLISM IN THE GAMMA-IRRADIATED COLEUS LEAF

Solon A. Gordon and Evelyn M. Buess

PURPOSE

If the Coleus leaf is excised and its petiole immersed in water, adventitious roots are formed at the petiole base; they emerge 5 to 6 days after excision. The blade controls the initiation of roots in the petiole by the rate at which it supplies carbohydrates, nitrogenous factors and the growth hormone, auxin. If the blade of the leaf is exposed to γ radiation, the petiole being heavily shielded, emergence of the roots is inhibited. The isolated leaf is, therefore, an abscopal system that can be used for the study of two aspects of radiation response: correlative effects in morphogenesis and biochemical loci of damage.

We have found that irradiation of the blade with exposures that halve root emergences in the shielded petiole base lowers significantly the petiolar RNA level within 12 hours.[1] The decrease becomes more pronounced by 24 hr, and occurs before histological differences are observed. In this same period there are no significant radiation-induced changes in levels of mono- and polysaccharides, soluble and protein N, and RNA synthesis. However, the loss of RNA can be directly correlated with a concomitant rise in gross ribonuclease activity in the petiole. In continuation, we have asked whether the DNA level of the petiole is also affected. And, since the leaf blade is a site of auxin production, does postirradiation supply of the growth hormone alter the radiation effects?

PROGRESS REPORT

Leaves were arranged along an isodose arc centering on a 6,000 or 12,000-curie ^{60}Co source. The petioles, with their bases in water, were shielded by 4 in of lead. The exposure rate was 250 R/min. After irradiation or sham irradiation, the petioles were placed in tap water with or without auxin (500 μg napthaleneacetic acid/l). At several times thereafter the 0.5-cm basal segments of the petioles were analyzed for RNA (E_{258}-E_{290} after removal of soluble nucleotides and DNA), DNA (diphenylamine reaction), and RNA synthesis (incorporation of uracil-2-^{14}C into RNA). Also, petioles were scored subsequently for number of roots.

First, we substantiate our previous observations that there is an abscopal reduction in root initiation that is preceded by a drop in the level of gross RNA soon after irradiation. Second, in the 36-hr period after exposure there is no significant effect of irradiation on incorporation of the ^{14}C-uracil into RNA or on gross DNA level. Third, supplying auxin to the petiole rapidly increases the levels of RNA and of RNA synthesis, subsequently of DNA, and later the number of roots per petiole. Fourth, auxin reverses the radiation-induced decreases in RNA content and root initiation. It can be suggested, therefore, that the correlative decrease in root emergence after irradiation of the lamina is associated with an antecedent drop in the RNA of the petiole, that the effect on RNA is mediated by a concomitant rise in ribonuclease activity,[1] and that the correlative agent is auxin.

The proposed role of auxin in the preceding hypothesis rests on several bases: auxin is required for root initiation, the production and the levels of the hormone in plants are lowered by ionizing radiation, and auxin reverses the decreases in rooting and in RNA content

induced by radiation. A demonstration that the radiation-induced rise of ribonuclease activity is also reversed by auxin would strengthen the hypothesis. Accordingly, lamina were exposed to 10 kR, as before, and the petioles then immersed in water or auxin solution for 24 hr. Cell-free homogenates of the petiole bases were then assayed for gross ribonuclease activity, using yeast RNA as the substrate and measuring the nucleotides released by spectrophotometry. The results show again a radiation-induced rise in ribonuclease activity. However, supplying auxin at a concentration of 1 or 10 mg/l *enhanced* ribonuclease activity. There was a synergistic interaction between the effects of radiation and of auxin.

On fractionation of the petiolar tissues into soluble and particulate fractions we find ribonuclease activity in each fraction. Possibly the two fractions respond differently to auxin, and one response masks the other. Factorial experiments between γ irradiation (10 kR) and post-irradiation auxin treatment (1 mg NAA/l) were repeated; this time the petiole bases were homogenized in isotonic media and the particulate fraction brought down by centrifugation at 110,000 $\times$ g for 90 min. Soluble and particulate ribonuclease activities were determined at 30 and 50°C at the pH optima determined for each fraction at each temperature. The analytical data show that the soluble enzyme has on the order of 10 times more activity than does the particulate, both on a tissue weight and protein basis. For the soluble enzyme activity on a tissue weight basis, both radiation and auxin increase the activity and interact synergistically. Irradiation did not increase activity of the particulate enzyme.

CONCLUSIONS

Despite the ability of auxin to reverse the radiation-induced decreases in rooting and RNA level, the enhancement of gross and soluble ribonuclease activity by radiation is not reversed by auxin. Therefore, we modify our hypothesis on the role of auxin and RNA in the radiation response as follows: The initiation of roots in the petiole is dependent on auxin in high ratio to other growth factors and to translations mediated by RNA. Irradiation of the leaf blade decreases the basipetal supply of auxin to the petiole, and decreases the level of RNA in the petiole by activation of the soluble ribonuclease. (Whether or not auxin is the correlative agent in this activation is not clear; if it is auxin, its action is not direct.) Root initiation is retarded. Postirradiation supply of auxin to the petiole, though it raises the activity of soluble ribonuclease, also enhances the rate of RNA synthesis. The net effect is a maintenance or rise in the level of RNA, and within 36 hr, an increase in DNA that is indicative of a stimulated cell division. The abscopal retardation of root initiation is thus reversed completely by the growth hormone.

REFERENCE

1. Gordon, S. A. and E. M. Buess. Argonne National Laboratory Biological and Medical Research Division Annual Report, 1965. ANL-7136, pp. 293–294.

DEVELOPMENT OF A CAPACITANCE AUXANOMETER FOR THE MEASUREMENT OF GROWTH RATES

Solon A. Gordon and William A. Dobra

PURPOSE

In studies on the hormonal physiology of phototropism it became necessary to determine the action spectrum for the photoinhibition of shoot growth. Preliminary action spectra using shadowgraphy showed no fine detail.[1] A more sensitive nondestructive method for measuring shoot elongation was needed, one that did not involve visible light or contact of the organ. We describe here an auxanometer, based on capacitance micrometry that was developed to fulfill the above requirements.

PROGRESS REPORT

Our approach was based on the idea that incremental intrusion of a shoot between plates of an air capacitor would change proportionately the capacitance by dielectric and electrode effects. Initially, vertically oriented parallel plates were used as the capacitor. The shoot of the oat seedling was placed between the plates so that its longitudinal axis was parallel to the plates and in normal orientation with respect to gravity. Though changes in capacitance proportional to shoot growth were observed, the system was unacceptably sensitive to lateral displacements of the seedling, to circumnutatory movements, and to rapid changes in ambient temperature and humidity. The present version of the micrometer is a two-capacitor network electrically shielded and thermally insulated from the surroundings. The 2 capacitors are a vertical stack of 3 *horizontal* parallel plates, spaced 55 mm apart. Alter-

nate measurements are made by switching between the upper (test) capacitor, and the (lower) monitor capacitor. Changes in capacitance unrelated to incremental elongation of the shoot are compensated for by treating the monitor as a blank. The capacitance change is due entirely to changes in the geometry of the plant, with the significant variable being the distance from the tip of the shoot to the bottom of the top plate.

To permit calibration of the system by optical measurement of growth rates, narrow slits are provided on opposite sides of the shielding for scan, under dim green light, with a traveling micrometer telescope. A shutter at the top of the shielding and a removable plug in the top plate of the test capacitor enables vertical irradiation of the shoot in the spectral studies.

The calibration curve is nonlinear; it ranges in slope from 5.5 attofarads/μm growth for a plant 10 mm tall to 30 aF/μm for a plant 25 mm tall. As the system is capable of measuring a change in capacitance of 10 aF, a change in shoot length of 1 μm is within the range of sensitivity with oat coleoptiles of working height. As such coleoptiles grow about 1 mm/hr, growth increments in 3 to 5 sec can be detected. Repeated experiments using coordinated electrical and optical measurements show that the capacitance gives plant height to within 10% and changes in height to within 1% of the values determined optically. The electric field of the capacitor is produced by a 1-kHz, 30-volt potential applied intermittently across the plates. Optical measurement of the growth rates of oat coleoptiles over 8-hour periods, with the field switched on and off, showed no significant effect of the field on growth rate.

Preliminary photoinhibition studies show that exposure of the dark-grown coleoptile to 1500 ergs/sec·cm^{-2} of 4800 A light for 4 sec caused an immediate decrease of elongation. After 10 min the initial growth rate was re-established but soon began to slow again, perhaps exponentially.

REFERENCE

1. Gordon, S. A. and G. A. Brown. Argonne National Laboratory Biological and Medical Research Division Annual Report, 1967. ANL-7409, pp. 92–93.

GROWTH AND CONSTITUENTS OF OAT PLANTS GROWN UNDER SINGLE- AND MULTIDIMENSIONAL GRAVITY COMPENSATION

Solon A. Gordon

PURPOSE AND METHODS

Emphasis is being placed on the clinostat as a substitute for the free-fall environment, or as an essential test situation preliminary to the free-fall experiment. Classically, clinostats are devices designed to reorient the organism continuously by rotation on a horizontal axis, so that the tropic effect of gravity direction is nullified or "compensated." The same principle may be applied to the compensation of the directional component of other field vectors. Where the field direction is not fixed, relative to the organism, or where there are multiple fields different in direction, then compensation requires clinostats with multiple axes of rotation; ideally, the device should move the organism about a fixed rotational center so that a uniform distribution about that center would be achieved for orientation, angular velocities, and angular accelerations. As a Laboratory interdivision effort, a solution to this problem in analytical mechanics of rigid body motion was derived by Cook,[1] and implemented by an electromechanical servosystem designed by Johanson, et al.[2] The apparatus was constructed at ANL. We term it a "4-Pi" compensator. Plants were grown in this 4-Pi compensator, and at the same time in single-axis clinostats whose rotational axes were either horizontal (HR) or vertical (VR). The present report summarizes several studies on the growth and constituents of oat seedlings so grown.

PROGRESS REPORT

Four seeds were planted on the flat surface of a hemispherical chamber filled with 1.5% agar, 2 with embryos inward, 2 with embryos outward, all within a radius of 1 cm from the center of rotation. A hemispherical cover was placed over the base and the assembly inserted into a 4-Pi compensator. Identical assemblies were placed on single-axis clinostats, one with rotational axis horizontal (HR), and the other with rotational axis vertical (VR) as a control for motion, with plants in normal, erect orientation. The rotational rates were 2 rpm. After growing for 72 hr at 25°C in continuous darkness, the seedlings were removed and the length and weight of their coleoptiles, mesocotyls, and roots rapidly measured. These organs were chilled and then lyophilized at −20°C over P_2O_5 for subsequent analysis for soluble sugar and starch (anthrone technique, checked by ceric sulfate titration of reduced ferricyanide), lignin (dichloroquinone reduction), per-

oxidase (H_2O_2 oxidation of guanicol), and polyphenolase (catechol oxidation) activities.

When plant shoots are tilted to the horizontal, they are subject to shear, compression, and extension forces. These forces change in direction as the plant is rotated, and are supplemented by torques. Physiological changes attributed to compensation could be partly a consequence of these ancillary forces, and not nullification of the geosensor stimulus. Accordingly, plantings were also made in the spherical growth chambers where the seedling was completely surrounded and supported by moist vermiculite.

Roots of seedlings grown in the 4-Pi and HR compensators were greater in length than those from plants rotated on a vertical axis. Only the 4-Pi treatment yielded significant increase of shoot growth, reflecting the sensitivity of the mesocotyl. The 4-Pi and horizontal rotation clearly differed in their effects on mesocotyl and shoot length. An influence of the medium (full vs. half-supportive) on the response to compensation was observed for coleoptile length. Essentially similar results were obtained when organ weight was used as the index of growth.

Though no material effect of or between the gravity treatments on the soluble sugar levels of the root was observed, these levels were raised in the shoot by compensation. The rise in sugars in the compensated shoot could have derived from an accelerated hydrolysis of the starch of the shoot. However, both 4-Pi and HR compensation increased rather than decreased starch levels of the shoot and of the root. From this elevation of starch content an explanation can be suggested for the enhancement of geosensitivity in shoots by gravity compensation. Hertel *et al.*[3] have examined the geosensitivity of the shoots of numerous mutants of maize, and demonstrated a high, direct correlation between sensitivity and amyloplast size and content. Thus, the enhancement of geotropic sensitivity in compensated organs may be derived from the rise in starch level induced by compensation. As yet we do not know whether it is amyloplast size or number that is affected.

Lignin, an oxidation polymer of polyphenols, is deposited in and rigidifies cell walls as the gravitational load on the plant increases. Similar polyphenolic condensation takes place in cells under mechanical stress. We anticipated that support of the shoot by the growth medium during compensation, and an accompanying reduction of flexing, would lead to a decrease in its lignin content. However, there was a greater drop in lignin levels relative to VR controls in unsupported shoots, and both types of compensation *decreased* the concentration of lignin. These results provide a supplementary explanation for the increase of tropic sensitivity, to gravity and to light, of gravity-compensated shoots, and why compensation increases the effectiveness of auxin in the growth of shoots. A decrease of rigidifying elements in cell walls would lower wall pressure, facilitate auxin-induced extension of cells, and magnify the effect of lateral differences in hormone content.

Significant differences were noted between the two types of compensation and supportive medium in their effects on peroxidase and polyphenolase activity of the root. Possibly related to the extent of flexing of the shoot, both methods of compensation increased the titer of shoot peroxidase and polyphenolase with the half-filled chambers.

CONCLUSIONS

Material differences between 4-Pi and single-axis compensation were observed for growth of the mesocotyl and entire shoot. Differences between the two types of compensation were also found for the levels of starch, lignin, peroxidase, and polyphenolase of the roots but not of the shoot. In some instances the response to compensation was influenced by the support medium. If we assume that the distribution of orientations in both types of compensator are adequate for nullification of the directional component of gravity, two, not mutually exclusive, explanations for the differences are: First, terrestrial fields other than gravity influence the growth of plants when the dominating effect of gravity direction is nullified. Second, the patterns of stress distribution accompanying the motion required for the directional compensation of gravity affect significantly the plant response to that compensation. If the second inference is correct, then the assumption that the clinostat, with its integration of gravitational force direction to null spread in time, is equivalent in biological effect to the free-fall, with its simultaneous null of force and hence direction, is of questionable validity.

Both 4-Pi and single-axis compensation increased the content of soluble sugars and starch of the shoot but lowered its lignin content. These observations provide explanations for the enhancement of tropic sensitivity and responsivity to growth hormone elicited in shoots by gravity compensation.

Contributing to the biological portion of these studies were Susan Barr, Evelyn Buess, Erma Cameron, and Ray Hinchman. This study was supported by the National Aeronautics and Space Administration.

REFERENCES

1. Cook, J. M. *Math. Biosciences* **5**, 353–364 (1969).
2. Johanson, E. W., W. P. McDowell, O. D. Despe and G. A. McGinnis. *ISA Trans.* **6**(1), 20–24 (1967).
3. Hertel, R., R. K. dela Fuente and A. C. Leopold. *Planta* **88**, 204–214 (1969).

COMPARATIVE MORPHOLOGY OF NORMAL AND CALLUS INITIATED CARROT ROOTS

Ray R. Hinchman

PURPOSE AND METHODS

Undifferentiated plant tissue cultures will, under a variety of culture conditions, differentiate to form shoots, buds, leaves, and most commonly, roots. Many workers report differentiated organs from plant tissue cultures as "roots" or "buds" or "shoots" by their external appearance, without actually examining these structures microscopically to determine if they correspond morphologically to the organs of normal plants. In the present study we examine the validity of this assumption for the externally normal roots differentiating from carrot callus tissue.

In an attempt to obtain suspensions of undifferentiated carrot callus cells, explants of vigorous, rapidly growing carrot callus were transferred to liquid media. Soon after transfer it was noted that roots were developing from some of the callus masses. This material offered an excellent opportunity for a comparative morphological study between the roots developed in culture from previously undifferentiated callus and the normal roots of soil-grown plants.

Undifferentiated callus tissue of the carrot was transferred to liquid medium and placed on a rotating shaker. In about 12 days roots began forming on the callus masses. The cultures were allowed to grow for 45 days and then were fixed in FPA under vacuum. Since the callus was continually initiating new roots, roots of various sizes and ages could be found in the cultures at this time. Seed from the same lot used to obtain callus tissue was planted in potting soil and placed in the greenhouse under natural illumination. Plants were harvested after 20, 30, and 40 days of growth and fixed as above.

PROGRESS REPORT

Roots differentiated from carrot callus tissue are about three times greater in diameter than roots grown in soil, and have an undeveloped and generally disorganized appearance in cross section. The large cortical cells, which constitute most of these roots, are arranged in a haphazard manner around a tiny, undeveloped stele, which infrequently contains a few primary xylem elements. The callus root stele also lacks phloem, cambium, pericycle, and all secondary tissues. Callus roots were never observed to form lateral (secondary) roots. Normal carrot roots form laterals in profusion.

Most of the nuclei of cells of the callus roots are polyploid and contain multiple nucleoli, as do the undifferentiated callus cell nuclei. The nuclei of soil grown roots are usually diploid; rarely do they have multiple nucleoli.

The apical meristems of callus roots are quite normal in gross morphology, although at least twice as large as any root meristem on the normal plant. This suggests that the morphogenesis of the meristem is controlled by a stable system, and that the culture conditions introduce a disorganizing influence on the enlargement, differentiation and ploidy of root cells.

CONCLUSIONS

Large, externally normal root-like organs differentiating on carrot callus tissues in liquid media were found to be morphologically disorganized and quite rudimentary in structure when compared to normal soil-grown carrot roots of the same age. The callus roots were generally polyploid. It is questionable whether these callus "roots" function as roots. It is suggested that differentiated structures developing on plant tissue cultures be examined microscopically to determine if they correspond morphologically to the structures they resemble superficially.

This study was supported by the National Aeronautics and Space Administration.

PLASTID MORPHOLOGY AND ONTOGENY IN THE OAT SEEDLING

Ray R. Hinchman and Solon A. Gordon

PURPOSE AND METHODS

Correlations between the movement of starch-containing organelles, the amyloplasts, and organ orientation in plants has led to the concept that the amyloplasts function as gravitational sensors. Intracellular displacement of "statolith" amyloplasts in cells of the coleoptile tip and root cap presumably initiate the geotropic response. To assess the role of the amyloplast in the plant gravity perception mechanism, an electron microscope study of plastids in the oat seedling was

initiated. Special emphasis was placed on amyloplast ontogeny and starch mobilization as they relate to patterns of geotropic response.

Seeds of *Avena sativa*, cv. Victory, were hydrated, cold-treated, grown under conditions of continuous light or total darkness, and harvested at 0, 24, 48, and 72 hr after planting. The roots and shoots were fixed in glutaraldehyde, post-fixed in osmium tetroxide, embedded in Epon-Araldite, sectioned and stained for electron microscopy.

PROGRESS REPORT

In embryos fixed immediately after soaking, all of the proplastids are quite similar in appearance and are structurally simple. These proplastids consist of a double membrane enclosing a granular stroma that often contains masses of a fibrillar protein. In soaked and cold-treated embryos the appearance of the proplastids is identical to that described above with the notable exception that most of the proplastids now contain small starch grains. Thus, even at 4°C the enzyme system responsible for starch deposition is active.

At 24 hr virtually all of the plastids in the shoots of both light- and dark-grown plants have become temporary amyloplasts and are distended with starch. In the light-grown plants, some of the plastids have begun to form photosynthetic lamellae, although the fresh coleoptiles are not visibly green.

At 48 hr the starch content of coleoptile and leaf plastids are markedly reduced, more so in the light-grown plants than in the dark-grown. At this time several distinct pathways of differentiation in the plastids are evident, depending on the experimental treatment and on the location of the plastids in the shoot. In the light-grown plants, the plastids of the leaf cells and of certain sub-epidermal parenchyma cells of the coleoptile have turned bright green and become chloroplasts with well-developed grana. In the corresponding cells in the dark-grown plants the plastids have developed prolamellar bodies. In some instances the lamellae lie within deep grooves eroded in the starch grain surface, suggesting a participation of the lamellae in the process of starch grain degradation. Similar phenomena, but accentuated, are observed in the seedling sampled at 72 hr.

In the two primary geoperceptive regions of the oat seedling (the coleoptile tip and the root cap) a quite different situation exists. In dark-grown plants from 24 hr on, there is a striking similarity of the amyloplasts from the two regions at the ultrastructural level. The amyloplasts of the geoperceptive cells are large and are distended with starch, usually in the form of a tetrad of polyhedral granula. The high starch/stroma ratio may explain why they sediment to a greater degree than other amyloplasts of the seedling. In light-grown plants the starch content of the coleoptile tip amyloplasts is considerably decreased. This is consistent with the observation[1] that light-grown coleoptiles are not as sensitive to gravity as dark-grown coleoptiles.

CONCLUSIONS

The ontogeny of all the differentiated plastid types of the oat seedling begins with a common precursor—a relatively simple proplastid. The proplastid is ontogenetically plastic, following several pathways of differentiation depending on its location in the plant and on external growth conditions.

Considering the amyloplast as a statolith implies that it acts passively as a graviprecipitatable body, initiating the geotropic response by a *physical* displacement. From the present observations that indicate starch mobilization in the statolith amyloplasts of the geoperceptive cells, it is suggested that the amyloplast starch could act in the active physiological sense as a localized (one side of the cell) intracellular source of sugars.

This study was supported by the National Aeronautics and Space Administration.

REFERENCE

1. Wilkins, M. G. *Ann. Rev. Plant Physiol.* **17**, 371–405 (1966).

PARTICIPATION OF GOLGI APPARATUS IN GEOTROPISM

Jane Shen-Miller and Carol Miller

PURPOSE AND METHODS

Our preliminary study[1] on the effect of geotropic stimulation upon the Golgi apparatus indicates that in a horizontal coleoptile the bottom half of a cell has more Golgi apparatus, and more active forms of Golgi, than does the top half. The difference in the number of the active Golgi is greater in the cells of the lower-half tissue (with respect to gravity) than those in the upper. These observations suggest that activity and localization of activity of the Golgi apparatus are correlated with the direction of the gravitational field. Since the latent period between gravity stimulation and the appearance of visible curvature is relatively short,[2] we proposed to determine whether Golgi dis-

tribution and activation could be related in time to the geotropic response.

Oat coleoptiles were geotropically stimulated for various periods of time up to 60 minutes. The tip and the 5th mm of the coleoptile were harvested at 6-min intervals. They were further divided longitudinally into upper and lower halves. The halves were fixed either in $KMnO_4$ or in glutaraldehyde solution (the fixation schedule for the latter was suggested by Dr. E. Vigil of the University of Chicago). The activity of the Golgi was arbitrarily classified into the *active*, *intermediate* and *inactive* forms[1] and tabulated. All tissues were coded to minimize bias during scoring. An average of 25 and 30 cell sections at each sampling time were scored for glutaraldehyde and $KMnO_4$-fixed tissues, respectively.

TABLE 50. AVERAGE NUMBER OF ALL FORMS OF GOLGI APPARATUS IN THE TOP (T) AND BOTTOM (B) HALF OF A CELL IN THE UPPER (U) AND LOWER (L) TISSUES OF OAT COLEOPTILES WITHIN 30 MINUTES OF GEOTROPIC STIMULATION

	$KMnO_4$		Glutaraldehyde	
	U	L	U	L
	Tip mm			
T	2.62	3.04	1.82	1.70
B	3.05	3.51	2.15	2.16
	5th mm			
T	2.75	2.96	1.95	1.82
B	3.09	3.27	2.19	2.10

PROGRESS REPORT

Glutaraldehyde does not fix membrane organelles as well as $KMnO_4$; we were not able to account for as many Golgi apparatus as in the $KMnO_4$-fixed cells (Table 50). Between 6 and 18 min after stimulation, the bottom half-cell begins to show an increasing accumulation of Golgi apparatus. The average total number of Golgi apparatus within 30 minutes of stimulation is consistently greater in the bottom (B) than in the top (T) half-cell. This trend is illustrated more clearly in Figure 45. In the 5th mm segment (Fig. 45a), the number of active Golgi is significantly different, at the 1% level, between the top and bottom half-cells, both in the upper and lower half-tissues. The data in Figure 45b and for the tip segments in Figure 45a are as yet not complete; therefore, they were

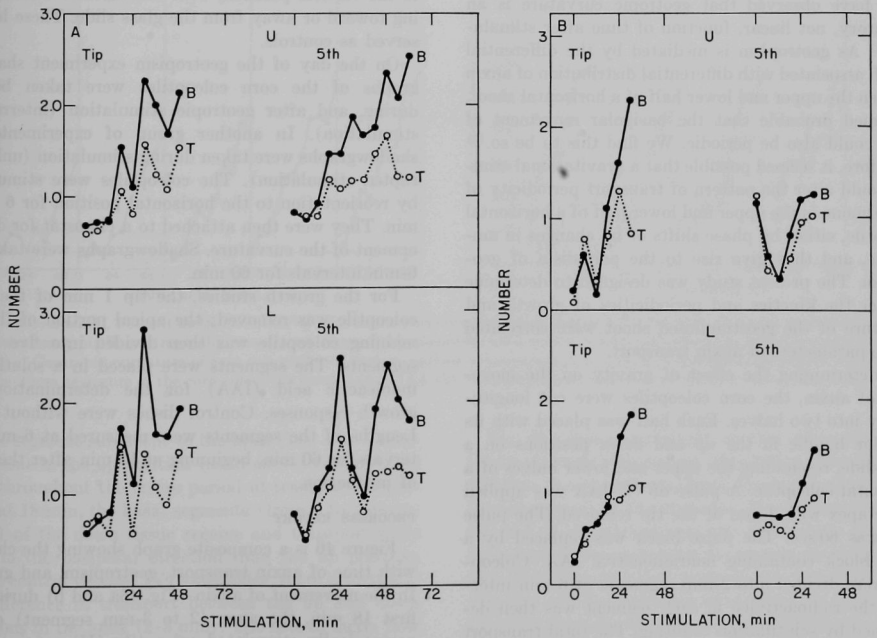

FIG. 45.—Distribution of "active" Golgi (intermediate plus active forms) between the top (T) and bottom (B) half of a cell in the upper (U) and lower (L) coleoptile tissue of oats that have been geotropically stimulated. a, $KMnO_4$ and b, glutaraldehyde fixed tissues.

not analyzed statistically. Regardless of the fixatives used, the number of active Golgi in the bottom half-cell also is consistently higher than in the top half. The difference between the two halves begins at about 12 min of stimulation. In geotropic curvature,[2] we find the appearance of visible geotropism occurring at about 30 min from the start of stimulation. If the Golgi apparatus is involved in the tropic curvature, it is reasonable that its activity change should precede the occurrence of actual curvature.

CONCLUSION

In the geotropically-stimulated oat coleoptile cell, the bottom half-cell has not only a greater total number of Golgi apparatus but also a greater number of the active form. The differences in Golgi distribution and morphology begins at about 12 min of geostimulation. The morphological changes in this organelle from the inactive to the more active form are compatible with the time constants for the occurrence of tropic curvature.

This study was supported by the National Aeronautics and Space Administration.

REFERENCES

1. Shen-Miller, J. and R. R. Hinchman. Argonne National Laboratory Division of Biological and Medical Research Annual Report, 1969. ANL-7635, pp. 320–322.
2. Shen-Miller, J., N. G. Noacke, and Judieth E. Baker. This report.

KINETICS AND PERIODICITY OF AUXIN TRANSPORT, GEOTROPIC CURVATURE AND GROWTH

Jane Shen-Miller, Neleen G. Noack, and Judieth E. Baker**

PURPOSE AND METHODS

We have observed that geotropic curvature is an oscillatory, not linear, function of time after stimulation.[1] As geotropism is mediated by the differential growth associated with differential distribution of auxin between the upper and lower half of a horizontal shoot, it seemed probable that the basipolar movement of auxin could also be periodic. We find this to be so.[2] Therefore, it seemed possible that a gravitational stimulus could alter the pattern of transport periodicity of the hormone in the upper and lower half of a horizontal coleoptile, either by phase shifts or by changes in amplitude, and thus give rise to the periodism of geotropism. The present study was designed to determine whether the kinetics and periodicities of growth and curvature of the geostimulated shoot were correlated to like parameters of auxin transport.

In determining the effect of gravity on the movement of auxin, the corn coleoptiles were cut longitudinally into two halves. Each half was placed with its vascular bundle in the *up* and *down* positions on a glass slide, resembling the upper and lower halves of a horizontal coleoptile. A pulse of ^{14}C-IAA was applied to the apex with 1 mm of the tip removed. The pulse time was 60 sec. The pulse block was replaced by a chase block containing nonradioactive IAA. Coleoptiles were divided into 2-mm segments at 6-min intervals; the radioactivity in each segment was then determined by scintillation counting. The total transport period was 60 min. We also placed halved coleoptiles in the vertical position, with the vascular bundle facing toward or away from the glass slide. These halves served as controls.

On the day of the geotropism experiment shadowgraphs of the corn coleoptiles were taken before, during, and after geotropic stimulation (interrupted stimulation). In another group of experiments, no shadowgraphs were taken during stimulation (uninterrupted stimulation). The coleoptiles were stimulated by reorientation to the horizontal position for 6 to 30 min. They were then attached to a clinostat for development of the curvature. Shadowgraphs were taken at 6-min intervals for 60 min.

For the growth studies, the tip 1 mm of the corn coleoptile was removed; the apical portion of the remaining coleoptile was then divided into five 2 mm segments. The segments were placed in a solution of indoleactic acid (IAA) for the determinations of growth responses. Control dishes were without IAA. Lengths of the segments were measured at 6-min intervals for 60 min, beginning at 12 min after the start of incubation.

PROGRESS REPORT

Figure 46 is a composite graph showing the changes with time of auxin transport, geotropism, and growth. In the movement of auxin (Fig. 46a and b) during the first 18 min, the apex (2 to 3-mm segment) of the geotropically stimulated coleoptile (H) retains more IAA in the tissue in the *down* position (dotted curve).

* Student Aide.

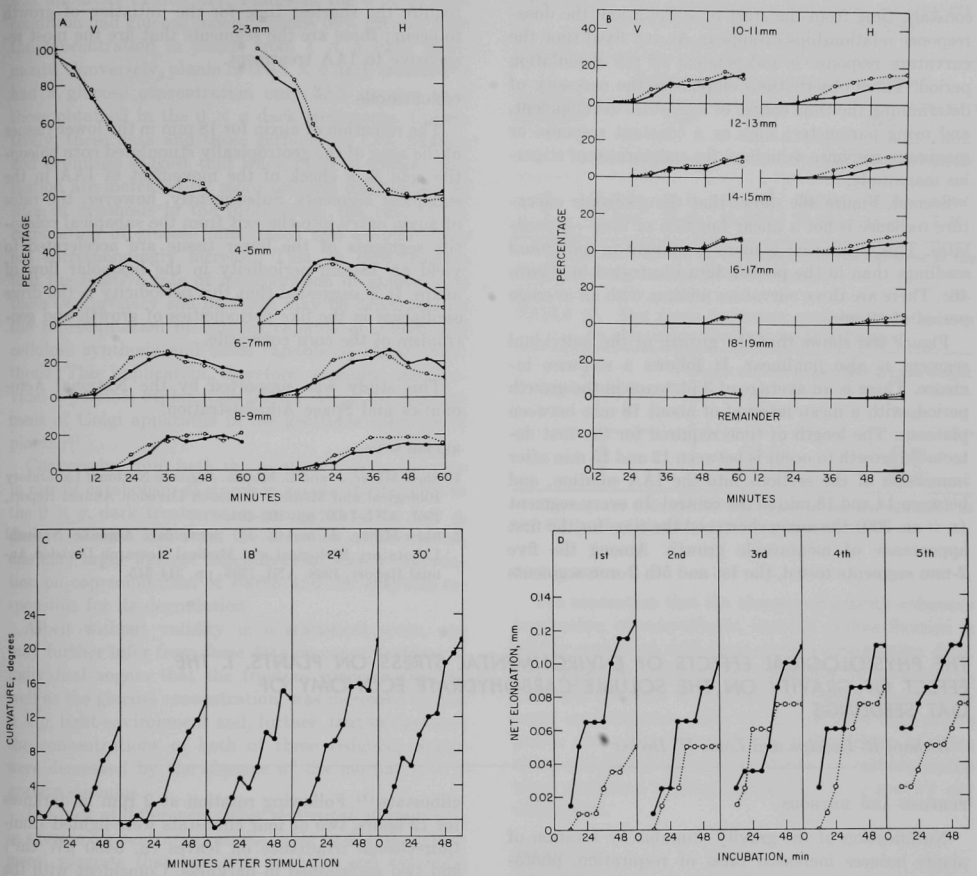

FIG. 46.—a and b. Percent distribution of ^{14}C-IAA in the various coleoptile segments from the apex (2–3 mm) to the basal region. V, vertical control; H, geotropically stimulated. Upper half coleoptile, solid curves; lower half coleoptile, dotted curves; $n = 9$ per datum. c. Geotropic curvature of corn coleoptiles of various periods of stimulation; $n = 20$. d. Representative growth curves of the various 2-mm segments of the corn coleoptile incubated in IAA (10^{-6} M, solid curve) and control (broken curve) solutions.

In the segment subjacent to the apex (i.e., 4 or 5 mm) the tissue in the *up* position (solid curve) retains more IAA throughout the entire period of transport. Beginning at 18 min, the basal segments (from 6 to 7 downward) of the *down* tissue receive and transport more IAA in the basipetal direction than the *up* position. In the control vertical (V) assemblies, there is virtually no difference in transport between the *up* and *down* positions in the apex (2–3 mm). The rate of auxin flow oscillates with a period of 18 to 20 min, though the oscillation is not as pronounced as that in the oat.[1]

Fig. 46c shows curvatures of corn coleoptiles after various periods of geotropic stimulation. This figure illustrates two phenomena. First, the degree of curvature is proportional to the stimulus. The interval between the end of stimulation and the appearance of curvature changes inversely with the magnitude of the stimulus. However, the time between the initiation of the stimulus and the initiation of curvature is a constant, about 27.5 min for the interrupted and 30.9 min for the uninterrupted type of stimulation. When the data (cf. Fig. 46c) are tabulated on the basis of curvature at a

constant time from the start of stimulation, the dose-response relationships disappear. At any fixed time the curvature response is independent of the stimulation period. These observations emphasize the necessity of determining the time course of curvature development, and using parameters such as a constant response or maximum response as indices for comparison of stimulus magnitude.

Second, Figure 46c shows that the geotropic curvature response is not a linear function of time—it oscillates. This oscillation is more prominent in individual seedlings than in the pooled data illustrated in Figure 46c. There are three curvature minima with an average period of 18 min.

Figure 46d shows that the growth of the individual segment is also nonlinear. It follows a stepwise increase. There is an average of 3 plateaus in the growth period, with a mean interval of about 18 min between plateaus. The length of time required for the first detectable growth to occur is between 12 and 15 min after immersion of the sections into the IAA solution, and between 14 and 18 min in the control. In every segment (n = ca. 200) the auxin shortened the time for the first appearance of measurable growth. Among the five 2-mm segments tested, the 1st and 5th 2-mm segments require the shortest time for the initiation of growth to occur; these are the segments that are the most responsive to IAA treatment.

CONCLUSIONS

The retention of auxin for 18 min in the lower tissues of the apex of the geotropically stimulated corn coleoptile acts as a check of the movement of IAA in the subapical segments. Subsequently, however, the rates of auxin entry into the exit from the subapical coleoptile segments of the lower tissue are accelerated to yield an 18-min periodicity in the basipolar flow of auxin. It is suggested that this periodicity is the drive oscillation in the like periodicities of growth and geotropism of the corn coleoptile.

This study was supported by the National Aeronautics and Space Administration.

REFERENCES

1. Shen-Miller, J. and L. Morris. Argonne National Laboratory Biological and Medical Research Division Annual Report, 1967. ANL-7409, pp. 102–104.
2. Shen-Miller, J. and E. G. Schneider. Argonne National Laboratory Biological and Medical Research Division Annual Report, 1968. ANL-7535, pp. 314–315.

THE PHYSIOLOGICAL EFFECTS OF ENVIRONMENTAL STRESS ON PLANTS. I. THE EFFECT OF GRAVITY ON THE SOLUBLE CARBOHYDRATE ECONOMY OF OAT SEEDLINGS

Richard R. Dedolph and Louis H. Decker

PURPOSE AND METHODS

Nullification of the gravity stimulus by rotation of plants induces increased rates of respiration, photosynthesis and net carbon fixation as measured by CO_2 uptake and evolution, during light and darkness. Heretofore, the effect of gravity force on the sugar content of plants has not been measured. Such measurements would provide confirmation of the results obtained when CO_2 measurement was used to index photosynthesis and respiration and further afford an inferential basis of the likely nutritional value of satellite-grown plants.

To obtain this information, oat plants were grown in special containers, under stationary conditions, for 7 days. Quartz sand, watered periodically with half-strength Hoagland's nutrient solution, was used as a rooting medium. When plants were of sufficient size containers with their plant complements were randomly selected and attached to special horizontal-axis clinostats.[1] Following rotation at 2 rpm in darkness for 12 hours, two of four clinostats were lighted (multidirectional irradiance on leaves ca. 3450 $\mu W/cm^2$) and two maintained in darkness. Coincident with the start of the different light regimes, one clinostat under each light condition was tipped so that its axis was vertical, placing plants on that clinostat in a normal gravity environment. The four environmental conditions ($0 \times g$, light; $1 \times g$, light; $0 \times g$, dark; $1 \times g$, dark) were then maintained for 9 hours, at which time the plants were harvested, weighed, separated as to tops and roots, and frozen for further analysis. Replication was obtained by repeating the described experiment. Sugar separation and quantitative analysis of these samples were performed by the methods described in the following contribution.[2]

RESULTS

A marked increase in glucose concentration in the plants subjected to a zero gravity stimulus under light

was apparent (Table 51). Plants in the 0 × *g*, light condition had glucose concentrations 68% greater than the concentration in plants from 1 × *g* light treatments. Conversely, plants in the 1 × *g* dark treatments had a glucose concentration only 35% greater than those obtained in the 0 × *g* dark treatments. Collectively, these data and those germane to CO_2 fixation and evolution suggest that when rates of glucose formation are increased by more uniform distribution of sites of synthesis in the protoplasm, the rate of incorporation of glucose into starch and cellulose does not correspondingly increase. This, in turn, implies that the relative rate of incorporation of glucose into these two primary end products may be dependent on the coprecipitation of entities capable of starch and cellulose synthesis and those capable of glucose synthesis. This implication, therefore, supports and provides a possible explanation for the suggested involvement of Golgi apparatus in the geotropic response of plants.[3]

Conversely, from both the relatively lesser increase in rate of catabolism of starch in plants attributable to the 0 × *g*, dark treatment as compared to the 1 × *g*, dark treatment and from the direction of this trend, one may argue against dependence of starch degradation on coprecipitation of starch and the enzymes responsible for its degradation.

Albeit without validity in a statistical sense, one may further infer from these data on concentrations of individual sugars that the fructose concentration, as well as the glucose concentration, was increased by the 0 × *g*, light environment and, further, that in darkness the concentrations of both of these reducing sugars were decreased by the absence of the normal 1 × *g* gravity stimulus.

The lack of difference, either statistical or apparent, in sucrose concentration attributable to gravity treatment, suggests that both the anabolic and catabolic metabolism of sucrose are gravity independent.

When the concentrations of these three sugars are summed (Table 52), the power of the statistical test employed is increased, and it is apparent that with adequate light, the absence of a gravity stimulus will increase plant sugar content.

TABLE 51. The Joint Influence of Light and Gravity on the Fructose, Glucose, and Sucrose Content of Oat Plants

Gravity stimulus, *g*	Sugar contents as μg sugar/g fresh weight*					
	Light			Dark		
	Fructose	Glucose	Sucrose	Fructose	Glucose	Sucrose
0	23.5cde	79.2a	12.7def	13.2def	35.9bc	8.0ef
1	17.4def	43.4b	13.8def	26.8cd	48.6b	7.3f

* Means not followed by the same letter are different at the 5% level of significance (F-test criterion).

TABLE 52. The Joint Influence of Light and Gravity on the Sugar Content of Oat Plants*

Gravity stimulus, *g*	Sugar content as μg sugar/g fresh weight	
	Light	Dark
0	115.5a	57.0c
1	74.7bc	82.8b

* Means not followed by the same letter are different at the 5% level of significance (F-test criterion).

CONCLUSIONS

The contention that the absence of gravity enhances respiration, photosynthesis, and net carbon fixation is wholly consonant with these sugar concentration data. The suggestion that Golgi apparatus is involved in geotropic response is similarly supported. From these sugar concentration data, we further infer that plants grown under conditions of free fall will be at least equal and likely superior as sources of carbohydrates when compared to plants grown in 1 × *g* gravity environments.

REFERENCES

1. Dedolph, R. R. and R. C. Waldbillig. Argonne National Laboratory Biological and Medical Research Division Annual Report, 1967. ANL-7409, pp. 105–106.
2. Dedolph, R. R. and L. H. Decker. This report.
3. Shen-Miller, J. and R. Hinchman. Argonne National Laboratory Biological and Medical Research Division Annual Report, 1969. ANL-7635, pp. 320–322.

THE PHYSIOLOGICAL EFFECTS OF ENVIRONMENTAL STRESS ON PLANTS. II. QUANTITATIVE EXTRACTION, SEPARATION, AND MEASUREMENT OF FRUCTOSE, GLUCOSE, AND SUCROSE IN PLANT TISSUE

Richard R. Dedolph, Louis H. Decker, and William Chorney

PURPOSE AND METHODS

Relative ease, rapidity, and economy, coupled with a high degree of accuracy of determination, renders the analysis scheme presented attractive as a method for determination of plant sugars.

Plant tissue, weighed and frozen at the time of harvest, was extracted with boiling 80% ethanol and then filtered through a 1.5-μ Millipore Solvinert filter. The alcohol was then evaporated from the extract on a steam bath and the aqueous solution remaining increased in volume. Protein present in this crude extract was precipitated with lead acetate, and the solution was filtered through a 0.25-μ Millipore filter. Lead was removed from the solution with Amberlite MB3 exchange resin. The exchange resin with adsorped lead was then removed by passing the fluid through a 1.5-μ Millipore filter; the aqueous filtrate was taken to dryness in a vacuum evaporator; and the dry residue was subsequently redissolved in 80% ethanol and brought to a convenient volume.

Aliquots of this solution containing 20 to 200 μg of each sugar along with a very small amount of ^{14}C-labeled fructose, glucose, and sucrose were spotted on Eastman Chromogram No. 6064 thin-layer sheets, using a micropipette and a Gelman spotting guide.

Chromatographs were developed with *n*-butanol: pyridine:water, 9:5:4 v/v in Gelman chambers. The Rf values were: fructose, 1.00; glucose, 0.85; and sucrose, 0.66. Best separation was achieved when the solvent was permitted to run to the end of the chromatograph (4- to 5-hr development time).

After they were developed and dried, the corners of the chromatographs were spotted with additional ^{14}C-labeled sugar, and they were radioautographed (Kodak No-Screen X-ray film, 24-hr exposure). Placing the developed X-ray film over the chromatograms permitted the exact location of the sugar spots on the chromatographs. Sugar spots were cut from the chromatographs, eluted with hot 95% ethanol, filtered through a 1.5-μ Millipore Solvinert filter, reduced to dryness, and the residue was redissolved in water (5 ml), and the sugar content was colorimetrically assessed following reaction with anthrone reagent (1.05 g anthrone in 500 ml glacial acetic acid 6.25 Na_2SO_3).

PROGRESS REPORT

Studies of the reproducibility of sugar contents so measured indicated that the variability between plant samples which had received the same treatment was 19.1 times greater than the variability between chemical determinations on the same sample. Radioactive assay of ^{14}C-labeled sugars added at the initial step in the analysis showed final recoveries near or in excess of 90%. Failure to recover all labeled sugar was independent of type of sugar and was found largely to be due to imperfect chromatographic elution.

CONCLUSIONS

Good separation of glucose, fructose, and sucrose can be obtained by utilizing a solvent developed for paper chromatography and Eastman Chromogram thin-layer cellulose sheets with relatively long development times. A nondestructive visualization technique, employing ^{14}C-labeled tracer sugars and autoradiography, enables the exact location of the separated sugars on the chromatographs. Following elution, the amounts of various sugars present may then be determined by sensitive colorimetric methods.

THE PHYSIOLOGICAL EFFECTS OF ENVIRONMENTAL STRESS ON PLANTS. III. THE PHYSICAL BASIS OF GRAVITY STIMULUS NULLIFICATION BY CLINOSTAT ROTATION*

Richard R. Dedolph and Merlin H. Dipert

The question of how rotation on a horizontal-axis clinostat removes plants from the influence of the gravitational stimulus is answered. It is shown that appropriate horizontal-axis clinostat rotation restricts the fall of intracellular particles to a quasi-circular path so that the position of the particle remains virtually stationary within cells. The displacement of the path of fall, due to centrifugal force, is then considered,

* Abstract of a paper submitted for publication in *Plant Physiology*.

and a method for determining the optimum rotation rate is developed from physical principles. This method selects the rotation rate which minimizes the volume of cytoplasm through which particles pass under the joint influence of centrifugal and gravitational forces. Recognizing that single-axis clinostats are ineffective with large plants or for long experiments, a new type of clinostat is proposed on which intracellular conditions can be rendered virtually identical to those of plants in satellite free fall, regardless of plant size or duration of the experiment.

It is shown that most low-gravity biological responses can be studied, using clinostats with only occasional satellite free fall experiments for verification. It is further suggested that most of these responses can be effectively and economically studied by computer simulation.

THE PHYSIOLOGICAL EFFECTS OF ENVIRONMENTAL STRESS ON PLANTS. IV. THE REMOVAL OF LEAD FROM AIR BY SOILS*

Richard R. Dedolph, Robert H. Stamps,† and William Chorney

Lead aerosols may be removed from air streams by passing them through a moist soil bed. The effect of flow rate, bed depth, and degree of water saturation on the efficiency of lead removal from air streams by soils suggest that lead removal depends upon adsorption of the metal on soil colloids. From these findings, the proposition that soil adsorption beds offer a practical and inexpensive method of removing lead and other heavy metals from exhaust streams of internal combustion engines, smelters, and other industrial processes is advanced.

* Abstract of paper prepared for submission to *Science*.

† ACM Undergraduate Honors Research Student.

THE PHYSIOLOGICAL EFFECTS OF ENVIRONMENTAL STRESS ON PLANTS. V. REST PERIOD REDUCTION IN NON-STORED ONION (ALLIUM CEPA) SETS*

Herbert J. Hopen,† Richard R. Dedolph, William F. Whiteside,† and William Chorney

Rest period reduction in non-stored onion (*Allium cepa*) sets is favored by postharvest temperatures of 5° and 25°C for periods of 1 to 10 days. A short-term postharvest temperature of 45°C favored rest period reduction, but periods over 24 hours at 45° did not reduce the rest period. Reduction of sprouting attributable to the 45° storage was more pronounced with the White Portugal cultivar than with yellow Ebenezer. Zero- to 800-rad γ irradiation did not significantly influence time of sprouting, but doses from 1,600 to 12,800 rads progressively decreased sprouting when followed by storage at 5° and 25°. Gibberellic acid (A_3) increased weights of plants grown from sets in the low postharvest storage temperature treatments. High postharvest storage temperatures (45°) negated the subsequent growth promoting effects of gibberellic acid. Prepublication application of these findings has resulted in commercial shipments of freshly harvested, non-stored onion sets under refrigeration.

* Abstract of a paper submitted for publication in the *Journal of the American Society for Horticultural Science*.

† University of Illinois, Urbana, Illinois.

PHOTOBIOLOGY STUDIES IN MAMMALS. I. X RADIATION AND THE CIRCADIAN THERMOPERIODICITY OF PEROGNATHUS PENICILLATUS

Solon A. Gordon, John L. Carrigan and James C. Liang**

PURPOSE AND METHODS

The pocket mouse, *Perognathus,* exhibits a circadian periodicity of body temperature between 35 and 36°C and ambient. Because of its well-defined and readily monitored temperature rhythms, its small size, and its lack of requirement for liquid water, the pocket mouse will be included in extraterrestrial probes to determine what happens to circadian rhythms in a mammal removed from the earth's rhythmic geophysical cycles. But organisms in such vehicles will be exposed to ionizing radiation, especially during periods of solar flare activity. If such radiation affects rhythms, it is possible that changes in periodicity under extraterrestrial conditions may not be a consequence of the diminution of an earth influence on the circadian clock, but a consequence of irradiation. The present experiments were initiated to determine if exposure of the pocket mouse to ionizing radiation will alter its thermoperiodicity.

Adult female *Perognathus penicillatus,* weighing approximately 20 g, were collected from the field in April, 1970. Body temperature was monitored by telemetry,[1] using a self-powered thermistor-modulated transmitter implanted into the peritoneal cavity. Each transmitter was individually calibrated by determining its pulse frequency at five temperatures within the range of interest, 19° to 39°C, and fitting a quadratic curve to these test points. Animals were scanned for 10 sec at 6-min intervals, using an electronic program interrogator. The number of pulses per individual scan was punch-coded on paper tape. These data were transferred to magnetic tape for processing by the S/360-75 computer. The pulse frequencies were translated to temperatures, using the previously determined calibration equations, and presented graphically as measured temperature vs. time for each animal. A smoothing function was also applied to the data, using the method of moving averages on successive sets of seven data points fitted by cubic polynomial; this step diminished the noise level and facilitated localization of the phase reference points.

PROGRESS REPORT

Two series of experiments were run. In series I, the aim was to expose mice to X radiation during free run under continuous darkness. The X-ray dosage was 210 R [250 kVp; HVL, 2 mm Cu], about 1/7 the LD_{50},[2] exposure rate 32 R/min. Three weeks after surgery, groups of animals were X irradiated at subjective Zeitgeber time (Z.t.) 0400, 0900, 1600, and 2100, so that the mice were exposed during the normothermic and hypothermic phases of the circadian rhythm. Controls were sham-irradiated by placing them on the irradiation turntable for a period equal to the exposure time. Midpoints of the normothermic and hypothermic periods were used as the phase reference points. Scanning was continued for 11 days after irradiation, maintaining continuous darkness. No significant departure from the established τ (23 to 25 hr) or its phasing in the free-running animals could be attributed to the irradiation; transients immediately after exposure were occasionally observed.

For experimental series II, entrained animals were used. Mice were maintained on an *LD 12:*12 (tungsten filament lamps, irradiance 450 $\mu W \cdot cm^{-2}$) for a period of 14 days after surgery and irradiated at Z.t. 1630. Retaining the same photoperiod, scanning was continued for a period of about 1 month. In one irradiated animal there was a shallow cycle the first day after irradiation and then a continuance of wide-range thermoperiodicity for the next 6 days. Shallow hypothermic periods characterized the next 3 circadian cycles, followed by a return, for 4 cycles, to wide-range thermoperiodicity. At this time, about 14 days after irradiation, the circadian rhythm disappeared completely for 1 week; the temperature of the animal remained at the normothermic level, retaining the 1- to 2-hour ultradian rhythms, and then rose to 39°. At about 3 weeks after irradiation circadian periodicity resumed, developed gradually into deep thermoperiodicity, and then disappeared again in hypothermia.

The extended circadian arhythmicity began over a week after X irradiation, and was accompanied by hyperthermia. For these reasons we believe that the arhythmicity may be a secondary component of the radiation syndrome. Delayed hyperthermia has been observed for the irradiated human[3] and the irradiated dog,[4] where it was attributed to concomitant septicemia.

Of the total of 4 mice irradiated and 4 control mice in series II, 2 of the irradiated mice had periods where there was an extended absence of circadian thermoperiodicity. On this basis, we suggest that ionizing radiation will add an additional equivocal factor in the interpretation of the effect of extraterrestrial flight on the patterns of circadian periodicity of the pocket

* Summer student aides.

mouse. We also suggest that the potential complication of radiation effect reduces the likelihood that presently planned extraterrestrial packages will resolve the intrinsic vs. extrinsic clock controversy.[5]

We are indebted to W. Eisler and D. LeBuis for their assistance with the telemetry equipment, to S. Tyler, M. Dipert, and J. Blomquist for aid in the programming and utilization of the computer, and to C. Poole for the lessons in surgery. This study was supported by the National Aeronautics and Space Administration.

REFERENCES

1. Jaroslow, B. N. and W. J. Eisler, Jr. Argonne National Laboratory Biological and Medical Research Division Annual Report, 1968. ANL-7535, pp. 103–105.
2. Gambino, J. J. and R. G. Lindberg. *Radiat. Res.* **22**, 586–597 (1964).
3. Bond, V. P., T. M. Fliedner, and J. O. Archambeau. *Mammalian Radiation Lethality.* Academic Press, New York, 1965, pp. 144 and 149.
4. Norris, W. P., T. E. Fritz, C. E. Rehfeld, and C. M. Poole. *Radiat. Res.* **35**, 681–708 (1968).
5. Brown, F. A., J. W. Hastings, and J. D. Palmer. *The Biological Clock; Two Views*, Academic Press, New York, 1970.

PHOTOBIOLOGY STUDIES IN MAMMALS. II. SPECTRAL SENSITIVITIES FOR THE PHASING OF CIRCADIAN TEMPERATURE RHYTHMS IN PEROGNATHUS PENICILLATUS*

Solon A. Gordon and Gerald A. Brown†

A number of circadian phenomena in plants are initiated or phased by red light. In view of the sensitivity of mammalian cells and organelles to this spectral region, we thought that circadian mammalian rhythms might respond similarly. To test this hypothesis, baselines of the thermoperiodicities of free-running and entrained pocket mice were determined by telemetry. These animals, located at various wavelength loci of the Argonne Biological Spectrograph, were then exposed to monochromatic light during the "dark," normothermic, phase of the rhythm. The wavelengths at which significant phase changes were observed were 550, 525, 500, 475, 450, and possibly 425 nm. We suggest that the most effective wavelengths for phase delay and perhaps for entrainment are not in the red spectral region but in the blue-green. The relatively higher effectiveness of the blue-green light is compatible with the proposition that the eye is the principal photoreceptive organ in the phasing of circadian rhythms of *Perognathus* by light, particularly in view of the predominant number and function of rods (rhodopsin receptors) in the eye of the mouse.

* Abstract of a paper to be published in the Proceedings of the Symposium on Biochronometry, Ed. M. Menaker, National Academy of Sciences, Washington, D. C.

† College of Veterinary Medicine, University of Illinois, Urbana.

PHOTOBIOLOGY STUDIES IN MAMMALS. III. THE INDUCTION OF CHROMOSOME ABERRATIONS IN PIG KIDNEY CELLS BY FAR-RED LIGHT*

Solon A. Gordon, Agnes N. Stroud,† and Chen H. Chen‡

Exposure of pig kidney cells in monolayer culture to far-red light (FRL), near 750 nm in wavelength, raises the frequency of chromatid aberrations. Dose-response curves for this effect of FRL reach a maximum at incident energies of ca. 50 millijoules·cm^{-2} and then decline. Lowering the temperature of the cells during exposure increases the aberration yield. When cells were exposed to FRL at various times after subculture, they showed peaks in the aberration yield when the intervals were about 16 and about 22 hours. These maxima correspond to the early S and G_2 stages of the cell cycle of the synchronized fraction of the population, as determined by pulse labeling with tritiated thymidine. The induction of chromosome damage by FRL is interpreted as a consequence of a decrease in repair of a high spontaneous aberration frequency or an impairment of chromosome synthesis.

* Abstract of a paper to be published in *Radiation Research.*

† Jet Propulsion Laboratory, Pasadena, California.
‡ South Dakota State University, Brookings.

Mammalian Genetics

DETERMINATION OF THE RADIATION INDUCED MUTATION RATE FOR SEX-LINKED LETHALS AND DETRIMENTALS IN THE MOUSE

Douglas Grahn, Ruth Ann Lea, and Jane L. Hulesch

PURPOSE AND METHODS

The mutation rate for sex-linked genes in the mouse is still a somewhat indeterminate value. A recently reported study employing a direct three-generation screening test with the mouse proved inconclusive for the induction of lethals by X-irradiation.[1] Other studies with mice and rats have generally relied on simple sex-ratio changes among the progeny of irradiated parents, although the element of direct screening has been incorporated in those studies involving sequential generations of irradiation and breeding.[2, 3] While some evidence for lethals is often detected, the overall results can be considered equivocal.

The situation is similar for studies on humans. The Hiroshima-Nagasaki data originally demonstrated evidence for the existence of sex-linked lethals among the progeny of irradiated parents,[4] but a subsequent analysis was negative.[5] A similar sequence of events was observed in a three-generation study of Italian families; a first report gave positive evidence of spontaneous lethals[6] while a later report was negative.[7]

Although several preliminary reports have been made on the study to be presented here,[8, 9] a final analysis has only been recently completed. The three-generation test system has been previously described in detail.[10, 11] Briefly, the procedure is to mate the irradiated (500 R) or control male to a female carrying the sex-linked, male-lethal, Tortoise (*To*) gene. The F_1 dam, with the marked chromosome now opposite the test chromosome, is outcrossed to produce second generation progeny that are scored for sex ratio, preweaning mortality, and *To* segregation ratio. A presumptive F_1 carrier dam for a new lethal mutant is initially recognized by a shift in sex ratio. As the expectation is normally 0.33 (number of males/total offspring), or 2 females to 1 male, due to the lethal effect of *To* in the male, a new lethal mutant on the unmarked X will cause the sex ratio to shift to 0.20, or 4 females to 1 male, if the lethal is $\geqslant$50 crossover units from *To*. The imbalance becomes calculably greater, if the lethal occurs closer to the *To* locus. Appropriate probability tests can be applied to permit consistent decision on the classification of a chromosome-at-risk as a suspect lethal-carrier or as a reject.

PROGRESS REPORT

Parent Generation

The irradiated males were held for 70 days to assure that only sperm from irradiated spermatogonial stages would be sampled. Both C57BL/6JGh and A/JGh males were used; the former showed nearly 50% sterility, though for both strains, fertile males were capable of being utilized for many months.

First Generation Progeny

Three genetically different sets of dams were used, the C57BL/6 and A strains, and a specially derived A:CF$\aleph$1 criss-cross hybrid. The parental crosses were always outcrosses to insure adequate hybrid vigor to the F_1 to overcome any possible synergistic lethal effect of the *To* gene in combination with any new lethal. Although litter size varied among the three F_1 sets, the average litter size reduction of 14.3% in irradiated families did not show significant heterogeneity. This reduction is nearly 3%/100 R to the 'gonia, and it does not vary significantly over 10 to 12 parities, though mean litter size steadily declines with parity.

There are no significant sex-ratio differences in this generation, and there is no manifestation of genetic damage as measured by postnatal mortality to 21 days of age. There is, in fact, a small but not significantly greater mortality among control progeny that is not a function of differences in mean litter size.

Second Generation Progeny

The individual chromosome-at-risk, or F_1 dam, ultimately becomes categorized in one of several classes:

1. Aparous or sterile.

2. Parous but discarded with insufficient progeny to meet minimum decision making criteria.
3. Reject as non-carrier of a lethal.
4. Preliminary suspect carrier that is finally rejected as a non-carrier (Type I error probability between 0.1 and 0.35; the probability of rejection as a false negative).
5. Suspect carrier that is accepted and subject to further genetic evaluation; Type I error of 0.35.

The data can be summarized in accordance with the above 5 categories:

Number of chromosomes at risk:	OR: 355;	500R:326	
Category 1—Aparous:	OR: 3.94%;	500R:3.99%	$p > 0.05$
" 2—Discard:	OR: 6.74%;	500R:10.54%	$p > 0.05$
" 3—Reject chromosomes:	OR: 275;	500R:227	
" 4—Suspect-reject:	OR: 11.32%;	500R:12.50%	$p > 0.05$
" 5—Suspect-test:	OR: 2.20%;	500R:6.43%	$p = 0.01$

If the difference between treated and control in category 5 is accepted as a measure of radiation induced lethals and detrimentals, then an estimate of the mutation rate can be made. This difference of $4.23 \pm 1.64\%$ gives an estimate of 8.5×10^{-5}/R/X [0.0423/500 R] with 95% confidence limits of 2.0×10^{-5} and 14.9×10^{-5}.

Significantly, the suspect class shows a litter size reduction of about 10% below the reject class. While this reduction is somewhat less than the 25% that would be predicted on the assumption that the shift in sex ratio from about 2:1 to 6:1 was entirely attributable to prenatal deaths of males, it is nevertheless positive evidence of the segregation of lethal or sublethal mutants. Strictly random deviations in sex ratio would not be expected to show an accompanying reduction in litter size.

There is also evidence of a slight but significant increase in postnatal mortality in the full second generation progeny array. Since both sexes show a small elevation of mortality in the first 21 days of life in families derived from the irradiated grandsire, the genetic damage may be largely autosomal. It also may be a reflection of induced genetic damage in the reproductive capability of the F_1 dam in the irradiated line.

Third and Later Generations

Most of the suspect F_1 dams had sufficient adult non-*To* daughters to permit further genetic analysis. Nearly all of the suspects proved negative in the third and fourth generations, but several are still under test in the fifth and sixth generations. None of the suspect chromosomes has yet been proved to carry a categorical lethal mutation. Although there is a reasonable expectation of random loss of any lethal mutation, the present results suggest that the X-chromosome of the mouse may efficiently eliminate most new lethals, possibly as zygotes or in early gestation. The suspect mutations, therefore, may be of sublethal or detrimental quality whose level of lethal expression may be rapidly modified through recombination and coadaptation. The new mutant may, therefore, be either eliminated *in utero*, or transmitted as a relatively minor detrimental gene.

CONCLUSIONS

A three-generation test system designed to detect lethal and detrimental mutations on the X-chromosome of the mouse gives an estimate of the radiation induced rate as 8.5×10^{-5}/R/X with 95% confidence limits of 2 and 15×10^{-5}. Associated evidence of reduced litter size confirms the occurrence of genetic damage in the form of lethals and detrimentals, but it has not been possible to identify or isolate a categorical lethal.

REFERENCES

1. Schröder, J. H. Proc. IVth International Congress of Radiation Research, Evian, France, 1970, in press.
2. Searle, A. G. *Mutation Res.* **1**, 99–108 (1964).
3. Havenstein, G. B., B. A. Taylor, J. C. Hansen, N. E. Morton, and A. B. Chapman. *Genetics* **59**, 255–274 (1968).
4. Schull, W. J. and J. V. Neel. *Science* **128**, 343–348 (1958).
5. Schull, W. J., J. V. Neel, and A. Hashizume. *Am. J. Human Genetics* **18**, 328–338 (1966).
6. Cavalli-Sforza, L. L. Demographic attacks on genetic problems. Some possibilities and results. *The use of vital and Health Statistics for Genetic and Radiation Studies*. United Nations, New York, 1962, pp. 221–231.
7. Cann, H. M. and L. L. Cavalli-Sforza. *Am. J. Human Genetics* **20**, 381–391 (1968).
8. Grahn, D., F. A. Verley, and W. P. Leslie. *Genetics* **54**, 336 (1966).
9. Grahn, D., W. P. Leslie, and R. Craggs. *Proc. XII Int. Congr. Genetics*, Vol. I, 1968, p. 96
10. Grahn, D., F. A. Verley, W. P. Leslie, K. F. Hamilton, and B. Slaughter. Argonne National Laboratory Biological and Medical Research Division Annual Report, 1965. ANL-7136, pp. 124-126.
11. Grahn, D., F. A. Verley, W. P. Leslie, and B. Slaughter. Argonne National Laboratory Biological and Medical Research Division Annual Report, 1966. ANL-7278, pp. 144–145.

GENETIC LOCATION OF A SEX CHROMOSOME CONTROLLER GENE ON THE NORMAL X OF THE MOUSE*

Douglas Grahn, Ruth Ann Lea and Jane L. Hulesch

Data have been presented on the genetic identification and location of a controller gene, *Cg*, on the normal X-chromosome of the mouse. The gene is identified by its enhancing action on the phenotypic expression of linked mutant genes. In this case, the genes Greasy (*Gs*) and Brindled (Mo^{br}) have been employed in a 3-point linkage test. The presence of *Cg* is recognized by extreme expression of the greasy coat characteristics and by the extensive occurrence of the grey-mottled hair color of Mo^{br}. Confirmation of the linkage has been accomplished by independent genetic tests with Blotchy (*Blo*), an allele of Mo^{br}. Significantly, the controller gene also expresses its enhancing action in the hemizygous male, thus indicating the action of *Cg* is at least not restricted to inducing non-random X-inactivation. Although the exact action of *Cg* is unclear, it does not seem to be a focal point from which a gradient of inactivation emanates. It may influence the original inactivation event, stimulate partial or complete reactivation, or possibly act, through a system of secondary activators, as a major regulator or sensor gene.

* Abstract of paper submitted to *Genetics*.

Microbial Genetics

THE GROWTH-DUPLICATION CYCLE. XII. THE DISTRIBUTION OF CELL GENERATION TIMES AND ITS RELATIONSHIP TO LINEAR CELL GROWTH*

Herbert E. Kubitschek

Two different distributions of generation times, lognormal and reciprocal normal, were compared by fitting them to experimental generation time distributions for bacteria, yeast, protozoa, and mammalian cells. In every case the reciprocal normal distribution gave the better agreement, whether the original frequency distributions or their cumulatives were compared. The lognormal distribution failed to give significant agreement for three of the original distributions. It is concluded that the reciprocal normal distribution of generation times or, more precisely, the truncated normal distribution of generation rates, is consistent with the published data for steady state populations of all kinds of cells that divide by regular binary fission. A model is suggested for this distribution of generation times, associating it with control of transport of materials into the cell, and with linear cell growth.

Figure 47 shows the distribution of cell generation times for this model, which is based upon the following assumptions:

1. All cells have the same mass, *M*, at birth, and the same mass, 2*M*, at division.
2. Each cell grows at a constant rate.
3. Growth rates of individual cells are described by a normal distribution.

As may be seen in this figure, this model leads to a skewed distribution of generation times. For each cell, the change in mass from birth to division, *M*, depends

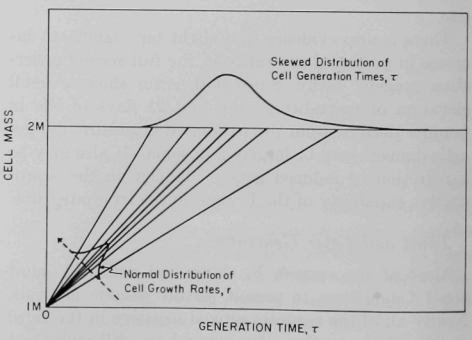

FIG. 47.—The relationship between linear cell growth and the generation time distribution. The population density is indicated by the normal distribution of cell growth rates on the dashed-line base. The frequency distribution of generation times is drawn just above the line labeled 2*M*.

* The first paragraph is the abstract of a paper to be published in *Cell and Tissue Kinetics*.

upon its growth rate, r, and its generation time, τ:

$$M = r\tau,$$

or

$$r = M(1/\tau).$$

Because M is a constant, the last equation shows that the *reciprocal* of the generation time $1/\tau$, must have the same distribution as that for growth rate, assumed above to be normally distributed. This prediction is compatible with experimental observations for bacteria, yeast, protozoa, and mammalian cells.

POTASSIUM UPTAKE IN E. COLI*

Herbert E. Kubitschek, Michael L. Freedman, and Simon Silver†

The uptake of potassium as ^{42}K during the cell growth-duplication cycle was examined in both synchronized and synchronous cultures of *E. coli*. In a synchronized culture, uptake rates were relatively constant during the first half of the initial cycle, doubled abruptly during the last half, and returned to the initial value when all cells had divided. There was no detectable deviation from a constant rate of uptake throughout the entire cycle in synchronous cultures. This constancy supports an earlier interpretation for steady state cultures, that uptake is limited in each cell by a constant number of sites for binding, transport, or accumulation of compounds from the growth medium, and that the average number of such uptake sites doubles late in each cycle. The abrupt doubling of the rate of uptake of potassium ^{42}K in the synchronized culture appears due to partial uncoupling of cell division and to activation or synthesis of these uptake sites.

In addition, preliminary findings indicate that the sites of action and the degree to which the action of SH poisons can be reversed are different for cell division and ^{42}K uptake. Cell-division blockage is not freely reversible, potassium uptake, although SH groups appear to play a role in the accumulation of ^{42}K, whether their function is primary, i.e., as the K-carrier, or secondary, i.e., as sites in an energy-producing process removed from the "potassium pump." Cells apparently killed by SH poisons can be restored to ^{42}K uptake competency. Further experiments are planned in which additional reagents will be used, such as glutathione, Ellman's reagent, cystine, spironolactone, and dithioerythritol, to determine the generality of the response of ^{42}K uptake to SH reagents and poisons.

* The first paragraph is the abstract of a paper submitted to the *Journal of Bacteriology*.

† Biology Department, Washington University, St. Louis, Missouri.

CHROMOSOME REPLICATION IN SLOWLY GROWING BACTERIA

*Herbert E. Kubitschek, Michael L. Freedman, and David Valdez**

PURPOSE AND METHODS

Although the pattern of DNA replication in rapidly growing bacteria appears to be well established,[1-3] conflicting patterns of chromosome synthesis have been observed in slowly growing cells. Replication appeared to occupy the first two-thirds of the generation cycle in cultures of *Escherichia coli* B/r,[3, 4] whereas in steady state cultures of *E. coli* 15 T^- synthesis of DNA was confined to the last half[5] or the final third[6] of the cycle.

In principle, one can distinguish between such divergent results by determining the average number of genomes per cell. If all cells had replicated their DNA just after birth, each would contain two genomes, and if replication occurred just prior to division, each would contain only one genome. Correspondingly, if DNA synthesis occupies the first two-thirds of the cycle[2] or only the final third[6], it can be shown that the average genome equivalents are 1.67 or 1.17, respectively.

We have measured the average rate of DNA synthesis, exposing culture samples to ^{3}H- or ^{14}C-thymidine, by extracting unincorporated thymidine with cold trichloracetic acid, and then by measuring residual radioactivity of incorporated thymidine. We also determined average amounts of DNA per cell, using the Burton diphenylamine method. Cells were grown at different rates in glucose-limited chemostats or in the exponential phase in batch cultures.

* Supported by Argonne Center for Educational Affairs.

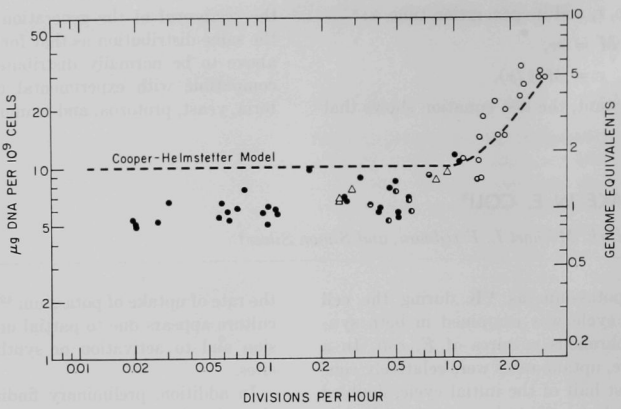

FIG. 48.—Average amount of DNA per cell in steady state cultures of *E. coli* B/r. ● and △, chemostat cultures; all others, batch cultures in the exponential growth phase.

PROGRESS REPORT

Values of thymidine incorporation per cell per generation were relatively constant at very slow growth rates, decreased to about a fourfold smaller minimum at about 0.3 division per hour, and then continually increased with growth rate. The results are inconsistent with our knowledge of the number of genome equivalents in these bacteria. The most slowly growing cells contain no fewer than one genome, and rapidly growing bacteria can contain several genome equivalents. Thus, the decrease in values for the middle growth region indicates the failure of the thymidine-labeling method for determining rates of synthesis of DNA.

This decreased incorporation of label supports the observation that *E. coli* produces an enzyme, thymidine phosphorylase, that breaks down thymidine to thymine, thereby reducing incorporation of thymidine.[7] Since adenosine inhibits the production of phosphorylase,[8] we tested for the presence of this enzyme by adding adenosine to chemostat cultures growing at about 0.3 division per hour. Thymidine incorporation increased, as expected, supporting the presence of the phosphorylase.

Average amounts of DNA per cell are shown in Figure 48. For comparison, the average number of equivalent genomes per cell, according to Cooper and Helmstetter's model, is indicated by the dashed line. Our values agree with theirs only over a limited region near 1 division per hour.

Our results do not support the Cooper-Helmstetter model:

1. Amounts of DNA per cell are smaller than predicted by about 40 to 50%, leading to theoretically impossible values of less than one genome equivalent at very slow growth rates.

2. Average DNA contents increase with growth rate, rather than remaining constant at rates below 1 division per hour.

The experimental results are in agreement with DNA synthesis only during the final portion of the cycle.[6] The most slowly growing cultures contain about the same amount of DNA per cell as that estimated for the single genome of *E. coli* B/r, 4.2×10^{-15} g DNA/cell.[2]

CONCLUSION

Chromosomes of slowly growing cells of *E. coli* B/r replicate only during the final portion of their generation cycles, contrary to earlier observations for synchronized cells of the same strain. Measurements of DNA synthesis by thymidine incorporation are unreliable over a range of growth rates in glucose-limited chemostat cultures.

REFERENCES

1. Helmstetter, C. E. *J. Mol. Biol.* **24**, 417–427 (1967).
2. Helmstetter, C. E., and S. Cooper. *J. Mol. Biol.* **31**, 507–518 (1968).
3. Cooper, S., and C. E. Helmstetter. *J. Mol. Biol.* **31**, 519–540 (1968).
4. Helmstetter, C., S. Cooper, O. Pierucci, and E. Revelas. *Quant. Biol.* **33**, 809–822 (1968).
5. Lark, C. *Biochim. Biophys. Acta* **119**, 517–525 (1966).
6. Kubitschek, E. E., H. E. Bendigkeit, and M. R. Loken. *Proc. Nat. Acad. Sci.* **57**, 1611–1617 (1967).
7. Rachmeler, M., J. Gerhart, and J. Rosner. *Biochim. Biophys. Acta* **49**, 222–225 (1961).
8. Yagil, E., and A. Rosner. *J. Bact.* **103**, 417–421 (1970).

REGULATION OF CHROMOSOME REPLICATION IN BACILLUS SUBTILIS: MARKER FREQUENCY ANALYSIS AFTER AMINO ACID STARVATION*

James C. Copeland

Marker frequency analysis of DNA isolated from amino acid starved *Bacillus subtilis* cells shows most chromosomes have not completed replication to the terminus. In strain W23 about 89% of the chromosomes have not completed replication after leucine starvation. Furthermore, the distribution of marker frequency ratios for different genetic markers on the chromosome shows that replication forks have stopped in a random fashion for those uncompleted chromosomes. The results are not compatible with regulation of chromosome replication at the initiation step only.

* Abstract of a paper to be published in *Science*.

REGULATION OF CHROMOSOME REPLICATION IN BACILLUS SUBTILIS: EFFECTS OF AMINO ACID STARVATION IN STRAIN W23*

James C. Copeland

Amino acid starvation allows limited synthesis of DNA in *B. subtilis* strain W23. DNA synthesis increased by about 30% after leucine starvation and by about 60% after histidine starvation. Genetic analysis by density transfer, and gradient analysis by transformation, on the DNA synthesized after amino acid starvation showed that all genetic markers examined have replicated, regardless of which amino acid was starved for. Initially all markers replicated equally, an observation consistent with the earlier result showing that chromosome replication stops randomly after amino acid starvation in this strain. It appears that chromosome replication simply resumes from the site where it had stopped once growth is restarted. It is interesting to note that upon further replication the *thr* to *cys*B and *arg*A to *lys* regions of the chromosome replicated ahead of their neighboring, proximal regions. A similar observation was noted in the reported study with strain 168. This could indicate that preferred stopping sites exist in these regions or additional sites from which replication can originate reside there. These results are not consistent with chromosome replication being controlled simply at the initiation event.

* Abstract of a paper published in the *Journal of Bacteriology* **105**, 595–603 (February 1971).

REGULATION OF CHROMOSOME REPLICATION IN BACILLUS SUBTILIS: MODULATION CONTROL OF DNA REPLICATION

James C. Copeland

PURPOSE AND METHODS

In previous studies I have shown that the initiation event can not account for control over chromosome replication in *B. subtilis* during amino acid starvation. Further analysis has revealed a strong correlation between the relationship of DNA/mass and the "stopping" and "starting" of chromosome replication during and after amino acid starvation.

PROGRESS REPORT

In Figure 49 is represented the change in amount of DNA and cell mass, as measured by optical density, during amino acid starvation and subsequent growth after starvation for 168 substrain BC 200. DNA synthesis stops after an increase of about 70% during starvation for leucine. The DNA/mass relationship shows that initially it increases to a value slightly above 1.2, where it plateaus and then increases again until it reaches a final value twice the first plateau, or about 1.4. Upon restart of growth, the DNA/mass relationship drops to 1.0 and stabilizes near that value, which represents the normal DNA/mass ratio for these cells grown in a glucose-mineral salts medium. The drop in DNA/mass on restart corresponds to a 50-minute delay in DNA synthesis during which time cell mass is continually increasing.

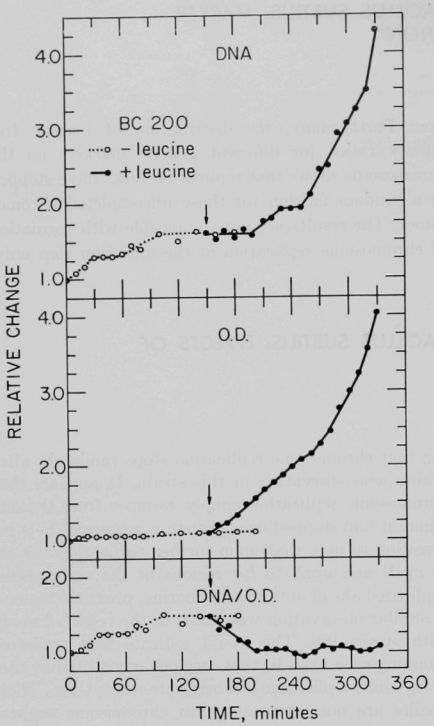

FIG. 49.—Relative changes in DNA and optical density during and after leucine starvation in the *B. subtilis* 168 substrain BC 200. The value during balanced growth in glucose-mineral salts medium is arbitrarily chosen as 1.0. The dotted line represents changes during leucine starvation. The solid line represents changes during restart of growth by addition of leucine to starved cells as indicated by the arrow.

Figure 50 shows these relationships for a W23 substrain BCW 503 during and after leucine starvation. In this substrain only 30% more DNA is synthesized during amino acid starvation, resulting in an increase of the DNA/mass ratio to a value near 1.2. Upon restart, the DNA/mass ratio drops back to 1.0 and remains near that value. The lag in DNA synthesis, on restart is short, about 10 to 20 minutes.

Finally, in Figure 51 are results obtained with another 168 substrain, BC 29, which synthesizes only about 15% more DNA during leucine starvation, resulting in a DNA/mass ratio of 1.1. In this substrain,

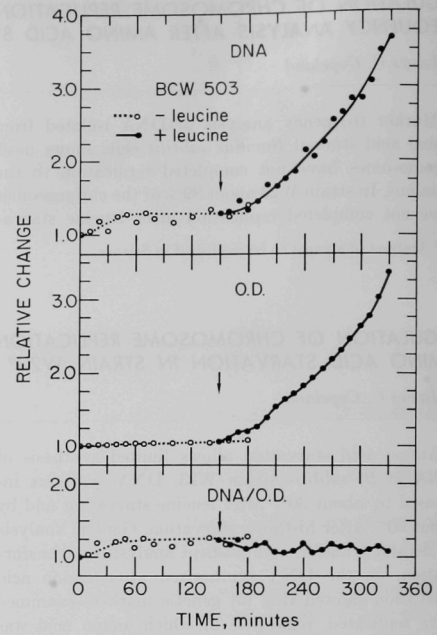

FIG. 50.—Relative changes in DNA and optical density during and after leucine starvation in the *B. subtilis* W23 substrain BCW 503. All conditions as in Figure 49.

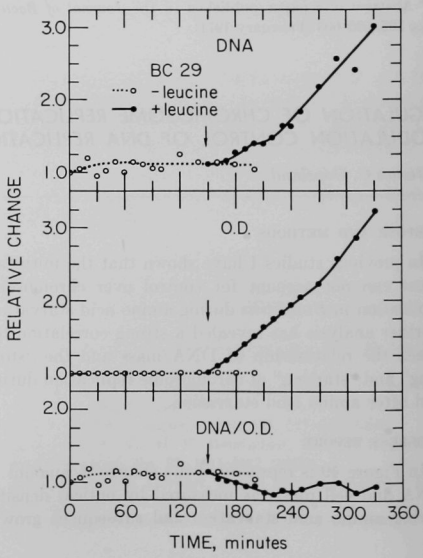

FIG. 51.—Relative changes in DNA and optical density during and after leucine starvation in the *B. subtilis* 168 substrain BC 29. All conditions as in Figure 49.

upon restart, there is a 10-minute lag in DNA synthesis. Initially the DNA/mass ratio drops below 1.0, but later this reduction is compensated and the DNA/mass ratio stabilizes at a value near 1.0.

CONCLUSION

Data in this report show that DNA replication strongly correlates with particular DNA/mass ratios. Results from the three substrains indicate that as a result of amino acid starvation, DNA replication stops at DNA/mass ratios that are multiples of the lower value, or at about 1.1, 1.2, or 1.4. Results of earlier studies indicate that cessation of DNA replication does not depend on any particular site on the chromosome. On restart of growth a lag in the renewal of DNA replication has been identified that is proportional to the amount of DNA synthesized during the starvation period. During this lag the DNA/mass ratio adjusts or eventually stabilizes at its normal value of 1.0. The earlier studies also indicated that interrupted replication forks simply continue from those sites where they had come to rest, once DNA replication resumes. All observations are consistent with a distinct regulatory circuit that acts to modulate DNA replication relative to cell mass changes or other cellular parameters that correlate with cell mass.

EVALUATION OF DIFFERENT SCINTILLATION COCKTAILS FOR THE COUNTING OF TRITIATED RIBONUCLEIC ACID SEPARATED BY SUCROSE GRADIENT CENTRIFUGATION*

Richard E. McDowell and James C. Copeland

Sucrose gradient centrifugation is widely used to fractionate nucleic acids and other macromolecules. Problems are encountered when this technique is used to fractionate tritiated ribonucleic acid (RNA) directly into certain scintillation cocktails. For example, counts are lost from tritium labeled RNA in the presence of sucrose. An examination of this counting problem demonstrated that count reduction by sucrose occurs only in specific scintillation fluids and when tritium is incorporated into RNA but does not occur when the tritium label is part of a small molecule like uridine. This observation had led to the evaluation of several frequently used scintillation cocktails and to the further characterization of another cocktail which counts ^{3}H-RNA in sucrose with a high efficiency and which is as effective as the sample oxidation technique.

* Abstract of paper submitted to *Analytical Biochemistry*.

REPAIR OF DAMAGE INDUCED BY NEAR UV AND VISIBLE RADIATIONS

Robert B. Webb, John R. Lorenz and Mickey S. Brown

PURPOSE AND METHODS

Lethal and mutagenic effects of near ultraviolet (UV) (330 to 390 nm) and visible light (390 to 750 nm), without added sensitizers, have been demonstrated in several biological systems.[1-3] Both lethal and mutagenic actions of near UV and visible light have been shown to be oxygen dependent, suggesting an indirect photosensitized process. Although a preliminary action spectrum for mutagenesis is consistent with the absorption spectrum of riboflavin, the endogenous chromophores have not been identified.

The purpose of this continuing study is the elucidation of mechanisms of action by radiations between 330 and 750 nm. Procedures largely have been given elsewhere.[2] Various strains of *Escherichia coli*, differing in repair capability, involving both excision repair and postreplication repair, were used in this study.

PROGRESS REPORT

Figure 52 shows the responses of stationary phase *E. coli* WP2 (repair sufficient) and *E. coli* K12 AB 2480 (excision-repair and postreplication-repair deficient) to 365 nm UV after plating them on nutrient agar in the absence and presence of 5 μg/ml acriflavine in the plating medium. When plated in the presence of acriflavine, *E. coli* WP2 was as sensitive as *E. coli* WP2hcr (excision-repair deficient) and *E. coli* K12 AB 2480 plated in the absence of acriflavine. Acriflavine had little effect on the sensitivity of K12 AB 2480. These results support damage to DNA as the basis of lethal action of near UV.

The responses of the 3 strains to 460-nm radiation after plating them in the absence and presence of 5 μg/ml acriflavine are shown in Figure 53. When plated without acriflavine, the relative response was qualita-

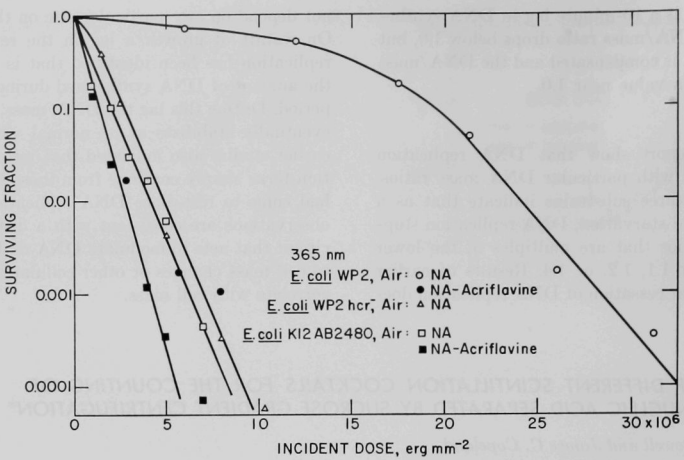

FIG. 52.—Dose-survival responses of 3 strains of *E. coli* differing in repair capability to 365-nm radiation.

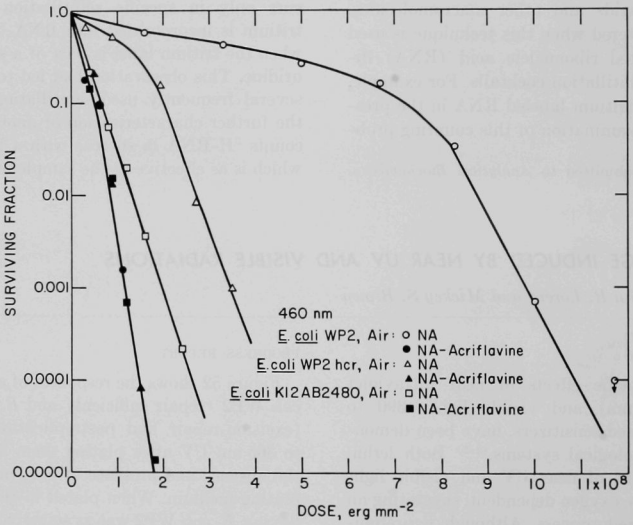

FIG. 53.—Dose-survival responses of 3 strains of *E. coli* differing in repair capability to 460-nm radiation.

tively the same as has been observed with 254-nm UV. However, the range of sensitivity was much less at 460 nm. When they were plated in the presence of acriflavine, the 3 strains showed identical responses, slightly more sensitive than strain K12 AB 2480, the most sensitive of the 3 strains. These results implicate DNA in the lethality by 460-nm radiation. These results also support the involvement of both excision repair and post-replication repair in 460 nm lethality.

At 550 nm and 650 nm, the 3 strains were much more resistant than they were at 460 nm or shorter wavelengths. Furthermore, they differ very little in their sensitivity to 550 nm and 650 nm radiations. Their resistance to very high irradiances of 550 nm

and 650 nm (5 to 9 × 10^4 ergs mm^{-2} sec^{-1}) eliminates local heating as the mechanism of inactivation at wavelengths shorter than 500 nm. Acriflavine had no more than a small sensitizing effect on any of the 3 strains at 550 nm and 650 nm.

CONCLUSIONS

Comparison of dose-survival curves of strains of *E. coli* of different repair capability provides indirect evidence for the action of both excision repair and post-replication repair on lethal damage by 365-nm and 460-nm radiation.

The very high, but almost equal, resistance to 550-nm and 650-nm radiations of the 3 strains studied eliminates local heating in the lethal response to shorter wavelength radiations.

Acriflavine sensitization of the repair-sufficient strain of *E. coli* to both 365 nm and 460 nm supports repair of lesions produced by these radiations in DNA.

REFERENCES

1. Spikes, J. D. *Photophysiology: Current Topics*, Vol. 3, Ed. A. C. Giese Academic Press, N. Y., 1968, pp. 33–64.
2. Webb, R. B. and J. R. Lorenz. *Photochem. Photobiol.* **12**, 283–289 (1970).
3. Webb, R. B. and M. M. Malina. *Photochem. Photobiol.* **12**, 457–468 (1970).

PHOTOREACTIVATION OF 365-NM LETHALITY

Mickey S. Brown and Robert B. Webb

PURPOSE AND METHODS

Although DNA is not known to absorb wavelengths above 330 nm, damage to DNA has been implicated in the lethal action of near UV (330–390 nm).[1] Also, mutagenesis by these wavelengths has been demonstrated in continuous cultures of bacteria.[2, 3] Both mutagenesis and lethal actions were shown to be oxygen dependent, suggesting an indirect photosensitized process. The endogenous chromophores have not been identified.

We investigated the possible role of pyrimidine dimers in the lethal action of near UV by testing for enzymatic photoreactivation (PR) after inactivation. As 365-nm radiation is within the efficient part of the action spectrum for enzymatic photoreactivation, photoreactivation would be expected to occur concomitantly with inactivation at this wavelength. Experiments were designed to separate inactivation from photoreactivation by 365-nm ultraviolet. *Escherichia coli* K12 AB 2480 (*uvr rec*), a strain deficient in both excision repair and postreplication repair, was chosen for this study.[4]

Complete survival curves were obtained, using 48-hr stationary state cultures grown at 37° on nutrient agar (Difco) plates. Procedures and radiation sources have been described.[1] Irradiances were measured with a General Electric Intensity Meter (for 254-nm UV) and YSI Kettering Model 65 Radiometer (for 365-nm UV and longer wavelengths). Photoreactivation was carried out with a 500-watt quartz iodine lamp filtered to give a wavelength range of 370 to 440 nm, with a peak at 400 nm.[5] Maximum photoreactivation routinely was obtained by using an irradiance of 200 ergs mm^{-2} sec^{-1} for 20 min at 25°C. This exposure caused no detectable inactivation in the unirradiated controls.

Survival curves were fitted empirically to the multitarget equation

$$S = 1 - (1 - e^{-kD})^n,$$

where S is the surviving fraction, D is the dose in ergs mm^{-2}, k is the inactivation constant, and n the Y axis intercept of the extrapolated straight line part of the survival curve.

PROGRESS REPORT

Initial experiments were designed to test for photoreactivation after inactivation of cells by near UV at a reduced temperature. Inactivation by 365 nm UV at 0°C in both the absence and presence of photoreactivation radiation at an irradiance of 200 ergs mm^{-2} sec^{-1} for 20 min is shown in Figure 54. The photoreactivation ratio (ratio of the inactivation constant k in the absence of maximum photoreactivation to k in its presence) for the first 2.5 decades of inactivation was 3.7. The 365-nm inactivation curve after maximum photoreactivation was a simple exponential, without a significant shoulder, over more than 3 decades of inactivation. In the absence of photoreactivation, deviations from a simple exponential response occurred below the second decade, which aproximately paralleled the survival curve after maximum photoreactivation. The survival point at which the break occurred was inversely related to the inactivating irradiance in a series of eight experiments. Eight sets of 365-nm survival curves obtained at irradiances of 952 to 4760 ergs mm^{-2} sec^{-1} were coincident, except for the positions

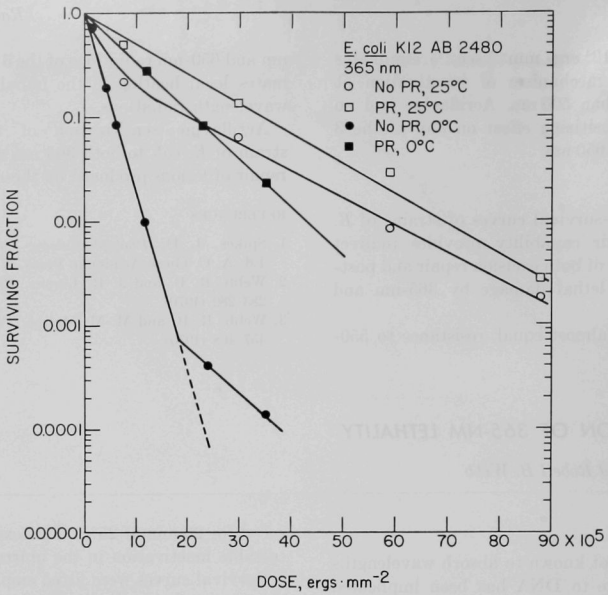

FIG. 54.—Dose-survival response and photoreactivation of *E. coli* K12 AB 2480 irradiated with 365-nm UV at 0°C and 25°C. Irradiance for inactivation was 2,000 ergs mm^{-2} sec^{-1}.

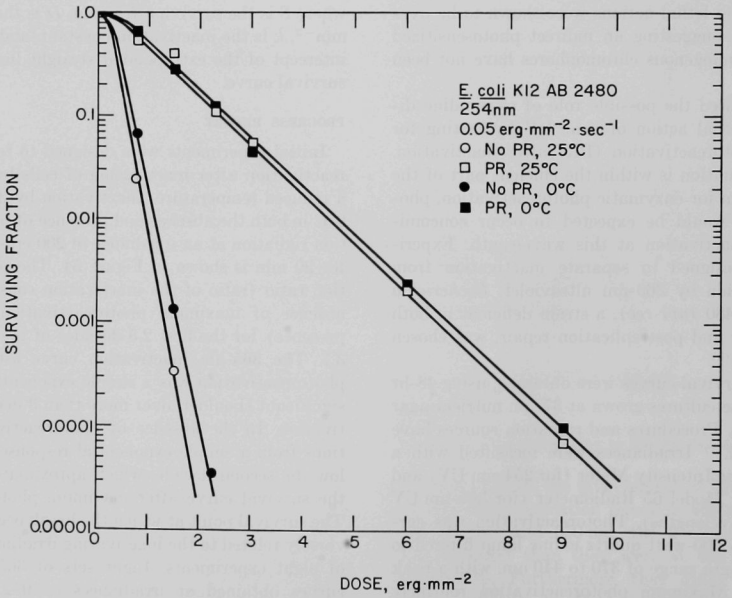

FIG. 55.—Dose-survival and photoreactivation of *E. coli* K12 AB 2480 irradiated with 254-nm UV at 0°C and 25°C. Irradiance for inactivation was 0.05 ergs mm^{-2} sec^{-1}.

of the break at low survival values. This demonstrated that survival is independent of dose rate over this range of irradiances.

Exposure to photoreactivating light after 365-nm inactivation at 25°C resulted in much less reactivation than at 0°C (Figure 54). This result is consistent with greater concomitant photorepair occurring at 25°C than at 0°C. The sensitivity to 365-nm UV after maximum photoreactivation was 60% greater at 0°C than at 25°C.

Inactivation by 254-nm UV at 0°C and 25°C in both the absence and presence of maximum photoreactivation (200 ergs mm^{-2} sec^{-1} for 20 min) is shown in Figure 55. The photoreactivation ratio was approximately 4.6 at both inactivation temperatures, a slightly larger value than the ratio of 3.7 observed after 365-nm inactivation. Photorepair after 365-nm inactivation closely parallels enzymatic photoreactivation after 254-nm inactivation. These parallels include: rate of reversal, irradiance at which saturation irradiance is reached, temperature dependence above saturation irradiance, and the extent of photoreversal after single flashes of reactivating light.

The small shoulders on the four survival curves shown in Figure 55 (extrapolation values, n, of 1.5 to 2.5) are typical of a large number of 254-nm survival curves we have obtained with this strain in the stationary state. In contrast, we have observed no shoulder ($n = 1.0$) on survival curves at 365 nm with this strain (Fig. 54). The sensitivity of the cells to 254-nm UV was slightly less at 0°C than at 25°C (Fig. 55). Comparison of responses of this strain to 254- and 365-nm dependence and shoulder size (n) suggests important differences in the *mechanism of induction* of the photoreactivable damage.

CONCLUSIONS

Oxygen dependence of 365-nm inactivation suggests that lethality from this radiation occurs through a photosensitized process involving a chromophore that occurs naturally in the cell. The identity and function of this compound is being sought.

Close parallels between photorepair after inactivation at 365 nm and 254 nm indicate that enzymatic photoreactivation of 365-nm lethality can occur. Enzymatic photoreactivation is highly specific for splitting pyrimidine dimers. Therefore, these results indicate that pyrimidine dimers are the major lethal lesion produced by near UV under the conditions of this study.

REFERENCES

1. Webb, R. B. and J. R. Lorenz. *Photochem. Photobiol.* **12,** 283–289 (1970).
2. Kubitschek, H. E. *Science* **155,** 1545–1546 (1967).
3. Webb, R. B. and M. M. Malina, *Science* **156,** 1104–1105 (1967).
4. Howard-Flanders, P. and R. Boyce. *Radiat. Res.* (*Suppl*) **6,** 156–189 (1966).
5. Davies, D. J. G., S. A. Tyler, and R. B. Webb. *Photochem. Photobiol.* **11,** 371–386 (1970).

THE LETHAL EFFECTS OF ^{125}I DECAY IN E. COLI AND IN BACTERIOPHAGES

Robert E. Kirsch, Sandra A. Drick, and Wayne T. Kickels

PURPOSE AND METHODS

^{125}I decays by electron capture, with a subsequent vacancy cascade and probable electrostatic disruption of the molecule harboring the decaying atom.[1] These disruptive local physical events which accompany ^{125}I decay lead to the expectation of severe biological effects from decays in DNA. The present study was undertaken to study these biological effects in microorganisms.[2] ^{125}I is incorporated into the DNA of *E. coli* and of bacteriophage T_1 in the form of iododeoxyuridine, a thymidine analogue.

PROGRESS REPORT

More accurate determinations of the lethal efficiency per decay of ^{125}I in the DNA of T_1 bacteriophage were made possible by direct measurements of the concentration of ^{125}I in phage preparations purified by a combination of enzyme treatment, dialysis, and sucrose gradient centrifugation.[3] These studies indicate that $(76 \pm 10)\%$ of all ^{125}I decays are lethal for T_1 phage during storage at −196°C, compared with only 5% lethality for ^{32}P decays under the same storage conditions.

More accurate determinations are also being made of the lethal efficiency per decay of ^{125}I in the DNA of *E. coli.* DNA is extracted from labeled cells, its concentration is measured by the diphenylamine reaction, and its radioactivity is measured by a gamma scintillation spectrometer. The number of ^{125}I atoms per bacterial genome is calculated directly from these data. Preliminary results for the relatively radiation-resist-

ant strain, *E. coli* 15THU indicate that (26 ± 11)% of ^{125}I decays are lethal during storage at −196°C, in agreement with our previously reported value[2] of approximately 20% from less direct measurements.

The finding that ^{125}I decay is considerably more lethal to phage T_1 than to *E. coli* 15THU is similar to the finding that ^{32}P nuclear recoil is much more lethal to phage than to bacteria. This similarity may be based on a common mechanism: an interruption of the transfer of part or all of a bacteriophage genome into a bacterial cell by a radioactive decay which cuts the phage genome in two. Studies are now in progress with the radiation-resistant strain of *E. coli*, B/r, as well as the radiation-sensitive, repair-deficient strains, B_{s-1} and K-12 AB2463. These experiments should show whether ^{125}I damage to bacterial DNA can be repaired and should also clarify the relationship between the lethal effects from ^{125}I decay in bacteria and in bacteriophage.

CONCLUSION

The more accurate determinations reported here, of the lethal effects of ^{125}I decay in T_1 *phage* and *E. coli* 15THU, confirm our earlier conclusion,[2] that ^{125}I decays in DNA are much more lethal to microorganisms than are ^{32}P decays. An ^{125}I decay in DNA is about three times more likely to be lethal to phage T_1 than to *E. coli* 15THU. Although the reason for this difference is not yet clear, studies comparing the effects of ^{125}I decay in normal and repair-deficient strains of *E. coli*, now in progress, are directed at solving this problem.

REFERENCES

1. Wexler, S. *Science* **156**, 901–907 (1967).
2. Krisch, R. E., B. A. Coombs, and W. T. Kickels. Argonne National Laboratory Biological and Medical Research Division Annual Report, 1969. ANL-7635, pp. 175–176.
3. Funk, F., S. Person, and R. C. Bockrath. *Biophys. J.* **8**, 1037–1050 (1968).

CHANGES IN THE MEAN CELL VOLUME OF ESCHERICHIA COLI AFTER BACTERIOPHAGE INFECTION

Michael L. Freedman and Robert E. Krisch

PURPOSE AND METHODS

This report covers continued work on enlargement of *E. coli* cells exposed to T-phage. The purpose and methods were reported previously[1] and are directed at determining the generality of the effect and its underlying mechanism.

PROGRESS REPORT

Bacteria undergo an increase in mean cell volume (MCV) after exposing sensitive strains, but not spontaneous phage-resistant revertants, of *E. coli* B/r and B_{s-1} to T-even bacteriophages. The effect is obtained with ultraviolet light (UV)-killed phage and with wild type and rapid lysis mutants. Ghosts, made by osmotically shocking T-even phage, also elicit a multiplicity-of-infection (MOI)-dependent cessation of cell division and a concomitant cell enlargement. T-odd phage, not reported to terminate host cell DNA, RNA, and protein synthesis after infection, neither abruptly halt cell division nor produce cell enlargement.

To determine the role of phage adsorption, we have used T4D 12⁻ carrying an amber mutation in a genetic locus coding for base-plate function. These phage, grown on B/r which lacks an amber suppressor, produce defective progeny which typically attach to the bacterium by their long tail fibers, but pull away from the would-be host when the sheath is contracted and DNA is injected. There is no irreversible attachment by these defective phage to the bacterium. Such viruses can have the defective gene 12 function complemented *in vitro* by a phage-free, cell-free extract made from infected bacteria in the latent period. Defective T4D 12⁻ phage neither caused cell division arrest nor enlargement, but, upon complementation to restore base-plate function, did elicit these responses.

Subsequent experiments elucidate the mechanism of the host cell's response to virus infection. First, the degree of enlargement 20 minutes after phage addition is dependent on MOI up to 4 (at which multiplicity each cell has adsorbed $\geqslant 1$ virus by Poisson distribution) and is constant above 4. The effect is temperature dependent, and between 22° and 37°C the MCV doubling rate has the same Q_{10} value as the number doubling rate of the cultures in exponential balanced growth, 2.4. The MCV increase is not reversed by hypertonic 15% sucrose, at which concentration plasmolysis commences.[2] There is no abrupt cell enlargement upon dilution into distilled water. The mean dry weight per cell does not increase as fast as the MCV after infection, causing a drop in mean cell density. This is substantiated by an experiment demonstrating a drop in turbidity at 450 nm, which reflects a drop in culture mass concomitant with the cell volume increase meas-

ured with the Coulter-counter multichannel-analyzer. The phage-produced enlargement is blocked by NaCN concentrations that reversibly inhibit energy metabolism and cell division, suggesting an energy-dependent component. Finally, *E. coli* K12 hosts that require diaminopimelic acid (DAP), a cell wall constituent, continue to take up DAP and incorporate it into acid-insoluble material after infection with T2 phage. The same is true for B/r infected with T2r; cell wall synthesis, as measured by DAP incorporation, continues at the pre-infection rate.

CONCLUSIONS

Results summarized above indicate that phage-sensitive bacteria stop dividing and begin to enlarge when they are infected with functional, wild type, or rapid lysis T-even phage, either live or UV killed, or with T-even phage ghosts. Injection of a functional phage genome is not necessary, but, normal irreversible phage adsorption and cell wall penetration are required. The effects of phage infection on host cell size do not appear to be exclusively osmotic, as hypothesized by Cohen,[3] but are attributed to a continuation of cell wall growth in the absence of cell division or other host cell macromolecular synthesis. This apparent tendency of the infected bacterium's surface to "outgrow" the cell's contents results in the observed sucrose effect, the temperature dependence and cyanide sensitivity, and the decrease in mean cell density.

REFERENCES

1. Freedman, M. L. and R. E. Krisch. Argonne National Laboratory Biological and Medical Research Division Annual Report, 1969. ANL-7635, pp. 171–173.
2. Bayer, M. E. *J. Gen. Microbiol.* **53,** 395–404 (1968).
3. Cohen, S. S. *Virus Induced Enzymes.* Columbia University Press, New York, 1968, p. 204.

TOXICITY AND METABOLISM OF RADIONUCLIDES: PROGRAM OBJECTIVES AND INTRODUCTION

William P. Norris

This program is an experimental study of biological effects produced by the radioactive products of nuclear fission. The study is done by using the purebred beagle dog—an animal that offers many experimental advantages, including that of sufficient body size for physiologic measurements.

During the last two years major emphasis has been on a study of dogs maintained continuously in a ^{60}Co γ-ray field at exposure rates low enough to allow survival for long periods of time. The exposure rates chosen have allowed us to view a wide range of hemopoietic responses and to relate their individual probability of occurrence to exposure rate and total exposure. The lowest exposure rate has produced no major damage to blood forming elements, hence we anticipate that other systems will predominate in the eventual causes of death. This study is important to the overall objective of assessing the effects of metabolized fission products because protracted radiation exposure is obtained with carefully controlled dosimetry.

We have maintained comprehensive records of the ancestry of each dog, and have now begun a data review to determine whether ancestry has a material effect on the radiation-induced responses that are observed.

A study of the beagle thyroid gland and the effect of radiation on it has been expanded. Methods that allow a more sensitive measure of thyroid integrity and response to ionizing radiations have been developed. These methods are beginning to be applied to dogs irradiated in the γ field as described above.

Chronic survivors of dogs given ^{137}Cs and ^{144}Ce 5 to 8 years ago are being observed. Mortality and incidence of degenerative disease and malignancies in these dogs are well in excess of those found in controls. Results, as reported previously, have not changed so appreciably as to indicate their inclusion in this report.

We continue our attempt to further characterize and identify the parameters of the normal beagle. This work has dealt largely with inherited characteristics, blood biochemistry, and bacteriology. The latter has been of especial importance in establishing the causal relationships in radiation-induced septicemias.

Studies of Radiation-Induced Changes

THE RESPONSE OF ANL BEAGLES TO PROTRACTED EXPOSURE TO ^{60}Co GAMMA RAYS AT 5 TO 35 R/DAY. I. SURVIVAL AND CLINICAL OBSERVATIONS

William P. Norris and Calvin M. Poole

PURPOSE AND METHODS

Our Annual Reports for 1968[1] and 1969[2] described the initiation and progress of an on-going study in which young adult dogs are maintained in a ^{60}Co γ-ray field until they die. Daily exposure rates are either 35, 17, 10, or 5 R/22-hr exposure day. These exposures are estimated to be equivalent to 25.40, 12.34, 7.26, or 3.63 rads/day, respectively.

The capacity of the ^{60}Co γ-ray facility is 52 dogs—4 at 35 R/day, 8 at 17 R/day, 16 at 10 R/day, and 24 at 5 R/day. As the dogs have died, they have been replaced by others, so the total number of dogs irradiated to date is in excess of 52.

Each dog is examined regularly for clinical abnormalities, with special attention to the eyes (for signs of retinal pathology and lens opacities) and body temperature (for indications of septicemia).[1] A complete hematologic work-up on each animal, including a differential white cell count, enumeration of platelets and reticulocytes, and measurement of certain biochemical parameters, is done at regular intervals. Bacteriologic examinations are performed at intervals on

blood specimens from living dogs, as well as on postmortem specimens, to define the significance of bacteremia in the overall response. All decedents are necropsied, and their tissues are collected for microscopic study.

During the last year, the exposures of selected groups were terminated when the accumulated dose had reached preselected levels. These dogs will be held for the duration of their lives to observe late manifestations of exposure to radiation.

PROGRESS REPORT

A summary of survival data obtained to date is contained in Table 53. At 35 R/day, death occurred after an average of 57 days' exposure—a total of 1995 R. As indicated in the next report, 600 R of this was "wasted," because the LD_{50} is reached after 40 days' exposure to 35 R/day (1400 R).

At 17 R/day, the mean survival time in decedents was 186 days (3162 R), but 2 animals are still surviving in apparent good health after 965 days (16,400 R).

At 10 R/day, the mean survival time in decedents was 415 days (4150 R), and 4 dogs are still surviving after 960 days exposure (9600 R).

Mortality is presented in Figure 56 as a function of total exposure for each of these different exposure-rate groups. The early wave of mortality is not strikingly different in the 35, 17, and 10 R/day groups. In each exposure class significant numbers of deaths occurred when the total exposure reached the vicinity of 2000 R. Data at 5 R/day are in sharp contrast; only in this group did mortality remain at a low level when the total exposure approached 5000 R.

TABLE 53. SURVIVAL OF YOUNG ADULT BEAGLE DOGS MAINTAINED IN A ^{60}Co γ-RAY FIELD

Exposure, R/day	Group	No. of dogs	Results to 10-15-70			
			Decedents		Survivors	
			Survival range, days	Mean	No. dogs	Survival to date, days
35	A & B	8	45–68	57	None	—
17	A	8	85–302	186	2	965
	B	5	131–416		None	
	C	6			6	235+23[a]
10	A	8	259–669	415	2	964
	B	8	209–929		2	950
	C	7	404		6	405+207[a]
	D	11			11	159
5	A	8	390–		7	963
	B & C	16	484–		15	918
Control		8	303–		7	965

[a] Terminated Exposures. First term is time in the γ field. Second term is survival to date after exposure was terminated. Total exposure was 4000 R in both cases.

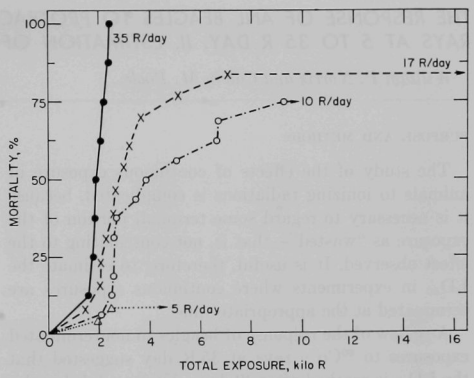

FIG. 56.—Mortality in beagle dogs exposed continuously to either 5, 10, 17, or 35 R/day in a ^{60}Co γ-ray field. The arrows indicate the total exposure reached at the time of this report.

Both Table 53 and Figure 56 illustrate the large variability in the response of individual dogs to protracted whole-body irradiation. In terms of the ratios of the extreme values of survival time in the γ field, this variability has reached a factor of 11.3 at 17 R/day, and 4.6 at 10 R/day. Such variability was not encountered in earlier experiments, where dogs were exposed at rates of 50 R/day or more. These findings, together with the hematologic data reviewed last year,[2] support the view that the threshold exposure rate for continued hematopoietic function is in the range of 10 to 20 R/day, and certainly above 5 R/day.

Causes of death in these animals have all been directly related to hematopoietic failure or damage. At 35 R/day, the direct cause of death was always septicemia—usually from microorganisms carried in the throat and upper respiratory tract. At 17 R/day septicemia occurred in some dogs, but others died of anemia and without septicemia. At 10 R/day, causes of death were marrow aplasia and myeloproliferative disease. The cause of death, therefore, varies as a function of exposure rate. The pathologic findings are discussed in another section of this report.

REFERENCES

1. Norris, W. P. and C. M. Poole. Argonne National Laboratory Biological and Medical Research Division Annual Report, 1968. ANL-7535, pp. 156–157.
2. Norris, W. P. and C. M. Poole. Argonne National Laboratory Biological and Medical Research Division Annual Report, 1969. ANL-7635, pp. 94–95.

THE RESPONSE OF ANL BEAGLES TO PROTRACTED EXPOSURE TO ^{60}Co GAMMA RAYS AT 5 TO 35 R/DAY. II. ESTIMATION OF THE LD_{50} AT 35 R/DAY

William P. Norris and Calvin M. Poole

PURPOSE AND METHODS

The study of the effects of continuous exposure of animals to ionizing radiations is complicated, because it is necessary to regard some terminal portion of the exposure as "wasted"—that is, not contributing to the effect observed. It is useful, therefore, to estimate the LD_{50} in experiments where continuous exposures are terminated at the appropriate time.

A review of the response of beagles to nonterminated exposures to ^{60}Co γ rays at 35 R/day suggested that the LD_{50} is reached after 40 days. Young adult beagles were given such an exposure in groups of 4. During the last 2 years, 55 dogs were irradiated in this manner.

PROGRESS REPORT

Mortality and survival data are presented in Table 54. Of the total of 55 dogs, 29 (52.7%) died acutely. Thirteen of the acute deaths preceded the end of the 40-day exposure period, while the remaining 16 animals survived an average of 14 days following termination of the exposure. In all of these acute deaths, the primary cause of death was septicemia.

In the 26 survivors, the time since irradiation was begun now ranges from 160 to 818 days. (This range reflects the time necessary to complete the exposures in groups of 4 dogs). None of these dogs has died. Twenty of these survivors will be kept for the duration of their lives to observe any chronic changes. The other 6 have been used in studies aimed at identifying latent, irreparable damage to thyroid tissue.

1400 R, delivered to these dogs at a rate of 35 R/22-hour day for 40 days, is a close approximation of the LD_{50} without "wasted" radiation.

TABLE 54. MORTALITY IN BEAGLE DOGS GIVEN PROTRACTED WHOLE-BODY EXPOSURE TO ^{60}Co γ RAYS AT 35 R/DAY FOR 40 DAYS

	No. dogs	Survival time,[a]	
		Range	Mean
Total dogs exposed	55		
Failed to survive the 40-day exposure period	13	31–40	37.5
Survived exposure period but died acutely	16	42–95	54.0
Surviving	26 (47.3%)		

[a] All times are computed from beginning of exposure. Data tabulated to 10-15-70.

THE RESPONSE OF ANL BEAGLES TO PROTRACTED EXPOSURE TO ^{60}Co GAMMA RAYS AT 5 TO 35 R/DAY. III. PATHOLOGIC CHANGES IN DOGS EXPOSED AT 10 R/DAY

Thomas E. Fritz, David V. Tolle, and Ruth C. Zeman

PURPOSE AND METHODS

During the past year, we have continued examinations and collection of specimens and data according to protocols described previously.[1] Our attention is focused on the 10 R/day group in this report since deaths continue to occur at this dose rate that are related to myeloproliferative disease.[2, 3]

PROGRESS REPORT

Three of the original 10 R/day dogs have died during the past year. All three had myeloproliferative disease as did two previous decedents.[2] The lesions included splenomegaly, mild hemorrhagic lymphadenopathy, edema of various tissues, scattered ecchymoses and petechiae of mucous membranes and serosal surfaces, and a characteristic brownish hyperplastic bone marrow. On microscopic examination, there were hyperplastic myeloid cells in the liver, spleen, and lymph nodes in addition to the marrow. Marrow examinations gave myeloid-erythroid ratios ranging from 5:1 to 60:1, with a predominance of immature myeloid cells. Lymph nodes from each had germinal centers with mitotic figures, suggesting that production of lymphocytes, as well as myeloid cells, was continuing at the time of death.

Table 55 lists the 12 decedents from the group of 16 that were exposed to γ radiation at 10 R/day. The terminal bone marrow pathology was of two separate and distinct types. One type occurred in the first 7 dogs which died at times less than 350 days in the radiation

TABLE 55. DOGS DYING DURING PROTRACTED EXPOSURE TO ^{60}Co γ RAYS AT 10 R/DAY

Dog No.	Total days irradiated	Interval between last hemogram and death, days	Cause of death	Erythrocytes/ $mm^3 \times 10^3$	Leukocytes/ mm^3	Thrombocytes/ mm^3
1474	209	0	Anemia, marrow aplasia	770	1,806	0
1362	249	1	Anemia, marrow aplasia	960	826	0
1434	258	5	Anemia, marrow aplasia	860	945	500
1341	259	11	Anemia, marrow aplasia	5,090	2,659	7,000
1467	259	0	Anemia, marrow aplasia	1,000	140	500
1348	268	0	Anemia, marrow aplasia	1,580	145	500
1351	345	0	Anemia, marrow aplasia	450	509	0
1397	383	9	Anemia, myeloproliferative disease	3,390	2,100	500
1462	504	0	Anemia, myeloproliferative disease	2,250	7,494	1,000
1210	662	0	Anemia, myeloproliferative disease	690	9,300	4,500
1382	669	1	Anemia, myeloproliferative disease	1,840	7,900	1,500
1386	929	9	Anemia, myeloproliferative disease	2,100	4,500	10,500
Control	965	—	—	7,450[a]	7,857[a]	360,050[a]

[a] Mean for 7 dogs.

field. They had anemia and bone marrow aplasia. The remaining 5 dogs all died at more than 350 days of irradiation and had myeloproliferative changes in the marrow. This time is approximately the same as the mean survival time (415 days) in decedents,[4] and indicates that only the more radiation-resistant segment of the experimental population developed myeloproliferative disease.

Table 55 also lists the final erythrocyte, leukocyte, and thrombocyte counts for each dog. These counts, separately, as well as collectively, appear to have some predictive value in arriving at a terminal pathologic diagnosis. Dogs with myeloproliferative disease typically had leukocyte, erythrocyte, and thrombocyte counts greater than those with marrow aplasia. Although cell counts within these two groups are variable, these variations appear to reflect proximity to the time of death that the final sample was collected. Dog 1341, for example, died with severe anemia on the 259th day of irradiation, but the final hemogram, measured 11 days before it died (Table 55), has blood values greater than expected for a dog dying with marrow aplasia. Postmortem examination indicated that these blood values were greatly reduced at the time of death. Similarly, the blood values shown for dog 1397 were collected 9 days before it died, when thrombocyte and leukocyte values were extremely low. The values may have changed significantly at times nearer death.

CONCLUSION

Of 16 dogs exposed continuously in a ^{60}Co γ-ray field at 10 R/day, 12 died between 209 and 929 days of exposure. Based on terminal bone marrow changes, there were two distinctly different causes of death. All 7 dogs that died between 209 and 345 days of exposure had marrow aplasia, and the primary cause of death was anemia. The other 5 dogs, that died after longer periods of exposure, had myeloproliferative lesions in the marrow and other tissues, including spleen, lymph nodes and liver.

REFERENCES

1. Fritz, T. E., R. C. Zeman, D. V. Tolle, and J. W. Williams. Argonne National Laboratory Biological and Medical Research Division Annual Report, 1968. ANL-7535, p. 161.
2. Fritz, T. E., R. C. Zeman, D. V. Tolle, and J. W. Williams. Argonne National Laboratory Biological and Medical Research Division Annual Report, 1969. ANL-7635, p. 102.
3. Fritz, T. E., W. P. Norris, C. E. Rehfeld, and C. M. Poole. *Myeloproliferative Disease of Animals and Man*, Ed. W. J. Clark, E. B. Howard and P. L. Hackett. U. S. Atomic Energy Commission Report CONF-680529 (1970), pp. 219–241.
4. Norris, W. P. and C. M. Poole. This report.

THE RESPONSE OF ANL BEAGLES TO PROTRACTED EXPOSURE TO ^{60}Co GAMMA RAYS AT 5 TO 35 R/DAY. IV. BONE MARROW CELL ULTRASTRUCTURE IN DOGS CONTINUOUSLY EXPOSED TO ^{60}Co GAMMA RAYS

Theodore N. Tahmisian, Rosemarie L. Devine, William P. Norris, Thomas E. Fritz, Ruth C. Zeman, and David V. Tolle

PURPOSES AND METHODS

The response of the beagle dog to protracted, whole-body irradiation is related primarily to damage to bone marrow. Other sections of this report[1, 2] demonstrate that marrow damage progresses slowly in dogs exposed to ^{60}Co γ rays at rates of 5 to 17 R/day, and that the primary causes of death, while directly related to marrow damage, are of at least 3 distinctly different types. At 35 R/day damage to marrow progresses rapidly and dogs die uniformly of septicemia after an average exposure of 57 days. It is necessary, therefore, to compare the ultrastructure of marrow from dogs exposed to γ rays at these exposure rates to establish if changes in marrow cells are related to dose rate and length of exposure.

In last year's annual report[3] we presented preliminary results of a study of bone marrow cells taken from normal, untreated, beagle dogs. This work has been extended to include marrow cells from dogs given whole-body exposures to ^{60}Co γ rays at a rate of 35 R/day. Samples of marrow taken from the right femur of dogs irradiated for 6, 12, 18, and 33 days at 35 R/day were compared with marrow from nonirradiated dogs. Tissues for electron microscopy were fixed in phosphate- or cacodylate-buffered glutaraldehyde, then post-fixed in osmium, dehydrated, and embedded by methods described previously.[3]

The same materials studied in the electron microscope also were prepared for light microscopy by conventional methods.

PROGRESS REPORT

Our electron microscopic studies of normal hemopoietic tissue have been concerned with: the identification of cell types, immature stages and cellular components, and the development of the various granules peculiar to certain cell types.

The use of two kinds of buffers has produced different results within the same cell type, and these comparisons aid in understanding the morphology and cytochemistry of cellular ulstrastructural components. Glycogen granules of maturing neutrophils are best seen in phosphate-buffered material, but are of low contrast in cacodylate-buffered materials. Ferritin aggregations and polysomes also are best seen in phosphate-buffered metarubricytes, but deposits of hemoglobin and the microfilamentous nature of the cytoplasm are best observed in cacodylate-treated metarubricytes.

Irradiated bone marrow cells showed changes from the normal. In the light microscope, differential counts of cells from irradiated dogs up to 18 days were not significantly changed. An increased number of degenerate cells, decrease of cellularity, and a slightly increased myeloid:erythroid ratio were observed. At 33 days, advanced degeneration and necrosis of cells and marked hypocellularity made differential counting of the marrow cells impossible.

In the electron microscope, the general appearance of the irradiated marrow is distinctly different from control bone marrow. The numbers of extracellular fat droplets had increased with increasing length of exposure. As a result of increased amounts of fat, the cells were pressed together and distorted in shape and were sometimes difficult to identify. At high magnification, intracellular aberrations were also revealed. Myelin-like figures were the most common aberration occurring in any part of the cell structure; these were more numerous in material irradiated for longer periods of time. The glycogen deposits of maturing neutrophils, distinctly particulate in control material, frequently appeared clumped in irradiated cells. The cisternae of the endoplasmic reticulum of plasma cells were atypically swollen, and the cells were often disrupted. The number of plasma cells and macrophages in irradiated bone marrow appeared to have increased in comparison with the control.

REFERENCES

1. Norris, W. P. and C. M. Poole. This report.
2. Fritz, T. E., D. V. Tolle, and R. C. Zeman. This report.
3. Tahmisian, T. N., R. L. Devine, B. J. Wright, W. P. Norris, T. E. Fritz, R. C. Zeman, and D. V. Tolle. Argonne National Laboratory Biological and Medical Research Division Annual Report, 1969. ANL-7635, pp. 110–114.

THE RESPONSE OF ANL BEAGLES TO PROTRACTED EXPOSURE TO ^{60}Co GAMMA RAYS AT 5 TO 35 R/DAY. V. BETA-HEMOLYTIC STREPTOCOCCI IN THE THROATS OF BEAGLES RECEIVING CONTINUOUS ^{60}Co GAMMA RADIATION

Patricia C. Brennan, Richard C. Simkins, and William P. Norris

PURPOSE AND METHODS

We have shown that β-hemolytic streptococci contribute to septicemia in dogs receiving continuous ^{60}Co γ radiation.[1] The source of these streptococci is the throat.[2] We began a study to determine if there are major shifts in throat microflora of dogs entering the intermediate γ ray facility. If shifts occur, they could be related to caging, irradiation, or both. We also wish to determine whether dogs carrying pathogenic organisms in their throats are less radioresistant than those that do not carry such organisms.

All dogs selected for entry into the γ room had throat cultures just before they were removed from the kennels for pre-exposure conditioning to metabolism cages. Cultures were repeated before the dogs were placed in the γ field.

All dogs exposed to 35 R/day had throat cultures taken at 7-day intervals after they entered the γ field until they died or, if removed from the field, until it was evident that they would survive.

All dogs exposed to 17, 10, and 5 R/day, and the controls, are being cultured at monthly intervals. When dogs are removed from the γ field at these exposure rates they are cultured at monthly intervals until they die, or it becomes evident that they will survive.

PROGRESS REPORT

We can make a few preliminary observations. Fourteen dogs have been consistently negative for β-hemolytic streptococci since we began this study in December 1969. All the negative dogs are in the 17 R, 10 R, and 5 R groups and in the controls. On the other hand, no dog in any group has been consistently positive for β-hemolytic streptococci, although dogs receiving 35 R/day have had more positive throat cultures than dogs in other groups. The overall recovery of β-hemolytic streptococci among the different dose rates is shown in Table 56. The recovery rate in dogs receiving 35 R/day is significantly higher than in dogs receiving 17, 10, or 5 R/day ($P < 0.05$), and the overall recovery rate in the γ field (25%) is significantly higher ($P < 0.01$) than in control dogs kept in the adjacent anteroom. It is of further interest that the recovery rate of β-hemolytic streptococci in these experimental dogs is significantly lower than the 65% incidence we found in the colony as a whole.[3]

TABLE 56. RECOVERY OF β-HEMOLYTIC STREPTOCOCCI FROM THE THROATS OF DOGS EXPOSED TO CONTINUOUS ^{60}Co γ RADIATION

Exposure rate, R/day	Number of cultures, positive/total	% positive
35	51/146	35.0
17	17/77	22.1
10	26/132	19.7
5	50/220	22.7
Control	5/70	7.1

REFERENCES

1. Brennan, P. C. and R. C. Simkins. Argonne National Laboratory Biological and Medical Research Division Annual Report, 1968. ANL-7535, pp. 159–160.
2. Brennan, P. C. and R. C. Simkins. *Proc. Soc. Exp. Bio. Med.* **134,** 566–570 (1970).
3. Brennan, P. C. and R. C. Simkins. This report.

EFFECTS OF IRRADIATION ON THE BEAGLE THYROID GLAND. I. EFFECT OF X IRRADIATION ON THE THYROID GLAND OF BEAGLES FED A RESTRICTED IODIDE DIET

Thomas E. Fritz, William P. Norris, James A. Taylor, and Norbert D. Kretz

PURPOSE AND METHODS

The thyroid gland has been described as highly resistant to damage from ionizing radiation. This apparent resistance is based upon failure to demonstrate changes in function and structure after irradiation—except when extremely high doses, that cause necrosis, are used.[1, 2] Recent studies, however, have demonstrated damage to the ability of the thyroid gland to respond to the acute hyperplastic stimulation of chemical goitrogens after irradiation of the thyroid gland with doses below 1000 R.[3, 4]

The objective was to determine the long-term effects

of a single, brief, localized exposure of the thyroid gland to X radiation.

Young adult beagles, previously fed a commercial diet estimated to provide at least 500 μg I^-/dog/day, were switched to a semisynthetic diet containing 25 μg I^-/100 g. Measurements of food consumption showed that total dietary iodide intake ranged from 50 to 75 μg/dog/day.

After a 75-day restricted iodide intake, the dogs were divided into 5 experimental groups and treated as follows:

Group 1. Experimental control (left and right thyroid lobes sham-irradiated)

Group 2. Unilateral X irradiation (left lobe X irradiated)

Group 3. Unilateral thyroidectomy (left thyroid lobe surgically removed)

Group 4. Bilateral X irradiation (left and right lobes X irradiated)

Group 5. Bilateral thyroidectomy (left and right lobes surgically removed).

Irradiated lobes received 2000 R, 250 kVcp X rays at a dose rate of 400 R/minute. The dogs were given test doses of ^{131}I at intervals over a period of more than a year to measure thyroidal uptake of ^{131}I and its subsequent rate of release from the gland. After these measurements, the dogs were killed serially and thyroid tissue was examined.

PROGRESS REPORT

When the iodide intake of the beagle dogs was reduced to 50 to 75 μg/day, thyroid glands of the control group responded by cellular hyperplasia and hypertrophy, loss of colloid, and increased weight. After about one year, the enlarged thyroid glands had accommodated to reduced dietary iodide and presented a normal histologic appearance.[5]

Dogs which had one thyroid lobe surgically removed showed changes in the remaining lobe similar to lobes of the control dogs.

When both lobes were exposed to 2000 R of 250 kVcp X rays, there was cellular hypertrophy and loss of colloid, but cellular hyperplasia and increased glandular size and weight did not occur. The irradiated glands did not regain a normal appearance, but did become fibrotic.

Three dogs from which both lobes had been surgically removed had small residual portions of hyperplastic thyroid tissue at the time of necropsy, regardless of the length of time they had been on the restricted iodide diet.

If only one lobe of the thyroid was irradiated, the unirradiated lobe responded normally to the change in iodide intake. This response was reflected in the irradiated lobe which also had cellular hypertrophy and loss of colloid, as well as fibrosis. When the enlarged unirradiated gland had reverted to a more normal histo-

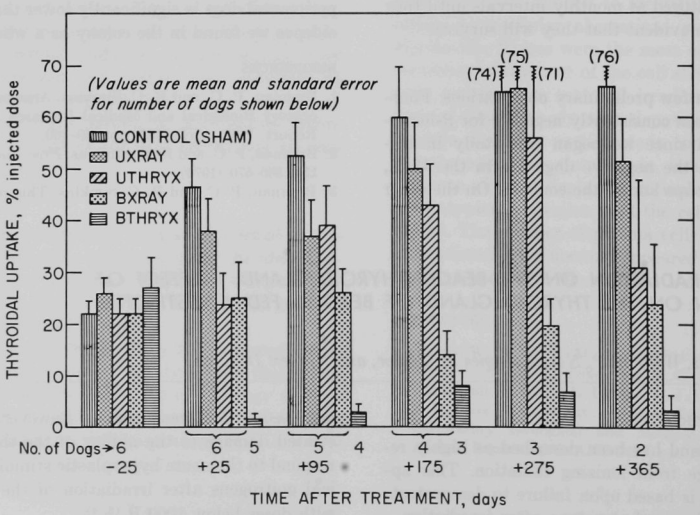

FIG. 57.—Effect of restricted iodide intake and X radiation on thyroidal ^{131}I uptake.

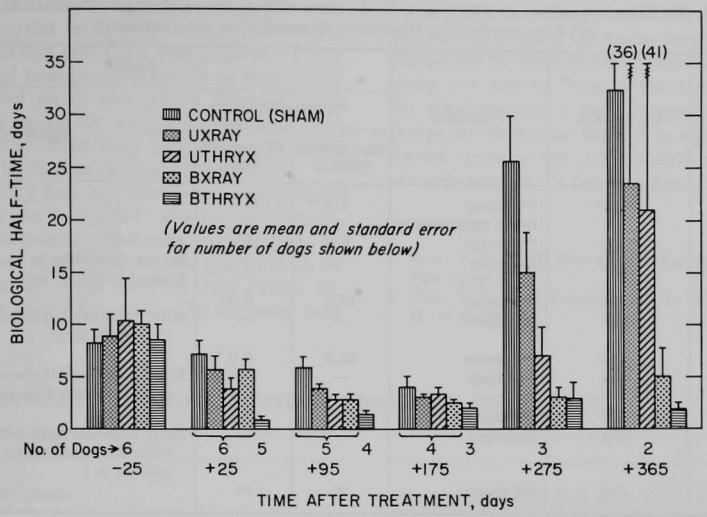

FIG. 58.—Effect of restricted iodide intake and X radiation on thyroidal ^{131}I release.

logic appearance, the irradiated lobe responded similarly, but was not increased in size.

All histologic changes correlated with changes in ^{131}I metabolism in the glands (Figures 57 and 58). Enlarged and hyperplastic glands (control, unilaterally X irradiated, and unilaterally thyroidectomized dogs 45, 95, and 175 days after treatment) accumulated more of the injected tracer doses of ^{131}I and also released it more rapidly than normal-appearing glands. With reversion to a more normal histologic appearance, ^{131}I metabolism in the enlarged glands of control, unilaterally X irradiated, and unilaterally thyroidectomized dogs 277 and 365 days after treatment, was characterized by a decrease in the rate ^{131}I was released but maximum percentages of intake were not affected.

CONCLUSION

Exposure of the thyroid gland to 2000 R of X radiation destroys the proliferative ability of thyroid epithelial cells but does not prevent residual cells from reacting to stimuli causing increased thyroid function.

REFERENCES

1. Rubin, P. and G. Cassarett. *Clinical Radiation Pathology*. W. B. Saunders, Philadelphia, 1968, pp. 749–767.
2. Hursh, J. B., P. A. Van Valkenburg, and J. B. Mahoney. *Radiology* **57**, 411–417 (1951).
3. Doniach, I. *Thyroid Neoplasia*, Ed. S. Young and I. Doniach. Academic Press, London, 1968, pp. 259–265.
4. Gibson, J. M. and I. Doniach. *Brit. J. Cancer* **21**, 524–530 (1967).
5. Norris, W. P., T. E. Fritz, and J. A. Taylor. *Am. J. Vet. Res.* **31**, 21–33 (1970).

EFFECTS OF IRRADIATION ON THE BEAGLE THYROID GLAND. II. THYROID RESPONSE TO PROTRACTED WHOLE-BODY EXPOSURE TO ^{60}Co GAMMA RAYS

William P. Norris, Thomas E. Fritz, and Norbert D. Kretz

PURPOSE AND METHODS

In another section of this report we demonstrated that a semisynthetic diet containing restricted amounts of iodide provides a stress to the thyroid gland that results in hypertrophy and hyperplasia of the follicular epithelium.[1] This response is suppressed by a single brief exposure to 2000 R of X rays localized to the thyroid. We intend to determine whether whole-body exposure to ^{60}Co γ rays at 35 R/day for 40 days (the LD_{50}) has an effect on the structure or function of

TABLE 57. SERIAL SACRIFICE OF DOGS ON A NO-I^- DIET. CORRELATIONS BETWEEN CHANGES IN ^{131}I METABOLISM AND HISTOLOGIC STRUCTURE OF THE THYROID

Group No. (3 dogs/group)	Days on diet	Procedures	Results		
			^{131}I Metabolism		Histology
			Max. uptake, mean %	$BT_{1/2}$, mean days	
1[a]	−14[a]	^{131}I tracer	1.5	18.0	—
1 through 8	0	Begin no-I^- diet	—	—	—
1 and 2	+7	^{131}I tracer	6.0	11.0	—
2	+21	Necropsy	—	—	Severe thyroiditis in 1 Normal histology in 2
1 and 3	+28	^{131}I tracer	19.0	5.0	—
3	+42	Necropsy	—	—	Mild follicular hypertrophy in 2; severe thyroiditis in 1
1 and 4	+49	^{131}I tracer	32.0	3.0	—
4	+63	Necropsy	—	—	Marked follicular hypertrophy in 2; moderate follicular hypertrophy in 1
1 and 5	+70	^{131}I tracer	(b)	(b)	
5	+84	Necropsy	—	—	Early follicular hyperplasia in 1; marked follicular hypertrophy in 1; severe thyroiditis in 1
1 and 6	+91	^{131}I tracer	(b)	(b)	

(a) This group is examined for ^{131}I uptake at each point in time along with dogs to be killed. It constitutes a subgroup, as indicated, for purposes of comparison.

(b) Measurements have been completed and data are available but have not been analyzed to determine mean maximum ^{131}I uptake and mean $BT_{1/2}$ for these groups.

the beagle thyroid. The response of thyroids of irradiated and unirradiated dogs that have been fed the semisynthetic diet is compared. The diet is modified to contain no added iodide. The I^- has been omitted from this diet to hasten the rate at which the thyroid gland will adapt to reduced iodide intake.

First, we have begun a serial-sacrifice experiment and serial measurement of ^{131}I metabolism in dogs switched from a commercial (high iodide) diet to the no-I^- diet. This series of measurements will provide data on the uptake and subsequent release [biological half-time ($BT_{1/2}$)] of ^{131}I, as well as endocrine weights, and material for histologic examination which will be examined by light and electron microscopy.

Other dogs fed the regular commercial (high I^-) diet, and irradiated for 40 days at 35 R/day, will be switched to the same no-I^- diet. Data from iodine-131 metabolism, endocrine weights, and thyroid histology will be compared with similar data obtained in the unirradiated serially sacrificed dogs.

Data from the serially sacrificed dogs are used to determine when thyroid hyperplasia begins. To determine whether irradiation during the hyperplastic phase has an effect different from that seen by irradiating the resting gland, other dogs, fed the no-I^- diet until hyperplasia begins, will also be irradiated at 35 R/day for 40 days. Data from dogs treated in this manner will be compared with data from those fed the diet but not irradiated and with data from dogs fed the diet after they were irradiated.

PROGRESS REPORT

The serial-sacrifice experiment has progressed to the stage where data on ^{131}I metabolism after 91 days on the no-I^- diet (Table 57) have been collected. The maximum uptake of the tracer doses of ^{131}I has increased from 1.5% on the commercial high iodide diet to 32% in group 1:4 after 49 days on the no-I^- diet. The $BT_{1/2}$ of ^{131}I at the same time has decreased progressively from 18 days in group 1, to 3 days in group 1:4.

Thyroid glands removed from groups 2 to 5 revealed increasing hypertrophy of the follicular epithelium with the addition of early, but obvious, hyperplasia in one dog in group 5, killed after 84 days on the no-I^- diet. Thyroiditis in groups 2, 3, and 5 was not unexpected because this disease occurs spontaneously in our colony with an incidence exceeding 20%.[2]

Based on analyses of these data, other dogs on the no-I^- diet will be sacrificed at still later times.

Eight dogs have received ^{60}Co γ radiation for 40 days at 35 R/day. Forty days after these dogs were removed from the γ-ray field they were switched to the no-I^- diet. Four of the eight have now been on

the no-I⁻ diet for 126 days, and the other four have been on the same diet for 84 days. After 90 days on the diet, each of the first group of 4 dogs received a tracer dose of ^{131}I, and measurements similar to those in the serially-sacrificed group were made. Although these data have not been fully analyzed, they appear to resemble those obtained from unirradiated dogs fed the no-I⁻ diet for 91 days (group 1:6, Table 57).

Two groups of 4 dogs also have been switched from the commercial diet to the no-I⁻ diet to induce hyperplasia before beginning irradiation. At the time of early hyperplasia of the thyroid, now judged to be 84 days, based on the serial sacrifice data (Table 57, group 5), these dogs will be placed in the γ-ray field at 35 R/day for 40 days and will receive the no-I⁻ diet. After the end of the 40-day irradiation, ^{131}I tracer studies will be conducted on an intermittent basis. One group of 4 dogs has been on the diet for 49 days and the other for only 7 days. Staggering the times the groups are started on the diet is required, because of limited space in the γ-ray facility and the logistics of conducting the ^{131}I tracer studies.

REFERENCES

1. Fritz, T. E., W. P. Norris, J. A. Taylor, and N. D. Kretz. This report.
2. Fritz, T. E., R. C. Zeman, and M. R. Zelle. *Exp. Mol. Path.* **12**, 14–30 (1970).

RADIATION DOSIMETRY IN BEAGLES GIVEN INTRAVENOUS DOSES OF ^{137}Cs

William P. Norris

PURPOSE AND METHODS

To interpret data from previous reports [1] properly, it has been necessary to compute the integrated radiation dose delivered by the decrementing ^{137}Cs burden of each animal, as well as the radiation dose rate at any point in time.

The problem pertains principally to the estimation of that portion of the radiation dose derived from the gamma radiation from the ^{137m}Ba daughter of ^{137}Cs. To date, computational methods for this calculation have not been entirely satisfactory. In the present study, the problem is complicated by the fact that there were appreciable changes in the body weights of the experimental animals.

PROGRESS REPORT

The retention of ^{137}Cs (Table 58) is dependent on age. In 5-month-old beagles, the age-dependent change in rate is sufficiently fast that ^{137}Cs retention must be described by the sum of 3 exponential terms. Two exponential terms were sufficient to describe ^{137}Cs retention in dogs older than 1 year.

TABLE 58. MEAN VALUES OF ^{137}Cs RETENTION CONSTANTS ± S.E. IN BEAGLE DOGS

	5-month old	13-month old	5-year old
C_1	0.1507±0.0277	0.2385±0.0141	0.2135±0.0130
λ_1	0.5751±0.0421	0.5990±0.0219	0.5750
C_2	0.6387±0.0310	0.7854±0.0135	0.7742±0.0160
λ_2	0.0583±0.0028	0.0320±0.0009	0.0187±0.0012
C_3	0.1839±0.0463		
λ_3	0.0256±0.0016		
$BT_{1/2}(\lambda_2)$-days			
Mean	11.9	21.6	37.0
Range	8.5–16.5	17.5–31.4	29.4–49.6

The decay scheme of ^{137}Cs and the energies of the associated radiations is as follows:

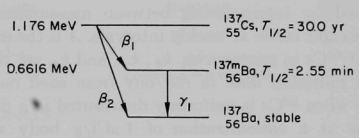

Source	Radiation	No./Dis.	Mean energy, MeV	Δ_i g·rad/ μCi·day
^{137}Cs	β_1	0.935	0.1749	9.7776
	β_2	0.065	0.4272	
^{137m}Ba	γ_1	0.840	0.6616	28.4088
	Internal conversion (*ic*)	0.095	0.6616	3.2208

The total integrated radiation dose, $\bar{D}$, delivered by injected ^{137}Cs is the sum of doses from the ^{137}Cs electrons and γ rays and internal conversion electrons from the ^{137m}Ba daughter. It is appropriate to compute the dose from the internal conversion electrons of ^{137m}Ba separately, because it has been reported that ^{137}Cs and ^{137m}Ba are not in radioactive equilibrium in the living animal.[2] Thus,

$$\bar{D} = \bar{D}_\beta + \bar{D}_\gamma + \bar{D}_{ic} . \quad (1)$$

The total integrated dose to time, t, in days, after an injection of ^{137}Cs is given by

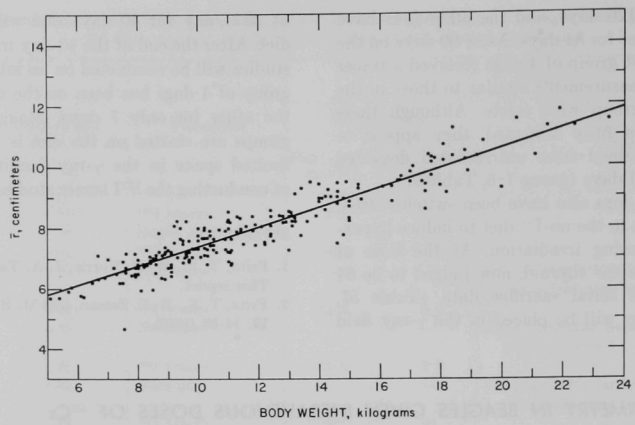

FIG. 59.—The relationship between mean body radius, $\bar{r}$, and body weight in 218 beagle dogs of both sexes.

$$\bar{D} = A\,(k_\beta + k_\lambda + k_{ic}) \int_0^t \frac{C_1 e^{-\lambda_1 t} + C_2 e^{-\lambda_2 t} + C_3 e^{-\lambda_3 t}}{W_t}\, dt, \qquad (2)$$

where C_1, C_2, and C_3 and λ_1, λ_2, λ_3 are the constants describing ^{137}Cs retention (Table 58) measured in each individual dog. W_t is body weight at time, t, and was obtained by interpolating between measurements of body weight made at weekly intervals. A is the injected dose of ^{137}Cs in microcuries. k_β, k_γ, and k_{ic} are the values of radiation dose in rad/day from each radiation source when ^{137}Cs is uniformly distributed in a dog-size volume at a concentration of 1 μCi/g body weight. Because the range of ^{137}Cs electrons in tissue is less than 3 mm, edge effects may be ignored and the values of k_β and k_{ic} become identical to those of Δ_i, computed for infinite homogeneous volumes containing ^{137}Cs. Thus,

$$k_\beta = 9.7776 \text{ g}\cdot\text{rad}/\mu\text{Ci}\cdot\text{day}$$

$$k_{ic} = 3.2208 \text{ g}\cdot\text{rad}/\mu\text{Ci}\cdot\text{day}.$$

k_γ is a complex value, however, and was computed using the method described in two papers by Hubbard and Williamson.[3, 4] It is necessary to approximate the volume of the dog by an equivalent cylinder.

The cylindrical approximation to beagles of varying size and weight was made from measurements of 111 female and 107 male anesthetized dogs. Body weights of these beagles ranged from 5.1 to 23.5 kg. Three circumferential measures—upper chest, at level of diaphragm, and lower abdomen—were made of each dog. In addition, there was a measure of body length from the shoulder to the base of the tail. The latter values ranged from 36.0 to 64.0 cm.

The three circumferential measures were averaged for each animal and then, assuming cylindrical proportions, this average was used to compute the mean radius, $\bar{r}$. A least squares fit of $\bar{r}$ against body weight, Figure 59, provided the relationship:

$$\bar{r} = 4.188 + 3.194 \times 10^{-4}\, W, \qquad (3)$$

where $\bar{r}$ is in cm and W is body weight in grams.

Small variations in cylinder length, L, have little effect on the fraction of gamma radiation absorbed. A review of the dimensions of the dogs given ^{137}Cs led us to conclude that the length of the equivalent cylinders representing these animals could be considered constant and equal to 44 cm.

From Hubbard and Williamson,

$$\frac{\Delta D_\gamma}{\Delta_t} \cong \frac{Ena\mu_{en}}{4\pi\rho}\,\bar{g}_\mu \left[1 - \frac{\mu_{en}^*}{\mu_{en}}\,(\mu - \mu_{en})\,\frac{1.03}{4\pi}\,\bar{g}_\mu^*\right]^{-1} \cdot \text{eV/g/day}. \qquad (4)$$

E is the energy of the primary photon in electron volts, n is photons per disintegration of ^{137}Cs, a is ^{137}Cs concentration in μCi/g, and ρ is the density of the medium. The average energy of the scattered photons, $\bar{E}_s^\gamma$, is

$$\bar{E}_s^\gamma = \frac{\mu - \mu_{en}}{\mu}\, E^\gamma = 0.41\text{MeV}$$

Values for the absorption coefficients[5] for a medium of unit density are as follows:

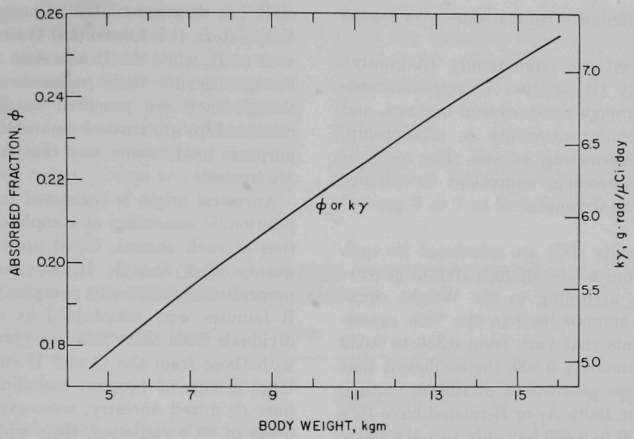

FIG. 60.—Computed values of k_γ and the absorbed fraction, ϕ, for the γ-rays of ^{137m}Ba derived from injected ^{137}Cs in beagle dogs.

Photon energy, MeV	
0.6616	$\mu = 0.08604$, $\mu_{en} = 0.0327$
0.41	$\mu^* = 0.106$, $\mu^*_{en} = 0.0328$

The quantities $\bar{g}_\mu$ and $\bar{g}^*_\mu$ are geometric factors related to the absorption of the primary and scattered photons, respectively, and are defined by Hubbard and Williamson.[4] Their values depend on the dimensions of the volume in which ^{137}Cs is distributed.

Solution of equation (4), above, with $\rho = 1.0$ and ^{137}Cs concentration, $a = 1\ \mu$Ci/g, together with appropriate constants to convert eV to rads gives

$$k_\gamma = \frac{16.81\bar{g}_\mu}{227.33 - \bar{g}^*_\mu}\ \text{g}\cdot\text{rad}/\mu\text{Ci}\cdot\text{day} \qquad (5)$$

Values of k_γ are plotted against body weight for dogs in Figure 60.

This computation of radiation dose was programed for a computer. Values of integrated dose and dose rate were calculated for each value of t to 200 days, at which time excretion has reduced the dose rate to a very small value. Although the fraction of the total dose attributable to each of the various radiations changes somewhat with animal size, their contributions to the total dose are well approximated as follows:

Source	Radiation	% Total dose
^{137}Cs	$\beta_1 + \beta_2$	51
^{137m}Ba	γ_1	32
^{137m}Ba	Internal conversion	17

REFERENCES

1. Poole, C. M., W. P. Norris, and T. E. Fritz. Argonne National Laboratory Biological and Medical Research Division Annual Report, 1968. ANL-7535, pp. 163–166.
2. Wasserman, R. H., A. R. Twardock, and C. L. Comar. *Science* **129**, 568–569 (1959).
3. Hubbard, L. B. and F. S. Williamson. *Phys. Med. Biol.* **14**, 255–267 (1969).
4. Hubbard, L. B. and F. S. Williamson. *Phys. Med. Biol.* In press.
5. Berger, M. J. *J. Nucl. Med.* (Supl.) **1**, 15–25 (1968).

BEAGLES: INBREEDING, ANCESTRY, AND RADIOSENSITIVITY

Carl E. Rehfeld and William P. Norris

PURPOSE AND METHODS

The project for the study of the toxicity and metabolism of radionuclides includes a beagle breeding program to produce the experimental animals. Planned inbreeding and avoidance of inbreeding are practiced simultaneously; the first produces greater uniformity, and the second insures continuance of the colony in the event inbreeding fails. A sufficient number of both inbred and comparatively non-inbred dogs have been included in certain phases of ^{60}Co experi-

ments to permit preliminary comparisons with regard to radiosensitivity.

Inbreeding produced one large family (A-family) and one small family (B-family). Although inbreeding was advanced through cousin-cousin matings, and other matings of similar proximity in relationship, there has been sibling-mating as well. The result is a wide range of inbreeding, equivalent in sibling-mating results to that accomplished in 1 to 7 generations.

Inbreeding coefficients (IC) are calculated for each dog in the colony from a base of six parental generations, when known, according to the Wright equation.[1] The inbred animals used in the ^{60}Co experiments have coefficients that vary from 0.336 to 0.632 but most are approximately 0.500, the coefficient that would result from two generations of sibling mating. Dogs that are neither 100% A- or B-related have IC's that range from 0.000 to 0.400 but only two are above the 0.150 level, and most are below the 0.090 level.

In avoidance of inbreeding, dogs that are neither 100% A- or B-related may be entirely unrelated to A or B, but they are related in part or entirely to O and U ancestors. It is known that O ancestors are unrelated to A or B, while the U ancestors are of undetermined lineage because their pedigrees are unavailable although they are purebred beagles. The O and U relationships are treated separately for computational purposes in the same way that A- and B-relatedness are treated.

Ancestral origin is registered in the ancestral composition,[2] consisting of complete familial identification of each animal, based upon the percentile frequency that the A, B, O, and U subpopulation progenitors appear in its pedigree. Although the A and B families were maintained as distinct entities, individuals from these families were frequently crossed with those from the O and U subpopulations. When large groups of beagles, including those with either pure or mixed ancestry, were exposed to challenging doses of ^{60}Co radiation, their wide range of response suggested that inbreeding and ancestry had influenced their radiosensitivity.

The ^{60}Co gamma exposures were varied as to total dose and dose rate; they include repeated, brief, near-lethal exposures and various dose rates protracted over 100-day and 32-month periods. In every exposure design the dogs were carefully randomized, within the limits of stock available at the time, according to sex, weight, degree of inbreeding and ancestry.

TABLE 59. REPEATED BRIEF EXPOSURES TO ^{60}Co (MORTALITY AND SURVIVAL)

Dog No.	Inbreeding coefficient	Percentage derivation from subpopulations				Parentage		First dose, R	Second dose, R	Third dose, R
		A	B	O	U	Dam	Sire			
808	0.274	75	22	3		329	541	275		
811	0.274	75	22	3		329	541	275		
821	0.057		48	8	44	50	433	325		
834	0.556	100				379	187	300		
801	0.008		56	3	41	394	459	275	275	
807	0.274	75	22	3		329	541	275	275	
809	0.274	75	22	3		329	541	325	275	
812	0.274	75	22	3		329	541	300	275	
817	0.0	50			50	42	469	325	275	
823	0.556	100				530	187	275	275	
826	0.099	25	36	8	31	229	433	300	275	
832	0.556	100				379	187	325	275	
805	0.008		56	3	41	394	459	325	275	275
818	0.0	50			50	42	469	275	275	275
819	0.057		48	8	44	50	433	300	275	275
830	0.556	100				379	187	275	275	275
831	0.556	100				379	187	300	275	275
833	0.556	100				379	187	275	275	275
802	0.008		56	3	41	394	459	275	275	275
803	0.008		56	3	41	394	459	300	275	275
804	0.008		56	3	41	394	459	300	275	275 [a]
806	0.008		56	3	41	394	459	325	275	275
828	0.099	25	36	8	31	229	433	325	275	275

[a] Survivors of all three exposures.

PROGRESS REPORT

The greatest variation in response observed occurs in one of the low-dose-rate experiments still in progress. In this example, where groups of dogs are exposed to 17 R/22-hr day until death, one dog survived only 85 days, others survived at least 118 days, but 2 dogs were still doing well in the γ field after 980 days. The earliest death (85 days) was a 100% A-related dog with an IC of 0.632, while the two survivors are not A-related and have IC's of 0.008 and 0.094. Data obtained with dogs at other low dose rates, over 900+ days, suggest on preliminary inspection that ancestry and inbreeding may also be important factors in survival or death.

Neither inbreeding nor ancestry appeared to influence survival when the dogs were exposed to a large dose of ^{60}Co radiation in a single 15-minute period; however, these factors did appear to influence survival when similar doses were given repeatedly (Table 59). There were 23 dogs divided into groups given either 275, 300, or 325 R; 4 dogs, 1 or 2 in each group, failed to survive this first exposure. Second and third doses of 275 R each eliminated another 14 dogs, including all remaining dogs that were 50% to 100% A-related and all of those with appreciable amounts of inbreeding. Of

the 5 dogs surviving all three exposures, 4 were siblings, the IC was either 0.008 or 0.099, and only one was A-related (25%). It must be added that there was no absolute distinction between decedent and survivor groups on the basis of inbreeding or ancestry, because 1 or 2 dogs in each of the decedent groups were similar or identical in these respects to the 5 survivors.

Final calculations of radiation dose to each animal will be made at the conclusion of the ^{60}Co experiments; these are necessary for additional analyses of the influence of inbreeding and ancestry upon radiosensitivity.

REFERENCES

1. Wright, S. *Am. Nat.* **56**, 330–339 (1922).
2. Rehfeld, C. E. *Am. J. Vet. Res.* **31**, 723–732 (1970).

COMPARISON OF CERTAIN HEMATOLOGIC EFFECTS IN BEAGLES GIVEN CESIUM-137, CERIUM-144, OR EXPOSED TO COBALT-60

Carl E. Rehfeld, Donald E. Doyle, and Donald L. Pearson

PURPOSE AND METHODS

Leukocyte levels and mean corpuscular volume (MCV) are the two hematologic values selected to compare both early and late effects from three sources of irradiation injury to beagles. Leukocyte levels are commonly used as sensitive measures of radiation toxicity. Increases in MCV were mentioned in some of the first assessments of radiation injury.[1, 2] Macrocytosis may be due to the increased number of cells that proceed to the reticulocyte stage without undergoing the last maturation division.[3, 4] There is evidence that humoral factors other than erythropoietin do affect erythropoiesis in radiation macrocytosis.[5] It will be seen here that macrocytosis is sustained over long periods of time with two forms of irradiation in dogs, so they could prove to be ideal subjects for a study in depth of radiation-induced macrocytosis and anemia.

Toxicological effects of ^{137}Cs, ^{144}Ce, and ^{60}Co irradiation are compared by means of hematologic data selected from dose levels that produce similar evidence of toxicity. Although a range of doses for each of these 3 forms of irradiation was studied, only one group of dogs from each range was of adequate size and similarity to allow preliminary comparison. The study of each radionuclide was initiated at a different time but this summary occurs at that point: 800 days after beginning continuous whole-body exposure of dogs to ^{60}Co; 2292 days after I.V. injection of ^{144}Ce (in citrate form); and 2661 days after I.V. injection of ^{137}Cs (as a chloride). Dose rates for ^{60}Co, ^{144}Ce, and ^{137}Cs were: 12.5 rads/22-hr day; approximately 15 rads/day; and, initially, 50 rads/day, respectively. The ^{60}Co dose/day is constant and the slowly decrementing ^{144}Ce is quite constant, by comparison with the rapidly decrementing ^{137}Cs; only approximate dose estimates are available for ^{144}Ce. Accumulated doses at 30 days and the times identified above are: for ^{60}Co, 375 rads and 10,000 rads; for ^{144}Ce, the doses are 450 rads at 30 days, and 5,300 rads to the skeleton and 10,000 to 15,000 rads to the liver after 2,300 days; for ^{137}Cs, the doses are 968 and 1,400 rads. The ratios of survivors/decedents for ^{60}Co, ^{144}Ce, and ^{137}Cs are 2/8, 2/18, and 9/10, respectively.

All blood samples were obtained from the jugular vein after food was withheld for about 18 hours. Erthyrocytes and leukocytes were enumerated by the electronic gating (Coulter) method, and Wintrobe tubes were used to determine hematocrits.

PROGRESS REPORT

The ^{137}Cs data are essentially a record of survival, while most deaths from ^{144}Ce occurred either within 100 days or after 1,000 days from the time of injection. Two apparently radioresistant dogs provide the leukocyte counts relative to ^{60}Co exposure beyond 260 days.

The temporal sequence of toxicological effects upon the hematopoietic system is relatively unique for each of the three sources of irradiation. Dogs injected with near-lethal doses of ^{137}Cs experience a severe leukopenia within the first 30 days, and those that survive this period recover to near their pre-exposure level within about 200 days. Lymphocytes are most affected, and failure to recover to pre-exposure levels indicates some permanent impairment of lymphopoiesis. Although initial leukopoietic depression (about 35 days) with ^{144}Ce is less severe, slow decrement of this nuclide prevents recovery to near normal until about 1,000 days when normal forms are supplemented by abnormal cells. Many of the late deaths resulting from the ^{144}Ce are due to myeloproliferative disorders that produce abnormally high cell counts periodically between 1,300 and 1,700 days. In continuous ^{60}Co ex-

posure, extreme depression of leukopoiesis occurs at about 120 days and recovery is very slow but continuous for the two dogs that survived beyond 260 days. Reductions in both neutrophils and lymphocytes are characteristic of ^{144}Ce and ^{60}Co exposure.

Erythrocytes were reduced in number by 35% or 40% at 175 days and again at 800 days during continuous ^{60}Co exposure, and at 1800 days after ^{144}Ce injection. These moderate anemias are more consistently associated with the deaths than with increases in MCV.

Radiation-induced macrocytosis was first observed in the ^{144}Ce-injected dogs. They had an average increase in MCV of about 21% at 85 days followed by a gradual return to normal at 500 days; a minor increase in the period from 900 to 1,100 days was followed shortly by a normal to subnormal period until 1,600 days, when MCV increased continuously until it attained a 28% increase at 1,800 days. Continuing with ^{144}Ce, there are unusually large differences among dogs, some having as little as a 3% increase and others as much as 40% or more. A microcytosis is almost invariably coincidental with the macrocytosis, so, in some instances, a marked macrocytosis is not reflected in the MCV where microcytes are too numerous.

The ^{60}Co-irradiated dogs had a marked macrocytosis beginning at 150 days, with even higher peaks at 300 days and 800 days; a relatively normal period of about 300 days occurred between the high peaks. In distinct contrast to the other two forms of irradiation, ^{137}Cs injection resulted in a definite and sustained reduction in MCV from 150 days to 2,500 days post-injection.

CONCLUSION

Comparison of hematopoietic effects caused by ^{137}Cs, ^{144}Ce, and ^{60}Co irradiation reveals some interesting parallels in production of leukopenia and macrocytosis even though the modes of irradiation are so different. The major differences in reaction are the times of appearance and recovery for leukopenia, anemia, and increased or decreased MCV. Exposure to ^{137}Cs, ^{144}Ce, and ^{60}Co results in a severe depression of leukopoiesis within 30 to 120 days, followed by rapid, intermediate, and slow recovery, respectively. At 800 days the ^{60}Co-irradiated dogs are at the half-point of their recovery with respect to number of leukocytes but many undoubtedly lack normal functional capacity. Between 1,000 and 2,300 days both ^{137}Cs- and ^{144}Ce-injected dogs have normal to near-normal numbers of leukocytes; cells of ^{137}Cs dogs appear normal, but many in ^{144}Ce dogs are grossly abnormal. These variations in response were expected because of differences among the three sources of radiation with respect to biological half-life, distribution within the body versus total-body exposure, and the dose rates.

If the same factors control erythrocyte maturation and release in dogs and man, the MCV increases identified with ^{144}Ce and ^{60}Co exposure are logical results of the irradiation at levels under discussion here. MCV increases in man are associated with hepatic and/or gastrointestinal disease. The liver is a target organ for ^{144}Ce; both liver and gastrointestinal tissues are subject to continuous insult from ^{60}Co exposure, 22 hours/day, over long periods of time. There is no logical explanation at the present time for the slight decrease in MCV associated with ^{137}Cs toxicity, but this unexpected reaction adds to the value of this system for a study of radiation-modified erythropoiesis.

REFERENCES

1. Jacobson, L. O., E. K. Marks, and E. Lorenz. *Radiology* **52,** 371–395 (1949).
2. Prosser, L., and M. C. Moore. *Biological effects of External X and Gamma Radiation*, Part 2. Ed. R. E. Zirkle U. S. Atomic Energy Commission Report TID-5220 1956, pp. 100–146.
3. Miller, M. and G. Sacher. *Radiat. Res.* **22,** 217 (1964).
4. Brecher, G. and F. Stohlman, Jr. *Erythropoiesis*, Ed. L. O. Jacobson. Grune and Stratton, New York, 1962. pp. 216–221.
5. Cederberg, A., E. Niskanen, and T. Rytoma. *Acta Physiol. Scand.* **70,** 147–157 (1967).

Characterization of the ANL Beagle

SOURCE OF BETA-HEMOLYTIC STREPTOCOCCI IN BEAGLE PUPS

Patricia C. Brennan, Richard C. Simkins, and William P. Norris

PURPOSE AND METHODS

In our previous reports[1, 2] we found that β-hemolytic streptococci were associated with bacteremia in dogs exposed to continuous ^{60}Co gamma radiation. We concluded that the streptococci originated in the throats of these dogs. Furthermore, when we studied the normal throat flora of unirradiated dogs from the beagle colony we found a high incidence of β-hemolytic streptococci and noted a similar incidence of β-hemolytic streptococci in young stock dogs and in breeding

adults.[3] Because young stock dogs are recent additions from the breeding kennel, it is possible that the pups become infected from the bitch soon after birth. We also have observed neonatal deaths associated with β-hemolytic streptococci in this beagle colony, further suggesting that pups become infected from the bitch. We began a study to determine whether the β-hemolytic streptococci in the throats of dogs in the colony can be traced to contact with infected bitches during the neonatal period.

Throat cultures were collected from pregnant bitches at a time estimated to be 7 to 10 days prior to whelping. Throat cultures were collected again from the bitches and from all pups of each litter when the pups were 10 days of age and when the pups were weaned at approximately 40 days of age. Methods for isolating streptococci have been described;[3] seventeen bitches and their litters have been examined.

PROGRESS REPORT

Only one bitch was negative for β-hemolytic streptococci at all three culture intervals, and her pups were similarly negative at 10 and 40 days of age. Nine bitches were negative before whelping; only two of these were negative when their pups were 10 days old, and these two were positive when their pups were weaned. The remaining seven were positive before whelping and also when their pups were 10 days old. Two of these were negative when the pups were weaned; the others were still positive. When the mother was positive for β-hemolytic streptococci ten days after whelping, the pups were also positive. These pups were still positive at weaning, regardless of whether β-hemolytic streptococci were recovered from the bitch at that time. The incidence of β-hemolytic streptococci among the pups was 65% when they were 10 days of age; this incidence decreased to 52% when they were weaned.

CONCLUSION

Pups become infected with β-hemolytic streptococci from contact with an infected mother during the neonatal period. The incidence in the pups is similar to the overall incidence in the colony.[4]

REFERENCES

1. Brennan, P. C. and R. C. Simkins. Argonne National Laboratory Biological and Medical Research Division Annual Report, 1968. ANL-7535, pp. 159–160.
2. Brennan, P. C. and R. C. Simkins. Argonne National Laboratory Biological and Medical Research Division Annual Report, 1969. ANL-7635, p. 99.
3. Brennan, P. C. and R. C. Simkins. *Proc. Soc. Exp. Biol. Med.* **134**, 566–570 (1970).
4. Brennan, P. C. and R. C. Simkins. This report.

CLINICAL CHEMISTRY OF THE NORMAL BEAGLE DOG

Lillian V. Kaspar and William P. Norris

PURPOSE AND METHODS

Since April 1965, blood samples for biochemical assay have been obtained from beagle dogs in this colony. Originally, total protein (TOPR), glucose (GLUC), and blood urea nitrogen (BUNI) were determined.[1] Cholesterol[2] (CHOL), alkaline phosphatase[3] (ALPH) and transaminase[4] (SGOT and SGPT) assays were added later. Data presented here were gathered from normal beagle dogs ranging in age from 13 months to more than 10 years.

PROGRESS REPORT

Table 60 lists mean values and standard deviations for the seven biochemical parameters assayed in normal, untreated beagle dogs in this colony. There are two partially inbred lines, designated as lines A and B. The majority of the colony remains outbred and is designated as line O. All parameters assayed, except BUNI, appear to be independent of age. Thirteen-month-old beagles have a mean BUNI value of 15 to 16 mg/100 ml serum; by an age of six years, this value drops to 10 to 11 mg/100 ml serum. (As data are still being analyzed, no values are listed in Table 60). When the other biochemical parameters were segregated on the basis of sex, and within this category on the basis of ancestral composition, certain groups of animals were recognized as different from others. Most striking are the higher cholesterol values of all females. Standard deviations of the cholesterol values of the females are also greater than those of the males. The few purebred B line dogs sampled have ALPH values half again as large as from dogs of other ancestral composition.

Our findings are being updated and we plan to more completely analyze the effects of ancestral composition,

TABLE 60. BIOCHEMICAL PARAMETERS OF THE NORMAL, UNTREATED BEAGLE DOG ARRANGED BY SEX AND ANCESTRAL COMPOSITION

Determination	All dogs		Ancestral composition	Males		Females	
	Units ± S.D.	No. of determinations		Units[a]	No. of determinations	Units[a]	No. of determinations
ALPH	0.95 ± 0.66	1108	All dogs	0.96 ± 0.49	567	0.93 ± 0.79	541
			O	0.97 ± 0.50	469	0.97 ± 0.86	437
			A	0.83 ± 0.43	91	0.74 ± 0.33	100
			B	1.49 ± 0.41	7	1.62 ± 0.64	4
CHOL	177.4 ± 53.7	237	All dogs	158.7 ± 38.9	125	198.7 ± 60.3	112
			O	158.7 ± 39.8	116	205.3 ± 62.5	89
			A	156.9 ± 25.8	8	173.5 ± 43.4	23
			B	174.2	1		0
GLUC	95.5 ± 17.8	1354	All dogs	95.5 ± 17.3	683	95.3 ± 18.2	671
			O	96.1 ± 17.4	558	95.6 ± 18.3	545
			A	90.8 ± 15.6	115	93.7 ± 17.8	122
			B	113.1 ± 14.6	10	93.1 ± 12.2	4
SGOT	23.6 ± 12.2	243	All dogs	23.6 ± 10.8	128	23.6 ± 13.8	115
			O	23.3 ± 10.9	119	23.7 ± 15.1	92
			A	26.7 ± 10.0	8	23.3 ± 6.6	23
			B	30.5	1		0
SGPT	29.0 ± 15.1	255	All dogs	28.9 ± 14.6	127	29.4 ± 15.8	128
			O	28.4 ± 14.1	118	30.6 ± 14.6	95
			A	38.1 ± 20.7	8	20.4 ± 5.0	23
			B	18.8	1		0
TOPR	6.1 ± 0.8	1308	All dogs	6.1 ± 0.9	658	6.1 ± 0.8	650
			O	6.2 ± 0.9	542	6.1 ± 0.8	530
			A	6.1 ± 0.7	106	6.2 ± 0.8	116
			B	5.8 ± 1.0	10	6.5 ± 0.4	4

[a] Units: ALPH, Bessey-Lowry units/ml serum. CHOL, mg/100 ml serum. GLUC, Mg/100 ml serum. SGOT and SGPT, Sigma-Frankel units/ml serum at 37°C. TOPR, g/100 ml serum.

sex, age, etc., on these and other blood biochemical parameters.

REFERENCES

1. Kaspar, L. V. and W. P. Norris. Argonne National Laboratory Biological and Medical Research Division Annual Report, 1966. ANL-7278, pp. 125–126.
2. Hycel Cholesterol Determinations, Hycel, Inc., Houston, Texas, 1964.
3. Sigma Technical Bulletin No. 104, Revised, 1963. Sigma Chemical Co., St. Louis, Mo.
4. Sigma Technical Bulletin No. 505, 1967. Sigma Chemical Co., St. Louis, Mo.

*ANALYSIS OF HERITABLE INFLUENCE ON MEAN ERYTHROCYTE VOLUME IN BEAGLES**

Carl E. Rehfeld, Max R. Zelle,† Donald E. Doyle, and Merlin H. Dipert

The mean corpuscular volume (MCV) of erythrocytes in normal dogs is reported to vary from 60.0 μ^3 to 77.0 μ^3, but the range of values in the Argonne beagles varies from 52.0 μ^3 to 89.1 μ^3. This colony includes two partially inbred subpopulations, and this suggests that the distribution of MCV for these subpopulations may differ enough to account for a larger variation than is normal. The MCV variations and alterations are of

* Abstract of paper submitted for publication in the *American Journal of Veterinary Research.*

† Present address: Department of Radiology and Radiation Biology, Colorado State University, Fort Collins, Colorado 80521.

particular interest because these beagles are used for radiation toxicology and MCV is frequently altered after their exposure to ionizing radiation.

Three MCV values for each dog are calculated from hemograms obtained at weekly intervals in the age period of 12 to 13.5 months; the average of the three values is the baseline MCV for each dog. The data sample for analyses includes the baseline values from 522 beagles; the mean of these values is 66.4 μ^3, and the median is 65.6 μ^3. Although the distribution curve for the 522 values is approximately symmetrical, the pattern of frequencies suggests the presence of two or more subpopulations. It was considered possible that the inbred subpopulations or families, termed A and B, influence the abnormal range of MCV by inheritance, so percentile values of A- and B-relatedness were carefully calculated.

Analyses of variances demonstrated significant differences in the MCV for various degrees of both A- and B-relatedness. Then, a series of regression equations were fitted to the data, using as variables the MCV, A-relatedness, and B-relatedness. Significant regressions indicated progressively that: there is a genetic effect on MCV; the abnormal variation in MCV is due primarily to A-relatedness; and there are large random or unknown factors also affecting MCV. Finally, the data analyses suggest a low heritability for MCV determination despite the existence of a highly significant genetic component.

HISTORY OF A BEAGLE COLONY*

Carl E. Rehfeld, Jeanne Blomquist, and Glenn N. Taylor†

A beagle colony is maintained by the Division of Radiobiology at the University of Utah to provide dogs of known ancestry and clinical history in an AEC sponsored study of bone-seeking radionuclide toxicity. Most of the foundation stock for this colony was purchased in 1950. Since that time this colony has provided substantial numbers of dogs for the development of other colonies used in AEC supported research. Argonne National Laboratory has acquired breeding stock from the Utah colony at several different times; as a result several hundred Argonne dogs are derived entirely, or in part, from Utah-bred stock. In following the policy of characterizing ANL beagles as fully as is possible and reasonable, it became necessary to study the history and genealogy of the Utah parent stock and offspring. This simultaneously provides a service to the Utah laboratory and other laboratories utilizing Utah-bred stock.

A total of 47 purebred beagles were purchased, or used temporarily, for the breeding program at Utah. Pedigree records published by the American Kennel Club were used extensively, and quite successfully, to determine the six parental generations for each of the original 47 dogs. This pedigree information was desirable for two reasons: first, to determine the nature and extent of relationships between the breeders, and, second, to calculate inbreeding coefficients.

Continuous inbreeding, where it occurs, is calculated as an accumulative process; therefore, it is necessary to either obtain accurate birth dates for all dogs or to find some means of arranging them in hierarchal order according to their appearance in sequential generations. Accurate birth dates were often unavailable, so a computer method was used to determine hierarchy among the ancestors of the foundation breeders. The next step involved the calculation of the inbreeding coefficient for each foundation animal, its ancestors, and descendents. These inbreeding coefficients also were calculated by a computer method and in this process the frequency of appearance of each parent or ancestor was tabulated at each generation level in which it appeared. The parent generation is designated P_1 while the grandparent generations are P_2 through P_6. The influence of each producing dog can be estimated from the number of times it appears in each generation from P_1 to P_6 in the pedigrees of dogs born at the laboratory.

Only 4 of the original 47 dogs appear in the P_6 generation (1851 times), indicating either that their offspring were most frequently selected as breeders, or that they were most prolific when selected. Eleven original dogs, including the 4 above, appear in pedigrees in the P_5 generation a total of 2275 times; these 11 dogs constitute the producing nucleus of the original colony.

A total of 1427 dogs were born at the Utah labora-

* Abstract of paper prepared for inclusion in the Twentieth Anniversary Symposium Volume, Division of Radiobiology, University of Utah.

† Division of Radiobiology, College of Medicine, University of Utah, Salt Lake City, Utah

tory between 09/15/51 and 07/19/70, and some degree of inbreeding was calculable for 550, or 38.5%. Inbreeding coefficients at the highest levels present were 0.25, 0.37, and 0.50 for 165, 11, and 14 dogs, respectively. Many dogs with coefficients of 0.25 to 0.50 may have been produced in the planned inbreeding program conducted on a very small scale in recent years. On preliminary examination there appear to be one or more inbred subpopulations of significance as regards interpretation of radiotoxicological data.

DETERMINATION OF ^{239}Pu AND ^{241}Am IN ANIMAL TISSUES BY LIQUID SCINTILLATION SPECTROMETRY*

Arthur Lindenbaum and Marguerite A. Smyth

Plutonium-239 or americium-241 in ashed samples of bone, liver, spleen, feces and urine, dissolved in 0.1 N HCl, was assayed by a liquid scintillation method, using Triton N-101-xylene-PPO. A commercially available liquid scintillation spectrometer was used, and essentially 100% counting efficiency was achieved. There was close agreement between analytical results obtained with this liquid scintillation method and with a previous one employing toluene-ethanol-PPO; also, between results obtained with liquid scintillation spectrometry (LS) as compared to proportional counting (PC). LS is generally superior to PC because it is less laborious and time-consuming, yields closer replication of analytical values, and permits more analyses per experiment because tissues low in activity can be counted individually, rather than pooled. The Triton N-101-xylene-PPO scintillation fluid has advantages over toluene-ethanol-PPO: It permits the use of larger volumes of aqueous samples, holds more insoluble matter in suspension (due to gelation), and, in most cases, allows vials to be stored indefinitely without apparent loss of activity. Simple instrumental methods of detecting and correcting occasional aberrant samples are described.

Addendum: When the quantity of organic residue is large, as with bone samples, prolonged overheating at the end of the ashing process may cake the residue into hard masses which may not disperse or dissolve in the scintillation fluid. This could result in a drop in counting efficiency and, consequently, an activity level below the true value. The best solution to this problem is avoidance. If necessary, the residue may be mechanically fragmented in the scintillation fluid with a flat-ended stirring rod. Another aid in dispersing larger quantities of inorganic residue is the dropwise addition, preferably *before* addition of scintillation fluid, of up to 0.5 ml of *colorless,* concentrated HNO_3. If, on counting the sample, this shifts the S value beyond the normal range, a higher gain setting alone usually will move the activity peak back into the preset window.

* Abstract of a paper to be published in *Organic Scintillators and Liquid Scintillation Counting,* Ed. Horrocks and Peng, Academic Press, New York.

METABOLIC AND THERAPEUTIC STUDIES OF PLUTONIUM AND AMERICIUM

Arthur Lindenbaum, Marcia W. Rosenthal, John J. Russell, Elizabeth S. Moretti, and Dorothy Chladek

PURPOSE AND METHODS

The broad objective of this program is to develop new approaches to the therapy of poisoning by radioactive and nonradioactive metals.[1] Plutonium-239 has received increasing emphasis during the last several years because of its importance as a radiological health hazard. The varying tendency of compounds of the actinide series (as well as other polyvalent heavy metals) to hydrolyze and polymerize, both in solution and *in vivo,* results in variable particulate characteristics which influence the deposition, retention, effectiveness of therapy, and delayed pathological effects of these nuclides. Thus, information obtained with plutonium and americium aids in understanding the behavior of other nuclides of the actinide, lanthanide, and rare earth series in living tissues. Plutonium compounds also provide useful information on the translocation and deposition of colloids and macromolecules in tissues.

Previous work has demonstrated the effectiveness of chelating agents, such as diethylenetriaminepentaacetic acid (DTPA), for removal of plutonium and related elements from blood, bone, and soft tissues; attention is now being directed toward other therapeutic approaches aimed at removal of that portion of the plutonium not readily removed by DTPA.

Related to the plutonium research is a concomitant program[2] concerned with calcium uptake and depletion and with biochemical transformations in the calcifying matrix of preosseous cartilage. The aim of this work is to achieve a better understanding of the uptake of normal (e.g. calcium) and abnormal (e.g. plutonium and strontium metals) in cartilage and bone.

This report summarizes 1) new information on a continuing comparative study of the long-term carcinogenic effects and tissue-distribution patterns of monomeric and polymeric plutonium in mice;[3] 2) preliminary results with rabbits, aimed at scale-up of the plutonium studies to larger animals; and 3) results of kinetic studies with monomeric and polymeric americium in mice.

PROGRESS REPORT

Metabolic and Therapeutic Studies of Plutonium. VI

Effects of the Physical Form of Plutonium (Polymeric vs Monomeric) on Lifetime Retention in the Soft Tissues of Mice.—Comparative lifetime information on the retention of monomeric and polymeric plutonium (or of any other actinide) in soft tissues is limited to the mouse liver. To obtain such information, and to relate lifetime plutonium concentration to the incidence of soft tissue and bone tumors in mice from a current experiment,[3] the terminal plutonium content of soft tissues has been determined after intravenous injection of graded doses of monomeric or polymeric plutonium. In addition to liver and spleen, analyses were carried out in kidneys, gastrointestinal tract, ovaries, uterus and oviducts, body musculature, heart, lymphatic tissue, lungs, adrenals, and salivary glands of mice dying between 141 and 742 days after injection. These data were compared with tissue levels of plutonium determined in groups of mice sacrificed at 6 and 90 days.

The following results are noted. 1) Liver: After polymeric plutonium, the initial high Pu burden in the liver decreased slowly over the first year ($T_{1/2}$ = 570 days), and more rapidly thereafter ($T_{1/2}$ = ~350 days). After monomeric plutonium, the liver burden decreased rapidly over the first 44 days ($T_{1/2}$ = 14 days), more slowly over the next 8½ months, and did not change thereafter. After either form of plutonium, the fraction retained by the liver was not dose dependent over the ranges injected. 2) Spleen: After polymeric plutonium, there was a linear, dose-dependent decrease throughout life; after monomeric plutonium (with lower concentrations) there was no decrease. 3) In most of the "minor" soft tissues, the initial deposition of plutonium was dependent on the form injected, as has been shown for liver, spleen, and bone. 4) During the first year (or less) after injection of monomeric plutonium there was a net loss of plutonium from most tissues, but no loss from ovaries and uterus. After polymeric plutonium there was a net gain of plutonium in ovaries, heart and lymphatic tissues (as well as bone), a loss of plutonium from lungs, and little change in the other tissues measured. 5) After about one year there appeared to be little or no change in the plutonium level of any of the "minor" soft tissues studied, throughout the remainder of the life span, after either form, or at any dose.

For eventual microdosimetric application, the deposition of plutonium at the cellular level in mouse liver is being measured by means of alpha-track autoradiography. Recent work, employing a standardized technique at light microscopic magnifications, indicates the possibility of achieving useful quantitative results, despite variations in the plutonium administered or in the length of time tissue sections are exposed to the photographic emulsion. A generally linear function was obtained when track counts were plotted against exposure times between 1 and 42 days.

Distribution of Monomeric and Polymeric Plutonium in Rabbits.—Because extrapolation to man is a long-range objective of this program, comparison of the metabolism of different physical-chemical forms of plutonium is being extended to larger species. Rabbits are now being used, both for distribution studies and for the adaptation of analytical techniques to larger tissues. Preliminary results obtained after intravenous injection indicate that: 1) Plutonium injected in monomeric form appeared to leave the rabbit liver more slowly than the mouse or rat liver. In this respect, the rabbit is more comparable to the dog, and probably to man. 2) After mid-range polymeric plutonium about one-half of the plutonium in the rabbit tibia was in the marrow, vs. about one-fourth in a comparable sample of mouse bone. 3) The concentration of polymeric plutonium in the marrow appeared to be highly variable among individual rabbits, and among different marrow samples in the same rabbit. This variability may be related to the proportions of erythropoietic and fatty marrow. Preliminary data indicate that the concentration of plutonium in predominantly erythropoietic marrow may be 10 to 20 times higher than in fatty marrow.

Deposition and Early Retention Patterns of Monomeric and Polymeric Americium-241 in Mice and Rats

For therapeutic and dosimetric applications, as well as for fundamental information, there is a need to determine whether there are significant differences be-

TABLE 61. TISSUE DISTRIBUTION OF TWO FORMS OF INTRAVENOUSLY INJECTED ^{241}Am IN CF1/ANL FEMALE MICE (% INJECTED DOSE)

Time after Am	Monomeric Am					Polymeric Am				
	Total skeleton	Tibial shaft		Liver	Spleen	Total skeleton	Tibial shaft		Liver	Spleen
		Marrow	Hard bone				Marrow	Hard bone		
1 hr	21.9	—	—	37.8	0.079	6.6	—	—	43.4	2.3
1 day	25.3	—	—	38.0	0.076	8.0	—	—	66.0	3.6
6 days	26.4	0.0057	0.315	24.2	0.115	9.8	0.047	0.067	55.0	3.8
90 days	22.6	0.0351	0.264	1.1	0.131	16.0	0.066	0.149	20.4	2.2

tween the metabolic behavior of plutonium and americium. Accordingly, a 200-day tissue distribution study is being carried out with 100-day-old CF1/Anl female mice injected intravenously with monomeric or polymeric americium-241 (100% and 1% ultrafilterable, respectively). This study was designed to parallel, as closely as possible, the experiment with plutonium-239 described above and previously.[3] In addition, tissue uptake at 1 and 8 hours was measured, and comparisons with CF1 mice from Carworth Farms, at 6 days, and with Sprague-Dawley rats, at 6 and 44 days, were made. Table 61 shows selected data to indicate major trends to date.

As found for plutonium, 1 to 6 days after monomeric americium less of the americium was deposited in liver, spleen, and marrow, and more in the skeleton, than after polymeric americium. After monomeric americium, however, the skeletal uptake at 1 to 6 days was about one-half that found after a comparable preparation of plutonium; the subsequent rate of skeletal loss up to 90 days was equal for both nuclides. In liver, the uptake and rapid loss of monomeric americium was comparable to the behavior of monomeric plutonium. After polymeric americium, there was a twofold higher skeletal uptake than after polymeric plutonium. As after polymeric plutonium, there was a gradual rise in skeletal (hard bone) burden between 1 and 90 days, which proceeded at approximately the same rate as after plutonium, and which was also accompanied by a depletion of the liver burden. However, liver depletion was more rapid after polymeric americium between 1 and 90 days (from 66% to 20% of the injected dose) than after polymeric plutonium (84% to 77%).

As with plutonium, the uptake of americium in the bone marrow was much higher after the polymeric than after the monomeric form. After monomeric americium, the marrow burden increased with time to a greater extent than after monomeric plutonium. It is estimated from tibial data that, after monomeric americium, the fraction of total skeletal americium incorporated in the marrow rose from 1% at 6 days to 7% at 90 days; after polymeric americium the marrow fraction of total skeletal americium is estimated to be about 20% at both intervals.

In rats, the distribution of monomeric and polymeric americium in liver, spleen, and bone at 6 and 44 days was generally comparable to that in CF1/Anl mice. In rat lung, however, there was lower incorporation of polymeric americium than in mouse lung (5% vs. 20% of the retained amount). In contrast to the high concentration of americium reported in the dog thyroid, the concentrations in both rat and mouse thyroids were low.

Comparison of the distribution of americium in the liver, spleen, and bone in Argonne and Carworth strains of CF1 female mice showed no essential differences at 6 days after injection of either form.

CONCLUSIONS

The initial deposition and the retention of plutonium in the "minor" soft tissues of mice over a period of one year (or less) after intravenous administration depends upon the particulate characteristics of the plutonium injected, as shown earlier for liver, spleen, and bone. Beyond one year, to the end of life, after either monomeric or polymeric plutonium, there is no apparent change in the plutonium burden of any soft tissue, except for a continuing loss of polymeric plutonium from liver and spleen.

Preliminary evidence in the rabbit of a greater uptake of polymeric plutonium in erythropoietic marrow than in fatty marrow, if confirmed, would have important dosimetric implications in man.

After intravenous injection of monomeric and polymeric americium, the distribution and retention patterns in mice up to 90 days are generally comparable to those reported after similar preparations of monomeric and polymeric plutonium. However, after monomeric americium, compared with monomeric plutonium, there is a lower early deposition in the skeleton and bone marrow, and a greater increase in marrow burden with time. After polymeric americium, com-

pared to polymeric plutonium, there is a somewhat higher deposition in bone, a lower uptake in liver, and a more rapid disappearance from the liver. Polymeric americium would appear to be less polymeric than polymeric plutonium, possibly as the result of more rapid depolymerization in the tissues. Polymeric americium and plutonium both undergo translocation from liver to hard bone.

REFERENCES

1. Lindenbaum, A. and M. W. Rosenthal. Argonne National Laboratory Biological and Medical Research Division Annual Report, 1965. ANL-7136, pp. 191–192.
2. Lindenbaum, A. and Egan, N. This report.
3. Lindenbaum, A., M. W. Rosenthal, J. J. Russell, E. S. Moretti, and M. A. Smyth. Argonne National Laboratory Biological and Medical Research Division Annual Report, 1969. ANL-7635, pp. 186–190.

BIOCHEMISTRY AND ION BINDING OF CONNECTIVE TISSUE. V.

Arthur Lindenbaum and Nancy Egan

PURPOSE AND METHODS

In the removal from the body of many toxic radioelements, including the polyvalent, heavy metals, such as plutonium, bone is the critical tissue. A better understanding of normal and abnormal physiological processes in bone, therefore, is of practical as well as fundamental importance. The overall objectives of this project are to investigate the biochemical changes taking place in cartilage during calcification and ossification, particularly with regard to changes in the protein-polysaccharide components, and to determine the involvement of such substances in the accumulation of normal and abnormal metals.

The objectives of present experiments are: 1) isolation, characterization, and quantitation of the protein-polysaccharide components of the organic matrix of calf scapula cartilage and bone, at various stages during calcification and ossification; 2) measurement of the binding of intact cartilage, and of isolated protein-polysaccharide components, with calcium and other metal ions; 3) investigation of the effect of these macromolecular substances on the precipitation of calcium phosphate salts from simulated physiological solutions.

PROGRESS REPORT

In previous investigations[1] the protein-polysaccharides were extracted from cartilage by a technique utilizing high-speed homogenization of cartilage in low-ionic-strength salt solution. The crude extract was fractionated into 4 water-soluble products, PPL-3, PPL-4, PPL-5, and PPL-6, on the basis of their sedimentability in various salt solutions.[2] A fifth hexuronate-containing fraction, PPL-2, was isolated from the cartilage residue by treatment with hydroxylamine; this fraction is thought to be more tightly bound to the cartilage matrix than the other, more readily extracted, protein-polysaccharides.

Other investigators[3] have suggested that the 5 fractions obtained from cartilage by this method might be, at least partially, artifacts of the high-shear homogenization used in the extraction. They, therefore, labeled this method "degradative," and introduced an alternate "dissociative" extraction method which involved the gentle agitation of cartilage in salt solutions of very high ionic strength and which resulted in the extraction of a single product which represented 85% of the total tissue hexuronate from bovine nasal cartilage.

TABLE 62. PROTEIN AND HEXURONATE IN PROTEIN-POLYSACCHARIDE FRACTIONS FROM 4 ZONES OF CALF SCAPULA OBTAINED BY TWO EXTRACTION TECHNIQUES[a]

Zone	Degradative method				Dissociative method			
	PPL-2		PPL-3		PPC-II		PPC	
	Protein	Uronate	Protein	Uronate	Protein	Uronate	Protein	Uronate
Resting cartilage	24.0	14.5	13.3	20.3	12.5	29.7	16.8	20.3
Transforming cartilage	23.5	14.0	9.7	17.1	14.7	25.3	23.2	26.6
Ossifying cartilage	35.7	13.6	2.5	19.7	10.0	27.3	38.5	18.5
New bone	7.0	9.1	3.2	15.1	29.5	16.0	24.3	20.4

[a] All values expressed as % of dried fraction.

Both methods were recently used to isolate corresponding protein-polysaccharides from 4 zones of calf scapular cartilage and bone. After extraction of cartilage samples by the dissociative method, each cartilage residue was also treated with hydroxylamine to obtain a product, termed PPC-II, representing remaining hexuronate. The resulting products were analyzed for protein and hexuronate content (Table 62).

Only in the resting zone of calf scapular cartilage were there similarities between PPL-3, the most abundant fraction of the degradative method, and PPC; in the zones actively being transformed into bone there were marked differences. The two products obtained by hydroxylamine extraction, PPL-2 and PPC-II, were distinctly different in all four zones.

CONCLUSIONS

The above work illustrates the complexities of cartilage and the difficulties in drawing correct inferences about the composition and functions of intact cartilage from data based on isolated components, obtained by procedures which may themselves make an artifactual contribution. At present, it is only possible to apply isolation procedures which yield reproducible cartilage components, with a minimum of artifact, on which generally standardized biochemical and physical-chemical measurements may be carried out. Investigation of the differences in the composition of ossifying and nonossifying cartilage, and the significance of such differences, will be continued, both for a better understanding of metal ion uptake in bone formation, and for therapeutic manipulation of radiounclides incorporated in bone.

REFERENCES

1. Lindenbaum, A. and Q. T. Smith. Argonne National Laboratory Biological and Medical Research Division Annual Report, 1969. ANL-7635, p. 191.
2. Pal, S., P. T. Doganges, and M. Schubert. *J. Biol. Chem.* **241**, 4261–4266 (1966).
3. Sajdera, S. W. and V. C. Hascall. *J. Biol. Chem.* **244**, 77–87 (1969).

SUPRALETHALLY X-IRRADIATED AMOEBAE TREATED WITH NONIRRADIATED, HOMOGENIZED PROTOPLASM*

Edward W. Daniels and Evelyn P. Breyer

Pelomyxa illinoisensis, giant carnivorous amoebae, die without mitosis or cell division within a week after an exposure to 30 kR X radiation. Those X-irradiated amoebae, injected by: (1) fusion with cytoplasm freed of nuclei; (2) a micropipette filled with nonirradiated protoplasm removed from donors in the absence of a homogenate medium, or (3) with homogenates made from nonirradiated amoebae, divide and produce cultures similar to those of the nonirradiated controls. Thus, the radiorestorative capacity of nonirradiated protoplasm has been maintained outside the cell long enough to demonstrate the feasibility of isolating the radiorestorative agents from donor protoplasm. It was also shown that cell membranes (plasmalemmae) of the donor amoebae are not required for radiorestoration.

* Abstract of manuscript to be published in *Radiation Research.*

ULTRASTRUCTURE OF SPERMATOZOA FROM THE AMERICAN OYSTER, CRASSOSTREA VIRGINICA GMELIN*

Edward W. Daniels, Arlene C. Longwell,† and Judith M. McNiff

The nucleus of the spermatozoon is ovoid with its long axis perpendicular to the flagellum. It is invaginated antero-posteriorly, enclosing the axial body, a relatively large amorphous mass containing many small vesicles. A centrally located filament extends from the base of the nuclear invagination to the apex of the acrosome. The latter, contained within its own membrane, caps the axial body and depresses the anterior rim of the nucleus. The head, middle piece, and tail are covered by the plasmalemma. A small fossa in the center of the distal surface of the nucleus is en-

* Abstract of manuscript to be submitted for publication in the *J. Ultrastructure Res.*

† U. S. Department of Commerce, National Oceanic and Atmospheric Administration, National Marine Fisheries Service, Biological Laboratory, Milford, Connecticut 06460.

closed within the two membranes of the nuclear envelope. The middle piece of the sperm contains 4 adjacent mitochondria radially arranged in a plane perpendicular to the flagellum. Two cylindrical centrioles are located in the center space between them. The sperm tail contains the 9 + 2 configuration of microtubules. The end piece of the tail is smaller in diameter than the body of the tail piece, and has 9 singlet microtubules radially arranged around a central doublet.

ULTRASTRUCTURE OF OOCYTES FROM THE AMERICAN OYSTER, CRASSOSTREA VIRGINICA GMELIN*

Edward W. Daniels, Arlene C. Longwell,† and Judith M. McNiff

Oocytes of *C. virginica* are characterized by numerous external villi (ca. 0.9 by 0.1 μm) embedded in a blanket of transparent matrix material. The nucleus or germinal vesicle (ca. 40 to 50 μm) contains an acentric nucleolus. The nuclear envelope has many blebs or evaginations of both membranes into the cytoplasm; some of these are branched. The nucleopores, about 160 nm from center to center, each have 8 subannuli and usually a central granule. The cytoplasm suspends the ribosomes, mitochondria, annulate lamellae, small vesicles of different types, as well as both lipid and yolk granules. The latter separate during centrifugation at 85,000 times gravity; the lipid accumulates at the centripetal pole and the yolk at the centrifugal pole. Also, this centrifugal force separated the dense, agranular portion of the nucleolus from the granular portion.

* To be submitted for publication.

† U. S. Department of Commerce, National Oceanic and Atmospheric Administration, National Marine Fisheries Service, Biological Laboratory, Milford, Connecticut 06460.

TREATMENT OF X- OR UV-IRRADIATED AMOEBAE WITH INJECTIONS OF HOMOGENATE MADE FROM NONIRRADIATED AMOEBAE AT 2°C.

Edward W. Daniels and Judith M. McNiff

PURPOSE AND METHODS

The radiosensitive amoebae, *Pelomyxa illinoisensis*, like those used in previous investigations on radiorestoration,[1] died, and none are available except in nature. Despite an extensive and continuing search, none have been recovered from the natural habitats sampled. Consequently, we returned to a study of the radioresistant amoeba, *Pelomyxa carolinensis*, which we found in Colorado.[2]

After a sublethal dose of X radiation, *P. carolinensis* recover their capacity to divide more rapidly if they are fused with small portions of nonirradiated donors.[3] In the present investigation, a homogenate of unirradiated amoebae was injected into supralethally X-irradiated amoebae to test its capacity to induce recovery. A homogenate was used in the hope of isolating radiorestorative agents like those described earlier.[1]

To extend this study, supralethally UV-irradiated amoebae (*P. carolinensis*) that also were injected with homogenate were compared with untreated, UV-irradiated controls. The sensitivity of this species to X rays and UV radiation in comparison with other species, especially *P. illinoisensis*, had to be studied, and the toxicities of different homogenate media had to be tested prior to radiorestoration experiments.

P. carolinensis from feeding cultures were X irradiated in buffer[1, 4] at 250 kVp at a rate of 44,000 R/min, or 1,100 R/min. The UV dose rate from a Pen Ray lamp at a distance of 9 cm was 50 ergs/mm^2/sec; reducing the target distance to 6.5 cm the dose rate was 100 ergs/mm^2/sec. Amoebae were fasted for 2 days, then UV irradiated in quartz vials under 6 mm of double distilled water. Photoreactivation effects, when present, were compensated by maintaining all UV-exposed amoebae, both experimentals and irradiated controls, in the same light.

The toxicity of the potential homogenate medium was tested by injecting it into stock amoebae. Tris-HCl buffer (50 mM, pH 7.2 and 8) was essentially nontoxic, and the amoebae quickly began to move after injection; they captured food organisms and divided normally. Other tests were done by injecting different amoebae with the following media: 5 mM $MgCl_2$ in glass distilled water; 5 mM $MgCl_2$ in Tris buffer (50

TABLE 63. SURVIVAL OF *PELOMYXA CAROLINENSIS* (COLORADO STRAIN) FOLLOWING X IRRADIATION AND HOMOGENATE INJECTION

Dose in kR		Number of amoebae isolated	Time between exposure and injection	Median survival in days	Cell divisions, %	Recovery, %	Homogenate media	Comment
(4,400 R/min)								
300	X-irrad. control	10	—	8	0	0	—	Median survival time of irradiated amoebae was reduced by treatment.
	X-irrad. injected	10	2 days	6.5	0	0	$MgCl_2$ 5 mM	
260	X-irrad. control	12	—	11	0	0	—	Median survival time of irradiated amoebae was reduced by treatment.
	X-irrad. injected	15	3 hr	2	0	0	$MgCl_2$ 10 mM KCl 50 mM Tris 50 mM	
260	X-irrad. control	16	—	8	0	0	—	Median survival time of irradiated amoebae was reduced by treatment.
	X-irrad. injected	25	2 days	3	0	0	$MgCl_2$ 5 mM	
250	X-irrad. control	18	—	16	0	0	—	Median survival time of irradiated amoebae was reduced by treatment.
	X-irrad. injected	44	1.5 days	10	0	0	$MgCl_2$ 5 mM	
200	X-irrad. control	100 (not isol.)	—	15 (estimate)	5	5	—	After 10 days each surviving amoeba had produced an average of 25 amoebae.
	X-irrad. injected	30	1 day	3	5	5	$MgCl_2$ 10 mM KCl 50 mM Tris 50 mM	
(1,100 R/min)								
125	X-irrad. control	10	—	—	80	80	—	After 10 days each surviving amoebae had produced an average of 23 amoebae.
	X-irrad. injected	25	1 day	—	96	96	$MgCl_2$ 5 mM KCl 1 mM Tris 1 mM	
0	Nonirrad. control	14	—	—	100	100	—	After 10 days, each amoeba had produced an average of 40 individuals.

and 10 mM); 10 mM $MgCl_2$ unbuffered; a combination of 50 mM Tris, 10 mM $MgCl_2$, and 50 mM KCl. None of these appeared to be toxic.

The amoebae were washed twice in the homogenate medium, then the supernatant was decanted, and the amoebae were ground by hand approximately 6 strokes in a Dounce homogenizer, which did not break nuclei. The homogenate was filtered through coarse fritted glass (which allowed nuclei to pass); it then was drawn into a glass micropipette which had a 20 to 25 μm tip. Irradiated amoebae were held in a micrurgy chamber between two glass slides and injected with the homogenate. The amount injected into each amoeba was equal to about 10% of its volume. Immediately after injection, the amoeba was transferred to a warm room (21°C), isolated in buffer,[4] and fed protozoans (chilomonads and paramecia). The nonirradiated and the irradiated controls were treated similarly, although

none were injected. All amoebae were observed and cared for daily until they either died or produced clones.

PROGRESS REPORT

X Radiation

Data obtained from our investigations, and some comments, are presented in Table 63. A dose of 250,000 R was necessary to kill all organisms in a culture of *P. carolinensis*, Colorado strain. Immediately after this dose, these amoebae were vacuolated and fragile, and for a day or two they could not be injected without disintegrating. Even when injected a day or two after exposure, they died more quickly than the irradiated, untreated controls (Table 63).

A lower dose of X radiation (125 kR) given at a slower rate (1,100 R/min) was much less damaging than were higher doses (200 to 300 kR), and when treated with homogenates of nonirradiated amoebae, more of the treated amoebae survived (96% vs. 80%).

UV Radiation

A dose of 25,000 ergs/mm^2 of ultraviolet radiation (254 nm) was given at the rate of 50 ergs/mm^2/sec to 32 amoebae. Twenty-two were injected with a homogenate made from nonirradiated donor amoebae in 5 mM $MgCl_2$ without a buffer at pH 7. The median survival time of the 10 UV-irradiated, noninjected controls was 3.5 days, while the median survival of those that were injected was 5 days. All amoebae in both groups were dead after 17 days, and there were no cell divisions in either group. Cell division occurred normally among 10 nonirradiated control amoebae that had been isolated. Thus, while homogenate treatment produced a therapeutic trend, its significance is not established.

REFERENCES

1. Daniels, E. W. and E. P. Breyer. *Int. J. Radiat. Biol.* **18,** 179 (1970).
2. Daniels, E. W., P. A. Sustarsic, and J. F. McClellan. *J. Protozool.* **16,** 182 (1969).
3. Daniels, E. W. *J. Exp. Zool.* **127,** 427 (1954).
4. Pace, D. M. and B. W. McCashland. *Proc. Soc. Exp. Biol. Med.* **76,** 165 (1951).

During 1970, a total of 26 college undergraduates received training in the Division of Biological and Medical Research, in cooperation with the Argonne Center for Educational Affairs. These students were in one of three programs, the Associated Colleges of the Midwest (ACM), the Central States Universities Incorporated (CSUI), or the Summer Student Training Program (SSTP). Four Student Aides also were employed during 1970.

In addition, one trainee in the Affirmative Action Program (AAP) and 15 high school students from Chicago, who were sponsored by the Neighborhood Youth Corps (NYC), U.S. Department of Labor, worked in the Division during the year.

The students, their schools, and their staff supervisors are listed below.

Student	School	Supervisor
ACM		
Barchas, Rebecca E.	Grinnell College	B. N. Jaroslow
Corbridge, Ann G.	Colorado College	C. Peraino
Durbahn, Camille M.	St. Olaf College	Y. E. Rahman
Lyman, Sherida E.	Grinnell College	R. J. M. Fry
Nelson, Donald M.	Cornell College	R. N. Feinstein
Phillips, Steven J.	Knox College	J. C. Copeland
Smith, Shelley D.	Grinnell College	H. E. Kubitschek
Stamps, Robert H.	Coe College	R. R. Dedolph
Thomsen, Robert J.	St. Olaf College Paracollege	R. E. Krisch
Zichal, Kenneth E.	Coe College	C. F. Ehret
CSUI		
Banks, Donald	Mansfield State College	W. E. Kisieleski
Bohl, Robert D.	Denison University	N. A. Frigerio
Boss, Peter	University of Redlands	E. J. Ainsworth
Cox, Alan	Buena Vista College	P. D. Klein
Dillon, David C.	Canisius College	A. M. Brues
Hatch, Lorraine	Marymount College	H. E. Kubitschek
Moskowitz, Joel M.	Brooklyn College	A. Lindenbaum
SSTP		
Baker, Judieth E.	Florida A & M University	J. S. Miller
Burkey, Thomas M.	Aquinas College	W. E. Kisieleski
Eatmon, Diane	N. Carolina Central University	Y. E. Rahman
Hughes, William H.	S. Carolina State College	G. Svihla
Kelley, Sandra F.	Paine College	S. Tyler
Pryor, Gail	Lawrence University	J. C. Copeland
Ryan, Homer W.	Morehouse College	R. J. M. Fry
Smith, David L.	Louisiana Polytechnic	Y. E. Rahman
Valdez, David	University of Illinois	H. E. Kubitschek
STUDENT AIDES		
Carrigan, John	Texas A & M University	S. A. Gordon
Liang, James C.	M.I.T.	S. A. Gordon
Noack, Nelleen G.	Mount Mary College	J. S. Miller
Wagner, Daniel R.	University of Missouri	C. M. Poole
AAP		
Reed, Sylvester		W. Eisler
NYC		
Bailey, Linda		C. Peraino
Chatman, Theatha		S. A. Gordon
Gillie, Joyce		A. H. Anderson
Goines, Carey		C. M. Poole
Henderson, Pat		M. Brown

Student	School	Supervisor
NYC—continued		
Hester, Rhonda R.		M. H. Dipert
House, Michael		R. R. Dedolph
Kiefer, Peter		K. Allen
McMiller, William		M. Brown
Mhoon, Patricia		J. W. Williams
Moore, Jean M.		L. Mabins
Sims, Carol		R. E. Ecker
Stratford, Michael		K. Hardman
Warfield, Myrtle		M. H. Dipert
Williams, Larry		R. R. Dedolph

JOURNAL ARTICLES

Bacchetti, S. and W. K. Sinclair. The relation of protein synthesis to radiation-induced division delay in Chinese hamster cells. *Radiat. Res.* **44,** 788–806 (1970).

Bell, C. L. and S. S. Danyluk. Solvent dependence of the chemical shifts and coupling constants of 1,2-dichlorofluoro-ethylenes. *J. Mol. Spectry.* **35,** 376–392 (1970).

Brennan, P. C., C. Peraino, R. J. M. Fry, and R. W. Swick. Immunofluorescent localization of ornithine aminotransferase in rat liver. *J. Histochem. Cytochem.* **18,** 264–267 (1970).

Brennan, P. C. and R. C. Simkins. Throat flora of a closed colony of beagles. *Proc. Soc. Exptl. Biol. Med.* **134,** 566–570 (1970).

Brockwell, P. J., M. D. MacLaren, and E. Trucco. Monte Carlo simulation of PLM-curves and collection functions. *Bull. Math. Biophys.* **32,** 429–433 (1970).

Brockwell, P. J. and E. Trucco. On the decomposition by generations of the PLM-function. *J. Theoret. Biol.* **26,** 149–179 (1970).

Buchal, R. N., D. L. Phillips, and E. Trucco. Area relations between labeling index curves from multicompartment cell kinetics models. *Cell and Tissue Kinetics* **3,** 67–81 (1970).

Chorney, W., E. Rakosnik, M. H. Dipert, and R. R. Dedolph. Rhythmic flowering response in cocklebur. *BioScience* **20,** 31–32 (1970).

Copeland, J. C. DNA synthesis during amino acid starvation in *Bacillus subtilis*. *Microbial Genetics Bull.* **30,** 14 (1969).

Copeland, J. C. The effect of amino acid starvation on chromosome replication in *Bacillus subtilis*. *Microbial Genetics Bull.* **32,** 19 (1970).

Daniels, E. W. and E. P. Breyer. Rescue of supralethally x-irradiated amoebae with nonirradiated cytoplasm. *Radiat. Res.* **41,** 326–341 (1970).

Daniels, E. W. and E. P. Breyer. Recovery of supralethally x-irradiated and nitrogen mustard (HN_2)-treated amoebae. *Int. J. Radiat. Biol.* **18,** 179–187 (1970).

Davies, D. B. and S. S. Danyluk. Assignment and conformational properties of the sugar-ring hydroxyl protons of the common nucleosides. *Can. J. Chem.* **48,** 3112–3115 (1970).

Davies, D. J. G., S. A. Tyler, and R. B. Webb. A sequential repair model of photoreactivation in bacteria. *Photochem. Photobiol.* **11,** 371–386 (1970).

Dedolph, R. R., G. Ter Haar, R. B. Holtzman, and H. F. Lucas. Sources of lead in perennial ryegrass and radishes. *Environ. Sci. Technol.* **4,** 217–223 (1970).

Dieterman, L. J., S. H. Wender, W. Chorney, and J. Skok. Incorporation of ^{14}C-quercetin into an isopropyl alcohol- and acid-insoluble fraction of tobacco. *Phytochemistry* **8,** 2321–2323 (1969).

Edmundson, A. B., M. K. Wood, M. Schiffer, K. D. Hardman, C. F. Ainsworth, K. R. Ely, and H. F. Deutsch. A crystallographic investigation of a human IgG immunoglobulin. *J. Biol. Chem.* **245,** 2763–2764 (1970).

Eisler, W. J. Jr. and R. B. Webb. Turbidimetric culture device. *Laboratory Equipment* **6,** 1 (1969).

Eisler, W. J. Jr., R. J. M. Fry, and D. LeBuis. A foot operated cell counter *Laboratory Practice* **18,** 761 (1969).

Etherton, B. Effect of indole-3-acetic acid on membrane potentials of oat coleoptile cells. *Plant Physiol.* **45,** 527–528 (1970).

Feinstein, R. N. and C. Peraino. Separation of soluble and particulate mouse liver catalase by isoelectric focusing. *Biochim. Biophys. Acta* **214,** 230–232 (1970).

Feinstein, R. N. Acatalasemia in the mouse and other species. *Biochem. Genetics* **4,** 135–155 (1970).

Fichtelius, K. E. and B. N. Jaroslow. Changes in the concentration of lymphocytes in the intestinal epithelium of hibernating ground squirrels (*Citellus tridecemlineatus*). *Acta Path. Microbiol. Scand.* **77,** 99–102 (1969).

Freedman, M. L. and R. E. Krisch. The effect of T-phage infection on host-cell size. *Microbial Genetics Bull.* **32,** 3 (1970).

Frigerio, N. A. Microdetermination of uranium in tissues. *Int. J. Appl. Radiat. Isotopes* **21,** 434–436 (1970).

Fritz, T. E., R. C. Zeman, and M. R. Zelle. Pathology and familial incidence of thyroiditis in a closed beagle colony. *Exptl. Mol. Pathol.* **12,** 14–30 (1970).

Fritz, T. E., W. P. Norris, and N. D. Kretz. Influence of lymphocytic thyroiditis on iodine metabolism in the beagle. *Proc. Soc. Exptl. Biol. Med.* **134,** 450–458 (1970).

Graff, G., P. Szczepanik, P. D. Klein, J. R. Chipault, and R. T. Holman. Identification and characterization of fully deuterated fatty acids isolated from *Scenedesmus obliquus* cultured in deuterium oxide. *Lipids* **5,** 786–792 (1970).

Grube, D. D., H. Auerbach, and A. M. Brues. Diurnal

variation in the labeling index of mouse epidermis. A double isotope autoradiographic demonstration of changing flow rates. *Cell and Tissue Kinetics* **3,** 363–373 (1970).

Han, A. and W. K. Sinclair. Sensitivity of synchronized Chinese hamster cells to ultraviolet light. *Biophys. J.* **9,** 1171–1192 (1969).

Huebner, L. G. and W. E. Kisieleski. A comparative evaluation of a combustion method for liquid scintillation assay of carbon-14 and tritium in biological materials. *Atompraxis* **16,** 1–5 (1970).

Kidwell, J. F., A. Howard, and A. K. Laird. The inheritance of growth and form in the mouse. II. The Gompertz growth equation. *Growth* **33,** 339–352 (1969).

Krisch, R. E. Comparison of the lethal effects of ^{32}P and ^{33}P decay in *E. coli* and in bacteriophages. *Int. J. Radiat. Biol.* **18,** 259–266 (1970).

Kubitschek, H. E., M. L. Freedman, and S. Silver. Potassium uptake in synchronized and synchronous cultures of *E. coli. Microbial Genetics Bull.* **32,** 3–4 (1970).

Kubitschek, H. E. Evidence for the generality of linear cell growth. *J. Theoret. Biol.* **28,** 15–29 (1970).

Kvetkas, M. J., R. E. Krisch, and M. R. Zelle. Genetic analysis of a large-cell, radiation-resistant strain of *Escherichia coli. J. Bacteriol.* **103,** 393–399 (1970).

Norris, W. P., T. E. Fritz, and J. A. Taylor. Cycle of accommodation to restricted dietary iodide in the thyroid gland of the beagle dog. *Am. J. Vet. Res.* **31,** 21–33 (1970).

Ortiz-Ortiz, L. and B. N. Jaroslow. Enhancement by the adjuvant, endotoxin, of the immune response induced *in vitro. Immunology* **19,** 387–399 (1970).

Peraino, C., S. Bacchetti, and W. J. Eisler. Automated continuous culture of mammalian cells in suspension. *Science* **169,** 204–205 (1970).

Perkins, J. H. and S. A. Gordon. Morphogenesis in *Schizophyllum commune.* II. Effects of monochromatic light. *Plant Physiol.* **44,** 1712–1716 (1969).

Powers, D. A. A numerical taxonomic study of Hawaiian reef corals. *Pacific Sci.* **24,** 180–186 (1970).

Rahman, Y. E., J. Verhagen, and D. F. M. v. d. Wiel. Evidence of a membrane-bound phospholipase A in rat liver lysosomes. *Biochem. Biophys. Res. Commun.* **38,** 670–677 (1970).

Rehfeld, C. E. Definition of relationships in a closed beagle colony. *Am. J. Vet. Res.* **31,** 723–732 (1970).

Rehfeld, C. E., G. J. Dammin, and W. J. Hester. Skin graft survival in partially inbred beagles. *Am. J. Vet. Res.* **31,** 733–745 (1970).

Schiffer, M. and A. B. Edmundson. Prediction of α-helices in glucagon. *Biophys. J.* **10,** 293–295 (1970).

Schiffer, M., K. D. Hardman, M. K. Wood, A. B. Edmundson, M. E. Hook, K. R. Ely. and H. F. Deutsch. A preliminary crystallographic investigation of a human L-type Bence-Jones protein. *J. Biol. Chem.* **245,** 728–730 (1970).

Schlenk, F., J. L. Dainko, and G. Svihla. The accumulation and intracellular distribution of biological sulfonium compounds in yeast. *Arch. Biochem. Biophys.* **140,** 228–236 (1970).

Schlenk, F. Deamination of adenosine and related compounds. *Biochimica Applicata* **17,** 105–116 (1970).

Schlenk, F. The destructive effect of some proteins on the yeast cell membrane. *Biochimica Applicata* **17,** 89–103 (1970).

Schlenk, F. and C. R. Zydek-Cwick. Enzymatic activity of yeast cell ghosts produced by protein action on the membranes. *Arch. Biochem. Biophys.* **138,** 220–225 (1970).

Shen-Miller, J. Notes after a conference on Great Lakes research. *BioScience* **20,** 1294–1296 (1970).

Shen-Miller, J. Some thoughts on the nuclear agro-industrial complex. *BioScience* **20,** 98–100 (1970).

Shen-Miller, J. Reciprocity in the activation of geotropism in oat coleoptiles grown on clinostats. *Planta* **92,** 152–163 (1970).

Sinclair, W. K. Synchronous tissue culture. *Laboratory Management* 20–21 (October 1970).

Smith, L. D. and R. E. Ecker. Uterine suppression of biochemical and morphogenetic events in *Rana pipiens. Develop. Biol.* **22,** 622–637 (1970).

Stearner, S. P. and E. J. B. Christian. Protection against early radiation injury to the microvasculature. *Microvascular Res.* **2,** 202–211 (1970).

Stearner, S. P. and M. H. Sanderson. Early vascular injury in the x-irradiated chick embryo: An electron microscope study. *J. Pathol.* **99,** 213–218 (1969).

Swick, R. W., S. L. Tollaksen, S. L. Nance, and J. F. Thomson. The unique distribution of ornithine aminotransferase in rat liver mitochondria. *Arch. Biochem. Biophys.* **136,** 212–218 (1970).

Taliaferro, W. H. and L. G. Taliaferro. Actinomycin D before and during primary and secondary anti-Forssman immunoglobulin hemolysin responses in rabbits. *Proc. Natl. Acad. Sci.* **66,** 1036–1043 (1970).

Taliaferro, W. H. and L. G. Taliaferro. Effects of irradiation on initial and anamnestic hemolysin responses in rabbits. Antigen injection before x-rays. *J. Immunol.* **104,** 1364–1376 (1970).

Taylor, G. N., C. E. Rehfeld, W. R. Christensen, and W. S. S. Jee. Influence of ^{226}Ra and ^{239}Pu on the dental root canal of the dog. *J. Dental Res.* **48,** 924–927 (1969).

Ter Haar, G. L., R. R. Dedolph, R. B. Holtzman, and H. F. Lucas, Jr. The lead uptake by perennial rye-

grass and radishes from air, water, and soil. *Environ. Res.* **2,** 267–271 (1969).

Thomson, J. F. and S. L. Nance. The time course of aconitate formation from isocitrate in H_2O and D_2O. *Arch. Biochem. Biophys.* **135,** 10–13 (1969).

Victor, T. A., F. E. Hruska, C. L. Bell, and S. S. Danyluk. A nuclear magnetic resonance study of the structure and interaction of Actinomycin D. Analysis and conformational properties. *Tetrahedron Letters* **53,** 4721–4724 (1969).

Webb, R. B. and J. R. Lorenz. Oxygen dependence and repair of lethal effects of near ultraviolet and visible light. *Photochemistry and Photobiology* **12,** 283–289 (1970).

Webb, R. B. and M. M. Malina. Mutagenic effects of near ultraviolet and visible radiant energy on continuous cultures of *Escherichia coli. Photochemistry and Photobiology* **12,** 457–468 (1970).

Yu, C. K. and W. K. Sinclair. Protection by cysteamine against mitotic delay and chromosomal aberrations induced by x rays in synchronized Chinese hamster cells. *Radiat. Res.* **43,** 357–371 (1970).

Zappia, V., C. R. Zydek-Cwick, and F. Schlenk. The specificity of S-adenosylmethionine derivatives in methyl transfer reactions. *J. Biol. Chem.* **244,** 4499–4509 (1969).

BOOKS, REPORTS, AND PROCEEDINGS

Brues, A. M. Implications and applications of radiation toxicity data to other environmental hazards. *Late Effects of Radiation,* Proc. Colloquium, Univ. of Chicago, May 1969, Ed. R. J. M. Fry et al. Taylor and Francis, London, 1970, pp. 265–271.

Brues, A. M. (Participant) *Cellular Dynamics,* Proc. 5th Interdisciplinary Conference on Cellular Dynamics, Princeton, New Jersey, Jan. 1967, Ed. L. D. Peachey. Gordon and Breach Science Publishers, New York, 1969, Vol. V, 551 pp.

Copeland. J. C. Molecular biology. Genetics. *Britannica Book of the Year,* 1969, pp. 532–533.

Copeland, J. C. Molecular genetics. *Britannica Yearbook of Science and the Future,* 1970, pp. 298–300.

Daniels, E. W. The cell. *Wonderland of Knowledge Encyclopedia,* Ed. E. E. Sentman. The United Educators, Inc., Chicago, 1970, Vol. 3, pp. C229–C232.

Ehret, C. E. and J. J. Wille. The photobiology of circadian rhythms in protozoa and other eukaryotic microorganisms. *Photobiology of Microorganisms,* Ed. Per Halldal. John Wiley, New York, 1970, pp. 369–416.

Frigerio, N. A. and M. H. Branson. Current research in depth dose calculations. Proc. Symp. on Neutrons in Radiobiology, Oak Ridge, Tenn., Nov. 1969, Ed. J. A. Auxier and M. J. Constantin. U. S. Atomic Energy Commission Report CONF-691106, 1970, pp. 95–115.

Fritz, T. E., W. P. Norris, C. E. Rehfeld, and C. M. Poole. Myeloproliferative disease in beagle dogs given protracted whole-body irradiation or single doses of ^{144}Ce. *Myeloproliferative Disorders of Animals and Man,* Proc. Symp., Richland, Washington, May 1968, Ed. W. J. Clarke, E. B. Howard, and P. L. Hackett. USAEC Report CONF-680529, 1970, pp. 219–241.

Fry, R. J. M., D. Grahn, M. L. Griem, and J. H. Rust, Editors. *Late Effects of Radiation.* Proc. Colloquium, Univ. of Chicago, May 1969. Taylor and Francis, London, 1970.

Fry, R. J. M., M. L. Griem, and W. H. Kirsten, Editors. *Normal and Malignant Cell Growth.* Springer-Verlag New York Inc., 1969, 233 pp.

Fry, R. J. M. (Participant) *Cellular Dynamics.* Proc. 5th Interdisciplinary Conference on Cellular Dynamics, Princeton, New Jersey, Jan. 1967, Ed. L. D. Peachey. Gordon and Breach Science Publishers, New York, 1969, Vol. V, 551 pp.

Grahn, D. Biological effects of protracted low-dose radiation exposure of man and animals. *Late Effects of Radiation.* Proc. Colloquium, Univ. of Chicago, May 1969, Ed. R. J. M. Fry et al. Taylor and Francis, London, 1970, pp. 101–138.

Grahn, D. Late effects of external irradiations in animals and the prediction of low-dose effects. *Biological Implications of the Nuclear Age,* Proc. Symp. Lawrence Radiation Lab., March 1969. U. S. Atomic Energy Commission Report CONF-690303, 1969, pp. 269–281.

Klein, P. D. Isotope effects and their consequences in liquid scintillation counting. *The Current Status of Liquid Scintillation Counting,* Proc. Symp., Boston, March 1969, Ed. E. D. Bransome. Grune and Stratton, New York, 1970, pp. 142–155.

Kubitschek, H. E. Repair of latent T5-resistant mutants in chemostat cultures. CIBA Foundation Symposium on Mutation as a Cellular Process, Ed. G. E. W. Wolstenholme and M. O'Connor. S and A. Churchill, Ltd., London, 1969, pp. 87–101.

Miller, M. and B. N. Jaroslow. Effects of irradiation on the changes in the immune response of aging mice. Proc. Symp. on Neutrons in Radiobiology, Oak Ridge, Tenn., Nov. 1969, Ed. J. A. Auxier and M. J. Constantin. U. S. Atomic Energy Commission Report CONF-691106, 1970, pp. 268–274.

Sacher, G. A., D. Grahn, R. J. M. Fry, and J. H. Rust. Epidemiological and cellular effects of chronic radiation exposure: A search for relationship. Proc. of the First European Symposium on Late Effects of Radiation, Comitato Nazionale per l'Energia Nucleare, Rome, 1970, pp. 15–38.

Sacher, G. A. Models from radiation toxicity data. *Late Effects of Radiation*. Proc. Colloquium, Univ. of Chicago, May 1969, Ed. R. J. M. Fry et al. Taylor and Francis, London, 1970, pp. 233–244.

Sacher, G. A. Allometric and factorial analysis of brain structure in insectivores and primates. *Advances in Primatology*, Ed. C. Noback and J. W. Montagna. Appleton-Century-Crofts, New York, 1970, pp. 245–287.

Schlenk, F., J. L. Dainko, and G. Svihla. Protein injury to the yeast cell membrane. *Yeast Protoplasts*, Proc. 2nd Int. Symp. on Yeast Protoplasts, Brno, Czechoslovakia, Aug. 1968, Ed. O. Nečas and A. Svoboda. Acta Fac. Med. Univ. Brno, 1970, pp. 25–31.

Sinclair, W. K. Methods and criteria of mammalian cell synchrony. *Normal and Malignant Cell Growth*, Ed. R. J. M. Fry, M. L. Griem, and W. H. Kirsten. Springer-Verlag New York Inc., 1969, pp. 90–103.

Sinclair, W. K. Sensitization by hydroxyurea and protection by cysteamine of Chinese hamster cells during the cell cycle. Proc. Int. Symp. on Radiosensitizing and Radioprotective Drugs, Rome, May 1969. Taylor and Francis, Ltd., London, 1970, pp. 201–210.

Sinclair, W. K. Dependence of radiosensitivity upon cell age. *Time and Dose Relationships in Radiation Biology as Applied to Radiotherapy*, Conf. at Carmel, Calif., Sept. 1969. U. S. Atomic Energy Commission Report BNL-50203(C-57), 1970, pp. 97–116.

Sinclair, W. K. (Chairman) *Linear Energy Transfer*. International Commission on Radiation Units and Measurements. ICRU Report 16, 1970.

Smith, L. D. and R. E. Ecker. Regulatory processes in the maturation and early cleavage of amphibian eggs. *Current Topics in Developmental Biology*. Academic Press Inc., New York, 1970, Vol. 5, pp. 1–38.

Smith, L. D. and R. E. Ecker. Foundations for the expression of developmental potential. *Problems in Biology: RNA in Development*, Ed. E. W. Hanly. University of Utah Press, Salt Lake City, 1969, pp. 355–379.

Stearner, S. P. and E. J. B. Christian. Early radiation injury to the microcirculation. Relation to mortality. *Radiation Biology of the Fetal and Juvenile Mammal*, Proc. 9th Annual Hanford Biol. Symp., Richland, Washington, May 1969. U. S. Atomic Energy Commission Report CONF-690501, 1969, pp. 341–355.

Taliaferro, W. H. and L. G. Taliaferro. The cellular reactions in the skin of normal and immune rabbits injected with trichinella with special reference to the hematogenous origin of macrophages. *Srivastava Commemoration Volume*, Ed. K. S. Singh. Indian Vet. Res. Inst., Izatnager, U. P., India, 1970, pp. 517–526.

Tyler, S. A., N. D. Kretz, and W. P. Norris. The dependence of ^{137}Cs retention on age in the fetal and juvenile beagle dog. *Radiation Biology of the Fetal and Juvenile Mammal*, Proc. 9th Annual Hanford Biol. Symp., Richland, Washington, May 1969. U. S. Atomic Energy Commission Report CONF-690501, 1969, pp. 191–205.

Williamson, F. S. The dosimetry of mixed fields of neutron and gamma radiation. A review. Proc. Symp. on Neutrons in Radiobiology, Oak Ridge, Tenn., November 1969, Ed. J. A. Auxier and M. J. Constantin. U. S. Atomic Energy Commission Report CONF-691106, 1970, pp. 3–11.

Zappia, V., R. Cortese, C. R. Zydek-Cwick, and F. Schlenk. The specificity of S-adenosylmethionine decarboxylase. Proc. of Accademia Nazionale Die Lincei. Estratto dal fasc. 2, Serie VIII, Vol. XLVI, 1969, pp. 191–195.

STAFF OF DIVISION OF BIOLOGICAL AND MEDICAL RESEARCH

ADMINISTRATION

Flynn, Robert J. (Assistant Director, Animal Facility)
Harrison, James W. (Executive Assistant)
Sinclair, Warren K. (Director)
Thomson, John F. (Associate Director)
Wolfgang, Robert W. (Editor)

PERMANENT STAFF

Ainsworth, Clinton F. (Scientific Assistant)
Ainsworth, E. John (Associate Biologist)
Allen, Katherine (Assistant Biologist)
Blomquist, Jeanne A. (Programmer)
Brennan, Patricia A. (Assistant Biologist)
Brown, Mickey S. (Scientific Assistant)
Brues, Austin M. (Senior Biologist)
Buess, Evelyn (Scientific Assistant)
Cameron, Erma C. (Scientific Assistant)
Cerny, Elizabeth (Scientific Assistant)
Chladek, Dorothy (Scientific Assistant)
Chorney, William (Assistant Biologist)
Christian, Emily J. (Scientific Assistant)
Chubb, G. Theodore (Scientific Assistant)
Cooke, Eugenia M. (Scientific Assistant)
Copeland, James C. (Associate Geneticist)
Dainko, Julia L. (Scientific Assistant)
Daniels, Edward W. (Associate Biologist)
Danyluk, Steven S. (Associate Chemist)
Decker, Louis H. (Scientific Assistant)
Dedolph, Richard R. (Associate Plant Physiologist)
Devine, Rosemarie L. (Scientific Assistant)
Dipert, Merlin H. (Assistant Mathematician)
Dobra, Arlene H. (Scientific Assistant)
Dobra, William A. (Scientific Assistant)
Doyle, Donald E. (Scientific Assistant)
Drick, Sandra A. (Scientific Assistant)
Ecker, Richard E. (Associate Biologist)
Edmundson, Allen B. (Associate Biochemist)
Ehret, Charles F. (Senior Biologist)
Eisler, William J. (Engineering Specialist)
Ellwanger, Paul W. (Scientific Assistant)
Ely, Katherine A. (Scientific Assistant)
Feinstein, Robert N. (Senior Biochemist)
Flynn, Robert J. (Senior Veterinarian)
Frigerio, Norman A. (Associate Biochemist)
Fritz, Thomas E. (Associate Veterinary Pathologist)
Fry, R. J. Michael (Senior Physiologist)
Gordon, Solon A. (Senior Plant Physiologist)
Grahn, Douglas (Senior Biologist)
Grube, Donald D. (Scientific Assistant)
Hardman, Karl (Assistant Biochemist)
Hinchman, Ray R. (Scientific Assistant)
Holmblad, Gordon L. (Scientific Assistant)
Howard, Judith B. (Scientific Assistant)
Hulesch, Jane S. (Scientific Assistant)
Januszyk, Rita M. (Scientific Assistant)
Jaroslow, Bernard N. (Associate Immunologist)
Jordan, Donn L. (Assistant Biologist)
Kaspar, Lillian A. (Scientific Assistant)
Keenan, William G. (Scientific Assistant)
Kisieleski, Walter E. (Associate Chemist)
Klein, Peter D. (Senior Biochemist)
Kokaisl, Gloria A. (Scientific Assistant)
Kostal, George (Assistant Technical Specialist)
Kretz, Norbert D. (Scientific Assistant)
Krisch, Robert E. (Assistant Biophysicist)
Kubitschek, Herbert E. (Senior Physicist)
Lea, Ruth A. (Scientific Assistant)
Lindenbaum, Arthur (Associate Biochemist)
Long, Melvin D. (Scientific Assistant)
Lorenz, John R. (Scientific Assistant)
McNiff, Judith M. (Scientific Assistant)
Miller, Carol J. (Scientific Assistant)
Miller, Jane Shen (Assistant Botanist)
Miller, Marietta (Assistant Biologist)
Moreton, Marilyn F. (Scientific Assistant)
Moretti, Elizabeth (Scientific Assistant)
Nance, Sharron L. (Scientific Assistant)
Norris, William P. (Associate Biochemist)
O'Malley, Mary P. (Scientific Assistant)
Pearson, Donald L. (Scientific Assistant)
Peraino, Carl (Associate Biochemist)
Polk, Patrick H. (Scientific Assistant)
Poole, Calvin M. (Associate Veterinarian)
Prapuolenis, Aldona M. (Scientific Assistant)
Racster, Grace (Scientific Assistant)
Rahman, Yueh-Erh (Assistant Biologist)
Rehfeld, Carl E. (Associate Veterinarian)
Rosenthal, Marcia W. (Associate Scientist)
Russell, John J. (Scientific Assistant)
Sacher, George A. (Senior Biologist)
Sallese, Anthony R. (Scientific Assistant)
Sanderson, Margaret (Assistant Biologist)
Schiffer, Marianne (Assistant Biochemist)
Schlenk, Fritz (Senior Biochemist)

Shotola, M. Anita (Scientific Assistant)
Simkins, Richard C. (Scientific Assistant)
Sinclair, Warren K. (Senior Biophysicist)
Soucek, Stephanie L. (Scientific Assistant)
Staffeldt, Everett F. (Scientific Assistant)
Stearner, S. Phyllis (Associate Biologist)
Suhrbier, Katherine M. (Scientific Assistant)
Svihla, George (Associate Biologist)
Szczepanik, Patricia (Scientific Assistant)
Tahmisian, Theodore N. (Senior Biologist)
Thomson, John F. (Senior Biologist)
Tollaksen, Sandra L. (Scientific Assistant)
Tolle, David V. (Scientific Assistant)
Trier, Joseph E. (Engineering Assistant)
Tyler, Sylvanus A. (Associate Mathematician)
Venters, Dace (Scientific Assistant)
Webb, Robert B. (Associate Bacteriologist)
Weber, Charlotte L. (Scientific Assistant)
Westholm, Florence A. (Scientific Assistant)
Williamson, Frank S. (Associate Physicist)
Wolfgang, Robert W. (Associate Biologist)
Wright, Betty J. (Scientific Assistant)
Yu, Chi-Kang (Assistant Cytologist)
Zeman, Ruth C. (Scientific Assistant)

FORMER PERMANENT STAFF DURING 1970

Auerbach, Harry (Associate Statistician)
Barton, A. Donald (Associate Biochemist)
Bunville, Lyle G. (Assistant Chemist)
Camden, Ronald W. (Assistant Veterinarian)
Glaser, Jane K. (Associate Technical Specialist)
Hutson, Nancy K. (Scientific Assistant)
Morris, Dale D. (Assistant Biologist)
Reiskin, Allan B. (Associate Biologist)
Robbins, Martha H. (Scientific Assistant)
Sampson, Martin J. (Scientific Assistant)
Smyth, Marguerite A. (Scientific Assistant)
Sutton, Harold G. (Assistant Biologist)
Trucco, Ernesto (Associate Mathematician)
Williams, John W. Jr. (Scientific Assistant)

TEMPORARY STAFF DURING 1970

Angerman, Neil S. (Postdoctoral Appointee)
Antipa, Gregory A. (Resident Associate)
Bacchetti, Silvia (Visiting Scientist)
Barnett, Audrey J. (Visiting Scientist)
Bell, Charles L. (Resident Associate)
Bennett, Basil T. III (Resident Associate)
Berngruber, Otto (Postdoctoral Appointee)
Bernhard, William A. (Postdoctoral Appointee)
Chapman, George E. (Postdoctoral Appointee)
Coley, Ronald F. (Resident Associate)
Cook, Harry (Resident Associate)
Cook, Kenneth M. (Resident Associate)
Davies, David B. (Postdoctoral Appointee)
Egan, Nancy E. (Resident Associate)
Freitag, Per (Resident Associate)
Freedman, Michael L. (Postdoctoral Appointee)
Harber, Phyllis A. (Resident Associate)
Harris, John W. (Resident Associate)
Killick, Kathleen A. (Postdoctoral Appointee)
Langford, George M. (Resident Associate)
Larson, Charles H. (Resident Associate)
Lehmann, Wilma H. (Resident Associate)
Leroy, Elie P. (Resident Associate)
Mackay, Donna J. (Resident Associate)
Maier, Siegried (Resident Associate)
McArdle, Eugene W. (Resident Associate)
McDonald, Shirley (Resident Associate)
McDowell, Richard E. (Resident Associate)
Mendoza, Guillermo (Resident Associate)
Mullman, Theodore M. (Resident Associate)
Powers, Dennis (Postdoctoral Appointee)
Silver, Simon D. (Resident Associate)
Sly, Dayle (Resident Associate)
Stoltze, Herbert J. (Resident Associate)
Victor, Thomas A. (Resident Associate)
Wittig, Gertraude (Resident Associate)
Wood, Mical (Postdoctoral Appointee)

Author Index

Ainsworth, Clinton F. 96, 98
Ainsworth, E. John 32, 33, 34, 36, 41, 44
Allen, Katherine 38
Auerbach, Harry 48, 50

Bacchetti, Silvia 79, 80
Baker, Judieth E. 108
Barnett, Audrey 91
Barton, Ambrose D. 54
Bell, Charles L. 86, 90
Berngruber, Otto W. 55, 56, 59, 60
Bernhard, William A. 84
Blomquist, Jeanne 147
Brar, Sarmukh S. 60, 61, 64
Brennan, Patricia C. 10, 12, 14, 15, 41, 44, 135, 144
Breyer, Evelyn P. 153
Brockwell, Peter J. 23
Brown, Gerald A. 115
Brown, Mickey S. 123, 125
Brues, Austin M. 48, 50
Buess, Evelyn M. 101

Camden, Ronald W. 11
Carrigan, John L. 114
Cerny, Elizabeth A. 60, 61, 64
Chapman, George E. 84, 87, 88
Chen, Chen H. 115
Chladek, Dorothy 149
Chorney, William 23, 112, 113
Christian, Emily J. B. 2, 3, 4, 7
Chubb, George T. 16
Cooke, Eugenia M. 36
Copeland, James C. 121, 123

Dainko, Julia L. 72
Dane, Charles W. 71
Daniels, Edward W. 153, 154
Danyluk, Steven S. 84, 85, 86, 87, 88, 90
Danziger, Rudy G. 55
Davies, David B. 84, 85, 86
Davies, David J. G. 24
Decker, Louis H. 110, 112
Dedolph, Richard R. 22, 23, 110, 112, 113
Devine, Rosemarie L. 134
Dipert, Merlin H. 6, 22, 23, 112, 146
Dobra, William A. 102
Doyle, Donald E. 143, 146
Drick, Sandra A. 127

Ecker, R. E. 73, 74, 75
Edmundson, Allen B. 94, 96, 99
Egan, Nancy 152
Ehret, Charles F. 90, 91, 101
Eisler, William J. 56, 59
Ely, Kathryn R. 94, 96
Engel, Milton B. 73

Faulhaber, Joann T. 67
Feinstein, Robert N. 11, 67, 68, 69, 70, 71
Flynn, Robert J. 10, 11, 12, 14, 16, 17, 18
Freedman, Michael L. 119, 128
Freitag, Per 73
Fritz, Thomas E. 10, 12, 14, 18, 132, 134, 135, 137
Fry, R. J. Michael 1, 23, 32, 33, 38, 40, 41, 51

Gordon, Solon A. 101, 102, 103, 105, 114, 115
Graff, Gustav 60
Grahn, Douglas 38, 116, 118
Griem, Melvin L. 1
Grube, Donald D. 48, 50

Han, Antun 79
Hardman, Karl D. 94, 96, 98
Haumann, Joseph 56, 88
Hinchman, Ray R. 105
Hofmann, Alan F. 55
Holman, Ralph T. 60
Holmblad, Gordon L. 26
Hopen, Herbert J. 113
Howard, Judith B. 67, 69, 70, 71
Hruska, Frank E. 86
Hulesch, Jane L. 116, 118
Hutson, Nancy K. 66

Jaroslow, Bernard N. 9, 67
Jordan, Donn L. 32, 41, 44

Kaspar, Lillian V. 145
Kickels, Wayne T. 127
Kisieleski, Walter E. 1, 33, 54
Klein, Peter D. 55, 56, 59, 60
Kotula, Bruno S. 88
Kretz, Norbert D. 135, 137
Krisch, Robert E. 127, 128
Kubitschek, Herbert E. 118, 119

Lea, Ruth Ann 38, 116, 118
Lester, Roger 59
Liang, James C. 114
Lindenbaum, Arthur 149, 152
Little, Joanna M. 59
Long, Melvin D. 78
Longwell, Arlene C. 153, 154
Lorenz, John R. 123

Mackevicius, Faustina 54, 60, 61, 64
Malkinson, Frederick D. 1
McArdle, Eugene W. 101
McDowell, Richard E. 75, 123
McNeill, James J. 59
McNiff, Judith M. 153, 154
Miller, Carol 106
Miller, Marietta 9, 36
Moretti, Elizabeth S. 149

Nance, Sharron L. 55
Nelson, Donald M. 60, 61, 64
Nelson, Donald Michael 68
Newlin, Janet E. 40
Noack, Neleen G. 108
Norris, William P. 130, 132, 134, 135, 137, 139, 141, 144, 145

O'Malley, Mary P. 32, 34, 36, 41, 44
Ortiz-Ortiz, Librado 9

Pearson, Donald L. 143
Peraino, Carl 51, 52, 53, 60, 61, 64, 71
Poole, Calvin M. 10, 11, 17, 18, 44, 130, 132
Powers, Dennis A. 96, 99

Rahman, Yueh-Erh 60, 61, 64
Rehfeld, Carl E. 141, 143, 146, 147
Rosenthal, Marcia W. 149
Ross, Dennis W. 76
Russell, John J. 149
Rust, John H. 38, 40

Sacco, Paul 59
Sacher, George 38
Sallese, Anthony R. 1, 32, 33
Sanderson, Margaret H. 3, 5
Savol, Rosanne 69, 71
Schiffer, Marianne 94, 96
Schlenk, Fritz 66, 72
Schoenfield, Leslie J. 55
Shen-Miller, Jane 106, 108
Silver, Simon 119
Simkins, Richard C. 15, 44, 135, 144
Sinclair, Warren K. 29, 76, 77, 78, 79, 80, 81, 82, 83
Sly, Dayle A. 96
Smith, L. Dennis 74, 75
Smyth, Marguerite A. 149
Staffeldt, Everett 40, 51
Stamps, Robert H. 113
Stearner, S. Phyllis 2, 3, 4, 5, 6, 7
Stroud, Agnes N. 115
Svihla, George 72, 73
Szczepanik, Patricia A. 55, 59, 60

Tahmisian, Theodore N. 60, 61, 64, 100, 134
Taylor, Glenn N. 147
Taylor, James A. 135
Thompson, Malcolm J. 60
Thomson, John F. 55
Tollaksen, Sandra L. 55
Tolle, David V. 12, 132, 134
Trier, Joseph E. 26
Trucco, Ernesto 19, 22, 23
Tyler, Sylvanus A. 6, 18, 22, 24

Valdez, David 119
Victor, Thomas A. 86

Wassermann, Friedrich 54
Webb, Robert B. 93, 123, 125
Weber, Charlotte L. 1
Westholm, Florence A. 96
Whiteside, William F. 113
Williamson, Frank 26, 32
Wille, John J., Jr. 90, 91
Wood, Mical K. 94, 96
Wright, Betty Jean 60, 61, 64, 100

Yu, C. K. 79, 82, 83

Zelle, Max R. 146
Zeman, Ruth C. 132, 134
Zydek-Cwick, Cynthia R. 66

ARGONNE NATIONAL LAB WEST
3 4444 00010859 7

B